Incorporating spatial and temporal dynamics into evaluations of fish populations and habitat

Julia Indivero

A dissertation

submitted in partial fulfillment of the

requirements for the degree of

Doctor of Philosophy

University of Washington

2025

Reading Committee:

Timothy E. Essington, Chair

Chelsea Wood

James T. Thorson

Program Authorized to Offer Degree:

Aquatic and Fishery Sciences

University of Washington

Abstract

Incorporating spatial and temporal dynamics into evaluations of fish populations and habitat

Julia L. Indivero

Chair of the Supervisory Committee:
Timothy E. Essington
School of Aquatic and Fishery Sciences

The ocean is rapidly changing, with impacts on both the physical environment and ecological systems. In my dissertation, I seek to understand how variations in fish populations over space and time are driven by environmental conditions in the ocean, and to improve statistical methods to accomodate this variation and thereby contribute to sustainable fisheries. In the following four chapters of my dissertation, I develop, test, and apply improved methodologies that link fish demographics to environmental conditions and address pressing management concerns. A spatio-temporal model of weight-at-age of walleye pollock improved our understanding of the dynamics of local and population-level demographic processes and can be used in future stock assessment models. I developed a statistical model that incorporated a physiological response to temperature and oxygen into distribution modeling to better capture this joint effect, in the context of predicting impacts of climate change on local fish densities. Because spatial statistical models rely on environmental data, I used statistical approaches to expand oxygen data available and test the sensitivity of ecological models to environmental data. Lastly, I applied these improved techniques in retrospective statistical models to evaluate evidence for oxygen limitation on the distribution of 32 groundfish species in the northeastern Pacific Ocean. Overall this dissertation advances statistical solutions for accomodating spatio-temporal data in estimates and predictions of fish ecological responses to environmental change.

TABLE OF CONTENTS

ACKNOWLEDGEMENTS

My grandparents, Anne and Jim Simon, instilled in all their kids and grandkids the value of education and generously supported all of us in pursuing it. They were loving, smart, and curious people, and I would not be where I am now without them. Thank you to my family—Mom, Gabi and Luke—for your limitless sense of humor and patience and for shaping me into the person I am. (Mom, thanks for taking care of my cat.) And thank you to my extended family—Uncle Jimmy and Aunt Cecilia, Uncle Steve and Aunt Heather, Madeleine, Adam, Nathaniel, Nancy, David, Jen, Dave, Max, Jakob, Jolli, and more—for so much love and support over the years.

While starting a PhD in Fall 2020 was tough for many reasons, it did mean I got to be part of the best cohort at SAFS. You are all spectacular scientists and friends, and I have been lucky to get to go through everything with you all the last five years. Emily (B) is the best lab buddy and friend I could have asked for through grad school. Thanks for the acrostic poem of my work strategy, so many winter Tuesdays spent at the climbing gym, and for talking on the phone basically every day. Jess, Arial, Zoe, and Laurel all kept me grounded, provided non-stop support, advice, and laughter, reminded me that we were all in this together. Markus, thanks for never letting me forget that my first chapter was about walleye pollock. Zoe, thank you for being my statistical phone-a-friend and sounding board. And to the rest of the SAFS graduate school community—Helena, Jezella (there's no one else I'd rather go to Medora's dance class with!), Callum, Amelia, Miranda, Emily (J), Emily (S) and dozens others that I am forgetting—you are what make this department a strong community. And thanks to my friends that are not fish scientists—Maddie, Heidi, Marissa, Megan, Caitlin, Cheryl, Cailene—for always being up for backpacking, traveling, and phone calls that got me out of my dissertation brain and back into the real world.

Science requires scientists, and scientists require funding. I was fortunate to be supported in my PhD from multiple sources. My deepest thanks to the Usha and S. Rao Varanasi Endowed Fellowship in Environmental and Marine Stewardship; H. Mason Keeler Endowment for Excellence; Richard T. Whiteleather, Fisheries B.S. 1935 Endowed Scholarship; The Hall Puget Sound Student Support Fund; Washington Sea Grant; the National Pacific Research Board; and the UW Cooperative Institute for Climate, Ocean, & Ecosystem Studies (CICOES) for providing fellowships and grants that funded my PhD.

My favorite part of science is getting to work with incredible people. A large scientific community made the work of this dissertation possible and have supported my career. Most importantly, an endless thank you to my advisor Tim. I cannot imagine a better person to get to work with for my PhD—I am grateful for the constant support on analysis, writing, and everything research related; for the the positive, collaborative, and compassionate lab culture that you foster; and for being a funny, kind, thoughtful, and helpful human. Between getting stuck on a boat in the Puget Sound a couple times and working through math on the whiteboard, it has been a joy to get to work with you. And thank you to my committee members—Jim Thorson, Chelsea Wood, Daniel Schindler, and Karin Martin—for always asking insightful questions that made me think more deeply about my research and how to be a better scientist.

My collaborators and coauthors Eric Ward, Sean Anderson, Jim Ianelli, Lewis Barnett, Sam Siedlecki, John Pohl, and Sean Rohan all contributed immense help throughout the research process, including on data wrangling, model fitting, and manuscript writing. Thank you to Owen Liu, Caitlin Allen-Akselraud, and Sofia Wasserman for help with data curation and analysis; Allen Hicks and Ian Stewart for help with the International Pacific Halibut Commission data; and to all participants of the bottom trawl survey for their important work collecting data that this dissertation used. Thank you to Sam Scherer, Michael Martinez, and the rest of the SAFS Admin office for make sure everything is running smoothly. Special thank you to Jenny Bigman and Alexa Fredston for being such helpful and encouraging friends and mentors.

Thank you to Nick Ward and Allison Myers-Pigg at PNNL for giving me the chance to do so much labwork, field work, analysis, and manuscript writing that prepared me for this PhD. And to the many teachers, professors, and supervisors over the years—Sonia Sultan and Michael Singer at Wesleyan University, Bree Yednock at South Slough National Estuarine Research Reserve—that encouraged me to continue pursuing this career. Lastly, I was incredibly fortunate to intern with the White House Office of Science and Technology Policy Climate & Environment team in 2023. Thank you to everyone there—Heather, Jane, Laura, Hila, Dave, and more—for the opportunity to learn and be part of it. It was inspiring to see what good people in government can do.

DEDICATION

To my grandparents, Anne and Jim Simon
זיכרונם לברכה

INTRODUCTION

Fisheries scientists have long recognized that fish demography and distribution are driven by environmental conditions in the ocean. There is extensive spatial complexity and heterogeneity of population density (Hutchings 1996, Sagarin & Gaines 2002, Sagarin et al. 2006, Barnett et al. 2021) and in population vital rates, such as in offspring survival (Langangen et al. 2016), density-dependence (Shima & Osenberg 2003, Johnson 2006), recruitment (Myers & Ca 1998) and growth (Kerrigan 1994, Marshall & Frank 1995, Taylor & Stefánsson 1999, Gust et al. 2001, Pardoe et al. 2008, Correa et al. 2021). This spatial and temporal variability is often tied to differences in local environmental conditions and habitat features, such substrate, depth, and food availability, over both space and time across a seascape (Hofmann and Powell 1998, Bergstad et al. 2008, Medeiros et al. 2010, Frederiksen et al. 2014, Kimirei et al. 2015, Vincenzi et al. 2018). For instance, fundamental physiological impacts of dissolved oxygen and temperature on fish influence size and growth (e.g. Portner and Knust 2007, Audzijonyte et al. 2018, Rubalcaba et al. 2020) and can limit species' ranges to their thermal tolerances (Ekman 1953). Changes in temperature over time can similarly cause shifts in spatial distributions (Rose et al. 2000, Perry et al. 2005) and can impact annual recruitment (DeYoung and Rose 1993, Johnson 2007, Mueter et al. 2011) and growth (Portner et al. 2001, Hurst and Abookire 2006).

Climate change will be a source of unprecedented environmental change in the ocean, including to the spatial and temporal patterning of marine environmental characteristics that will impact marine fish. Over the next century many regions are likely to experience rising temperatures (Cheng et al. 2019) and widespread decline in dissolved oxygen (Diaz and Rosenberg 2008). Differences in the magnitude of these shifts at the regional and at a local level (Garcia-Soto et al. 2021) will change the spatial makeup of environmental conditions. Increasing frequency of extreme events such as heatwaves (Frölicher et al. 2018) will also change temporal dynamics of the environment. Overall, variability in marine environmental conditions is projected to increase under climate change, in turn increasing environmental heterogeneity (Boyd et al. 2016).

These environmental changes will likely have complex and varied impacts to demographic processes and spatial distributions. Temperature and oxygen, two key environmental conditions directly altered in climate change, are central to fundamental physiological processes in marine fishes. There is early documentation of biological patterns linked to temperature, such as in species' occurrences (Ekman 1953), range edges (Grinnell 1917), fluctuations in population size (Hjort 1914), and latitudinal clines in body size (Bergmann 1847). In addition to these broad biogeographic patterns, early research recognized that metabolism (aerobic, i.e. oxygen consumption) of individual organisms scaled with body mass (Kleiber 1932; Rubner 1883) and temperature (Ege & Krogh 1914; Murray 1908), and that fish avoided low oxygen (Shelford & Allee 1914). Observed natural patterns were subsequently described by mathemetical expressions rooted in fundamental laws of physics and chemistry: the mechanical forces and geometry behind morphology (Thompson 1917); that metabolic rates, as chemical reactions, are dependent on temperature (Arrhenius 1889); and geometric scaling of surface to volume ratios (Kleiber 1832, Rubner 1883). These physical and chemical laws, for instance, underlay the mathematical expression of growth developed in von Bertalanffy (1938) that is widely used. Application of these principles additionally underpinned early theorizing of oxygen and temperature limitations for fish (Fry 1947). Sustained empirical experimental laboratory studies have been a primary focus to

measure the temperature scaling of metabolic rates, and therefore oxygen demand, for numerous species (Beamish 1964; Fry & Hart 1948; Gardner et al. 1922; Ultsch et al., 1978; see Rogers et al. 2016 for meta-analysis of 96 published studies).

Further research to develop mechanistic understandings and unified frameworks has continued to build widespread theoretical and empirical support for physiological impacts of temperature and oxygen on marine species. For instance, von Bertalanffy growth has been applied to develop mechanistic hypotheses on how oxygen limitation stems from morphological constraints on the proportion of gill area to body size (Pauly 1981). Physical and chemical principles and empirical research on metabolic rates discussed above were similarly formally unified into the Metabolic Theory of Ecology (Brown et al. 2004; Gillooly et al. 2001). By conceptually and mathematically linking temperature, body size, and metabolic rates, this theory provides a framework for understanding temperature-driven patterns from individual to biogeographic scales, and has been empirically demonstrated to help explain individual growth (Lindmark et al. 2022), trophic dynamics (O'Gorman et al. 2016), ecosystem metabolism (Enquist et al. 2003), and biogeographic gradients in larval dispersal (O'Connor et al. 2007) and biomass (van Denderen et al. 2023). Metabolic theory has additionally been integrated into indices that provide a way to statistically evaluate the effects of changing oxygen and temperature on fish distribution (e.g. Deutsch et al. 2015) and growth (e.g. Clarke et al. 2021; Lindmark et al. 2022). For instance, combining insights from metabolic theory with von Bertalanffy indicates that higher temperatures and lower oxygen will lead to smaller fishes and changes in abundance and distribution (Cheung et al., 2012).

Together with direct physiological impacts of temperature and oxygen described above, climate change is influencing fish population dynamics via a range of ecological mechanisms, such as changes in food availability, predator—prey interactions and species assemblage, and phenology (Brander 2007). Together these changes are impacting demographic processes, such as growth and size (e.g. Huang et al. 2021, Sheridan and Bickford 2011, Audzijonyte et al. 2020) and recruitment (e.g. Shoji et al. 2011). Additionally, there will likely be shifts in fish distributions, and some shifts have already been observed (Mueter et al. 2011, Pinsky et al. 2020, Rooper et al. 2020, Campana et al. 2020). For instance, species in the northeast U.S. have moved northeastward on average 20 kilometers per decade (Pinsky et al. 2013), and Atlantic cod have moved significantly northward and deeper in the North Sea since the 1940s (e.g. Engelhard et al. 2013).

These impacts of rapid environmental change on fish demographic rates have implications for fisheries conservation and management. While many countries may have research programs related to impacts on climate change or consider ecosystem impacts of climate change, climate is not explicitly considered in policy or in stock assessments of any of the countries examined in one review (Bryndum-Buchholz et al., 2021). Yet stock assessment models used to make management decisions are sensitive to changes in demographic rates (Thorson et al. 2015b) that are impacted by environmental conditions. Additionally, population-level demographic rates used in stock assessment models consist of local-scale responses of fish to environmental conditions (Fredericksen et al. 2014; Horodysky et al. 2015; Thorson et al. 2020). Stock assessment models often do not incorporate the extent of variation in demographic characteristics, such as growth, both over time and spatially over a species' geographic range (Cadrin et al. 2020, Gruss et al. 2021, Punt et al. 2021). Not considering this spatial variation can

lead to biased and imprecise estimates of population status (Hamilton et al 2011,Thorson et al., 2015, Barnett et al. 2021). If climate change alters the prevailing environment, and demographic rates consequently change, the outcomes of a stock assessment will be inaccurate if they fail to take into account this variation. Being able to explore how demographic rates may respond to environmental change is therefore crucial for incorporating the effects of climate change into stock assessment models (Punt et al. 2021) and fisheries management (Holbrook and Johnson 2014).

Similarly, distributional shifts due to climate change may cause challenges for existing fisheries management regimes. Allocation and management boundaries are often static geographic areas that are based on historical adult distributions during a particular season (e.g., one that is easily surveyed or the primary fishing component). As species shift in or out of these boundaries across seasons and/or years, there are various possible governance challenges. It may increase inter-state conflict, as it did in the case of the "mackerel wars" (Spijkerss & Boonstra 2017) or cause mismatch between existing monitoring, survey, and allocation regimes (Sumaila et al. 2011, Pinsky et al., 2018, Baudron et al. 2020). Even within jurisdictional boundaries, shifts in distribution may constrain or expand fishing opportunities at a local level through changes in the location of target species relative to existing ports and processing facilities, gear type, and the presence of co-occurring protected bycatch species (e.g. Astthorsson et al. 2012, Pinsky and Mantua 2014, Hare et al. 2016, Kleisner et al. 2017, Liu et al 2023). Anticipating possible changes in species distribution will enable management to pre-emptively plan, such as establishing transboundary agreements (Oremus et al. 2020, Pentz & Klenk 2023), quota reallocation (Costello et al. 2008, Bell et al. 2020, Palacios-Abrantes et al. 2022) and survey design and data processing (e.g. O'Leary et al. 2020). Forecasting these shifts also facilitates adaptation in the fishing industry, such as identifying new fishing options (Bell et al. 2020, Fulton et al. 2021), changing permit rules (McIlgorm et al. 2010, Mills et al. 2013, Farady & Bigford 2019) new markets and post-harvest value (Bell et al. 2020), moving or building new infrastructure (Bell et al. 2020), developing insurance programs (Hotta 1999, Mumford et al. 2009) and permit banks (Bell et al. 2020) and eliminating harmful fisheries subsidies (Cisneros-Montemayor et al. 2020). Evaluating the need for these management and industry options requires understanding the extent and pace of change to fish population dynamics and distributions for that specific region and species.

Incorporating environmental variation to predict fish population demography and distribution has therefore been an ongoing effort in fisheries research (e.g. Haltuch et al. 2019, Thompson et al. 2023); however, it still faces several challenges to implement. For one, it is often difficult to identify the specific environmental characteristics that explain current fish population dynamics (Thorson et al. 2017, Dambrine et al. 2020). For example, environment-recruitment relationships are notoriously difficult to establish (Myers & Cadigan 1998, Punt et al. 2014, Schindler & Hilborn, 2015) and a regime shift in the North Pacific in 1976-1977 was not identified until decades later because of high interannual variation that masked it (Wooster & Zhang 2004). There are complexities inherent in ecological systems that complicate analysis: overlapping processes operating across different time scales (Levin 1992, Tommasi et al. 2017), regional differences in how climate and oceanographic conditions are related (Hunt et al. 2002, Huntington et al. 2020), confounding environmental changes (temperature, oxygen, pH, etc.)

(Scheutz et al. 2019), and underlying spatial and temporal variation that is unaccounted for in environmental covariates (Thorson et al. 2015, Maunder et al. 2020, Breivik et al. 2021).

Additionally, specific features of climate change exacerbate these ecological complexities and the analytical challenges for forecasting species responses to environmental changes. Populations face cumulative impacts (Pinsky and Mantua 2014) from multiple stressors (Brander 2007)—that is, numerous physical changes, such as to temperature, oxygen, acidification, sea level, ocean circulation, and related ecosystem effects, such as to food availability and species interactions. Second, the pace and magnitude of climate change is anomalously high and in some regions is creating novel environmental conditions outside historical conditions in at least the past 1500 years (e.g. Marshall et al. 2017, Smith et al. 2022). This may cause systems to behave differently than in the past (Palacios-Abrantes et al. 2022), as systems often exhibit changing relationships between the environment and population dynamics over time (Asch et al. 2022). Predictions of fish distribution based on relationships during the modern era (i.e., past 500 years) may consequently break down when used in forecasting (Muhling et al 2020, Barnes et al. 2022). Relatedly, there are probably nonlinear responses to these novel conditions, such as tipping points, threshold values, and rapid state shifts (Selkoe et al. 2015) that challenge forecasting. Lastly, there is a high degree of uncertainty in forecasting climate change responses. This is due to added uncertainty from both the projections of earth system models and in the emissions scenarios (e.g. Brodie et al. 2022, Davies et al. 2023), on top of the inherent uncertainty in fish response to the environment stemming from the challenges discussed previously.

This dissertation advances solutions to these challenges by: 1) incorporating spatial and temporal variation of demographic traits and 2) linking changes in environmental characteristics to local fish densities, in the contexts of important management questions. I developed a spatio-temporal model of weight-at-age of walleye pollock, a data-rich and commercially important fishery, for a new approach to be used in the stock assessment (*Chapter 1*). To enable better predictions of effects of environmental change, I tested a new approach to incorporate physiological effects of oxygen and temperature on fish responses in spatial models (*Chapter 2*). I expanded the underlying environmental data available for physiological thresholds and distributional responses to local conditions and evaluated the sensitivity of these estimates to the source of environmental data (*Chapter 3*). Lastly, I applied these improved fish distribution models to a broad geographic and species assemblage to identify groundfish species with a threshold response to oxygen along the U.S. West Coast (*Chapter 4*). Overall this dissertation improves methodologies to link fish demographic rates and distribution to environmental conditions and to address pressing management concerns to improve the sustainable management of fisheries.

References

Arrhenius, S. (1889). Über die Reaktionsgeschwindigkeit bei der Inversion von Rohrzucker durch Säuren. *Zeitschrift Für Physikalische Chemie*, *4*(1), 226–248.

Astthorsson, O. S., H. Valdimarsson, A. Gudmundsdottir, and G. J. Óskarsson. 2012. Climate-related variations in the occurrence and distribution of mackerel (Scomber scombrus) in Icelandic waters. *ICES Journal of Marine Science* 69:1289–1297. https://doi.org/10.1093/icesjms/fss084

Audzijonyte, A., Barneche, D., Baudron, A., Belmaker, J., Clark, T., Marshall, C., Morrongiello, J., van Rijn, I. 2018. Is oxygen limitation in warming waters a valid mechanism to explain decreased body sizes in aquatic ectotherms? *Global Ecology and Biogeography* 28: 64-77. https://doi.org/10.1111/geb.12847

Audzijonyte, A., Richards, S.A., Stuart-Smith, R.D. *et al.* (2020). Fish body sizes change with temperature but not all species shrink with warming. *Nat Ecol Evol* 4: 809–814. https://doi.org/10.1038/s41559-020-1171-0

Barnes, C., Essington, T., Pirtle, J., Rooper, C., Laman, E., Holsman, K., Aydin, K., and Thorson, J. 2022. Climate-informed models benefit hindcasting but present challenges when forecasting species-habitat associations. *Ecography* e01689. https://doi.org/10.1111/ecog.06189

Barnett, L. A. K., Ward, E. J., & Anderson, S. C. (2021). Improving estimates of species distribution change by incorporating local trends. *Ecography*, *44*(3), 427–439. https://doi.org/10.1111/ecog.05176

Baudron, A.R., Brunel, T., Blanchet, M.-A., Hidalgo, M., Chust, G., Brown, E.J., Kleisner, K.M., Millar, C., MacKenzie, B.R., Nikolioudakis, N., Fernandes, J.A. and Fernandes, P.G. 2020. Changing fish distributions challenge the effective management of European fisheries. *Ecography* 43: 494-505. https://doi.org/10.1111/ecog.04864

Beamish, F. W. H. (1964). Standard oxygen consumption: Influence of weight and temperature on respiration of several species. *Can. J. Zool*, *42*, 177–188.

Bell, R. J., Odell, J., Kirchner, G., & Lomonico, S. (2020). Actions to Promote and Achieve Climate-Ready Fisheries: Summary of Current Practice. *Marine and Coastal Fisheries*, *12*(3), 166–190. https://doi.org/https://doi.org/10.1002/mcf2.10112

Begg, G. and Marteinsdottir, G. 2002. Environmental and stock effects on spatial distribution ad abundance of mature cod Gadus morhua. Marine Ecology Progress Series 229: 345-262.

Bergmann, C. (1847). Ueber die verhäitnisseder wärmeökonomie der thiere zu ihrer grösse. *Go ttinger Studien*.

Bergstad, O., Menezes, G., and Hoines, A. 2008. Demersal fish on a mid-ocean ridge: Distribution patterns and structuring factors. *Deep Sea Research Part II: Topical Studies in Oceanography* 55(1-2): 185-202. https://doi.org/10.1016/j.dsr2.2007.09.005

Boyd, P., Cornwall, C., Davison, A., Doney, S. Fourquez, M., Hurd, C., Lima, I., McMinn, A. 2016. Biological responses to environmental heterogeneity under future ocean conditions. *Global Change Biology* 22(8): 2633-2650. *https://doi-org.offcampus.lib.washington.edu/10.1111/gcb.13287*

Brander, K. M. (2007). *Global fish production and climate change*. www.pnas.orgcgidoi10.1073pnas.0702059104

Breivik, O., Aanes, F., Sovik, G., Aglen, A., Mehl, S., and Johnsen, E. 2021. Predicting abundance indices in areas without coverage with a latent spatio-temporal Gaussian model. *ICES Journal of Marine Science* 78(6), 2031-2042. https://doi.org/10.1093/icesjms/fsab073

Brown, J., Gillooly, J., Allen, A., et al. 2004. Toward a metabolic theory of ecology. *Ecology* (85): 1771-1789. https://doi.org/10.1890/03-9000

Bryndum-Buchholz, A., Tittensor, D. P., & Lotze, H. K. (2021). The status of climate change adaptation in fisheries management: Policy, legislation and implementation. *Fish and Fisheries*, *22*(6), 1248–1273. https://doi.org/10.1111/faf.12586

Cadrin, S., Maunder, M., and Punt, A. 2020. Spatial Structure: Theory, estimation and application in stock assessment models. Fisheries Research 229: 105608. https://doi.org/10.1016/j.fishres.2020.105608

Campana, S.E., Stefánsdóttir, R.B., Jakobsdóttir, K. *et al.* 2020. Shifting fish distributions in warming sub-Arctic oceans. *Sci Rep. (10):* 16448. https://doi.org/10.1038/s41598-020-73444-y

Cheng, L., Abraham, J., Hausfather, Z., and Trenberth, K.E. 2019. How fast are the oceans warming? *Science* 363(6423): 128-129. https://10.1126/science.aav7619

Cheung, W.W.L., Sarmiento, J.L., Dunne, J., Frölicher, T.L., Lam, V.W.Y., Deng Palomares, M.L., Watson, R., and Pauly, D. 2012. Shrinking of fishes exacerbates impacts of global ocean changes on marine ecosystems. Nature Climate Chang, 3: 254-258. https://doi.org/10.1038/NCLIMATE1691

Cisneros-Montemayor, A. M., Ota, Y., Bailey, M., Hicks, C. C., Khan, A. S., Rogers, A., Sumaila, U. R., Virdin, J., & He, K. K. (2020). Changing the narrative on fisheries subsidies reform: Enabling transitions to achieve SDG 14.6 and beyond. *Marine Policy*, *117*. https://doi.org/10.1016/j.marpol.2020.103970

Clarke, T. M., Wabnitz, C. C. C., Striegel, S., Frölicher, T. L., Reygondeau, G., & Cheung, W. W. L. (2021). Aerobic growth index (AGI): An index to understand the impacts of ocean warming and deoxygenation on global marine fisheries resources. *Progress in Oceanography*, *195*, 102588. https://doi.org/https://doi.org/10.1016/j.pocean.2021.102588

Correa, G. M., McGilliard, C. R., Ciannelli, L., & Fuentes, C. (2021). Spatial and temporal variability in somatic growth in fisheries stock assessment models: evaluating the consequences of misspecification. *ICES Journal of Marine Science*, *78*(5), 1900–1908.

Dambrine, C., Woillez, M., Huret, M., and de Pontual, H. 2020. Characterising Essential Fish Habitat using spatio-temporal analysis of fishery data: A case study of the European seabass spawning areas. *Fisheries Oceanography* 30: 413-428.

Davies, S.C., Thompson, P.L., Gomez, C., Nephin, J., Knudby, A., Park, A.E., Friesen, S.K., Pollock, L.J., Rubidge, E.M., Anderson, S.C., Iacarella, J.C., Lyons, D.A., MacDonald, A., McMillan, A., Ward, E.J., Holdsworth, A.M., Swart, N., Price, J. and Hunter, K.L. .2023. Addressing uncertainty when projecting marine species' distributions under climate change. *Ecography*: e06731. https://doi.org/10.1111/ecog.06731

Deutsch, C., A. Ferrel, B. Seibel, H. O. Portner, and R. B. Huey. 2015. Climate change tightens a metabolic constraint on marine habitats. *Science* 348:1132–1135. https://doi.org/10.1126/science.aaa1605

Deutsch, C., J. L. Penn, and B. Seibel. 2020. Metabolic trait diversity shapes marine biogeography. *Nature* 585:557–562. https://doi.org/ 10.1038/s41586-020-2721-y

DeYoung, B. and Rose, G. 1993. On recruitment and distribution of Atlantic Cod (Gadus morhua) off Newfoundland. *Canadian Journal of Fishery and Aquatic Sciences* 50: 2729-2741.

Diaz, R. J., and R. Rosenberg. 2008. Spreading dead zones and consequences for marine ecosystems. *Science* 321:926–929. https://doi.org/10.1126/science.1156401

Ege, R., & Krogh, A. (1914). On the Relation between the Temperature and the Respiratory Exchange in Fishes. *Internationale Revue Der Gesamten Hydrobiologie Und Hydrographie*, *7*(1), 48–55. https://doi.org/https://doi.org/10.1002/iroh.19140070105

Ekman, S. (1953). *Zoogeography of the sea*.

Engelhard, G.H., Righton, D.A. and Pinnegar, J.K. 2014. Climate change and fishing: a century of shifting distribution in North Sea cod. Glob Change Biol, 20: 2473-2483. https://doi.org/10.1111/gcb.12513

Enquist, B. J., Economo, E. P., Huxman, T. E., Allen, A. P., Ignace, D. D., & Gillooly, J. F. (2003). *Scaling metabolism from organisms to ecosystems*. www.nature.com/nature

Farady, S. E., & Bigford, T. E. (2019). Fisheries and Climate Change: Legal and Management Implications. *Fisheries*, *44*(6), 270–275. https://doi.org/10.1002/fsh.10263

Frederiksen, M., Lebreton, J-D., Pradel, R., Choquet, R., and Gimenez, O. 2014. Identifying links between vital rates and environment: a toolbox for the applied ecologist. Journal of Applied Ecology 51:71-81. https://doi.org/10.1111/1365-2664.12172

Frölicher, T., Fischer, E., and Gruber, N. 2018. Marine heatwaves under global warming. *Nature* 560: 360-364. https://doi.org/ 10.1038/s41586-018-0383-9

Fry, F. (1947). Effects of the environment on animal activity. *Publ. Out. Fish. Res. Lab.*, *55*(68), 1–62.

Fry, F. & Hart, J. S. (1948). The relation of temperature to oxygen consumption in the goldfish. *The Biological Bulletin*, *94*(1), 66–77.

Gardner, J. A., King, G., & Powers, E. B. (1922). The respiratory exchange in fresh water fish. III. Gold-fish. *Biochemical Journal*, *16*(4), 523.

Garcia-Soto, C., Cheng, L., Caesar, L., Schmiddtko, S., Jewett, E. et al. An Overview of Ocean Climate Change Indicators: Sea Surface Temperature, Ocean Heat Content, Ocean pH, Dissolved Oxygen Concentration, Arctic Sea Ice Extent, Thickness and Volume, Sea Level and Strength of the AMOC (Atlantic Meridional Overturning Circulation). *Frontiers in Marine Science. https://doi.org/10.3389/fmars.2021.642372*

Gillooly, J., Brown, J., West, G., Savage, V., & Charnov, E. (2001). *Effects of size and temperature on metabolic rate*. https://digitalrepository.unm.edu/biol_fsp

Grinnell, J. (1917). Field tests of theories concerning distributional control. *The American Naturalist*, *51*(602), 115–128.

Gruss, A., Thorson, J.T., Stawitz, C.C., Reum, J.C.P., Rohan, S.K., and Barnes, C.L. 2021. Synthesis of interannual variability in spatial demographic processes supports the strong influence of cold-pool extent on eastern Bering Sea walleye pollock (Gadus chalcogrammus). *Progress in Oceanography*, 194:102569. https://doi.org/10.1016/j.pocean.2021.102569

Gust, N., Choat, J. H., & McCormick, M. I. (2001). Spatial variability in reef fish distribution, abundance, size and biomass: a multi scale analysis. *Marine Ecology Progress Series*, *214*, 237–251. https://www.int-res.com/abstracts/meps/v214/p237-251/

Haltuch, M., A'mar, Z., Bond, N., Valero, J. 2019. Assessing the effects of climate change on US West Coast sablefish productivity and on the performance of alternative management strategies, *ICES Journal of Marine Science*: Volume 76(6): 1524-1542, https://doi.org/10.1093/icesjms/fsz029

Hare, J. A., W. E. Morrison, M. W. Nelson, M. M. Stachura, E. J. Teeters, R. B. Griffis, M. A. Alexander, J. D. Scott, L. Alade, R. J. Bell, A. S. Chute, K. L. Curti, T. H. Curtis, D. Kircheis, J. F. Kocik, S. M. Lucey, C. T. McCandless, L. M. Milke, D. E. Richardson, E. Robillard, H. J. Walsh, M. C. McManus, K. E. Marancik, and C. A. Griswold. 2016. A Vulnerability Assessment of Fish and Invertebrates to Climate Change on the Northeast U.S. Continental Shelf. *PLOS ONE* 11:e0146756 https://doi.org/10.1371/journal.pone.0146756

Hjort, J. (1914). *Fluctuations in the great fisheries of northern Europe viewed in the light of*

biological research.

Hofmann, E. and Powell, T. 1998. Environmental variability effects on marine fisheries: Four case histories. *Ecological Applications* 8(1): S23-S32.

Holbrook, N. and Johnson, J. 2014. Climate change impacts and adaptation of commercial marine fisheries in Australia: a review of the science. *Climatic Change* 124:703-715. https://doi.org/10.1007/s10584-014-1110-7

Hotta, M. (1999). *Fisheries insurance programmes in Asia: experiences, practices and principles*.

Huang, M., Ding, L., Wange, J., Ding, C., Tao, J. 2021. The impacts of climate change on fish growth: A summary of conducted studies and current knowledge. *Ecological Indicators* 121: 106976. https://doi.org/10.1016/j.ecolind.2020.106976

Hunt, G. L., P. Stabeno, G. Walters, E. Sinclair, R. D. Brodeur, J. M. Napp, and N. A. Bond. 2002. Climate change and control of the southeastern Bering Sea pelagic ecosystem. *Deep-Sea Research II* 49:5821–5823. https://doi.org/10.1016/S0967-0645(02)00321-1

Huntington, H. P., S. L. Danielson, F. K. Wiese, M. Baker, P. Boveng, J. J. Citta, A. De Robertis, D. M. S. Dickson, E. Farley, J. C. George, K. Iken, D. G. Kimmel, K. Kuletz, C. Ladd, R. Levine, L. Quakenbush, P. Stabeno, K. M. Stafford, D. Stockwell, and C. Wilson. 2020. Evidence suggests potential transformation of the Pacific Arctic ecosystem is underway. *Nature Climate Change* 10:342–348. https://doi.org/10.1038/s41558-020-0695-2

Hurst, T. and Abookire, A. 2006. Temporal and spatial variation in potential and realized growth rates of age-0 year northern rock sole. *Journal of Fish Biology* 68: 905-919. https://10.1111/j.1095-8649.2006.00985.x

Hutchings, J. A. (1996). Spatial and temporal variation in the density of northern cod and a review of hypotheses for the stock's collapse. *Canadian Journal of Fisheries and Aquatic Sciences*, *53*(5), 943–962. https://doi.org/10.1139/f96-097

Johnson, D. W. (2006). Predation, Habitat Complexity, and Variation in Density-Dependent Mortality of Temperate Reef Fishes. In *Source: Ecology* (Vol. 87, Issue 5).

Johnson, D. 2007. Habitat complexity modifies post-settlement mortality and recruitment dynamics of a marine fish. *Ecology* 88(7): 1716-1725.

Kerrigan, B. A. (1994). Post-settlement growth and body composition in relation to food availability in a juvenile tropical reef fish. *Marine Ecology Progress Series. Oldendorf*, *111*(1), 7–15.

Kimirei, I., Nagelkerken, I., Slooter, N., Gonzalez, E., Huijbers, C., Mgaya, Y., and Rypel, A.

2015. Demography of fish populations reveals new challenges in appraising juvenile habitat values. *Marine Ecology Progress Series* 518: 225-237. https://doi.org/10.3354/meps11059

Kleiber, M. (1932). Body size and metabolism. *Hilgardia*, *6*, 315.

Kleisner, K. M., M. J. Fogarty, S. McGee, J. A. Hare, S. Moret, C. T. Perretti, and V. S. Saba. 2017. Marine species distribution shifts on the U.S. Northeast Continental Shelf under continued ocean warming. *Progress in Oceanography* 153:24–36. https://doi.org/10.1016/j.pocean.2017.04.001

Langangen, Ø., Ottersen, G., Ciannelli, L., Vikebø, F. B., & Stige, L. C. (2016). Reproductive strategy of a migratory fish stock: implications of spatial variations in natural mortality. *Canadian Journal of Fisheries and Aquatic Sciences*, *73*(12), 1742–1749.

Laufkötter, C., Zxjceischler, J., and Frölicher, T. 2020. High-impact marine heatwaves attributable to human-induced global warming. *Science* 369(6511): 1621-1625. https://doi.org/ 10.1126/science.aba0690

Levin, S.A. 1992. The Problem of Pattern and Scale in Ecology. *Ecology*, 73: 1943-1967. https://doi.org/10.2307/1941447

Lindmark, M., Audzijonyte, A., Blanchard, J. L., & Gårdmark, A. (2022). Temperature impacts on fish physiology and resource abundance lead to faster growth but smaller fish sizes and yields under warming. *Global Change Biology*, *28*(21), 6239–6253. https://doi.org/10.1111/gcb.16341

Marshall, C. and Frank, K. 1995. Density-dependent habitat selection by juvenile haddock (Melanogrammus aeglefinus) on the southwestern Scotian Shelf. Canadian Journal of Fisheries and Aquatic Sciences 52: 1007-1018.

Maunder, M., Thorson, J., Xu, H., Oliveros-Ramos, R., Hoyle, S., Tremblay-Boyer, Lee, H., Kai, M., Chang, S., Kitakado, T., Albertsen, C., Minte-Vera, C., Lennert-Cody, C., Aires-da-Silva, A., and Piner, K. 2020. The need for spatio-temporal modeling to determine catch-per-unit effort based indices of abundance and associated composition data for inclusion in stock assessment models. *Fisheries Research* 229: 105594. https://doi.org/10.1016/j.fishres.2020.105594

McIlgorm, A., Hanna, S., Knapp, G., Le Floc'H, P., Millerd, F., and Pan, M. 2010. How will c climate change alter fishery governance? Insight from seven international case studies. *Marine Policy* 34(1): 170-177. https://doi.org/10.1016/j.marpol.2009.06.004

Medeiros, P, Souza, A., and Ilarri, M. 2010. Habitat use and behavioural ecology of the juveniles of two sympatric damselfishes (Actinopterygii: Pomacentridae) in the south-western Atlantic Ocean. *Journal of Fish Biology* 77(7): 1599-1615. https://doi.org/10.1111/j.1095-8649.2010.02795.x

Mills, K. E., Pershing, A. J., Brown, C. J., Chen, Y., Chiang, F. S., Holland, D. S., Lehuta, S., Nye, J. A., Sun, J. C., Thomas, A. C., & Wahle, R. A. (2013). Fisheries management in a changing climate: Lessons from the 2012 ocean heat wave in the Northwest Atlantic. *Oceanography*, *26*(2). https://doi.org/10.5670/oceanog.2013.27

Mumford, J. D., Leach, A. W., Levontin, P., & Kell, L. T. (2009). Insurance mechanisms to mediate economic risks in marine fisheries. *ICES Journal of Marine Science*, *66*(5), 950–959.

Mueter, F. J., Bond, N.A., Ianelli, J.N., and Hollowed, A.B. 2011. Expected declines in recruitment of walleye pollock (Theragra chalcogramma) in the eastern Bering Sea under future climate change. *ICES Journal of Marine Science*, 68(6): 1284-1296. https://doi.org/10.1093/icesjms/fsr022

Murray, S. J. (1908). The distribution of organisms in the hydrosphere as affected by varying chemical and physical conditions. *Internationale Revue Der Gesamten Hydrobiologie Und Hydrographie*, *1*(1-2), 10–17.

Myers, R. A., & Ca, R. M. (1998). When do environment±recruitment correlations work? In *Reviews in Fish Biology and Fisheries* (Vol. 8).

O'Connor, M. I., Bruno, J. F., Gaines, S. D., Halpern, B. S., Lester, S. E., Kinlan, B. P., & Weiss, J. M. (2007). *Temperature control of larval dispersal and the implications for marine ecology, evolution, and conservation*. www.pnas.org/cgi/content/full/

O'Gorman, E. J., Ólafsson, Ó. P., Demars, B. O. L., Friberg, N., Guðbergsson, G., Hannesdóttir, E. R., Jackson, M. C., Johansson, L. S., McLaughlin, Ó. B., & Ólafsson, J. S. (2016). Temperature effects on fish production across a natural thermal gradient. *Global Change Biology*, *22*(9), 3206–3220.

Oremus, K. L., Bone, J., Costello, C., García Molinos, J., Lee, A., Mangin, T., & Salzman, J. (2020). Governance challenges for tropical nations losing fish species due to climate change. *Nature Sustainability*, *3*(4), 277–280. https://doi.org/10.1038/s41893-020-0476-y

Ottersen, G., Planque, B., Belgrano, A., Post, E., Reid, P., and Stenseth, N. 2001. Ecological Effects of the North Atlantic Oscillation. *Oecologica* 128(1):1-14.

Palacios-Abrantes, J., Frölicher, T. L., Reygondeau, G., Sumaila, U. R., Tagliabue, A., Wabnitz, C. C., & Cheung, W. W. L. (2022). Timing and magnitude of climate-driven range shifts in transboundary fish stocks challenge their management. *Global Change Biology*, *28*(7), 2312–2326. https://doi.org/10.1111/gcb.16058

Pardoe, H., Thórdarson, G., & Marteinsdóttir, G. (2008). Spatial and temporal trends in condition of Atlantic cod Gadus morhua on the Icelandic shelf. *Marine Ecology Progress Series*, *362*, 261–277.

Pauly, D. (1981). The relationship between gill surface area and growth performance in fish: a generalization of von Bertalanffy's theory of growth. *Meeresforsch*, *28*, 251–282.

Pentz, B., & Klenk, N. (2023). Will climate change degrade the efficacy of marine resource management policies? *Marine Policy*, *148*. https://doi.org/10.1016/j.marpol.2022.105462

Perry, A., Low, P., Ellis, J. and Reynolds, J. 2005. Climate change and distribution shifts in marine fishes. *Science* 308(5730): 1912-1915. https://doi.org/10.1126/science.1111322

Pinsky, M. L., Worm, B., Fogarty, M. J., Sarmiento, J. L., & Levin, S. A. (2013). Marine taxa track local climate velocities. Science 341: 1239.-1242. https://doi.org/10.1126/science.1239352

Pinsky, M. L., and N. J. Mantua. 2014. Emerging Adaptation Approaches for Climate-Ready Fisheries Management. *Oceanography* 27:146–159.

Pinsky, M. L., Reygondeau, G., Caddell, R., Palacios-Abrantes, J., Spijkers, J., & Cheung, W. W. L. (2018). Preparing ocean governance for species on the move. *Science*, *360*(6394), 1189–1191.

Pinsky, M., Selden, R., and Kitchel, Z. 2019. Climate-driven shifts in marine species ranges:

Scaling from Organisms to Communities. *Annual Review of Marine Science* 12: 153-79. https://doi.org/10.1146/annurev-marine-010419-010916

Portner, H. and Knust, R. 2007. Climate change affects marine fishes through the oxygen limitation of thermal tolerance. *Science* 315: 95-97. https://doi.org/10.1126/science.1135471

Portner, H., Berdal, B., Blust, R., Brix, O., Wachter, B., Guiliani, A., Joahnsen, T., Fischer, T., Knust, R., Lannig, G., Naevdal, G., Nedenes, A., Nyhammer, G., Sartoris, F., Serendero, I., Sirabella, P., Thorkildsen, S., and Zakhartsev, M. 2001. Climate induced temperature effects on growth performance, fecundity, and recruitment in marine fish: developing a hypothesis for cause and effect relationships in Atlantic cod (Gadus morhua) and common eelpout (Zoarces viviparus). Contintental Shelf Research 21(18-19): 1975-1997. https://doi.org/10.1016/S0278-4343(01)00038-3

Punt, A. E., A'Mar, T., Bond, N. A., Butterworth, D. S., De Moor, C. L., De Oliveira, J. A. A., Haltuch, M. A., Hollowed, A. B., & Szuwalski, C. (2014). Fisheries management under climate and environmental uncertainty: Control rules and performance simulation. *ICES Journal of Marine Science*, *71*(8), 2208–2220. https://doi.org/10.1093/icesjms/fst057

Punt, A.E., Dalton, M. G., Cheng, W., Hermann, A.J., Holsman, K.K., Hurst, T.P., Ianelli, J. N., Kearney, K. A., McGilliard, C.R., Pilcher, D.J., and Veron, M. 2021. Evaluating the impact of climate and demographic variation on future prospects for fish stocks: An application for northern rock sole in Alaska. *Deep Sea Research Part II: Topical Studies in Oceanography*, 189-190: 104951. https://doi.org/10.1016/j.dsr2.2021.104951

Rogers, N. J., Urbina, M. A., Reardon, E. E., McKenzie, D. J., & Wilson, R. W. (2016). A new analysis of hypoxia tolerance in fishes using a database of critical oxygen level (P crit). *Conservation Physiology*, *4*(1), cow012.

Rooper, C., Ortiz, I., Hermann, A., Laman, N. Cheng, W., Kearney, K. and Aydin, K. 2021. Predicted shifts of groundfish distribution in the Eastern Bering Sea under climate change, with implications for fish populations and fisheries management. *ICES Journal of Marine Science* 78(1) 220-234. https://doi.org/10.1093/icesjms/fsaa215

Rose, G., DeYoung, B., Kulka, D., Goddard, S. and Fletcher, G. 2000. Distribution shifts and overfishing the northern cod (Gadus Morhua): a view from the ocean. Canadian Journal of Fishery and Aquatic Science 57: 644-663.

Rosenberg, A., Bigford, T., Leathery, S., Hill, R., and Bickers, K. 2000. Ecosystem approaches to fishery management through essential fish habitat. *Bulletin of Marine Science* 66(3): 535-542.

Rubalcaba, J., Verberk, W., Hendriks, A. Saris, B., and Woods, H. 2020. Oxygen limitation may affect the temperature and size dependence of metabolism in aquatic ectotherms. *PNAS* 117(50): https://doi.org/10.1073/pnas.2003292117

Rubner, M. (1883). Über den einfluss der körpergrösse auf stoff-und kraftwechsel. *Zeitschrift Für Biologie*, *19*, 536.

Sagarin, R. D., & Gaines, S. D. (2002). The 'abundant centre'distribution: to what extent is it a biogeographical rule? *Ecology Letters*, *5*(1), 137–147.

Sagarin, R. D., Gaines, S. D., & Gaylord, B. (2006). Moving beyond assumptions to understand abundance distributions across the ranges of species. *Trends in Ecology & Evolution*, *21*(9), 524–530.

Shelford, V. E., & Allee, W. C. (1914). Rapid modification of the behavior of fishes by contact with modified water. *Journal of Animal Behavior*, *4*(1), 1.

Schindler, D. E., & Hilborn, R. (2015). Prediction, precaution, and policy under global change. *Science* (Vol. 347, Issue 6225, pp. 953–954). American Association for the Advancement of Science. https://doi.org/10.1126/science.1261824

Selkoe, K. A., Blenckner, T., Caldwell, M. R., Crowder, L. B., Erickson, A. L., Essington, T. E., Estes, J. A., Fujita, R. M., Halpern, B. S., Hunsicker, M. E., Kappel, C. V, Kelly, R. P., Kittinger, J. N., Levin, P. S., Lynham, J. M., Mach, M. E., Martone, R. G., Mease, L. A., Salomon, A. K., … Zedler, J. (2015). Principles for managing marine ecosystems prone to tipping points. *Ecosystem Health and Sustainability*, *1*(5), 1–18. https://doi.org/https://doi.org/10.1890/EHS14-0024.1

Schmidtko, S., Stramma, L. and Visbeck, M. 2017. Decline in global oceanic oxygen content during the past five decades. *Nature* 542: 335-339. https://doi.org/10.1038/nature21399

Sheridan, J., Bickford, D. 2011. Shrinking body size as an ecological response to climate change. *Nature Clim Change* 1: 401–406 (2011). https://doi.org/10.1038/nclimate1259

Shima, J. S., & Osenberg, C. W. (2003). Cryptic Density Dependence: Effects of Covariation between Density and Site Quality in Reef Fish. *Ecology*, *84*(1), 46–52. http://www.jstor.org/stable/3107996

Shoji, J., Toshito, S., Mizuno, K., Kamimura, Y. Hori, M., and Hirakawa, K. Possible effects of global warming on fish recruitment: shifts in spawning season and latitudinal distribution can alter growth of fish early life stages through changes in daylength, *ICES Journal of Marine Science*: 68(6): 1165–1169, https://doi.org/10.1093/icesjms/fsr059

Spijkers, J., & Boonstra, W. J. (2017). Environmental change and social conflict: the northeast Atlantic mackerel dispute. *Regional Environmental Change*, *17*(6), 1835–1851. https://doi.org/10.1007/s10113-017-1150-4

Sumaila, U. R., Cheung, W. W. L., Lam, V. W. Y., Pauly, D., & Herrick, S. (2011). Climate

change impacts on the biophysics and economics of world fisheries. *Nature Climate Change*, *1*(9), 449–456.

Taylor, L. and Stefansson, G. 2013. Growth and maturation of haddock (Melanogrammus aeglefinus) in Icelandic Waters. *Journal of Northwest Atlantic Fishery Science* 25: 101-114.

Thompson, D. (1917). *On Growth and Form*. Cambridge University Press.

Thorson, J.T., Shelton, A.O., Ward, E.J., Skaug, H.J. 2015. Geostatistical delta-generalized linear mixed models improve precision for estimated abundance indices for West Coast groundfishes. *ICES Journal of Marine Science* ,72(5): 1297-1310. https://doi.org/10.1093/icesjms/fsu243

Thorson, J. T., Skaug, H. J., Kristensen, K., Shelton, A. O., Ward, E. J., Harms, J. H., & Benante, J. A. 2015a. The importance of spatial models for estimating the strength of density dependence. In *Source: Ecology* (Vol. 96, Issue 5).

Thorson, J.T., Monnahan, C., and Cope, J. 2015b. The potential impact of time-variation in vital rates on fisheries management targets for marine fishes. *Fisheries Research* 169: 8-17. https://dx.doi.org/10.1016/j.fishres.2015.04.007

Thorson, J.T. and Minte-Vera, C. 2016. Relative magnitude of cohort, age, and year effects on size at age of exploited marine fishes. *Fisheries Research* 180: 45-53. https://dx.doi.org/10.1016/j.fishres.2014.11.016

Thorson, J.T., Ianelli, J. N., and Kotwicki, S. 2017. The relative influence of temperature and size-structure on fish distribution shifts: A case-study on Walleye pollock in the Bering Sea. *Fish and Fisheries* 18: 1073-1084. https://doi.org10.1111/faf.12225

Trowborst, A. 2009. International Nature Conservation Law and the Adaptation of Biodiversity to Climate Change: a Mismatch? *Journal of Environmental Law* 21(3): 419-442. https://doi.org/10.1093/jel/eqp024

Ultsch, G. R., Boschung, H., & Ross, M. J. (1978). Metabolism, Critical Oxygen Tension, and Habitat Selection in Darters (Etheostoma). *Ecology*, *59*(1), 99–107. https://doi.org/https://doi.org/10.2307/1936635

Wooster, W. S., & Zhang, C. I. (2004). Regime shifts in the North Pacific: early indications of the 1976–1977 event. *Progress in Oceanography*, *60*(2), 183–200. https://doi.org/https://doi.org/10.1016/j.pocean.2004.02.005

van Denderen, D., Maureaud, A. A., Andersen, K. H., Gaichas, S., Lindegren, M., Petrik, C. M., Stock, C. A., & Collie, J. (2023). Demersal fish biomass declines with temperature across productive shelf seas. *Global Ecology and Biogeography*, *n/a*(n/a). https://doi.org/https://doi.org/10.1111/geb.13732

Vincenzi, S., Jesensek, D., and Crivelli, A. 2018. A framework for estimating the determinants of spatial and temporal variation in vital rates and inferring the occurrence of unobserved extreme events. *Royal Society Open Science* 5: 171087. http://dx.doi.org/10.1098/rsos.171087

von Bertalanffy, L. (1938). A Quantitative Theory of Organic Growth (Inquiries on Growth Laws II). *Human Biology*, *10*(2), 181–213. http://www.jstor.org/stable/41447359

Chapter 1. INCORPORATING DISTRIBUTION SHIFTS AND SPATIO-TEMPORAL VARIATION WHEN ESTIMATING WEIGHT-AT-AGE FOR STOCK ASSESSMENTS: A CASE STUDY INVOLVING BERRING SEA POLLOCK (*GADUS CHALCOGRAMMUS*)

Publication history: This study was co-authored with James N. Ianelli, James T. Thorson, and Timothy E. Essington. At the time this dissertation was submitted, a version of this chapter was published in *ICES-Journal of Marine Science* (https://doi.org/10.1093/icesjms/fsac236).

1.1 ABSTRACT

Environmental conditions can create spatial and temporal variability in growth and distribution processes, yet contemporary stock assessment methods often do not explicitly address the consequences of these patterns. For example, stock assessments often assume that body weight-at-age (i.e. size) is constant across the stocks' range, and may thereby miss important spatio-temporal patterns. This is becoming increasingly relevant given climate-driven distributional shifts, because samples for estimating size-at-age can be spatially unbalanced and lead to biases when extrapolating into unsampled areas. Here, we jointly analyzed data on the local abundance and size of walleye pollock (Gadus chalcogrammus) in the Bering Sea, to demonstrate a tractable first step in expanding spatially unbalanced size-at-age samples while incorporating fine-scale spatial and temporal variation for inclusion in stock assessments. The data come from NOAA's bottom trawl survey data and were evaluated using a multivariate spatio-temporal statistical model. We found extensive variation in size-at-age at fine spatial scales, though specific patterns differed between age classes. In addition to persistent spatial patterns, we also documented year-to-year differences in the spatial patterning of size-at-age.. Intra-annual variation in the population-level size-at-age (used to generate the size-at-age matrix in the stock assessment) was largely driven by localized changes in fish size, while shifts in species distribution had a smaller effect. The spatio-temporal size-at-age matrix led to marginal improvement in the stock assessment fit to the survey biomass index. Results from our case study suggests that accounting for spatially unbalanced sampling improved stock assessment consistency. Additionally, it improved our understanding on the dynamics of how local and population-level demographic processes interact. As climate change affects fish distribution and growth, integrating spatiotemporally explicit size-at-age processes with anticipated environmental conditions may improve stock-assessment forecasts used to set annual harvest limits.

1.2 INTRODUCTION

Fisheries managers depend on stock assessments to make informed decisions about conservation and management measures (Methot 2009). State-of-the-art methods typically involve fitting an age-structured population dynamics model to evaluate the current and projected status of the resource including biomass and fishing mortality (Hilborn and Walters 1992). The population dynamics model relies on data from surveys and fisheries to estimate survival patterns and age-specific demographic rates, including growth, mortality, recruitment, and maturation. Key stock characteristics estimated from assessment models are sensitive to changes in these demographic rates (Thorson et al. 2015). Therefore, the accuracy and precision of the data ultimately impact the value of stock assessments for managers, especially when assumptions such as constant growth rates can be avoided (Methot 2009, Francis 2011).

Survey and fishery data on catch rates and composition inevitably have biases and gaps that present challenges to using them in stock assessments (Thorson 2014, Breivik et al. 2021, Ducharme-Barth et al. 2022). While well-designed fishery-independent surveys attempt to account for known sources of variation with standardized protocols (Gunderson 1993), there are inevitable disruptions in survey implementation and unobservable sources of variation that make this challenging (Kimura and Somerton 2007). For instance, sampling intensity may not be equally distributed across a species' range (Thorson 2014), there may be aberrant extreme catches (Thorson et al. 2011), and the catchability of survey gear may vary (Kotwicki and Ono 2018). Resource limitations and weather conditions may contribute to unforeseen gaps in spatial coverage (Adams et al., 2021). In 2020, for instance, many planned surveys were canceled due to COVID-19 restrictions (e.g., NOAA 2020a-d). As fish distributions shift due to climate change (Mueter et al. 2011, Pinsky et al. 2020, Rooper et al. 2020), available data may increasingly fail to align with species' actual ranges (Link et al. 2010; O'Leary et al. 2020) and will exacerbate the challenge of handling biases and gaps in data.

Spatio-temporal models are being used more commonly to address these issues (Maunder and Punt 2004, Francis 2011(Breivik et al. 2021, Maunder et al. 2020, O'Leary et al. 2020, Ducharme-Barth et al. 2022). By accounting for persistent spatial differences (i.e., spatial variation) and spatial differences that change over time (i.e., spatio-temporal variation) in the catch rate data, these models can provide better estimates of annual abundance in areas with missing data (e.g. Breivik et al. 2021), extrapolate to unsampled years (e.g. O'Leary et al. 2020), and correct for differences in sampling intensity across the range (e.g. Maunder et al. 2020). Spatio-temporal models have begun to similarly be applied to age composition data (Thorson 2014, O'Leary et al. 2020, Thorson and Haltuch 2018). These models provide a way to predict fish density by standardizing catch rates by the area sampled ("area-weighting") and to predict composition information, such as age and size, by standardizing composition data by the fish density ("density-weighting") of each location (Thorson et al. 2020). Spatio-temporal models were found to improve prediction and accuracy of abundance estimates over other standardization methods (Gruss et al. 2019, Zhou et al. 2019, Thorson et al. 2015b).

However, spatio-temporal models have rarely been applied to standardizing size-at-age (here defined as weight-at-age), another critical component of assessment models. While there are different methods used to incorporate growth rates in stock assessment models (Helser and

Brodziak 1998, Clark and Hare 2002, Whitten et al. 2013, Minte-Vera 2004, Thorson and Minte-Vera 2016), often an annual size-at-age is derived from size measurements of survey or fishery data in an empirical size-at-age matrix (e.g. Kuriyama et al. 2016, Ianelli et al. 2021). Standardizing data for size-at-age is inherently more complicated than standardizing catch rate for abundance indices because size data results from the interplay between variation in two processes: growth (and resulting size) within different habitats, and the stock abundance in those habitats. First, environmental differences in food availability, temperature, or oxygen may impact local growth rates, resulting in variation in local size-at-age (DeVries and Frie 1996). Second, fish populations are distributed in space via movement processes that are constrained by physiological limits and dispersal capability. This can lead to spatial mis-matches between local food conditions and prey availability, as in the case in the Baltic Sea where expansion of hypoxic water has concentrated cod into the remaining suitable habitat that lacks their main prey (Casini et al. 2016). The size of cod in this area has consequently drastically declined, at the same time that cod abundance in the same area has increased (Casini et al. 2016). Thus, spatio-temporal variation in both local habitat conditions and population distributions must both be considered when standardizing size-at-age. Given these multiple mechanisms, it can be helpful to attribute variation in annual size-at-age to the various processes contributing to them (e.g. Thorson et al. 2017), in this case spatial and spatio-temporal variation and local size versus local abundance.

In this study, we used walleye pollock (*Gadus chalcogrammus*) in the Bering Seas as a data-rich case study in using a spatio-temporal model to incorporate local-scale spatial and temporal variation in size (i.e. weight) and abundance to estimate population-level size-at-age (i.e. a size-at-age matrix for use in a stock assessment). We evaluate the pattern of size over space and time, whether these patterns are persistent or transient (i.e., varying among years), and their implications for the stock assessment. This fishery is particularly relevant to test a spatio-temporal size-at-age model. Bering Sea walleye pollock is the world's second-largest single-species fishery by catch weight (FAO 2021), with an average catch of 1.2 million tons since 1979 and first-wholesale value of $1.55 billion in 2019 (Ianelli et al. 2021). The stock is sampled with extensive fishery-independent surveys, providing a rich data set to evaluate spatio-temporal variability in size-at-age. Finally, size-at-age is an important component of the stock assessment because it converts numbers of fish (which forms the basis of the model dynamics) to biomass and catch recommendations. Although the stock assessment is already transitioning to using spatio-temporal models for estimates of a biomass index and age composition (O'Leary et al. 2020), these models have yet to be applied to size-at-age.

Additionally, climate change is predicted to cause significant shifts in the physical and biological regime (Hunt et al. 2008; Whitehouse et al. 2021) that will greatly impact the spatial distribution of walleye pollock (O'Leary et al. 2020). As the pollock range shifts out of the historical survey footprint, spatial gaps in survey data will increase (O'Leary et al. 2020, O'Leary et al., 2022). In addition to incorporating local-scale variation in growth processes and compensating for local abundance, this spatio-temporal model could therefore also enable better predictions of the pollock stock under future climate change by providing a way to extrapolate to unsampled regions as spatial distributions shift. Further research could explore the impact of including covariates and correlation between ages and hauls, as well as short-term forecasting skill. However, we focus here on the first step (showing how model-based estimators compare with existing methods for expanding size-at-age data) and leave these other topics for future research.

It is often difficult to identify the specific environmental features that cause observed variation in fish populations (Thorson et al. 2017, Dambrine et al. 2021). Because of this, here we constrained our analysis to quantifying latent spatial and spatio-temporal variation and to retrospective size-at-age data to determine the best analysis protocols, to establish an operating model framework, and to ensure that it could replicate existing estimators and be applied in the stock assessment before delving into covariates and forecasts. Here we focus on an initial assessment of the pattern of spatial and temporal variation in size-at-age in Bering Sea pollock, the demographic processes contributing to this variation, and how this model impacts outcomes of the stock assessment.

We seek to answer the following questions:

1. How does size-at-age vary spatially and temporally, both locally and at the aggregated population-level (i.e. the size-at-age matrix used in the stock assessment)?
2. How do local spatial and spatio-temporal variation impact the size-at-age matrix?
3. How does local variation in size versus abundance contribute to the size-at-age matrix?
4. How does our spatio-temporal model of the size-at-age matrix affect the stock assessment predictions of population biomass compared to a simple empirical estimate?

To do so, we develop a spatio-temporal model for size-at-age and fish density, and use this to calculate the population-level size-at-age, i.e. the "size-at-age matrix", that is used as input within many stock-assessment models worldwide (e.g. Kuriyama et al. 2016). We then evaluate the drivers within the model and explore its inclusion in a stock assessment compared to a simple empirical estimate.

1.3 METHODS

We aimed to estimate annual time series of population size-at-age (i.e. a size-at-age matrix) for Bering Sea walleye pollock that incorporated local spatial variability in size-at-age while also compensating for shifts in the relative density of areas with small and large fishes. This required an estimate of two response variables—average size and fish density—for each age class for each year in distinct locations across the Bering Sea. Then, to aggregate the local size-at-age at each location up to the population level, we area-expanded fish density to abundance and weighted the size-at-age at each location by the local abundance-at-age in that year to calculate the population-level "size-at-age matrix". We therefore sought to estimate density and size in a joint model. To accommodate estimating both response variables in a single joint model, we used a flexible model structure (a Poisson-link delta approach to a generalized linear mixed model) that predicts density-at-age $n_{a,y,g}$ and size-at-age $w_{a,y,g}$ for each year y and age a for distinct locations in space g, while accounting for annual effects and spatial fields that cover spatially and temporally dynamic latent variables. We then evaluated how these estimates might affect key outcomes in a stock assessment model.

1.3.1 *Data compilation*

The model was fitted to data collected from the NOAA Groundfish Bottom Trawl Survey from 1982—2019. Estimating size-at-age relied on the specimen age a_i (years), weight v_i (grams), and

length l_i (millimeters) measurements that are sub-sampled as part of hauls in the survey. Surveys were not conducted in 2020, and completed survey data from 2021 was not available at the time of this study. Surveys from 1984—1998 did not measure individual fish weights because motion-compensating scales were not widely available at that time (e.g. Wilson and Armestead 1991, Walters 1997, Nebenzahl and Goddard 2000). After 1991, specimen weights were sampled sporadically, and were consistently measured from 1999 onwards. For 1984—1999 weight was estimated from measured lengths using sex-specific weight-length conversion parameters (Ianelli et al. 2021) (Appendix A). Individual fish from the northern Bering Sea survey were not aged by the time this study was completed. Additionally, there was no specimen data available for age-14 in 2018 and age-15+ in 1986 and 2019. The density-at-age data that we used is the age-stratified, density-dependence-corrected catch-per-unit-effort (CPUE) per haul (numbers of fish hectare^{-1}) c_i (see Kotwicki et al. (2014) for details). Figure 1 shows the spatial distribution of survey data for a subset of years, and the general geographic extent of CPUE and specimen weight or length data is similar. See Appendix B Figure 1 for full time series of locations of specimen weight and length data and Appendix B Figure 2 for CPUE data.

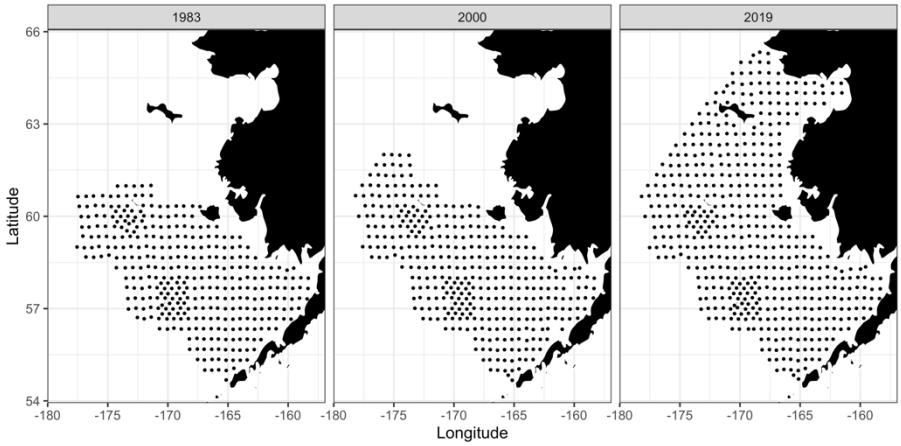

Figure 1. Bottom trawl survey locations in the Bering Sea for subset of years to show extent of survey over time.

1.3.2 *Model structure*

Average local size $w_{g,a,y}$ for each year y and age a for distinct locations in space g was estimated using a log-linked generalized linear mixed model. The model includes a single linear predictor that contains terms for temporal variation β, spatial variation ω, and spatio-temporal variation ε.

$$\log(w_{g_i,a_i,y_i}) = \underbrace{\beta_{a_i,y_i}}_{Temporal\ variation} + \underbrace{\omega_{g_i,a_i}}_{Spatial\ variation} + \underbrace{\varepsilon_{g_i,a_i,y_i}}_{Spatio-temporal\ variation} \quad [1]$$

Temporal variation was estimated as a fixed effect for each age a and year y, and represents a fixed intercept for each age and year. Spatial and spatio-temporal variation were estimated as Gaussian random effects with mean 0 and were assumed to follow a multivariate normal distribution with covariance matrices $\sigma_\omega^2\mathbf{R_\omega}$ and $\sigma_\varepsilon^2\mathbf{R}_\varepsilon$**.** Covariance matrices include the correlation between

locations, calculated using a Matérn function in the correlation matrices $\mathbf{R}_{\boldsymbol{\omega}}$ and $\mathbf{R}_{\varepsilon}$, which are governed by a shared decorrelation rate κ (i.e. the distance that locations are uncorrelated), and the estimated marginal variances σ_{ω} and σ_{ε}. Spatio-temporal variation also follows an auto-regressive process, governed by the autocorrelation parameter ρ_{ε}.

$$\boldsymbol{\omega}_{\boldsymbol{a}} \sim \mathrm{MVN}(\mathbf{0}, \sigma_{\omega}^2 \mathbf{R}_{\boldsymbol{\omega}}) \quad [2]$$

$$\boldsymbol{\varepsilon}_{\boldsymbol{a,y}} \sim \begin{cases} \mathrm{MVN}(\mathbf{0}, \sigma_{\varepsilon}^2 \mathbf{R}_{\varepsilon}) & \text{if } t = 1 \\ \mathrm{MVN}\left(\rho_{\varepsilon} \boldsymbol{\varepsilon}_{\boldsymbol{a,y-1}}, \sigma_{\varepsilon}^2 \mathbf{R}_{\varepsilon}\right) & \text{if } t > 1 \end{cases} \quad [3]$$

The measured size v_i is assumed to follow a lognormal distribution, with log-mean $\log\left(w_{g_i,a_i,y_i}\right)$ and log-variance σ_{v}^2.

$$\Pr(V = v_i) = \mathrm{lognormal}(v_i | \log\left(w_{g_i,a_i,y_i}\right), \sigma_{\mathrm{v}}^2) \quad [4]$$

In order to weight the local size estimates from this size-at-age model by the local abundance at each location in each year, we additionally needed a similar spatio-temporal model of density-at-age $n_{g,a,y}$ for each year *y* and age *a* for distinct locations in space *g*. However, catch rates contain many zeroes for certain ages in certain years (Martin et al. 2005). To accommodate for zero-inflation in the model of abundance, we used a Poisson-link delta approach to a generalized linear mixed model (Thorson 2018). This approach calculates the probability of encounter $r_{1,i}$ from a Poisson distribution whose rate parameters are governed by linear predictor $p_{1,i}$ (i.e., a complementary log-log link function), and the density if encountered $r_{2,i}$ from the Poisson distribution modeled as $p_{1,i}$, and a gamma-distributed multiplier of counts whose mean and variance are determined by a linear predictor $p_{2,i}$. Thus, the encounter rate $r_{1,i}$ and density if encountered $r_{2,i}$ equal:

$$r_{1,i} = 1 - e^{-e^{p_{1,i}}} \quad [5]$$

$$r_{2,i} = \frac{e^{p_{1,i}}}{r_{1,i}} \times e^{p_{2,i}} \quad [6]$$

Final estimated density n_i is then the product of $r_{1,i}$ and $r_{2,i}$, such that $\log(n_i) = p_{1,i} + p_{2,i}$.

Because both linear predictors are included in the calculation of positive catch rates $r_{2,i}$, including the three variation terms in the first linear predictor includes them in both $r_{1,i}$ and $r_{2,i}$. To simplify the model for computational efficiency, temporal, spatial, and spatio-temporal variation are included in the first linear predictor, $p_{1,i}$, while only temporal variation was included in the second linear predictor. When using the Poisson-link delta model, the variance associated with the second linear predictor is typically small, and we can assume that excluding the terms in the second linear predictor will have negligible impacts on the model estimates (see Thorson et al. 2018).

$$p_{1,i} = \underbrace{\beta_{1,a_i,y_i}}_{Temporal\ variation} + \underbrace{\omega_{g_i,a_i}}_{Spatial\ variation} + \underbrace{\varepsilon_{g_i,a_i,y_i}}_{Spatio-temporal\ variation} \quad [7]$$

$$p_{2,i} = \underbrace{\beta_{2,a_i,y_i}}_{Temporal\ variation} \quad [8]$$

The probability of not encountering an age-class in a given sample [i.e. Pr(C_i=0)] equals $1 - r_{1,i}$, and the positive catch rates C_i >0 were assumed to follow a gamma distribution, governed by shape parameter k and scale parameter θ, with mean $r_{2,i}$ and coefficient of variation σ_r, where $k = \frac{1}{\sigma_r^2}$ and $\theta = r_{2,i} \times \sigma_r^2$.

$$\Pr(C = c_i) = \begin{cases} 1 - r_{1,i} & \text{if } c = 0 \\ r_{1,i} \times \text{gamma}\{c | r_{2,i}, \sigma_r^2\} & \text{if } c > 0 \end{cases} \quad [9]$$

We implemented this joint spatio-temporal size- and density-at-age model using the R package VAST version 3.8.2 (Thorson 2019). This package allows the flexibility to do a multivariate spatio-temporal model, essentially treating each size- and density-at-age as a different response variable (i.e. category). Each category is specified with its probability distributions and link function, and separate spatial (i.e. omega term) and spatio-temporal (i.e. epsilon term) variation are estimated for each size- and density-at-age. Spatial and spatio-temporal terms are not correlated across ages. This package also allowed the flexibility to estimate both size- and density-at-age by using a Poisson-link delta approach that estimated density-at-age as in Equations 5—9, but essentially fixed the encounter probability for size-at-ages at 1 (i.e. 100% encountered) to ultimately estimate size-at-age by a single linear predictor. For additional details on how this joint model was coded in VAST, see Appendix D. Additional information on code and documentation of the VAST package is available at https://github.com/James-Thorson-NOAA/VAST.

Ultimately, the model extrapolated size and abundance by predicting density-at-age $n_{g,a,y}$ and size-at-age $w_{g,a,y}$ for each year y and age a for distinct locations in space g. The model estimated spatial and spatio-temporal effects across 500 points (i.e. termed "knots" in VAST) that were uniformly distributed across the Bering Sea and used bilinear interpolation to cover the entire geographic extent of the model (in this case, the Bering Sea) between these points with 51,769 distinct locations (i.e. grid cells g). We established that 500 knots was sufficient by qualitatively comparing model predictions over a range of knots. Density- and size-at-age were estimated for each of the years 1982—2019 at each of these 51,769 locations spanning the region. Approximating the multivariate normal distribution was accomplished using the SPDE method (Lindgren et al., 2011), and the matrices involved were calculated using R-INLA (Lindgren & Rue, 2015). See Appendix Figure 3 for the map of the SPDE mesh and Appendix Table 2 for estimated model parameters.

1.3.3 *Annual population size-at-age*

From these 51,769 local estimates of size-at-age for each year, we wanted an average annual population-level size-at-age (i.e. "size-at-age matrix") that incorporated local variation in size and compensated for the local abundance. This is because the stock assessment model requires a size-at-age matrix with dimensions age x year. To that end, for each year we calculated a weighted average of size-at-age, weighted by the local abundance. First, the modeled density $n_{g,a,y}$ per age

a, year y, and grid cell g (in number of fish hectare^{-1}) was expanded by the area A_g of the grid cell (in kilometers^2) to calculate area-expanded abundance $\hat{n}_{g,a,y}$ (with units numbers of fish) using Equation 10. $\hat{n}_{g,a,y}$was then summed across all grids per year and per age to calculate the annual, population-level area-expanded abundance $\hat{n}_{a,y}$.

$$\hat{n}_{a,y} = \sum_{g=1}^{G}(n_{g,a,y} \times A_g) \quad [10]$$

Second, a weighted-average of size for each age class and year, $\widehat{w}_{a,y}$, was calculated by weighting size-at-age $w_{a,y,g}$ by the abundance associated with this extrapolation point $n_{g,a,y} \times A_g$.

$$\widehat{w}_{a,y} = \sum_{g=1}^{g}[w_{g,a,y} \times (\frac{n_{g,a,y} \times A_g}{\hat{n}_{a,y}})] \quad [11]$$

1.3.4 *Question 1: Spatial and temporal patterns of size-at-age*

We descriptively evaluated spatial and temporal patterns in the model predictions of size and abundance at the local level and in population-level size-at-age matrix. We also calculated the coefficient of variation (CV) in size for each age class to quantify the extent of variation and compare patterns in size-at-age.

We were also interested in comparing our spatio-temporal model of the size-at-age matrix to a non-spatially explicit simple estimate. For this simple empirical estimate, we calculated the weighted average of size-at-age per year from the observed size data, weighting mean size-at-age in each haul by catch-at-age in that haul from the survey data. (See Appendix C for detailed equations.)

1.3.5 *Question 2: Impact of spatial and spatio-temporal variation on size-at-age matrix*

We sought to compare how much spatial versus spatio-temporal variation impacted the model predictions of the size-at-age matrix used in the Bering Sea walleye pollock stock assessment. A greater contribution of spatio-temporal variation indicates that there are important transient annual changes in habitat suitability. To do so, we used a method similar to adjusted predictions or marginal effects (e.g Williams 2012, Bornmann and Williams 2013, Mize 2019) and to the counterfactual approach in Thorson et al. (2017), where model predictions are compared when some variables in the model are held constant while the variable of interest fluctuates as a way to evaluate the effect of each variable within the model. In our study, the spatial term $\omega_{g,a}$ and spatio-temporal term $\varepsilon_{g,y,a}$ from each grid cell was each alternately replaced with the respective mean to calculate a reduced model (i.e. no spatial or no spatiotemporal variation term) of population size-at-age $\widehat{w}_{a,y}$ for the size-at-age matrix. Because spatial and spatio-temporal terms are random effects with means of 0, this essentially "zeroes out" the term and allows us to see from the change in model prediction the relative impact of spatial or spatio-temporal variation in the model. We used this approach, rather than compare predictions between alternative model fits, because we aimed to compare the relative strength of each type of variation within our model structure when both spatial and spatio-temporal variation are estimated. Our approach allows us to quantify the

effect of each model component when used in the inverse-link transformed linear predictor, and hence provides a more useful summary that simply interpreting the estimated standard deviation of each model component as its "importance". The percent difference between $\widehat{w}_{a,y}$ in the reduced model (i.e. no-spatial or no-spatiotemporal variation) from the full model (i.e. all forms of variation) was then calculated for each year. We interpreted the greater percent difference between the simplified and full model as indicating a greater impact of that source of variation.

1.3.6 *Question 3: Contribution of local variation in size versus abundance to size-at-age matrix*

We similarly evaluated how the size-at-age matrix was impacted by accounting for the local variation in size and by local abundance. To do so, we alternately replaced the grid-level abundance-at-age and grid-level size-at-age with their average across all years, and re-calculated the size-at-age matrix using these values. Specifically:

- To isolate the impact of correcting for local abundance, the local area-expanded abundance $\hat{n}_{g,a,y}$ was replaced with the mean abundance-at-age for each grid cell across all years, $\bar{\hat{n}}_{g,a}$.
- Alternately, to isolate the effect of local size-at-age, the local size, $w_{g,a,y}$, was replaced with the average size for each grid cell for each age class $\overline{w}_{\mathrm{g,a}}$ across years and subsequently used to calculate annual size-at-age $\widehat{w}_{a,y}$.

The percent difference between $\widehat{w}_{a,y}$ in the reduced model (i.e. no local temporal variation in size or no local temporal variation in density) from the full model was calculated for each year.

1.3.7 *Question 4: Stock assessment comparison*

We evaluated how using our spatio-temporal model to calculate the size-at-age matrix $\widehat{w}_{a,y}$ — incorporating local spatio-temporal variation in size and weighting by abundance—impacts outcomes of the stock assessment. We did so by comparing the walleye pollock stock assessment model (see Ianelli et al. 2021) using our spatio-temporal size-at-age matrix compared to using the simple empirical estimate (see above). Because there was no specimen data available for age-14 in 2018 and age-15+ in 1986 and 2019, we used average values since there were no model estimates for those age classes in those years. We ran the Bering Sea walleye pollock stock assessment model using each size-at-age matrix method and compared the total estimated biomass and the predicted numbers of fish in the stock from the stock assessment model. We compared the fit of the stock assessment model using each size-at-age method to the trawl survey biomass using Akaike Information Criteria (AIC), where a value of <2 is weak, >10 is very strong, and between these is intermediate (Burnham and Anderson 2002) .

Table 3. Variable names and symbols used in data processing and model outputs

Name	**Symbol**	**Units**
Indices		

Specimen (data)	i	--
Haul (data)	h	--
Age (data and model)	a	year
Year (data and model)	y	--
Grid cell (model)	g	--
Data Inputs		
Fish specimen size (weight)	v_i	grams
Fish specimen fork length	l_i	Millimeters
Catch rate (density-corrected catch-per-unit-effort)	c_i	Number of fish hectare^{-1}
Model Components		
Temporal variation	β	--
Spatial variation	ω	--
Spatio-temporal variation	ε	--
Linear predictor	p	--
Encounter probability	r_1	--
Density if encountered	r_2	--
Autocorrelation for spatio-temporal variation	ρ_ε	--
Spatial correlation matrix for spatio-temporal variation	$\mathbf{R}_\varepsilon$	--
Spatial correlation matrix for spatio-temporal variation	$\mathbf{R}_\omega$	--
Shape parameter of gamma distribution	k	--
Scale parameter of gamma distribution	θ	--
Model Outputs		
Fish density (i.e. density)	n	Number of fish hectare^{-1} (or km^{-2})
Abundance	$\hat{n}$	Number of fish

Size (i.e. weight)	w	Grams
Abundance-weighted size	$\widehat{w}$	Kilograms
Area	A	Kilometer^2

1.4 RESULTS

1.4.1 *Question 1: Spatial and temporal patterns of size-at-age*

Size-at-age varied across the Bering Sea and among years. Across the Bering Sea, we found some persistent spatial patterns (i.e. spatial variation). For instance, age-1 pollock size reached 30-40g in the western extent of its range, while averaging only 10-20g in the eastern extent of the range (Figure 2). Age-9 pollock were typically larger at the eastern end of the range than the western, reaching 2000g in some years in the eastern end while less than half that size in the western end (Figure 2). However, the spatial patterns of size differed among years (i.e. spatio-temporal variation). For example, an area of particularly higher age-1 size appeared in the northeast in 2019 (Figure 2), and some years exhibited more variability in size across the region. For example, while there was great spatial variation and stratification of size in age-9 pollock in 1982 and 2000, there was a more uniform size-at-age across the entire Bering Sea in 1990 and 2019.

The overall magnitude of spatial variation in size also differed among age classes. The youngest age classes showed the greatest variation across grid cells (Figure 3), with a CV of 42% for age-1 and 39% for age-2 pollock. There was a marked decline in variation for older ages. CV dropped to 30% for age-3 and further declined to ~18-22% for each age classes 4-15+.

There was also a trend of declining size-at-age over the study period for all but the youngest age classes at both the local and population level (i.e. the size-at-age matrix). Beginning in 2015 through 2019, there was a distinct, uniform decline in weight for age-8 pollock and older across the entire Bering Sea, while this was not evident in younger ages (e.g. see Appendix E Figure 4). At the population level, size-at-age from the first modeled year (1982) to the last modeled year (2019) declined by 24% for age-1 pollock, increased by 12—60% for age-2 through age-5 pollock, and declined by 15—30% for age classes 6—8, and 35—50% for age classes 9 and older (e.g. Figure 4 and Appendix E Figure 5).

Our spatio-temporal size-at-age matrix differed from the simple empirical estimate (i.e. the non-spatially explicit, simple empirical average) of size-at-age. Though this non-spatial estimate somewhat tracked fluctuations in the model size-at-age, it often fell outside the confidence range (Figure 4 and Appendix E Figure 5).

1.4.2 *Question 2: Impact of spatial and spatio-temporal variation on size-at-age matrix*

The size-at-age matrix was impacted by both spatial and spatiotemporal variability. Both latent persistent spatial and transient spatio-temporal patterns in size across the Bering Sea contributed to the fluctuations in the population-level size-at-age matrix. Population-level size-at-age that excluded spatial or spatio-temporal variation differed from the full model (Figure 5 and Appendix E Figure 6), though the magnitude of the impact varied between age classes. Spatial variation had the largest impacts in age-1 and ages 5-7, with 10-25% average impact on annual size-at-age. However for the remaining age classes, the impact of spatial variation was relatively minor, with an average difference of 8-14% for age-8—14, and almost zero impact on age-3 and age-15. Spatio-temporal variation had an overall lower impact on more age classes, ranging from 2-8% for age-1 and age 4—15, and only had a larger impact on age-2 and age-3 pollock (14% and 20%, respectively). Overall, spatial and spatio-temporal variation had relatively similar magnitude of impact on the size-at-age matrix.

1.4.3 *Question 3: Contribution of location variation in size versus abundance to size-at-age matrix*

Annual fluctuations in the weight-at-age matrix were almost entirely due to changes in local size between years, rather than shifts in local fish abundance (Figure 6). Inter-annual fluctuations in size-at-age were markedly dampened when local variation in size-at-age was removed, but were not substantially changed when local variation in abundance was removed. Incorporating local variation in abundance-at-age but holding local size constant caused an 11-19% average difference (Figure 6 and Appendix E Figure 7). Including local changes in fish size while holding local abundance-at-age constant on average caused only a 2-8% average difference (Figure 6). Overall, accounting for the changes in local size-at-age processes year-to-year had a substantial impact when extrapolating to the population level, while compensating for local changes in fish density did not greatly change the size-at-age matrix value.

1.4.4 *Question 4: Stock assessment comparison*

The spatio-temporal size-at-age matrix did marginally change estimated annual biomass and numbers of fish from the walleye pollock stock assessment (Figure 7) compared to the simple empirical mean. The stock assessment model using our spatio-temporal size-at-age resulted in a slightly improved fit than a model using the simple empirical estimate (ΔAIC=3.6). In particular, the spatio-temporal model resulted in marginally better predicted biomass in year 2003 (Figure 7), when the observed biomass in the bottom trawl survey was anomalously higher than the model estimates for that year. The spatio-temporal model was able better avoid the underestimation and capture the higher biomass that was a closer fit to the survey observation. A similar pattern is seen in 1991, though there is less divergence between the model and observation than 2003. The spatio-temporal size-at-age matrix generally estimated lower size-at-age than the simple empirical estimate in 1991, except for much higher estimates in the oldest age-classes of 13—15+. In 2003 size-at-age was also higher in the spatially explicit model in the oldest age classes, but also in some younger ages (Appendix E Figure 5). There was essentially no difference in the estimated numbers

of fish in the stock by the assessment model between size-at-age methods until the most recent several years (2015—2021), when the numbers of fish estimated using the spatio-temporal size-at-age are consistently higher than the simple empirical estimate (Figure 4). This suggests that local-scale variation in weight did manifest in the demographic patterns of the population, and that accounting for these structures scaled up to impact the estimation of population-level metrics.

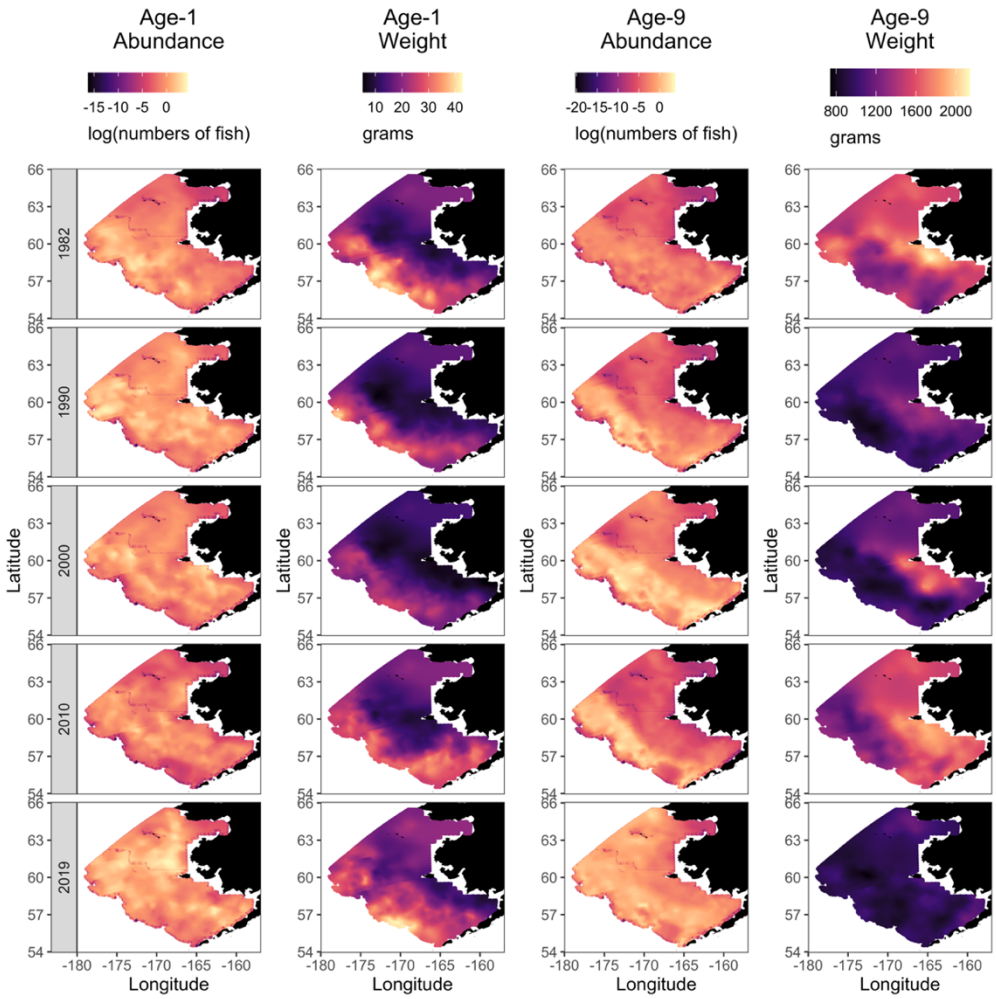

Figure 2. Model estimates of area-expanded abundance (log(abundance, numbers of fish) and weight (grams) for age-1 and age-9 walleye pollock (*Gadus chalcogrammus*) for subset of years (1982, 1990, 2000, 2010, and 2019).

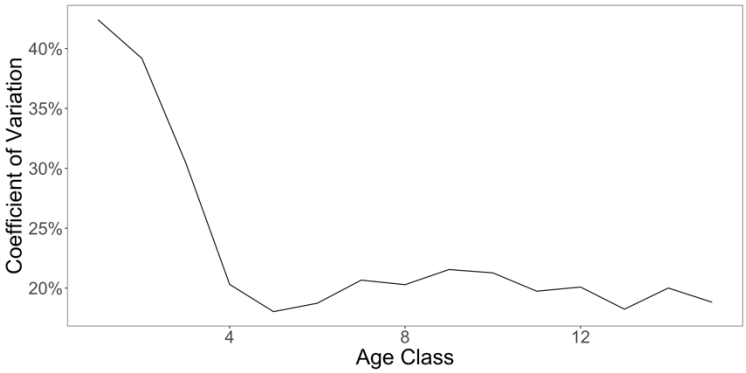

Figure 3. Spatial coefficient of variation of estimated size-at-age of walleye pollock (*Gadus chalcogrammus*) in the Bering Sea for each age class, calculated as the standard deviation across all grid cells and all years divided by the mean across grid cells and years.

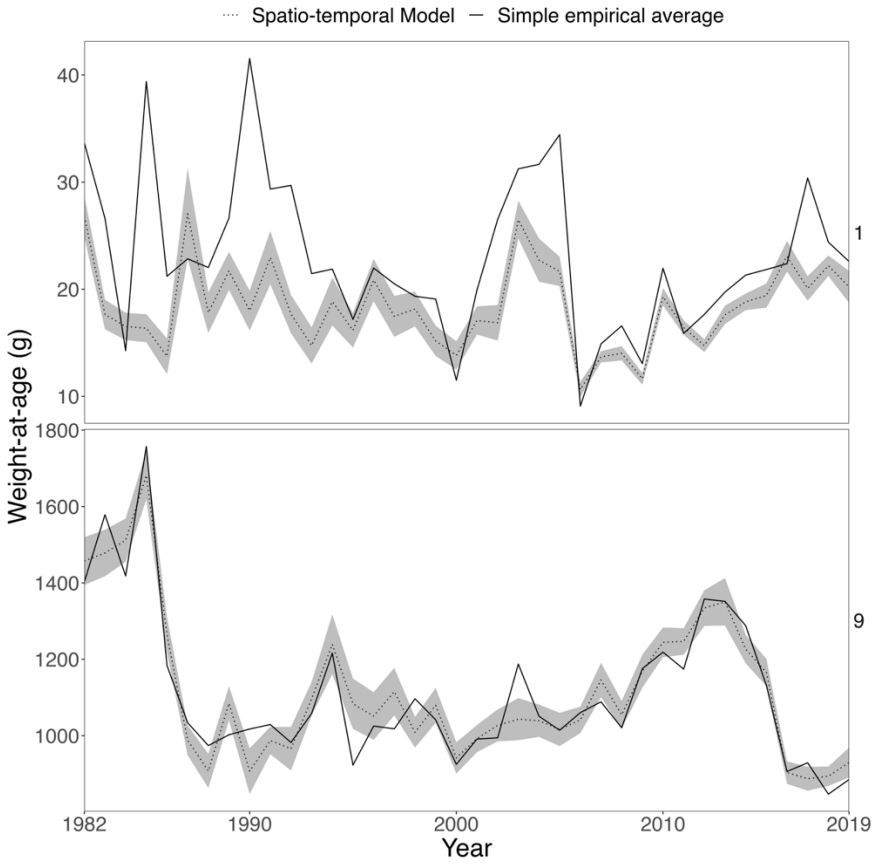

Figure 4. Size-at-age matrix (i.e. annual abundance-expanded population size-at-age) from model estimates (dashed line) and standard error (grey shaded), compared to the simple empirical estimate (i.e. the simple empirical average, a non-spatially explicit weighted average of observations) (solid black line) for ages 1 (top panel) and 9 (bottom panel) walleye pollock. See Appendix E Figure 4 for all age classes.

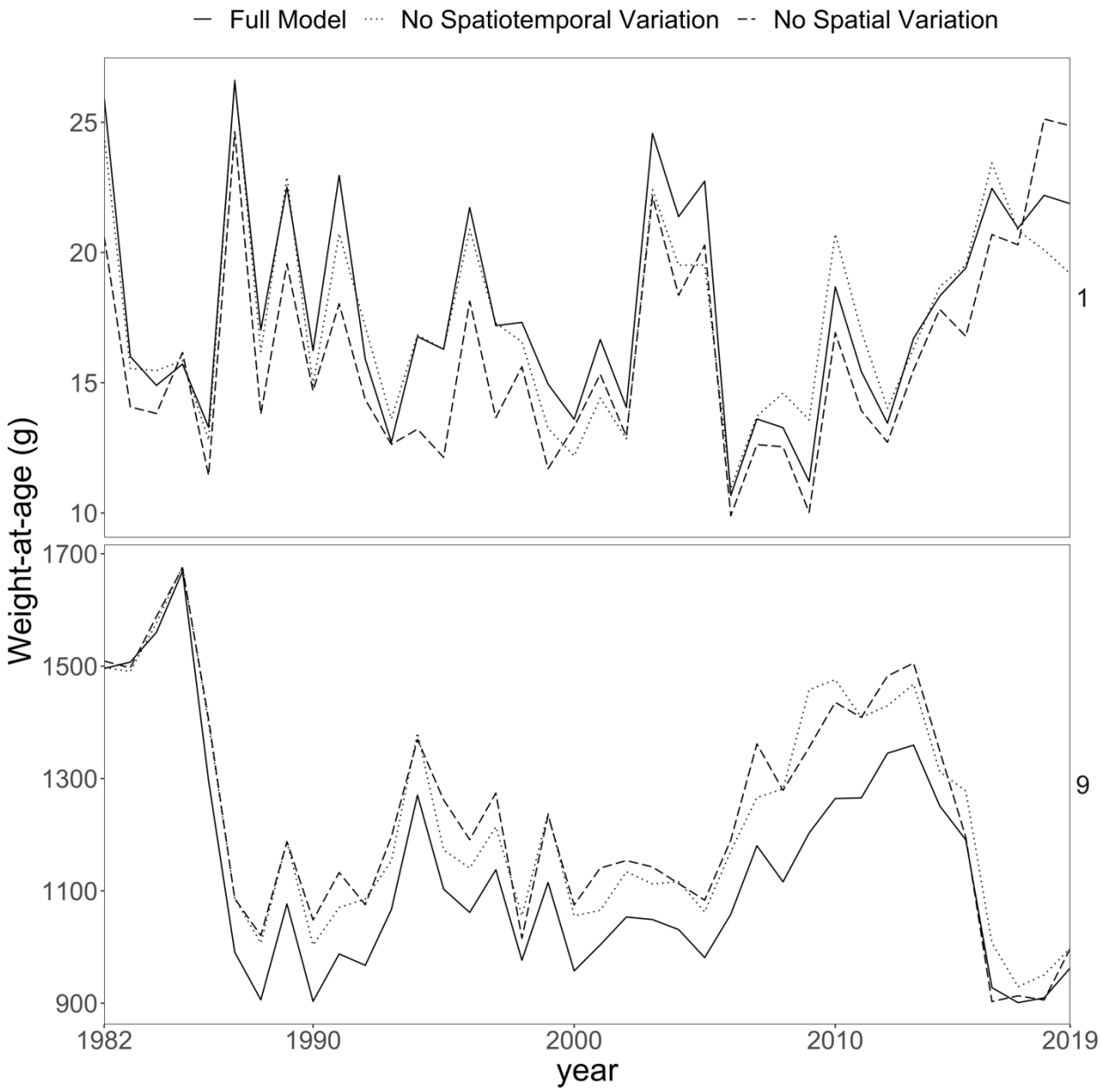

Figure 5. The size-at-age matrix (i.e. annual abundance-expanded population size-at-age) from the full model, including spatial, spatio-temporal, and temporal variation (solid black line) compared to 1) removing spatial variation (dashed line) and 2) removing spatio-temporal variation (dotted line). See Appendix E Figure 5 for all age classes.

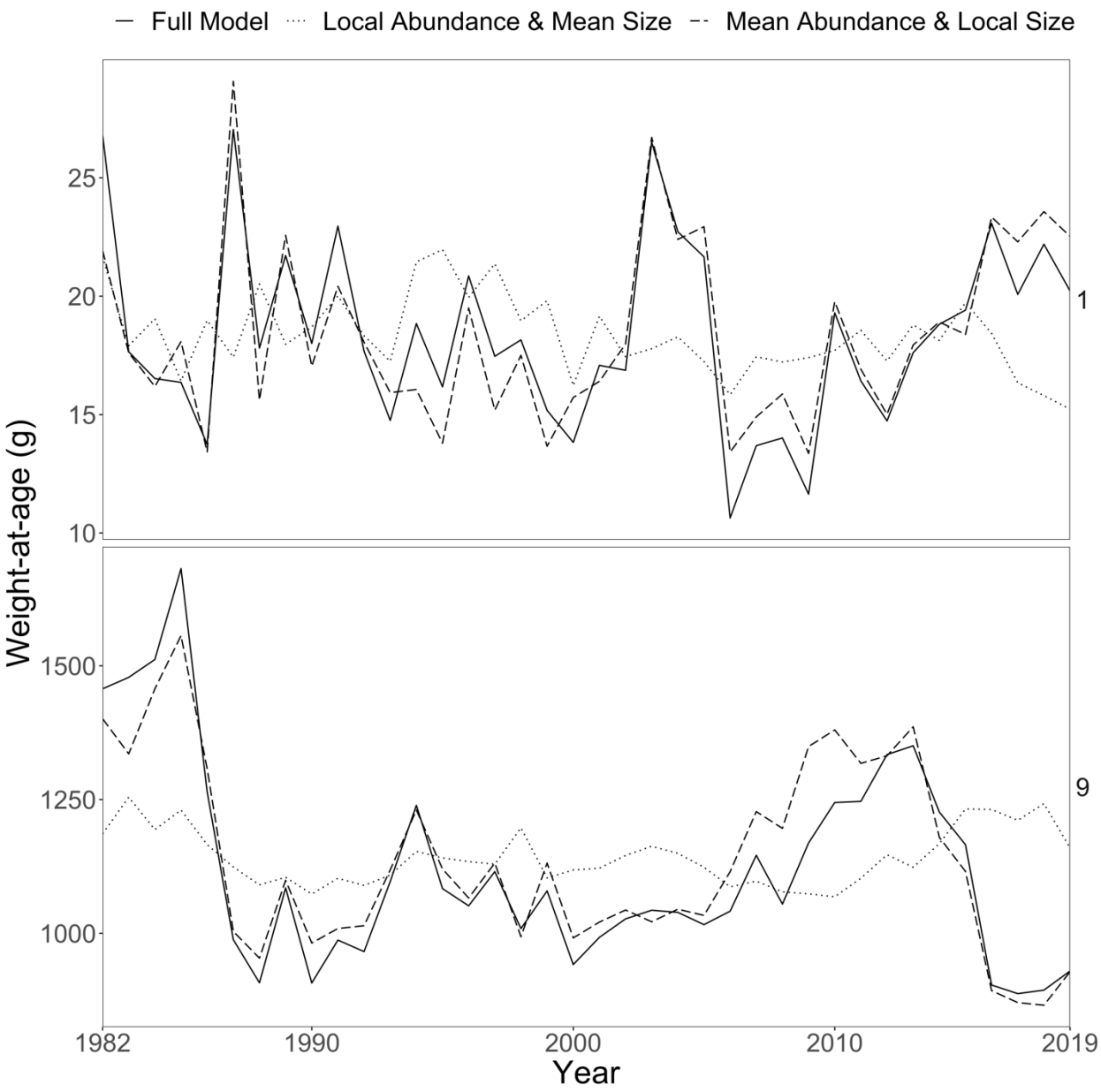

Figure 6. The population size-at-age matrix from the full model (i.e. calculating the abundance-expanded size-at-age with both local size-at-age and local abundance-at-age) (solid black line) compared to the size-at-age matrix calculated using: 1) local abundance but mean size-at-age (i.e. showing the contribution of local size-at-age) (dotted line), and 2) mean abundance but local size-at-age (i.e. showing the contribution of local abundance) (dashed line). See Appendix E Figure 6 for all age classes.

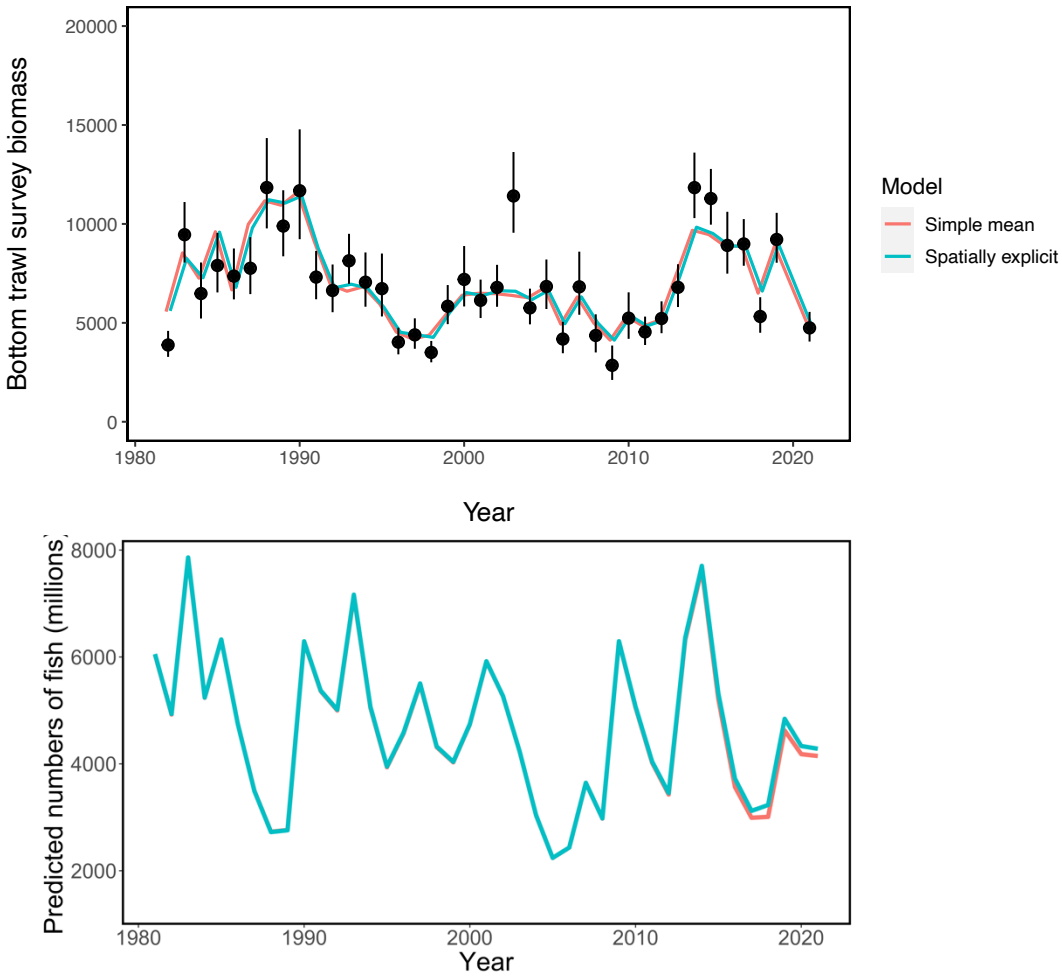

Figure 7. Walleye pollock biomass from bottom trawl survey (top) and predicted numbers of fish (bottom) estimated from stock assessment model (Ianelli et al. 2021) using spatio-temporal size-at-age matrix (blue) and from the simple empirical estimate (a non-spatially explicit weighted average of observations) (red), compared to observed biomasses (black points).

1.5 DISCUSSION

We developed and demonstrated a population-level size-at-age matrix that accounts for both inherent differences in size-at-age between habitats across the region and movement of fish (i.e. shifts in distribution) among patches with smaller or larger size. Local spatial variation in size-at-age, rather than local changes in abundance, largely governed variability in the resulting weight-at-age matrix. Accounting for spatial and spatio-temporal variation in local size-at-age therefore considerably impacts the estimated population size-at-age. Spatio-temporal models, such as with VAST as done here, of abundance (e.g. Fenske et al. 2020) and age composition (e.g. O'Leary et al. 2020, Thorson and Haltuch 2018) have been used in stock assessments previously, but to our knowledge this is the first example of the approach being applied to size-at-age. While the stock assessment in our study was relatively robust to the method used to calculate survey size-at-age, climate change will make it increasingly important for fisheries to account for the rapid pace of

distribution shifts and environmental changes that species are likely to experience. The overall framework implemented here (spatio-temporal estimation and abundance-expansion of size-at-age) could be widely applied to other systems and stock assessments to evaluate the sensitivity of estimates to changing species distributions and local changes in productivity and growth.

This study highlights large decreases in size-at-age for pollock. Our model showed a general trend of a decline in size-at-age between the beginning and end of the study period in all but the youngest age classes of pollock. While age-2 through age-5 pollock did not see a decline, sizes of age-1 and ages-6—15+ in the final year of the study period (2019) were 15—50% lower than at the beginning (1982). This aligns with recent reports from fishers, who noted smaller than usual pollock in 2020 and 2021 catches (Ianelli et al. 2021).

This decline may be due to changes in environmental conditions or size-selective fishing. Declines in fish growth and size with ocean warming are expected due to increased metabolic demand and reduced oxygen availability in higher sea temperatures (Daufresene et al. 2009, Gardner et al. 2011) and have been widely documented (e.g. Baudron et al. 2014, van Rijn et al. 2017). For instance, Pacific halibut mean size-at-age has declined at a similar magnitude to our study (Holsman et al. 2018), and has been attributed to both sea temperature (Holsman et al. 2018) as well as interspecific competition, density-dependent effects, and size-selective fishing (Clark and Hare 2002, Sullivan et al. 2018). Higher temperatures are also likely to reduce body size in larger and older individuals more than smaller and younger individuals (Ikpewe et al. 2020, Lindmark et al. 2022, Oke et al. 2022). Over the last several years (~2016—2021), the Bering Sea has experienced warmer than average temperatures (Ianelli et al. 2021). The age-class patterns we observed and recent environmental conditions of the Bering Sea would be consistent with an age-specific growth response to environmental conditions.

Size-selective fishing may also have contributed to the decline in size-at-age. Fishery-induced declines in size-at-age have been documented in numerous fisheries (Sharpe and Hendry 2009) such as Pacific halibut (Sullivan 2016, Sullivan 2018) and northern cod (Krohn and Kerr 1997). Size-selective fishing can lead to smaller body size through evolutionary pressure (e.g. Jorgensen et al. 2009, Swain et al. 2007) causing heritable genetic change (Uusi-Heikkila et al. 2015), phenotypic plasticity (Fenberg and Roy 2008), or the higher removal of faster-growing individuals of a population (i.e. the "Rosa Lee phenomen", Kraak et al. 2019). In the Bering Sea pollock fishery, vessel operators pursue pollock that are optimal for cost-efficient processing and market demand and some vessels have modified gear to exclude smaller pollock (Ianelli et al. 2021). Further exploration of the links between spatio-temporal variation in size-at-age of walleye pollock in the Bering Sea and environmental conditions would help clarify the possible cause of declining size-at-age.

This spatio-temporal model of size-at-age can improve stock assessments in several ways. Our estimated weight-at-age matrix incorporated the extensive local variation in size across the eastern Bering Sea. By jointly estimating size and abundance at a fine spatio-temporal scale, we also compensated for uneven distributions in fish abundance and shifts in distribution of fish throughout the region when expanding the local size estimates to the population size-at-age matrix. While the stock assessment was not substantially impacted by the method for generating the size-at-age matrix, the spatio-temporal and abundance-expanded size-at-age matrix did slightly improve the

fit of the model to the biomass survey data. For instance, the spatio-temporal size-at-age was able to slightly improve the model's ability to capture the anomalously high biomasses observed in the bottom trawl survey in 2003 (and to a lesser extent in 1991). Lastly, a spatio-temporal model as done in this study can help extrapolate in time and space to account for shifting survey and stock extents (Adams et al., 2021; O'Leary et al., 2020, 2022). For instance, in this study weight observations of pollock in the northern Bering Sea were not available, and there is sparse data from that region because of limited surveys. Additionally, our joint modelling approach allows the size-at-age matrix to include both uncertainty in estimates of size and uncertainty in estimates of abundance. Spatio-temporal approaches have become more common practice in some components of the stock assessment (such as biomass and age composition). While we did not see a marked change in the stock assessment outcome from our spatio-temporal method to size-at-age, accounting for spatio-temporal variation in other demographic metrics, such as size-at-age in this study, are the logical next step and will improve methodological consistency across a stock assessment.

Extending our spatio-temporal framework of size-at-age to fishery size data could be particularly beneficial because fishery-dependent data tends to have more pronounced spatial variation in fishing effort. There are differences in selectivity between fleets (e.g. gear characteristics such as depth of fishing) and unbalanced sampling in areas of higher, or lower, fish abundance due to fishers preferentially targeting areas based on convenience, safety, profitability, etc. (Maunder et al. 2020). A spatio-temporal model of size-at-age from fishery data consequently would require additionally accounting for catchability and selectivity when weighting size-at-age by catch (Thorson et al. 2020, Maunder et al. 2020). Stock assessments can be sensitive to how fishery size-at-age is estimated (Punt and Smith 2001). An accurate fishery size-at-age is necessary for correctly determining the number of fish caught by the fishery when landings are measured in weight, and consequently how actual fishing mortality compares to management limits (Ianelli et al. 2021). This study shows that it is feasible to take the grid-level output of size and abundance estimates from VAST and calculate a population average size-at-age, first weighting density by area and then weighting size by abundance. Including catchability covariates and weighting size by catch and fitting to fishery data would be a tractable extension of the model used in this study.

Our model showed extensive local-scale differences in size-at-age across the region and across years, suggesting that there is significant variation in local growth processes. Certain areas may have intrinsic conditions that make them more or less favorable for growth (e.g. Williams et al. 2003, Begg and Martensdottir 2002), contributing to the persistent spatial differences seen. Spatial patterns in pollock size have been previously observed; for instance, pollock in the northwest area have typically been found to be smaller than those in the southeast (Ianelli et al. 2020). Additionally, we saw annual differences in the spatial patterns that may indicate more transient changes in habitat conditions. We also saw some evidence of local shifts in abundance, though this was not as predominant as local variation in size-at-age. Passive dispersal and habitat selection can impact size-at-age if fish move to optimize foraging resources, to access spawning grounds, or to avoid competition or predators (Hanselman et al. 2015). Fish may also make dynamic migratory decisions based on energetic status, resulting in larger individuals migrating to different habitats than smaller individuals, such as has been seen in sablefish (Hanselman et al. 2015). In this study, however, local changes in growth processes, rather than shifts in distribution, seemed to be the principal driver of size-at-age.

Our spatio-temporal model of size-at-age also informs our understanding of how these local spatial and temporal patterns in size affect population-scale productivity. This has been identified as a "Grand Habitat Challenge" (Thorson et al. 2021b). Here, we developed a model of local size at a fine spatial scale, and expanded it to population-level abundance and productivity through the stock assessment. We show that persistent habitat conditions (spatial variation) and annual fluctuations in the suitability of a habitat for growth (spatio-temporal variation) caused local-scale variation in size-at-age over space and between years. Incorporating the variation in local size-at-age was the main driver of the annual population size-at-age (i.e. the size-at-age matrix). This suggests that variation in local growth processes across years did have an impact on population-level demographic metrics. In this study we therefore show a feasible approach to incorporate fine-scale local demographic processes into population-level assessments.

Being able to predict how demographic rates, such as growth and size, may respond to environmental change will also be crucial for incorporating the effects of climate change into stock assessment models (Punt et al. 2021). In the Bering Sea, climate change is likely to alter environmental conditions known to impact walleye pollock demographics. Declining sea ice cover and associated declines in zooplankton may reduce food availability and impact growth processes (Hunt et al. 2008, Mueter and Litzow 2008, Hunt et al. 2022) and recruitment (Mueter et al. 2011), and reduced bottom sea temperatures (i.e. the "cold pool extent) impacts a suite of demographic characteristics (Gruss et al. 2021). A model that can estimate size-at-age at fine spatial and temporal scales will enable better predictions of size-at-age, and the associated impacts on yield-per-recruit and other elements of the stock assessment, under future climate scenarios. For simplicity, in this study we did not integrate environmental or catchability covariates or forecast future size-at-age. Rather, we focused on an initial assessment of the feasibility of applying spatio-temporal models to size-at-age and abundance for stock assessments. It can often be difficult to identify the specific environmental features that cause observed variation in fish populations (Thorson et al. 2017, Dambrine et al. 2021), and addressing the latent spatio-temporal as done here was a tangible first step. The framework presented here can be expanded to incorporate environmental covariates and used for short-term forecasting.

1.6 ACKNOWLEDGEMENTS

We would like to specifically thank Cecilia O'Leary and Caitlin Allen-Akelsrud for their help and guidance on pulling together the various data sources. Special thanks to the bottom trawl survey team and Age and Growth Program at the NOAA Alaska Fisheries Science Center for the data that make this work possible. We also thank Paul Spencer and Christine Stawitz and the two anonymous reviewers for helpful comments on a previous draft. This publication was partially funded by the Cooperative Institute for Climate, Ocean, & Ecosystem Studies (CIOCES) under NOAA Cooperative Agreement NA20OAR4320271, Contribution No. 2022-1205 and by the National Pacific Research Board Grant #1805. J.I. was supported partly by a CICOES Graduate Student Award (Contribution No. 2022-1205) and by the National Pacific Research Board Grant #1805.

1.7 REFERENCES

Adams, C., Brooks, E., Legault, C., Barrett, M., and Chevrier, D. 2021. Quota allocation for stocks that span multiple management zones: analysis with a vector autoregressive spatiotemporal model. *Fisheries Management and Ecology* https://doi.org/10.1111/fme.12488

Baudron, A., Needle, C., Rijnsdorp, A., and Marshall, C. 2014. Warming temperatures and smaller body sizes: synchronous changes in growth of North Sea fishes. *Global Change Biology* 20: 1023-2031. https://doi.org/10.1111/gcb.12514

Begg, G. and Marteinsdottir, G. 2002. Environmental and stock effects on spatial distribution and abundance of mature cod Gadus morhua. *Marine Ecology Progress Series* 229: 345-262.

Bornmann, L. and Williams, R. 2013. How to calculate the practical significance of citation impact differences? An empirical example from evaluative institutional bibliometrics using adjusted predictions and marginal effects. *Journal of Informetrics* 7:562-574. http://dx.doi.org/10.1016/j.joi.2013.02.005

Breivik, O., Aanes, F., Sovik, G., Aglen, A., Mehl, S., and Johnsen, E. 2021. Predicting abundance indices in areas without coverage with a latent spatio-temporal Gaussian model. *ICES Journal of Marine Science* 78(6), 2031-2042. https://doi.org/10.1093/icesjms/fsab073

Burnham, K. and Anderson, D. 2002. *Model Selection and Inference*. Springer-Verlag, New York. http://dx.doi.org/10.1007/b97636

Casini, M., Kall, F., Hansson, M., Plikshs, M., Baranova, T., Karlsson, O., Lundstrom, K., Neuenfeldt, S., Gardmark, A., and Hjelm, J. 2016. Hypoxic areas, density-dependence and food limitation drive the body condition of a heavily exploited marine fish predator. *Royal Society Open Science* 3(10): 160416. https://doi.org/10.1098/rsos.160416

Clark, W. and Hare, S. 2002. Effects of climate and stock size on recruitment and growth of Pacific Halibut. *North American Journal of Fisheries Management* 22: 852-862. https://10.1577/1548-8675(2002)022<0852:EOCASS>2.0.CO;2

Dambrine, C., Woillez, M., Huret, M., and de Pontual, H. 2021. Characterising Essential Fish Habitat using spatio-temporal analysis of fishery data: A case study of the European seabass spawning areas. *Fisheries Oceanography* 30: 413-428. https://doi.org/10.1111/fog.12527

Daufresne, M., Lengfellner, K., and Sommer, U. 2009. Global warming benefits the small in aquatic ecosystems. *PNAS* 106(31): 12788-12793. https://doi.org/10.1073/pnas.0902080106

DeVries, D.R. and Frie, R.V. 1996. Determination of age and growth. In: Murphy, B.R., Willis, D.W. (Eds.), *Fisheries Techniques*. 2nd edition. American Fisheries Society, Bethesda, MD, pp. 483–512.

Ducharme-Barth, N., Gruss, A., Vincent, M., Kiyoofuji, H., Aoki, Y., Pilling, G., Hampton, J. and Thorson, J. 2022. Impacts of fishery-dependent spatial sampling patterns on catch-per-unit-effort standardization: A simulation study and fishery application. Fisheries Research 246: 106169. https://doi.org/10.1016/j.fishres.2021.106169

FAO. 2021. *FAO Yearbook. Fishery and Aquaculture Statistics* 2019. Rome: FAO. https://doi.org/10.4060/cb7874t

Fenberg, P. and Roy, K. 2008. Ecological and evolutionary consequences of size-selective harvesting: how much do we know?. *Molecular Ecology* 17:209-220. https://doi.org/10.1111/j.1365-294X.2007.03522.x

Fenske, K., Hulson, P., Williams, B., and O'Leary, C. 2020. Assessment of the Dusky Rockfish stock in the Gulf of Alaska. https://repository.library.noaa.gov/view/noaa/20258

Francis, R. I. C. 2011. Data weighting in statistical fisheries stock assessment models. Canadian Journal of Fisheries and Aquatic Sciences, 68: 1124–1138. https://doi.org/10.1139/f2011-025

Gardner, J., Peters, A., Kearney, M., Joseph, L., and Heinsohn, R. 2011. Declining body size: a third universal response to warming? *Trends in Ecology & Evolution* 26(6): 285-291. https://doi.org/10.1016/j.tree.2011.03.005

Gruss, A., Walter, J., Babcock, E., Forrestal, F., Thorson, J., Lauretta, M., and Schirripa, M. 2019. Evaluation of the impacts of different treatments of spatio-temporal variation in catch-per-unit-effort standardization models. *Fisheries Research* 213: 75-93. https://doi.org/10.1016/j.fishres.2019.01.008

Gruss, A., Thorson, J.T., Stawitz, C.C., Reum, J.C.P., Rohan, S.K., and Barnes, C.L. 2021. Synthesis of interannual variability in spatial demographic processes supports the strong influence of cold-pool extent on eastern Bering Sea walleye pollock (Gadus chalcogrammus). *Progress in Oceanography*, 194:102569. https://doi.org/10.1016/j.pocean.2021.102569

Gunderson, D. R. 1993. *Surveys of Fisheries Resources*. New York: John Wiley & Sons.

Hanselman, D., Heifetz, J., Echave, K., and Dressel, S. 2015. Move it or lose it: movement and mortality of sablefish tagged in Alaska. *Canadian Journal of Fisheries and Aquatic Sciences* 72(2): 238-251. https://doi.org/10.1139/cjfas-2014-0251

Helser, T. and Brodziak, J. 1998. Impacts of density-dependent growth and maturation on

assessment advice to rebuild depleted US siler hake (Merluccius bilinearis) stocks. *Canadian Journal of Fishery and Aquatic Sciences* 55: 882-892. https://doi.org/10.1139/f97-290

Hilborn, R., and Walters, C. J. 1992. *Quantitative Fisheries Stock Assessment - Choice, Dynamics and Uncertainty*, 1st edn. Springer, Norwell ,Massachusetts.

Holsman, K., Aydin, K., Sullivan, J., Hurst, T., and Kruse, G. 2018. Climate effects and bottom-up controls on growth and size-at-age of Pacific halibut (Hippoglossus stenolepis) in Alaska (USA). *Fisheries Oceanography* 28(3): 345-358. https://doi.org/10.1111/fog.12416

Hunt, G., Stabeno, P., Strom, S., and Napp, J. 2008. Patterns of spatial and temporal variation in the marine ecosystem of the southeastern Bering Sea, with special reference to the Pribilof Domain. *Deep-Sea Research II* 55:1919-1944. https://doi.org/10.1016/j.dsr2.2008.04.032

Hunt, G., Yasumiishi, E., Eisner, L. Stabeno, P., and Decker, M. 2022. Climate warming and the loss of sea ice: the impact of sea-ice variability on the southeastern Bering Sea pelagic ecosystem. *ICES Journal of Marine Science* 79(3): 937-953. https://doi.org/10.1093/2 3 53 icesjms/fsaa206

Ianelli, J., Fissel, B., Stienessen, S., Honkalehto, T., Siddon, E., and Allen-Akselrud, C. 2021. Chapter 1: Assessment of the Walleye Pollock Stock in the Eastern Bering Sea. https://www.fisheries.noaa.gov/resource/data/2021-assessment-walleye-pollock-stock-eastern-bering-sea

Ikpewe, I., Baudron, A., Ponchon, A., and Fernandes, P. 2020. Bigger juveniles and smaller adults: Changes in fish size correlated with warming seas. *Journal of Applied Ecology* 58(4): 847-856. https://doi.org/10.1111/1365-2664.13807

Jorgensen, C., Ernande, B., and Oyvind, F. 2009. Size-selective fishing gear and life history evolution in the Northeast Arctic cod. *Evolutionary Applications* 2: 366-370. https://doi.org/ 10.1111/j.1752-4571.2009.00075.x

Kimura, D. and Somerton, D. 2007. Review of statistical aspects of survey sampling for marine fisheries. Reviews in Fisheries Science 14(3): 245-283. https://doi.org/10.1080/10641260600621761

Kraak, S., Haase, S., Minto, C., and Santos, J. 2019. The Rosa Lee phenomenon and its consequences for fisheries advice on changes in fishing mortality or gear selectivity. *ICES Journal of Marine Science* 76(7): 2179-2192. https://doi.org/ 10.1093/icesjms/fsz107

Kristensen, K., Nielsen, A., Berg, C., Skaug, H., Bell, B. 2016. "TMB: Automatic Differentiation and Laplace Approximation." Journal of Statistical Software 70(5): 1–21.

https://doi.org/10.18637/jss.v070.i05.

Krohn, M. and Kerr, S. 1997. Declining weight-at-age in northern cod and the potential importance of the early years and size-selective fishing mortality. *Science Council Studies* 29:43-50.

Kotwicki, S., Ianelli, J., and Punt, A. 2014. Correcting density-dependent effects in abundance estimates from bottom-trawl surveys. *ICES Journal of Marine Science* 71(5): 1107-1116. https://doi.org/10.1093/icesjms/fst208

Kotwicki, S. and Ono, K. 2018. The effect of random and density-dependent variation in sampling efficiency on variance of abundance estimates from fishery surveys. Fish and Fisheries 20: 760-774. https://doi.org/10.1111/faf.12375

Kuriyama, P., Ono, K., Hurtado-Ferro, F., Hicks, A., Taylor, I., Licandeo, R., Johnson, K., Anderson, S., Monnahan, C., Rudd, M., Stawitz, C., and Valero, J. 2016. An empirical weight-at-age approach reduces estimation bias compared to modeling parametric growth in integrated, statistical stock assessment models when growth is time varying. *Fisheries Research* 190: 119-127. https://doi.org/10.1016/j.fishres.2015.09.007

Lindgren, F. and Rue, H. 2015. Bayesian spatial modelling with R-INLA. *Journal of Statistical Software*, 63(19): 1–25. https://doi.org/10.18637/jss.v063.i19

Lindgren, F., Rue, H., and Lindstrom J. 2011. An explicit link between Gaussian fields and Gaussian Markov random fields: the stochastic partial differential equation approach**.** *Statistical Methodology* 73(4): 423-498. https://doi.org/10.1111/j.1467-9868.2011.00777.x

Lindmark, M, Ohlberger, J., and Gardmark, A. 2022. Optimum growth temperature declines with body size within fish species. *Global Change Biology* 28)7): 2259-2271. https://doi.org/10.1111/gcb.16067

Link, J., Nye, J., and Hare, J. 2010. Guidelines for incorporating fish distribution shifts into a fisheries management context. Fish and Fisheries 12(4): 461-469. 10.1111/j.1467-2979.2010.00398.x

Martin, T., Wintle, B., Rhodes, J., Kunert, P., Field, Sa., Low-Choy, S., Tyre, A., Possingham, H. 2005. Zero tolerance ecology: improving ecological inference by modelling the source of zero observations. *Ecology Letters* 8: 1235-1246.

Maunder, M. and Punt, A. 2004. Standardizing catch and effort data: a review of recent approaches. Fisheries Research 70: 141-159 https://doi.org/10.1016/j.fishres.2004.08.002

Maunder, M., Thorson, J., Xu, H., Oliveros-Ramos, R., Hoyle, S., Tremblay-Boyer, Lee, H., Kai, M., Chang, S., Kitakado, T., Albertsen, C., Minte-Vera, C., Lennert-Cody, C., Aires-da-Silva, A., and Piner, K. 2020. The need for spatio-temporal modeling to determine catch-per-unit effort based indices of abundance and associated composition data for inclusion

in stock assessment models. *Fisheries Research* 229: 105594. https://doi.org/10.1016/j.fishres.2020.105594

Methot, R. 2009. Stock Assessment: Operational Models in Support of Fisheries Management. R.J Beamish and B.J. Rothschild (eds.). *The Future of Fisheries Science in North America*. Chapter 9. 137-165. https://doi.org/10.1007/978-1-4020-9210-7_9

Minte-Vera, C. 2004. Meta-analysis of density-dependent growth. Ph. D. Thesis, University of Washington, Seattle, 1-204.

Mize, T. 2019. Best practices for estimation, interpreting, and presenting nonlinear interaction effects. *Sociological Science* 6: 81-117. https://doi.org/10.15195/v6.a4

Mueter, F. and Litzow, M. 2008. Sea ice retreat alters the biogeography of the Bering Sea continental Shelf. *Ecological Applications* 18(2): 309-320. https://doi.org/10.1890/07-0564.1

Mueter, F. J., Bond, N.A., Ianelli, J.N., and Hollowed, A.B. 2011. Expected declines in recruitment of walleye pollock (Theragra chalcogramma) in the eastern Bering Sea under future climate change. *ICES Journal of Marine Science*, 68(6): 1284-1296. https://doi.org/10.1093/icesjms/fsr022

National Oceanic and Atmospheric Administration. May 22, 2020a. NOAA Fisheries Will Cancel Five Alaska Research Surveys for 2020. Media Release. https://www.fisheries.noaa.gov//media-release/noaa-fisheries-will-cancel-five-alaska-research-surveys-2020

National Oceanic and Atmospheric Administration. Aug 27, 2020b. NOAA Fisheries Cancels 2020 Southeast Fishery-Independent Survey (SEFIS). Media Release. https://www.fisheries.noaa.gov//agency-statement/noaa-fisheries-cancels-2020-southeast-fishery-independent-survey-sefis

National Oceanic and Atmospheric Administration. Aug 3, 2020c. NOAA Fisheries Cancels Three West Coast Surveys for 2020. Agency Statement. https://www.fisheries.noaa.gov//agency-statement/noaa-fisheries-cancels-three-west-coast-surveys-2020

National Oceanic and Atmospheric Administration. Aug 3, 2020d. NOAA Fisheries Cancels Three West Coast Surveys for 2020. Agency Statement. https://www.fisheries.noaa.gov/agency-statement/noaa-fisheries-cancels-four-fisheries-and-ecosystem-surveys-2020

Nebenzahl, D. and Goddard, P. (Compilers). 2000 Bottom Trawl Survey of the Eastern Bering Sea Continental Shelf. AFSC Processed Rep. 2000-10. Alaska Fish. Sci. Cent., NOAA, Natl. Mar, Fish. Serv., 7600 Sand Point Way NE, Seattle WA 98115.

Oke, K., Mueter, F., and Litzow, M. 2022. Warming leads to opposite patterns in weight-at-age for young versus old age classes of Bering Sea walleye pollock. *Canadian Journal of Fisheries and Aquatic Sciences.* https://doi.org/10.1139/cjfas-2021-0315

O'Leary, C., Thorson, J., Ianelli, J., and Kotwicki, S. 2020. Adapting to climate-driven distribution shifts using model-based indices and age composition from multiple surveys in the walleye pollock (Gadus chalcogrammus) stock assessment. Fisheries Oceanography 29(6): 541-557. https://doi.org/10.1111/fog.12494

O'Leary, C., DeFilippo, L., Thorson, J., Kotwicki, S., Hoff, G., Kulik, V., Ianelli, J., and Punt, A. 2022. Understanding transboundary stocks' availability by combining multiple fisheries-independent surveys and oceanographic conditions in spatiotemporal models. *ICES Journal of Marine Science* 79(4): 1063-1074. https://doi.org/10.1093/icesjms/fsac046

Pinsky, M., Selden, R., and Kitchel, Z. 2020. Climate-driven shifts in marine species ranges: Scaling from Organisms to Communities. *Annual Review of Marine Science* 12: 153-79. https://doi.org/10.1146/annurev-marine-010419-010916

Punt, A. and Smith, D. 2001. Assessments of species in the Australian South East Fishery can be sensitive to the method used to convert from size- to age-composition data. *Marine & Freshwater Research* 52: 683-690. https://doi.org/10.1071/MF99129

Punt, A.E., Dalton, M. G., Cheng, W., Hermann, A.J., Holsman, K.K., Hurst, T.P., Ianelli, J. N., Kearney, K. A., McGilliard, C.R., Pilcher, D.J., and Veron, M. 2021. Evaluating the impact of climate and demographic variation on future prospects for fish stocks: An application for northern rock sole in Alaska. *Deep Sea Research Part II: Topical Studies in Oceanography*, 189-190: 104951. https://doi.org/10.1016/j.dsr2.2021.104951

Rooper, C., Ortiz, I., Hermann, A., Laman, N. Cheng, W., Kearney, K. and Aydin, K. 2021. Predicted shifts of groundfish distribution in the Eastern Bering Sea under climate change, with implications for fish populations and fisheries management. *ICES Journal of Marine Science* 78(1) 220-234. https://doi.org/10.1093/icesjms/fsaa215

RStudio Team. 2020. RStudio: Integrated Development for R. RStudio, PBC, Boston, MA URL http://www.rstudio.com/.

Sullivan, J. 2016. Environmental, ecological, and fishery effects on growth and size-at-age of Pacific halibut (Hippoglossus stenolepis). Dissertation. University of Alaska Fairbanks. https://www.proquest.com/dissertations-theses/environmental-ecological-fishery-effects-on/docview/1814754668/se-2

Sullivan, J., Kruse, G., and Mueter, F. 2018. Do Environmental and Ecological Conditions Explain Declines in Size-at-age of Pacific Halibut in the Gulf of Alaska. In F.J. Mueter, M.R. Baker, S.C. Dressel, and A.B. Hollowed (eds.), *Impacts of a Changing Environment*

on the Dynamics of High-latitude Fish and Fisheries. Alaska Sea Grant, University of Alaska Fairbanks. https://doi.org/10.4027/icedhlff.2018.06

Swain, D., Sinclair, A., and Hanson, J. 2007. Evolutionary response to size-selective mortality in exploited fish population. *Proceedings of the Royal Society B* 274(1613): 1015-1022. https://doi.org/ 10.1098/rspb.2006.0275

Thorson, J., Stewart, I., and Punt, A. 2011. Accounting for fish shoals in single- and multi-species survey data using mixture distribution models. *Canadian Journal of Fisheries and Aquatic Sciences* 68(9): 1681-1693. https://doi.org/10.1139/f2011-086

Thorson, J. 2014. Standardizing compositional data for stock assessment. *ICES Journal of Marine Science* 71(5): 1117-1128. https://doi.org/ 10.1093/icesjms/fst224

Thorson, J., Monnahan, C., and Cope, J. 2015. The potential impact of time-variation in vital rates on fisheries management targets for marine fishes. *Fisheries Research* 169: 8-17. https://dx.doi.org/10.1016/j.fishres.2015.04.007

Thorson, J., Shelton, A.O., Ward, E.J., Skaug, H.J. 2015b. Geostatistical delta-generalized linear mixed models improve precision for estimated abundance indices for West Coast groundfishes. *ICES Journal of Marine Science* ,72(5): 1297-1310. https://doi.org/10.1093/icesjms/fsu243

Thorson, J. and Minte-Vera, C. 2016. Relative magnitude of cohort, age, and year effects on size at age of exploited marine fishes. *Fisheries Research* 180: 45-53. https://dx.doi.org/10.1016/j.fishres.2014.11.016

Thorson, J., Ianelli, J. N., and Kotwicki, S. 2017. The relative influence of temperature and size-structure on fish distribution shifts: A case-study on Walleye pollock in the Bering Sea. *Fish and Fisheries* 18: 1073-1084. https://doi.org10.1111/faf.12225

Thorson, J. 2018. Three problems with the conventional delta-model for biomass sampling data, and a computationally efficient alternative. *Canadian Journal of Fisheries and Aquatic Sciences* 75: 1369-1382. https://doi.org/dx.doi.org/10.1139/cjfas-2017-0266

Thorson, J. and Haltuch, M. 2018. Spatiotemporal analysis of compositional data: increased precision and improved workflow using model-based inputs to stock assessment. *Canadian Journal of Fisheries and Aquatic Sciences* 75(3): 401-414. https://doi.org/10.1139/cjfas-2018-0015

Thorson, J. 2019. Guidance for decisions using the Vector Autoregressive Spatio-Temporal (VAST) package in stock, ecosystem, habitat and climate assessments. *Fisheries Research* 215: 143-150. https://doi.org/10.1016/j.fishres.2018.10.013

Thorson, J., Maunder, M., and Punt, A. 2020. The development of spatio-temporal models of

fishery catch-per-unit-effort data to derive indices of relative abundance. *Fisheries Research* 230:105611. https://doi.org/10.1016/j.fishres.2020.105611

Thorson, J., Barbeau, S., Goethel, D., Kearney, K., Laman, E., Nielsen, J., Siskey, M., Siwicke, K., and Thompson, G. 2021. Estimating fine-scale movement rates and habitat preferences using multiple data sources. *Fish and Fisheries* 22: 1359-1376. https://doi.org/ 10.1111/faf.12592

Thorson, J., Hermann, A., Siwicke, K., and Zimmermann, M. 2021b. Grand challenge for habitat science: stage-structured responses, nonlocal drivers, and mechanistic associations among habitat variables affecting fishery productivity. *ICES Journal of Marine Science* 78(6): 1956-1968. https://doi.org/10.1093/icesjms/fsaa236

Uusi-Heikkila, S., Whiteley, A., Kuparinen, A., Matsumura, S., Venturelli, P., Wolter, C., Slate, J., Primmer, C., Meinelt, T., Killen, S., Bierbach, D., Polverino, G., Ludwig, A., and Arlinghaus, R. 2015. The evolutionary legacy of size-selective harvesting extends from genes to populations. *Evolutionary Applications* 8: 597-620. https://doi.org/10.1111/eva.12268

Walters, G. 1997. 1993 Bottom Trawl Survey of the Eastern Bering Sea Continental Shelf. AFSC Processed Rep. 97-09. Alaska Fish. Sci. Cent., NOAA, Natl. Mar, Fish. Serv., 7600 Sand Point Way NE, Seattle WA 98115.

Whitehouse, G., Aydin, K., Hollowed, A., Holsman, K., Cheng, K., Faig, A., Haynie, A., Hermann, A., Kearney, K., Punt, A., and Essington, T. 2021. *Bottom-up impacts of forecasted climate change on the eastern Bering Sea food web. Frontiers in Marine Science* 8: 624301. https://doi.org/10.3389/fmars.2021.624301

Whitten, A., Klaer, N., Tuck, G., and Day, R. 2013. Accounting for cohort-specific variable growth in fisheries stock assessments: a case study from south-eastern Australia. *Fisheries Research* 142: 27-36. https://doi.org/10.1016/j.fishres.2012.06.021

Williams, R. (2012). Using the Margins Command to Estimate and Interpret Adjusted Predictions and Marginal Effects. *The Stata Journal* 12(2): 308–331. https://doi.org/10.1177/1536867X1201200209

Wilson, M. and Armistead, C. 1991. NOAA Technical Memorandum NMFS F/NWC-212. Alaska Fish. Sci. Cent., NOAA, Natl. Mar, Fish. Serv., 7600 Sand Point Way NE, Seattle WA 98115.

Zhou, S., Campbell, R., and Hoyle, S. 2019. Catch per unit effort standardization using spatio-temporal models for Australia's Eastern Tuna and Billfish Fishery. *ICES Journal of Marine Science* 76(6): 1489-1504. https://doi.org/10.1093/icesjms/fsz034

van Rijn, I., Buba, Y., DeLong, J., Kiflawi, M., and Belmaker, J. 2017. Large but uneven

reduction in fish size across species in relation to changing sea temperatures. *Global Change Biology* 23(9): 3667-3674. https://doi.org/10.1111/gcb.13688

VAST. Version 3.8.2. https://github.com/James-Thorson-NOAA/VAST

Chapter 2. ESTIMATING A PHYSIOLOGICAL THRESHOLD TO OXYGEN AND TEMPERATURE FROM MARINE MONITORING DATA REVEALS CHALLENGES AND OPPORTUNITIES FOR FORECASTING DISTRIBUTION SHIFTS

Publication history: This study was co-authored with Sean C. Anderson, Lewis A.K. Barnett, Eric J. Ward, and Timothy E. Essington. At the time this dissertation was submitted, a version of this chapter was published in *Ecography* (https://doi.org/10.1111/ecog.07413).

2.1 ABSTRACT

Species distribution modeling is increasingly used to describe and anticipate consequences of a warming ocean. These models often identify statistical associations between distribution and environmental conditions such as temperature and oxygen, but rarely consider the mechanisms by which these environmental variables affect metabolism. Oxygen and temperature jointly govern the balance of oxygen supply to oxygen demand, and theory predicts thresholds below which population densities are diminished. However, parameterizing models with this joint dependence is challenging because of the paucity of experimental work for most species, and the limited applicability of experimental findings *in situ*. Here we ask whether the temperature-sensitivity of oxygen can be reliably inferred from species distribution observations in the field, using the U.S. Pacific Coast as a model system. We developed a statistical model that adapted the metabolic index—a compound metric that incorporates these joint effects on the ratio of oxygen supply and oxygen demand by applying an Arrhenius equation—and used a non-linear threshold function to link the index to fish distribution. Through simulation testing, we found that our statistical model could not precisely estimate the parameters due to inherent features of the distribution data. However, the model reliably estimated an overall metabolic index threshold effect. When applied to case studies of real data for two groundfish species, this new model provided a better fit to spatial distribution of one species, sablefish (*Anoplopoma fimbria*),than previously used models, but did not for the other, longspine thornyhead (*Sebastolobus altivelis*). This physiological framework may improve predictions of species distribution, even in novel environmental conditions. Further efforts to combine insights from physiology and realized species distributions will improve forecasts of species' responses to future environmental changes.

2.2 INTRODUCTION

Range shifts of aquatic and terrestrial species are widespread, although the velocity and magnitude vary with taxa and system (Lenoir et al., 2020). Anticipating how species

distributions might shift under future climate conditions can enable more effective conservation and natural resource actions. Predicting these range changes can inform disease and parasite risk analysis (Polley & Thompson, 2009; Rohr & Cohen, 2020), invasive species control (Beaury et al., 2020; Smith et al., 2022), protected area design (Monzón et al., 2011; Hoffmann et al., 2019), and harvest management (Baudron et al., 2020; Bell et al., 2020).

However, there are limits to our ability to forecast species range shifts. For instance, correlative species distribution models (SDMs), a type of habitat suitability model (Hirzel & Le Lay, 2008), have been a common approach to predict species responses to climate change (Franklin, 2010; Warton & Shepherd, 2010; Swanson et al., 2013; Melo-Merino et al., 2020). These models identify historical associations between species densities and relevant environmental conditions to explain past shifts and forecast future shifts. Relying on correlations from the past may provide unskillful forecasts as climate change pushes environmental conditions far outside those seen in the past (Williams & Jackson, 2007; Marshall et al., 2017; Rollinson et al., 2021; Smith et al., 2022). Ecological systems may have novel responses to these anomalous conditions (Williams & Jackson, 2007; Hobbs et al., 2009) and often exhibit changing relationships over time (e.g. Myers 1998; Asch et al., 2022). For instance, the temperature-recruit relationship for Pacific sardine (*Sardinops sagax*) used in operational stock assessments was no longer significant when re-evaluated with more recent data (McClatchie et al., 2010). Predictions based on historical relationships may consequently break down when used in forecasting (Veloz et al., 2012; Muhling et al., 2020; Barnes et al., 2022), especially in novel environments (Waldock et al., 2022).

Incorporating mechanistic relationships into SDMs is one approach to include biological realism and improve inference and forecasting ability (Kearney & Porter, 2009; Martínez et al., 2015; Urban et al., 2016; Urban, 2019; Briscoe et al., 2023). For marine taxa, one possible mechanistic pathway for predicting responses to climate change is considering the joint effect of temperature and oxygen on metabolism (e.g. Methorst et al., 2017; Duncan et al., 2020). Due to climate change, ocean temperatures are projected to to increase (Cheng et al., 2019), and extreme heatwave events are becoming more frequent (Frölicher et al., 2018; Laufkötter et al., 2020). There will also likely be widespread oxygen depletion (Diaz & Rosenberg, 2008). Temperature governs metabolic rate and therefore oxygen demand (Gillooly et al., 2001; Brown et al., 2004). Temperature and oxygen may therefore jointly govern tolerances to environmental conditions through these metabolic requirements (Pörtner & Knust, 2007, Pörtner 2010, Verberk et al., 2016a, Pörtner et al., 2017, Leiva et al., 2019), though there is ongoing debate on the exact way and extent to which limitations may occur (e.g. see Verberk et al., 2016b, Lefevre et al., 2017, Jutfelt et al., 2018, Seibel and Deutsch 2020, Verberk et al., 2020, Scheuffele et al., 2021, Atkinson et al. 2022). Yet overall, parameterizing the interactive effect of temperature and oxygen in the metabolic index, rather than separately or linearly, can provide a framework rooted in physiological theory to explain historical effects of temperature and oxygen on distributions. This can help better identify habitats important for fish population processes (i.e. for designating essential fish habitat, Rosenberg et al., 2000; Moore et al., 2016) and predict future range shifts, contractions, or expansions.

One way to capture how the interaction between oxygen and temperature shapes species' distribution is the "metabolic index" (ϕ) a compound metric that incorporates the joint effects of

temperature and oxygen on the ratio of oxygen supply to oxygen demand (Deutsch et al., 2015). Theory predicts a ratio below which aquatic taxa are likely to avoid due to insufficient temperature-oxygen conditions for metabolic functioning (Deutsch et al., 2015). We recognize that there are other possible frameworks for combining the effects of oxygen and temperature on fish (e.g. the aerobic growth index in Clarke et al. 2021, Moreé et al. 2023; Ern 2019), yet comparison of different frameworks is beyond the scope of this study. The metabolic index was found to closely align with species distributions across biogeographic scales to define species' range limits (Deutsch et al., 2020; Sunday et al., 2022) and has been used to explain contemporary distributions (Franco et al., 2022, Penn & Deutsch, 2024), past extinction events (Penn & Deutsch, 2022), and predict future marine habitat shifts (Chen et al., 2024).

Using the metabolic index (or a similar ecophysiological metric) in statistical species distribution models may improve predictions of distribution shifts under future climate regimes. However, implementing this approach is often challenged by the paucity of information on how the ratio of oxygen demand and supply scale with temperature. Most data to estimate the metabolic index are derived from laboratory studies. Because of the time and logistical demands of such studies, such information is only available for a small number of marine taxa. A recent empirical meta-analysis used taxonomic imputation of data from 74 marine taxa to evaluate the parameters of the metabolic index across species (Essington et al., 2024). This approach (see Penone et al., 2014; Debastiani et al., 2021; Thorson et al., 2021b) is a rigorous statistical model that accounts for phylogenetic relationships to predict traits for unmeasured species. The empirical meta-analysis found that the temperature-sensitivity of oxygen tolerance was highly variable across taxa and could not be precisely predicted for unmeasured species from existing data. Moreover, the applicability of experimental findings to explain distributions *in situ* is limited (e.g. Essington et al., 2022; Bandara et al., 2023) owing to the wide range of physiological acclimations and potential for local adaptation.

Here, we evaluate the reliability of a new approach to estimate a physiologically-based (i.e. metabolic index) temperature-dependence of oxygen tolerance from species distribution data within a statistical model, using the U.S. Pacific coast as a model system. This approach aims to overcome limitations of laboratory studies by estimating this component of the metabolic index (the temperature-dependence of oxygen tolerance) from widely available data (e.g. species distribution data collected from the field). While our approach is not directly mechanistic, we aim to (1) improve existing methods by basing the response of fish to temperature and oxygen in a more physiologically and ecologically realistic relationship than considering temperature and oxygen independently or linearly, and (2) illustrate data limitations and gaps in estimating metabolic responses.

We first developed a statistical model that simultaneously estimates relevant metabolic index parameters and estimates the effect of temperature and oxygen (metabolic index) on local fish density (i.e. estimates parameters that describe this function). We then used simulation testing to evaluate whether our new model could accurately recover parameters, a standard practice when developing quantitative methods. For this, we simulated data of fish density and distribution from our model with specified parameters, fit our new model, and then compared estimated parameter estimates with the known values (i.e., those used in simulation). Finally, we fit the model to real-world data of two Pacific coast demersal fish species as case studies to evaluate

model performance and behavior, and to demonstrate how the model can be used to evaluate the extent to which oxygen, temperature, or the metabolic index governs fish distributions.

2.3 METHODS

2.3.1 *Model structure*

We modified a geostatistical generalized linear mixed effects model (GLMM) widely used for correlative SDMs that estimates local population densities as a function of observed and latent environmental variables. This approach is generic and could be extended to other models consistent with a GLMM framework. These modifications were twofold. First, we introduced an additional term that would allow for an asymptotic effect of oxygen on local abundance, which recognizes that oxygen is a limiting factor. Second, we accounted for the interactive effect of $p\mathrm{O}_2$ and temperature as described by the metabolic index. We describe these steps in detail below and provide a graphical summary of the modeling framework in Figure 1.

The SDM is a generalized linear mixed effects model (Eq. 1) that estimates the expected density μ of observation i with a log link

$$\log(\mu_i) = b_{year[i]}t_i + b_2 d_i + b_3 d_i^2 + \omega_i \quad \text{Eq.1}$$

where b_{year} are independent year effects for each year t_i, b_2 and b_3 are the estimated effects of scaled log(depth) (d_i) and its square (d_i^2), and ω_i is a spatial random effect that accounts for spatially structured latent variables. Depth is included because fish have depth preferences separate from other environmental conditions (e.g. sablefish in Sogard and Berkely 2017). We model spatial effects using the stochastic partial differential equation (SPDE) approximation to Gaussian random fields via Gaussian Markov random fields (GMRFs) (Lindgren et al., 2011) as implemented in TMB (Kristensen et al., 2016). The random effects describing the spatial field are estimated at a set of vertices or knots and then projected to the locations of observed data with bilinear interpolation, assuming spatial covariance is modeled using a GMRF with a Matérn covariance function and anisotropy. The approach allows modelling a sparse precision matrix of a GMRF, which is considerably more efficient than modelling the covariance matrix of a Gaussian random field directly (Lindgren et al., 2011). Given that observations in catch-per-unit-effort (CPUE) data typically include positive continuous values and zeros, we assumed the observed process followed a Tweedie distribution (Shono, 2008, Tweedie 1984) so that the i_{th} observation is drawn from a Tweedie distribution with mean μ_i, power parameter p, and scale parameter σ.

We made two adjustments to the linear structure of the above model (Eq. 1), depicted visually in Figure 1. One, the model uses oxygen and temperature and estimates the parameter E_0 to generate the portion of the metabolic index (the temperature-dependence of oxygen tolerance) that can be uniquely estimated in this statistical modelling framework ($\Phi_{eco,i}$) (see Appendix A). The symbol Φ_{eco} is defined as the terms of the metabolic index that depend on $p\mathrm{O}_2$ and temperature (see Appendix A for derivation, Eqs. S5—S7):

$$\Phi_{eco,i} = pO_{2,i} \exp\left[\frac{E_0}{k_b}\left(\frac{1}{T_i} - \frac{1}{T_{ref}}\right)\right] \quad \text{Eq. 2}$$

where E_0 is an estimated parameter that describes the temperature dependence of the ratio of oxygen supply to demand, k_b is Boltzmann's constant, and T_{ref} is a reference temperature (here chosen as 12 C). Both T and T_{ref} are in Kelvin units in Eq. 2.

Second, we defined a function f($\Phi_{eco,i}$) that takes the calculated $\Phi_{eco,i}$ and estimates parameters that governs the predicted mean density at a sample site, and is added to the suite of linear predictors in equation 1:

$$\log(\mu_i) = b_{year[i]}t_i + b_2 d_i + b_3 d_i^2 + \omega_i + f\left(\Phi_{eco,i}\right) \quad \text{Eq. 3}$$

Here, $f(\Phi_{eco})$, when exponentiated, acts as a multiplier to diminish predicted mean density when oxygen and temperature conditions are estimated to be physiologically stressful. We expected this to be a monotonically increasing function that asymptotes at 1, i.e. there is no additional benefit of oxygen and temperature on density once oxygen and temperature exceed limiting values, following typical fish responses to environmental conditions (Farrell & Richards, 2009). We therefore needed to choose a functional form for $f(\Phi_{eco})$ such that $e^{f(\Phi_{eco})}$ is asymptotic and bounded between 0 and 1. The following function meets these criteria:

$$f(\Phi_{eco}) = \psi\left(\frac{1}{1+\exp(-\alpha_0-\alpha_1\Phi_{eco})} - 1\right) \quad \text{Eq. 4}$$

where $\alpha_0$and α_1 are parameters describing a sigmoidal curve (based on a modified logistic function) and ψ scales the function (example plot of this function shown in Figure 1). We re-parameterized Eq. 4 to both work in the log-linear model framework and to have more easily interpretable parameters (see Appendix A, Eqs. S1—S4): the value of Φ_{eco} at which the exponentiated value of the function $f(\Phi_{eco})$ equals 0.5, $s50$ (i.e. the value of Φ_{eco} that reduces fish density by 50%) and the value of Φ_{eco} where the exponentiated value of the function equals 0.95, $s95$ (i.e. the value of Φ_{eco} that reduces fish density by 5%). All parameters of the model are estimated simultaneously using maximum marginal likelihood.

To implement this model, we have added a feature within the widely used sdmTMB package (Anderson et al., 2024) that requires a simple addition to the model formula (see [github link will be provided for publication after peer-review process is completed] for example vignette.

2.3.2 *Simulation testing*

To evaluate whether our model could accurately estimate the metabolic-index parameter E_0 and parameters of $f(\Phi_{eco})$, we used simulation testing, a standard practice for testing model performance. This involves specifying values of all model parameters in an operating model, simulating data as if the model were "true", and passing simulated data to the estimation routine. In this way, bias and precision of parameter estimates can be evaluated because the "true" parameter values are known. Our goals of this simulation were to ask: 1) How accurately could the model estimate key parameters relating local density to oxygen and temperature (E_0 and $s50$)? 2) How accurately could the model estimate a response of local density to the combined

temperature and oxygen function $f(\Phi_{eco})$? 3) Does constraining model estimation with prior information on E_0 improve accuracy? 4) How robust are parameter estimates to a hypothetical model mis-specification?

We simulated data for fish density and distribution, using the U.S. Pacific coast as a model system. Our objective was to replicate the distribution of a hypothetical fish species that inhabits a broad range of depths, specifically extending through its oxygen minimum zone. For instance, sablefish and longspine thornyhead can both be found in habitat up to 1250 m deep (Appendix B Fig S5). We used year effects and a quadratic response to depth for sablefish based on the estimated parameters in Essington et al., (2022). We simulated datasets for two cases, reflecting contrasting effects of the temperature-dependence of oxygen tolerance. The first (i.e. "typical case") represented a case where the simulated species' temperature-dependence of oxygen tolerance (Eq. 2) was close to the median value from the empirical meta-analysis for a generic teleost (E_0=0.3) in Essington et al. (2024), as described above. The second (i.e. "unusual case") represents a case in which the simulated species' temperature-dependence of oxygen sensitivity deviates greatly from the expected value (i.e. the median of the meta-analysis) and is roughly equal to the upper 90% of the meta-analysis distribution (E_0=0.7). A higher value of E_0 indicates a steeper sensitivity of oxygen tolerance to changes in temperature.

For both cases, the $f(\Phi_{eco})$ threshold function parameters were selected to generate a reasonably shaped sigmoidal curve, where ~30% of observations fell below the $s50$ threshold (see Appendix B Table S1 for full values used in data generation and all equations and Fig S3 for simulated $f(\Phi_{eco})$ response for typical and unusual cases). We used the actual latitude/longitude and temperature, oxygen, and depth of each haul from the West Coast Bottom Trawl Survey (WCBTS) data from 2010-2015, rather than simulating random locations, bathymetry, and environmental conditions. We wanted to retain the covariances and confounding effects of environmental conditions and space from the real data, thus challenging the model's ability to fit to data resembling real-world environmental and biological characteristics (see Appendix B Fig S2 for covariation plots). The WCBTS is a standardized trawl survey of the U.S. portion of the California Current (spanning the Pacific coast waters of Washington, Oregon, and California). It uses a random stratified design and has had consistent sampling procedures since 2003 (Keller et al. 2017). Using this environmental data and the specified parameter values, fish densities were then generated following Eq. 2-4 using sdmTMB (Anderson et al., 2024) for 250 unique datasets (Appendix B Fig S1). Each iteration was a randomized realization (varying in the specific year effects, spatial variation, and observation error) of the same true structure. We evaluated the number of iterations to ensure that it was sufficient for stable results (Appendix B Fig S4).

To evaluate how well parameters could be recovered, we then fit a perfectly specified model to each simulated dataset (i.e., the fitted model was identical to the data generating model, Eq. 3), using sdmTMB (Anderson et al., 2024). To evaluate parameter estimation, we calculated overall accuracy (root mean squared error (RMSE) across all data iterations of each generating-fitting scenario); bias (difference between the maximum likelihood estimate (MLE) and the true value), and precision (standard deviation of the MLEs across all data iterations). To evaluate the accuracy of the estimated temperature-oxygen effect compared to the true effect size used to simulate data, we calculated the conditional effect of $f(\Phi_{eco})$ for each data iteration (Eq. 4) and the RMSE compared to the true value. We evaluated the support for the "true" model in

comparison to alternative models (see models in Table 1) by calculating and comparing the marginal Akaike Information Criterion (AIC) (Akaike, 1974) for each iteration of generated data. This also provided an assessment of how well a standard model selection procedure could identify the correct model as the one most supported by the data.

To assess the impact of using empirical information about physiological parameters on model performance, we repeated the same model fitting procedure for each simulated dataset as described above (i.e. "unconstrained model"), but applied a prior probability via a likelihood penalty on estimated E_0 (i.e. "constrained model"). The penalized likelihood was based on the distribution expected for teleosts from the empirical meta-analysis of laboratory data (Essington et al., 2024), which followed a normal distribution of mean=0.3422 and standard deviation=0.1455. This approach is one way to integrate information from multiple sources; if empirical data on a related species are available, that could provide an informative prior to constrain the values of E_0 estimated from realized distribution data. By comparing model fit with and without a prior to both simulated species, we evaluated the ability of the data to estimate the $f(\Phi_{eco})$ parameters versus the reliance on a prior and whether, and to what extent, a prior improves estimation.

We also evaluated the robustness of model performance against one hypothetical model mis-specification. In the first two model fittings above, the estimation model was perfectly matched to the covariate structure of the generating model. We challenged the model estimation by mis-specifying the covariate structure in Eq. 3 fit to the simulated datasets by using only a linear depth term rather than a quadratic (i.e. "mis-specified model"), using unconstrained E_0 estimation (i.e. with no prior).

2.3.3 *Application to case studies*

After the simulation testing allowed us to understand how the model performed with known parameters, we then used empirical distribution data to assess how well this new model structure with the $f(\Phi_{eco})$ term performed relative to other models that either did not consider oxygen or that considered oxygen and temperature as separate predictor variables. While this analysis does not allow us to assess precision or accuracy (because the true values of parameters are not known), it does illustrate the application of the method in a realistic context. For this assessment, we used species distribution data on two groundfish species— sablefish (*Anoplopoma fimbria*) and longspine thornyhead (*Sebastolobus altivelis*)— in the northeast Pacific coast that inhabit a wide range of habitats that include those with low oxygen over a range of temperatures and depths (Appendix B Fig S5). There is not laboratory data sufficient to derive the metabolic index following Deutsch et al. (2015) for these or other demersal fish species important to the region. For each species, we modeled the observed CPUE (kg km^{-2}) from the West Coast Bottom Trawl Survey data. We restricted analysis to the catch rate of intermediate-sized fish following the method in Essington et al., (2022) so that the data represented a narrow range of fish sizes. We did this because coast fish distributions are often size-structured, and physiological sensitivity to oxygen is also size-dependent (Rubalcaba et al., 2020).

We used multi-model inference to judge the weight of evidence for our new model (Eq. 3) compared to other parameterizations of oxygen or temperature, as well as not including them at

all. Including a null model with no temperature and oxygen terms provided a comparison to evaluate if a species' distribution is not bound by these environmental conditions, rather than assuming they are a constraint. Models denoted with "breakpoint" function use the following structure to relate a slope β on a predictor variable, x, up until the breakpoint of the predictor variable x_{bp}, on the expected value of the response variable:

$$g(x) = \begin{cases} x\beta & if\ x < x_{bp} \\ x_{bp}\beta & otherwise \end{cases} \quad \text{Eq. 5}$$

The full suite of alternative models is provided in Table 1.

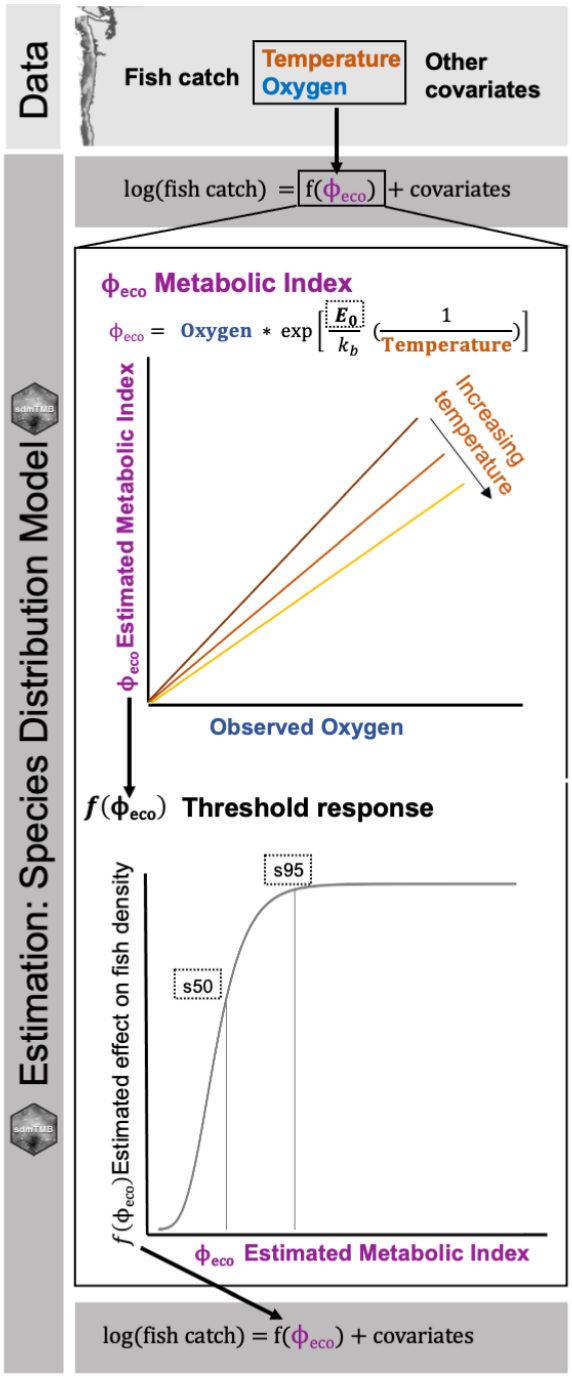

Figure 1. Conceptual diagram showing the data inputs and estimation model. The data required is spatially explicit temperature, oxygen, and fish catch, and any additional environmental covariates (e.g. depth). The model is a commonly used spatial generalized linear mixed model (GLMM), implemented using the R package sdmTMB (Anderson et al. 2024). This model is flexible to allow optional temporal, spatial, and spatio-temporal random variation, as well as environmental covariates. We have added a feature within the standard GLMM estimation procedure that simultaneously estimates 1) a modified form of the metabolic index from temperature and oxygen data, and 2) a sigmoidal threshold function that estimates an asymptotic effect of oxygen on local abundance when oxygen becomes a limiting factor. Dashed line boxes indicate the estimated parameters.

2.4 RESULTS

Our simulation testing revealed limited accuracy of estimated metabolic index parameters and thresholds when they were estimated from species distribution data. The parameter E_0, which defines the temperature-dependency of oxygen tolerance of the metabolic index (Eq. 2), was estimated with relatively low bias, but low precision (Fig 2A). The average estimate of E_0 was only 0.04 less (-13%) than the true value for the typical case (E_0=0.3) and 0.03 higher (+4%) than that of the unusual case (E_0=0.7). However, across the 250 iterations of generated data there was a wide range of estimates, for instance ranging from negative values to almost 1 for the typical case. A similar pattern was seen for the threshold parameter $s50$ (Fig 2B): the average estimate was closely estimated to the true value, but there was wide variability in the estimate across data iterations.

A key reason for this low precision is the high covariance between these two parameters (Fig 3A), caused in part by limited information in the data. Because the model can produce the same overall $f(\Phi_{eco})$ shape by estimating multiple combinations of values E_0 and $s50$, so that precision in any one parameter is low (Fig 3B). Across all simulations, the estimated $f(\Phi_{eco})$ were consequently close to the true function (Fig 3B). There are two reasons underlying this covariance. One, the model internally estimates a covariate Φ_{eco} (via E_0) and the effect of that covariate $f(\Phi_{eco})$ on the local density. Two, the environmental data do not have enough contrast in temperature and pO_2 near the true threshold value (Fig 3C). There was only a narrow band of temperatures (6.5 – 10 C) where observed pO_2 values were above and below the threshold. However, as the overall function $f(\Phi_{eco})$ was well estimated across a range of E_0 estimates (Fig 3B), predictions of fish response to novel climate conditions (e.g. a +1.5 C increase in temperature) were generally similar among simulations with different parameter estimates (Fig 3D). The true model was also consistently identified as the most parsimonious model against the alternative models that were fit to the simulated data by a large margin (ΔAIC=20—300, Appendix Table S2).

We then asked whether, and to what extent, constraining E_0 based on empirical laboratory data on metabolic index traits would improve the accuracy of estimation. We specified the prior as the median value expected for a teleost from the empirical meta-analysis using taxonomic imputation (Essington et al., 2024), as this represents the best estimate for a generic fish with no laboratory data available. For a typical case, where the mean of this prior was close to the true

value of the species, accuracy was improved (Fig 4A). However, in an unusual case, where a fish had a temperature-dependence of oxygen tolerance far from that expected from empirical data, the overall accuracy was largely unchanged because precision improved while bias increased (Fig 4A). For the unusual species, the median of the MLEs was 0.48, higher (+68%) than the prior median (0.331) and lower (-68%) than the true value (0.7) (Fig 4A). In both cases, the distributions of maximum likelihood estimates were distinct from the prior (Fig 4A).

Estimation accuracy was reduced by a hypothetic model mis-specification. When we omitted the quadratic effect of log(depth) from the estimation model, parameter estimates were highly biased in both the typical and unusual cases, leading to a 5 – 7 fold increase in RMSE (Appendix C Fig S6A). For instance, for the typical species, E_0 was underestimated by 1.45 (-300%) (Appendix C Fig S6A), compared to 0.04 (+13%) in the correctly specified model (Fig 2A). While the RMSE of the estimated function $f(\Phi_{eco})$ also increased, the magnitude of change was relatively small with an RMSE of 0.14±0.009 for a typical case and 0.26±0.14 for an unusual case (Appendix C Fig S6C). Despite reduced accuracy, the model that included $f(\Phi_{eco})$ was still most commonly identified as the most-supported model for the simulated data for the typical case and for the majority of simulated datasets for the unusual case.

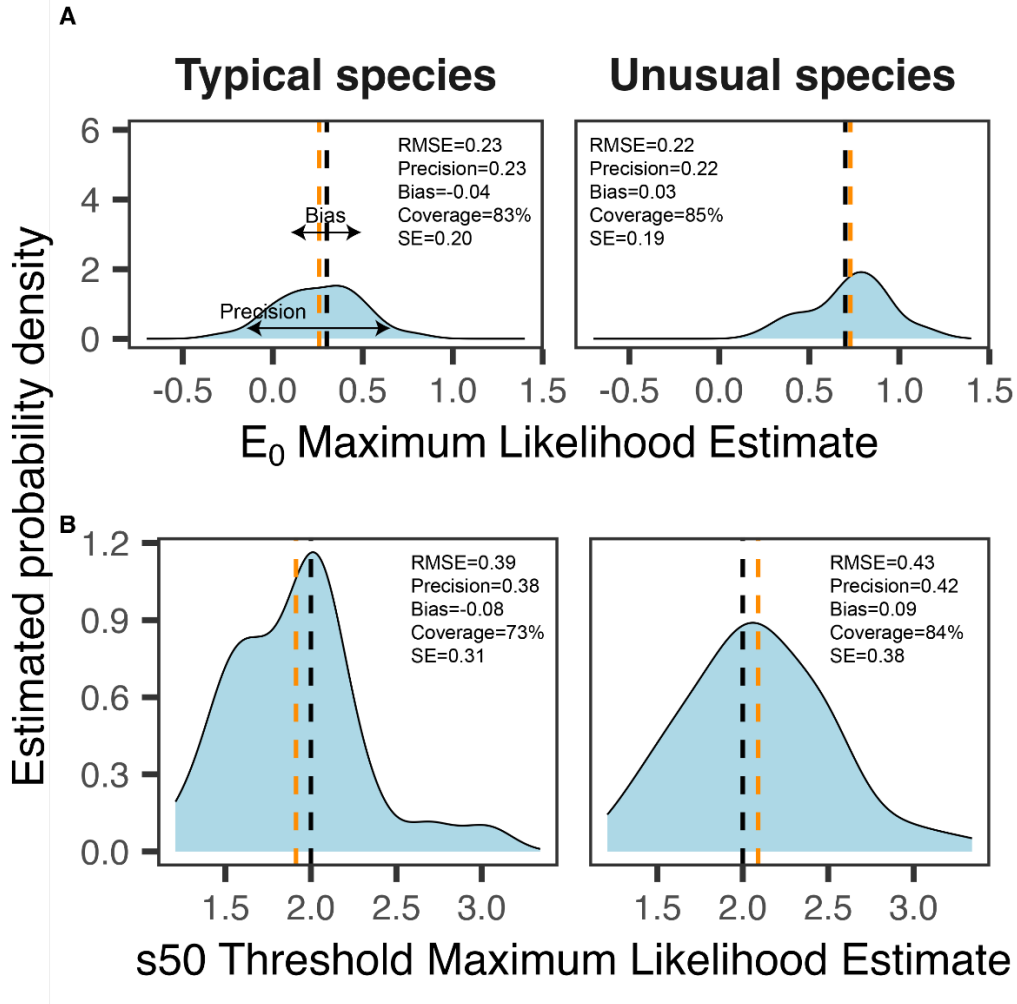

Figure 2. Comparison of maximum likelihood estimates for (A) the temperature-dependence of oxygen sensitivity parameter E_0 from the derived metabolic index and (B) *s50*, a parameter in

the sigmoidal threshold function, for each of the two data generating scenarios (a typical case, left and an unusual case, right) for the unconstrained model (estimated with no prior on E_0) across all 250 data simulation iterations. The typical case represents a simulated species' temperature-dependence of oxygen tolerance that is close to the median value from the empirical meta-analysis for a generic teleost (E_0=0.3), and the unusual case where a simulated species' temperature-dependence of oxygen sensitivity deviates greatly from the expected value (i.e. the median of the meta-analysis) and is roughly equal to the upper 90% of the meta-analysis distribution (E_0=0.7). The blue curves show a fitted kernel density smoother across the maximum likelihood estimates (MLEs) for all 250 simulated data iterations. The black dashed line shows the true parameter value specified to generate the simulated data, and the orange line shows the average maximum likelihood estimate across all iterations of simulated data. The upper left figure shows the interpretation of bias and precision. Bias is calculated as the difference between the average MLE and the true value, and precision is the standard deviation of MLEs across all iterations (proportional to the width of the blue kernel density). RMSE is the Root Mean Squared Error, which gives a single metric of accuracy.

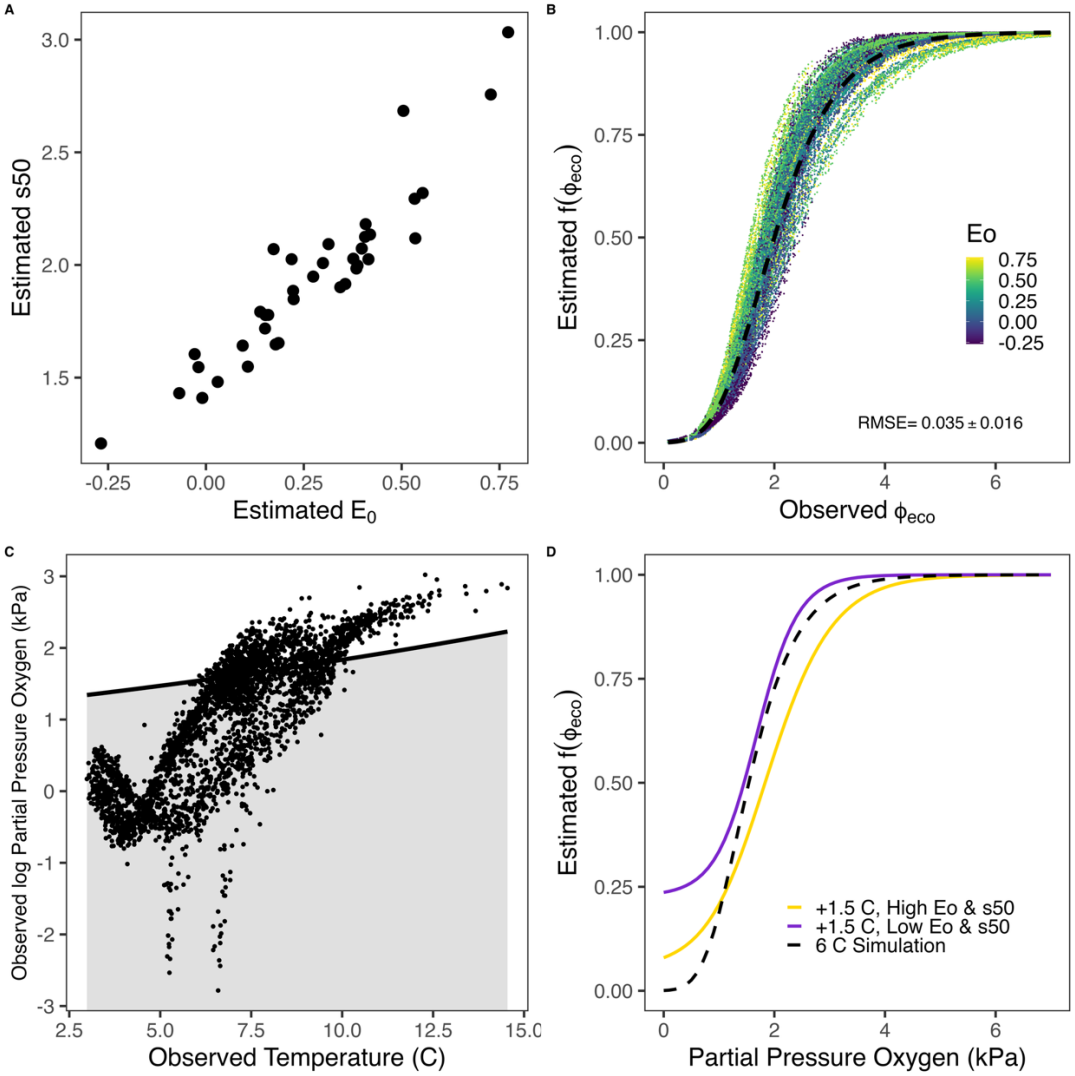

Figure 3. (A) Maximum likelihood estimates of derived metabolic index parameter E_0 and sigmoidal threshold parameter $s50$ for each simulated data set. (B) Estimated synergistic

temperature-oxygen effect $f(\Phi_{eco})$ from each model fit to each of 250 simulated data sets, with color indicating the value of the maximum likelihood estimate of the derived metabolic index Φ_{eco}parameter E_0, and the dashed line the true effect specified in the simulated data. Root mean squared error, shown as the average RMSE±SD of iterations, shows the mean and spread of accuracy across iterations. RMSE for the unusual species was similar, 0.032±0.016. (C) The temperature and pO_2 values from the data (points), and the combinations of temperature and pO_2 where Φ_{eco} equals the $s50$ threshold value (black line). Grey shaded area depicts combinations below this threshold. (D) The estimated synergistic temperature-oxygen effect from two model fits, one high (E_0=0.77, $s50$=3.03, yellow) and one low (E_0=0.03, $s50$=1.48, blue) metabolic index and sigmoidal threshold parameters given a hypothetical 1.5 C increase in bottom temperature (compared to the true response at a base reference temperature of 6 C, dashed line) across a range of plausible observed oxygen values.

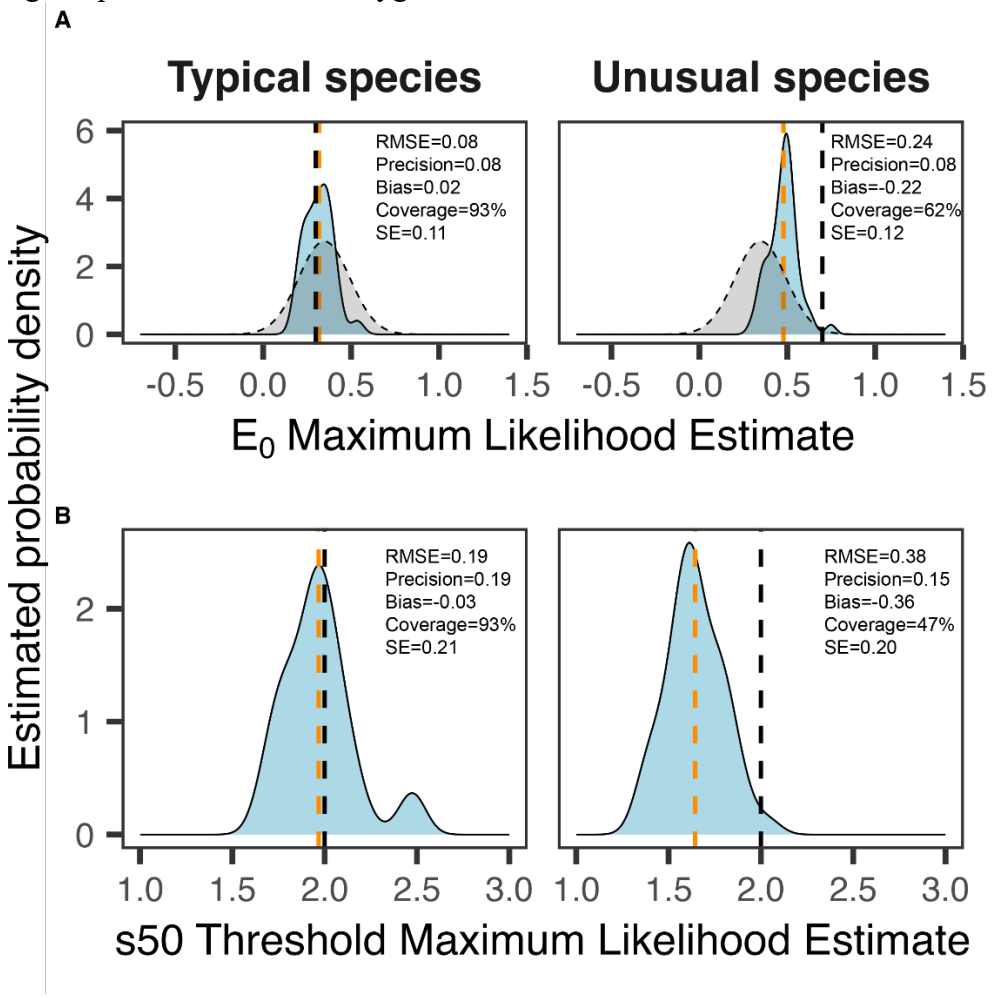

Figure 4. Comparison of maximum likelihood estimate for (A) the temperature-dependence of oxygen sensitivity parameter E_0 from the derived metabolic index and (B)$s50$, a parameter in the sigmoidal threshold function from each of the two data generating scenarios (a typical case, in the left column, and an unusual case, right). The typical case represents a simulated species' temperature-dependence of oxygen tolerance that is close to the median value from the empirical meta-analysis for a generic teleost (E_0=0.3), and the unusual case where a simulated species' temperature-dependence of oxygen sensitivity deviates greatly from the expected value (i.e. the

median of the meta-analysis) and is roughly equal to the upper 90% of the meta-analysis distribution (E_0=0.7). Model estimation included a prior constraint on E_0 via a penalized likelihood. The blue curves show the fitted kernel density smoother across the maximum likelihood estimates (MLEs) for all 250 simulated data iterations (narrower densities translates to more precision). Gray curves show the prior distribution used to constrain E_0 based on the empirical model. The black dashed line shows the true parameter value specified to generate the simulated data, and the orange line is the average maximum likelihood estimate across all iterations of simulated data.

2.4.1 *Estimation of temperature-oxygen synergistic effect in case studies*

When applied to two groundfish species, we found mixed support for our new model compared to alternative models. For sablefish, our new model provided the most parsimonious fit by a large margin over a sigmoidal model of pO_2 alone (ΔAIC=20) (Table 1). However, for longspine thornyhead the new model and the model with sigmoidal(pO_2) as a predictor had roughly equivalent support (ΔAIC of new model=0.77) (Table 1). For both species, the new models provided a substantially better fit than any other alternative model of temperature and/or oxygen and of the null model (i.e., oxygen linearly or as a breakpoint, temperature linearly, or both oxygen and temperature combined as separate linear terms or as an interactive term) (Table 1). Because the simulation testing showed that $s50$ and E_0 could not be estimated precisely, we focus on the estimated $f(\Phi_{eco})$ (Fig 3B). (See Appendix Table S3 for parameter estimates). Only a small percentage of longspine thornyhead observations were below the $f(\Phi_{eco})$ $s50$ or $s95$ threshold and were therefore predicted to be restricted by low oxygen and high temperature (Fig 4B). Yet for sablefish, 3% of hauls were below the $s50$ and 18% below $s95$ (Fig 4A). A primary reason why the new model was strongly supported for sablefish, but not longspine thornyhead, is that there were more sablefish catches where density was constrained by the estimated Φ_{eco}.

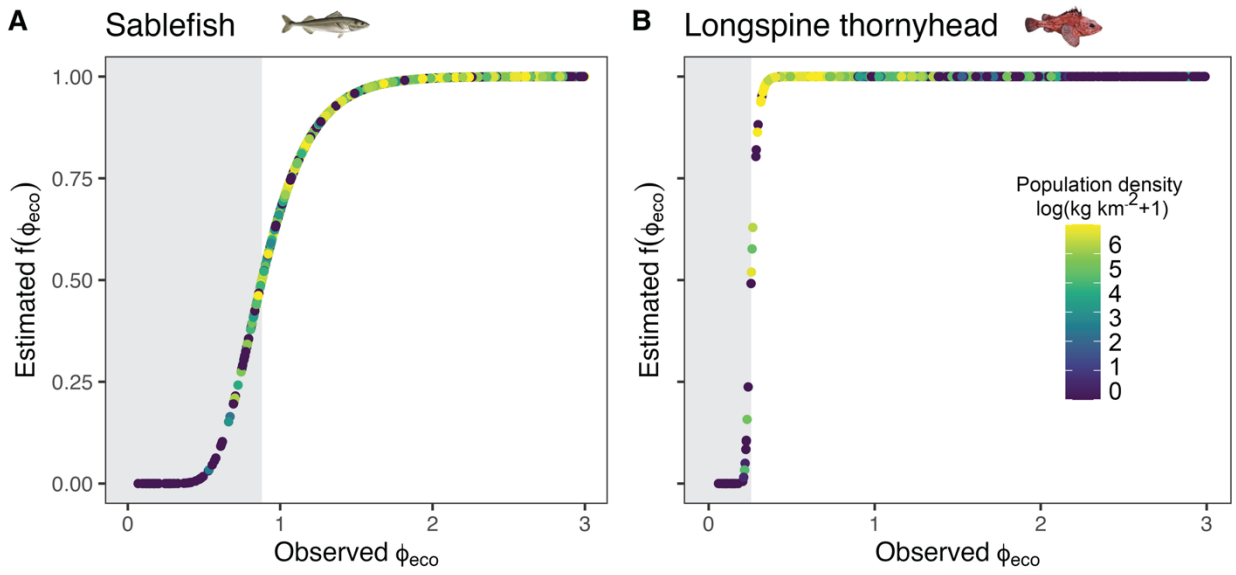

Figure 5. Estimated marginal effect of the synergistic temperature-oxygen term $f(\Phi_{eco})$ on fish density for A) sablefish (*Anoplopoma fimbria*) and B) longspine thornyhead (*Sebastolobus*

altivelis), for each Φ_{eco} calculated as the observed oxygen and temperature and estimated parameter E_0. Color indicates the observed catch per area sampled, and the grey shaded areas indicate the values Φ_{eco} where fish would be restricted by low oxygen and high temperature.

Table 1. Model selection for alternative models fit to sablefish and longspine thornyhead data. $f(\Phi_{eco})$ refers to the new model described in Eq. 2-4, including degrees of freedom (df), log-likelihood, and ΔAIC. Null refers to the base model only, which included independent means by year, a quadratic effect of depth, and a spatial random field.

		Sablefish		Longspine thornyhead	
Model	df	Log-likelihood	ΔAIC	Log-likelihood	ΔAIC
+ $f(\Phi_{eco})$	18	-14477.61	0	-74441.266	0.8
+logistic(pO_2)	17	-14488.85	20.5	-7441.887	0
+breakpoint(pO_2)	16	-14495.00	32.7	-7469.342	52.9
+Temperature * pO_2	17	-14500.74	50.9	-7460.328	46.1
+Temperature + pO_2	16	-14505.06	51.9	-7466.307	44.3
+ temperature	15	-14509.76	56.3	-7505.677	122.2
+ pO_2	15	-14506.56	58.3	-7466.385	123.3
Null	14	-14509.77	44.3	-7506.110	36.0

2.5 DISCUSSION

We developed a statistical model that estimates the temperature-dependence of oxygen tolerance (metabolic index) using the spatiotemporal distribution of a species, rather than laboratory data, by simultaneously estimating the value of the metabolic index and its effect on fish density. Using simulation testing, we evaluated the performance of the new model and then applied it to empirical data from two groundfish species. Our findings reveal both opportunities and challenges for this approach. Generally, historical distributions were estimated accurately, even when models were mis-specified. Additionally, these models were sufficient for forecasting responses to simulated changes in environmental conditions, even though the statistical model could not uniquely estimate two covarying parameters: the temperature-dependence of oxygen sensitivity, and the threshold value of the index at which species densities decline. The addition of priors provided some benefits, but these came with the risk of increasing bias when taxa's oxygen limits had unusual temperature dependence.

Our findings demonstrate the possible benefit of this approach for predicting species' responses to climate change. Our full model provided the most parsimonious fit to simulated data and for empirical Pacific coast sablefish distribution, and was a more parsimonious fit than a null model or models with temperature and oxygen alone for longspine thornyhead. The full model remained the most parsimonious fit in simulation testing even with a mis-specified covariate, though we did not test robustness against all possible mis-specifications. As our approach is a

correlative model, it may still be subject to a common critique of correlative models, namely that an improved fit to historical data does not necessarily translate to better prediction, especially when extrapolating to unobserved environmental conditions (Barnes et al., 2022; Brodie et al., 2022). However we found that our approach could reliably generate a unique effect of a change in oxygen for a given temperature change. A key benefit of our approach is that by rooting in physiology, it constrains extrapolation toward more biologically realistic responses by encompassing novel combinations of changes in two dimensions—oxygen and temperature—into a single value (the metabolic index) that can be interpolated along a known response curve. In our study region, bottom temperatures are projected to increase 0.5—2.5 C by 2100, and oxygen levels to drop by 0-30 mmol/m^3 (Liu et al., 2023), producing a range of new conditions. These effects may be mapped to identify areas or habitats that are facing higher risks associated with climate change (Parouffe et al., 2023).

However, there are still limitations with the approach. We caution that each parameter (E_0 and $s50$) should not be used in isolation for prediction outside of this model structure, since the covariance in estimation means that it did not reliably delineate between the temperature-sensitivity of oxygen (i.e. Φ_{eco}) versus the threshold of temperature-corrected oxygen (i.e. $\mathrm{s50}$). Additionally, it is necessary to consider this model in a suite of alternative configurations of temperature and oxygen, including a null model to ensure that a response to temperature and oxygen is best supported by the data, rather than assuming that they are constraining distribution. The estimated response also needs to be properly interpreted for the body size structure of each dataset and population, as metabolic rate scales with body size (Deutsch et al., 2015; Rubalcaba et al., 2020). For instance, biomass, rather than numerical abundance, data should be used, and the size structure of the fish catch needs to be considered. Here, we restricted fish densities to only biomass of intermediate-sized fish (see Methods), and therefore interpret the metabolic index to be estimated and density predicted for intermediate-sized fishes. Overall properly quantifying and incorporating uncertainty in the metabolic index response (Brodie et al., 2022; Davies et al., 2023) will help reflect the parameter imprecision and range of possible fish distribution outcomes under future conditions.

Some of the estimation challenges we encountered were a result of inherent characteristics of the environmental data. For one, the range of environmental conditions present in the data was limited, providing insufficient contrast around the threshold. If the data had provided more combinations of temperature and pO_2 that produced a Φ_{eco} above and below the threshold (e.g. high temperature and low pO_2, or low temperature and high pO_2), it is possible that the precision of the threshold estimation would have been improved. Truncated environmental data, with a restricted representation of possible conditions—particularly relative to the variation and extremes observed on shorter timescales—is an ongoing challenge in forecasting distributions (Thuiller et al., 2004; Hannemann et al., 2016; Charney et al., 2021). Seeking out datasets, or combining data across a broader geographic range, that can expand the range of training data to capture a wider range of conditions (Bandara et al., 2023) and reduce extrapolation (Davies et al., 2023; Brodie et al., 2022; Waldock et al., 2022) may allow better estimation of responses to temperature and oxygen. This would additionally help identify whether a species (such as longspine thornyhead here) with a poor fit of this model and with density estimated to be constrained only at a very low metabolic index value, is due to the dataset only including environmental conditions within a species' tolerance, versus a species whose distribution is truly

not constrained by temperature and oxygen. This finding supports the need for increased monitoring to better characterize thresholds: advanced ocean observing instrumentation that can collect environmental data with greater spatial and temporal resolution and extent, and additional biological survey efforts that focus on sampling environmental extremes and complement existing stratified random sampling designs.

Second, there was spatial structure in—and covariation between—the environmental variables of interest (temperature and oxygen) and other environmental features, such as bathymetry. We recognize that the species distribution model (a generalized linear mixed model with latent spatial fields) and underlying data (point densities) we used here are only one of many possible frameworks for evaluating and predicting distributions in response to environmental change. Yet other model approaches and distribution data in other environmental systems likely face similar challenges, for instance as seen in: spatial confounding in Bayesian approaches (Mäkinen et al., 2022); spatial bias in presence-only data (Phillips et al., 2009; Baker et al., 2022); spatial dependence and bias in maximum entropy (Kramer-Schadt et al., 2013; Halvorsen et al., 2016); and the impact of spatial autocorrelation in various methods including boosted regression trees, generalized additive models, mixed effects models, maximum entropy, and others (e.g.; Santika & Hutchinson, 2009; Crase et al., 2014; Brodie et al., 2020). Other efforts to apply the metabolic index by parameterizing directly from laboratory data have seen similar limitations when fitting to realized distributions, such as a restricted range of environmental conditions in the data (Bandara et al., 2023) and confounding spatial features (Essington et al., 2022). Estimating these temperature-oxygen relationships directly from the distribution data itself did not fully resolve these issues. Combining distribution data from a wider geographic area, such as across the entire northeastern Pacific range for sablefish, may provide enough contrast in the relationships between environmental variables to overcome challenges of spatial structure and covariance, since correlations between bathymetry, oxygen, and temperature differ between regions.

Our findings highlight a well-recognized difficulty in identifying causal pathways from distribution data (e.g. Thorson et al., 2021a; Addicott et al., 2022). Here, we were able to flag uncertainty in the parameter estimates because our estimation model included latent spatial fields and other covarying environmental features (depth). If we had not included these effects, we may have wrongly identified a temperature-oxygen impact on distribution that was actually due to other factors. It is important to note that there are other possible impacts on density that were not included in the model (such as food availability or predator presence) that may not have been captured by the latent spatial field and may have impacted the estimated response to the metabolic index. Additionally, fish may show no threshold response to oxygen and temperature and not be bound by these environmental constraints. In some cases, there may be an advantage to not use spatial random fields, as they may absorb too much of the variation and dampen the effect of the environmental variable of interest (Hodges & Reich, 2010). This reinforces the need to properly consider model structure to avoid spuriously attributing species distribution to environmental conditions (e.g. Bahn & McGill, 2007; Chapman, 2010; Brodie et al., 2022). By accounting for additional physical and biotic factors beyond temperature and oxygen that may exert more influence on population densities at fine spatiotemporal scales (Whittaker et al., 2001), our approach may improve the explanatory and predictive skill of the metabolic index, which has previously been challenging (e.g. Essington et al., 2022, Bandara et al., 2023). Analyses conducted at broader biogeographic scales to evaluate range limits have attributed

much of the observed patterns to the metabolic index while ignoring additional drivers (e.g. Deutsch et al., 2015, Penn & Deutsch, 2024). Considering multiple dimensions of control on species distribution, not solely the variables of interest, and comparing to more complex models to test robustness (Oster 2016) can ensure proper attribution to the temperature-oxygen response of interest.

Improving methods for combining physiological responses and the information from realized distributions will support forecasting the effects of climate change on marine species (e.g. Meineri et al., 2015; Peterson et al., 2015; Gamliel et al., 2020; Tourinho & Vale, 2023). For the metabolic index, resolving the temperature-sensitivity of oxygen will be a particular challenge. Empirical laboratory data and spatial comparisons show high variation in E_0 across species and regions (Essington et al., 2024, Penn & Deutsch, 2024). Here, distribution data similarly did not provide a reliable estimate of E_0 alone, but could estimate a combined threshold effect. Applying empirical data to inform a prior on the E_0 parameter also did not resolve this challenge, as it can greatly bias estimates if species' realized behavior greatly differs from that theoretically expected. While we adopted the metabolic index for this study, other physiological frameworks of how fish respond to oxygen and temperature (e.g. Ern 2019; Clarke et al. 2021) and other mechanisms, could similarly be tested. Estimating sensitivities to oxygen and temperature from responses beyond distribution, such as growth and size (e.g. van Denderen et al. 2020; Dimarchopoulou & Tsikliras, 2022), may also be informative. Limited availability or applicability of data for parameterization is a common problem for incorporating mechanistic responses into species distribution models (e.g. Gamliel et al., 2020). For identifying mechanistic parameters from distribution data in other cases, our study highlights the need for simulation testing (also see DiRenzo et al., 2023) to validate that the mechanistic parameters can be reliably estimated, given the unique spatial structure, range of environmental conditions, and confounding covariates specific to that dataset and model structure. Additionally, evaluating multiple distribution models specified with alternative parameter values spanning a plausible range informed by empirical data (e.g. similar to the "ecotype" approach in Chen et al., 2024), rather than assuming a single parameterization, could help capture uncertainty in the mechanistic response (Brodie et al., 2022). Other modeling approaches—such as space- or time-varying coefficients (Barnett et al., 2021), a fully Bayesian method (e.g. Talluto et al., 2016; Gamliel et al., 2020; Morera-Pujol et al., 2023), empirical dynamic modeling (e.g. Wang et al., 2020) and structural equation modeling (Liu et al., 2005; Thorson et al., 2021a)—may also provide an improved framework to estimate mechanistic responses and combine insights from empirical laboratory work and realized species distributions.

2.6 Data Availability Statement

Data are available from the Dryad Digital Repository: https://doi.org/10.5061/dryad.47d7wm3pb (Indivero et al. 2024). The data and code are also available at https://github.com/jindivero/estimating_mi_from_distribution2.

2.7 ACKNOWLEDGEMENTS

This publication was partially funded by Washington Sea Grant grant number R/SFA-12, and from the Lowell E. Wakefield Professorship. We thank the West Coast Groundfish Bottom Trawl survey participants. We also thank Jenny Bigman and three anonymous reviewers for their helpful comments.

2.8 REFERENCES

Addicott, E. T., Fenichel, E. P., Bradford, M. A., Pinsky, M. L., & Wood, S. A. (2022). Toward an improved understanding of causation in the ecological sciences. In *Frontiers in Ecology and the Environment* (Vol. 20, Issue 8, pp. 474–480). John Wiley and Sons Inc. https://doi.org/10.1002/fee.2530

Akaike, H. (1974). A new look at the statistical model identification. *IEEE Transactions on Automatic Control*, *19*(6), 716–723. https://doi.org/10.1109/TAC.1974.1100705

Anderson, S. C., Ward, E. J., English, P. A., Barnett, L. A. K., Thorson J.T. (2024). sdmTMB: an R package for fast, flexible, and user-friendly generalized linear mixed effects models with spatial and spatiotemporal random fields. *BioRxiv*, 2022.03.24.485545. https://doi.org/10.1101/2022.03.24.485545

Asch, R. G., Sobolewska, J., & Chan, K. (2022). Assessing the reliability of species distribution models in the face of climate and ecosystem regime shifts: Small pelagic fishes in the California Current System. *Frontiers in Marine Science*, *9*. https://doi.org/10.3389/fmars.2022.711522

Atkinson, D., Leighton, G., & Berenbrink, M. (2022). Controversial Roles of Oxygen in Organismal Responses to Climate Warming. *The Biological Bulletin*, *243*(2), 207–219. https://doi.org/10.1086/722471

Bahn, V., & McGill, B. J. (2007). Can niche-based distribution models outperform spatial interpolation? *Global Ecology and Biogeography*, *16*(6), 733–742. https://doi.org/10.1111/j.1466-8238.2007.00331.x

Baker, D. J., Maclean, I. M. D., Goodall, M., & Gaston, K. J. (2022). Correlations between spatial sampling biases and environmental niches affect species distribution models. *Global Ecology and Biogeography*, *31*(6), 1038–1050. https://doi.org/10.1111/geb.13491

Bandara, R. M. W. J., Curchitser, E., & Pinsky, M. L. (2023). The importance of oxygen for explaining rapid shifts in a marine fish. *Global Change Biology*, *30(1),* e17008. https://doi.org/10.1111/gcb.17008

Barnes, C. L., Essington, T. E., Pirtle, J. L., Rooper, C. N., Laman, E. A., Holsman, K. K., Aydin, K. Y., & Thorson, J. T. (2022). Climate-informed models benefit hindcasting but present challenges when forecasting species–habitat associations. *Ecography*, *2022*(10). https://doi.org/10.1111/ecog.06189

Barnett, L. A. K., Ward, E. J., & Anderson, S. C. (2021). Improving estimates of species distribution change by incorporating local trends. *Ecography*, *44*(3), 427–439. https://doi.org/10.1111/ecog.05176

Baudron, A. R., Brunel, T., Blanchet, M., Hidalgo, M., Chust, G., Brown, E. J., Kleisner, K. M., Millar, C., MacKenzie, B. R., & Nikolioudakis, N. (2020). Changing fish distributions challenge

the effective management of European fisheries. *Ecography*, *43*(4), 494–505. https://doi.org/10.1111/ecog.04864

Beaury, E. M., Fusco, E. J., Jackson, M. R., Laginhas, B. B., Morelli, T. L., Allen, J. M., Pasquarella, V. J., & Bradley, B. A. (2020). Incorporating climate change into invasive species management: insights from managers. *Biological Invasions*, *22*(2), 233–252. https://doi.org/10.1007/s10530-019-02087-6

Bell, R. J., Odell, J., Kirchner, G., & Lomonico, S. (2020). Actions to Promote and Achieve Climate-Ready Fisheries: Summary of Current Practice. *Marine and Coastal Fisheries*, *12*(3), 166–190. https://doi.org/10.1002/mcf2.10112

Briscoe, N. J., Morris, S. D., Mathewson, P. D., Buckley, L. B., Jusup, M., Levy, O., Maclean, I. M. D., Pincebourde, S., Riddell, E. A., Roberts, J. A., Schouten, R., Sears, M. W., & Kearney, M. R. (2023). Mechanistic forecasts of species responses to climate change: The promise of biophysical ecology. *Global Change Biology*, *29*(6), 1451–1470. https://doi.org/10.1111/gcb.16557

Brodie, S. J., Thorson, J. T., Carroll, G., Hazen, E. L., Bograd, S., Haltuch, M. A., Holsman, K. K., Kotwicki, S., Samhouri, J. F., Willis-Norton, E., & Selden, R. L. (2020). Trade-offs in covariate selection for species distribution models: a methodological comparison. *Ecography*, *43*(1), 11–24. https://doi.org/10.1111/ecog.04707

Brodie, S., Smith, J. A., Muhling, B. A., Barnett, L. A. K., Carroll, G., Fiedler, P., Bograd, S. J., Hazen, E. L., Jacox, M. G., Andrews, K. S., Barnes, C. L., Crozier, L. G., Fiechter, J., Fredston, A., Haltuch, M. A., Harvey, C. J., Holmes, E., Karp, M. A., Liu, O. R., … Kaplan, I. C. (2022). Recommendations for quantifying and reducing uncertainty in climate projections of species distributions. *Global Change Biology*, *28*(22), 6586–6601. https://doi.org/10.1111/gcb.16371

Brown, J. H., Gillooly, J. F., Allen, A. P., Savage, V. M., & West, G. B. (2004). Toward a metabolic theory of ecology. *Ecology*, *85*(7), 1771–1789. https://doi.org/10.1890/03-9000

Chapman, D. S. (2010). Weak climatic associations among British plant distributions. *Global Ecology and Biogeography*, *19*(6), 831–841. https://doi.org/10.1111/j.1466-8238.2010.00561.x

Charney, N. D., Record, S., Gerstner, B. E., Merow, C., Zarnetske, P. L., & Enquist, B. J. (2021). A Test of Species Distribution Model Transferability Across Environmental and Geographic Space for 108 Western North American Tree Species. *Frontiers in Ecology and Evolution*, *9*. https://doi.org/10.3389/fevo.2021.689295

Chen, Z., Siedlecki, S., Long, M., Petrik, C. M., Stock, C. A., & Deutsch, C. A. (2024). Skillful multiyear prediction of marine habitat shifts jointly constrained by ocean temperature and dissolved oxygen. *Nature Communications*, *15*(1). https://doi.org/10.1038/s41467-024-45016-5

Cheng, L., Abraham, J., Hausfather, Z., & Trenberth, K. E. (2019). How fast are the oceans warming? *Science*, *363*(6423), 128–129. https://doi.org/10.1126/science.aav7619

Clarke, T. M., Wabnitz, C. C. C., Striegel, S., Frölicher, T. L., Reygondeau, G., & Cheung, W. W. L. (2021). Aerobic growth index (AGI): An index to understand the impacts of ocean warming and deoxygenation on global marine fisheries resources. *Progress in Oceanography*, *195*, 102588. https://doi.org/10.1016/j.pocean.2021.102588

Clarke, T. M., Wabnitz, C. C. C., Frölicher, T. L., Reygondeau, G., Pauly, D., & Cheung, W. W. L. (2022). Linking observed changes in pelagic catches to temperature and oxygen in the Eastern Tropical Pacific. *Fish and Fisheries*, *23*(6), 1371–1382. https://doi.org/10.1111/faf.12694Crase, B., Liedloff, A., Vesk, P. A., Fukuda, Y., & Wintle, B. A. (2014). Incorporating spatial autocorrelation into species distribution models alters forecasts of climate-mediated range shifts. *Global Change Biology*, *20*(8), 2566–2579. https://doi.org/10.1111/gcb.12598

Davies, S. C., Thompson, P. L., Gomez, C., Nephin, J., Knudby, A., Park, A. E., Friesen, S. K., Pollock, L. J., Rubidge, E. M., Anderson, S. C., Iacarella, J. C., Lyons, D. A., MacDonald, A., McMillan, A., Ward, E. J., Holdsworth, A. M., Swart, N., Price, J., & Hunter, K. L. (2023). Addressing uncertainty when projecting marine species' distributions under climate change. *Ecography*, *2023*(11), e06731. https://doi.org/10.1111/ecog.06731

Debastiani, V. J., Bastazini, V. A. G., & Pillar, V. D. (2021). Using phylogenetic information to impute missing functional trait values in ecological databases. *Ecological Informatics*, *63*, 101315. https://doi.org/10.1016/j.ecoinf.2021.101315

Deutsch, C., Ferrel, A., Seibel, B., Pörtner, H.-O., & Huey, R. B. (2015). Climate change tightens a metabolic constraint on marine habitats. *Science*, *348*(6239), 1132–1135. https://doi.org/10.1126/science.aaa1605

Deutsch, C., Penn, J. L., & Seibel, B. (2020). Metabolic trait diversity shapes marine biogeography. *Nature*, *585*(7826), 557–562. https://doi.org/10.1038/s41586-020-2721-y

Diaz, R. J., & Rosenberg, R. (2008). Spreading Dead Zones and Consequences for Marine Ecosystems. *Science*, *321*(5891), 926–929. https://doi.org/10.1126/science.1156401

Dimarchopoulou, D., & Tsikliras, A.C. (2022). Linking growth patterns to sea temperature and oxygen levels across European sardine (*Sardina pilchardus*) populations. *Environmental Biology of Fishes,* 105: 1335–1345. https://doi.org/10.1007/s10641-022-01229-5

DiRenzo, G. V, Hanks, E., & Miller, D. A. W. (2023). A practical guide to understanding and validating complex models using data simulations. *Methods in Ecology and Evolution*, *14*(1), 203–217. https://doi.org/10.1111/2041-210X.14030

Duncan, M. I., James, N. C., Potts, W. M., & Bates, A. E. (2020). Different drivers, common mechanism; the distribution of a reef fish is restricted by local-scale oxygen and temperature constraints on aerobic metabolism. *Conservation Physiology*, *8*(1), coaa090. https://doi.org/10.1093/conphys/coaa090

Ern, R. (2019). A mechanistic oxygen-and temperature-limited metabolic niche framework. *Philosophical Transactions of the Royal Society B*, *374*(1778), 20180540. https://doi.org/10.1098/rstb.2018.0540

Essington, T. E., Anderson, S. C., Barnett, L. A. K., Berger, H. M., Siedlecki, S. A., & Ward, E. J. (2022). Advancing statistical models to reveal the effect of dissolved oxygen on the spatial distribution of marine taxa using thresholds and a physiologically based index. *Ecography*, *2022*(8), e06249. https://doi.org/10.1111/ecog.06249

Essington, T.E., Thorson, J.T., and Deutsch, C. (2024). Remarkable similarity in oxygen tolerance among taxonomically diverse marine taxa revealed through hierarchical analysis. *bioRxiv* 2024.08.23.606857. https://doi.org/10.1101/2024.08.23.606857.

Farrell, A. P., & Richards, J. G. (2009). Chapter 11 Defining Hypoxia: An Integrative Synthesis of the Responses of Fish to Hypoxia. In J. G. Richards, A. P. Farrell, & C. J. Brauner (Eds.), *Fish Physiology* (Vol. 27, pp. 487–503). Academic Press. https://doi.org/10.1016/S1546-5098(08)00011-3

Franco, A. C., Kim, H., Frenzel, H., Deutsch, C., Ianson, D., Sumaila, U. R., & Tortell, P. D. (2022). Impact of warming and deoxygenation on the habitat distribution of Pacific halibut in the Northeast Pacific. *Fisheries Oceanography*, *31*(6), 601–614. https://doi.org/10.1111/fog.12610

Franklin, J. (2010). Mapping Species Distributions: Spatial Inference and Prediction. In *Ecology, Biodiversity and Conservation*. Cambridge University Press. https://doi.org/10.1017/CBO9780511810602

Frölicher, T. L., Fischer, E. M., & Gruber, N. (2018). Marine heatwaves under global warming. *Nature*, *560*(7718), 360–364. https://doi.org/10.1038/s41586-018-0383-9

Gamliel, I., Buba, Y., Guy-Haim, T., Garval, T., Willette, D., Rilov, G., & Belmaker, J. (2020). Incorporating physiology into species distribution models moderates the projected impact of warming on selected Mediterranean marine species. *Ecography*, *43*(7), 1090–1106. https://doi.org/10.1111/ecog.04423

Gillooly, J., Brown, J., West, G., Savage, V., & Charnov, E. (2001). Effects of size and temperature on metabolic rate. *Science* 293: 2248-2251. https://doi.org/10.1126/science.1061967

Halvorsen, R., Mazzoni, S., Dirksen, J. W., Næsset, E., Gobakken, T., & Ohlson, M. (2016). How important are choice of model selection method and spatial autocorrelation of presence data for distribution modelling by MaxEnt? *Ecological Modelling*, *328*, 108–118. https://doi.org/10.1016/j.ecolmodel.2016.02.021

Hannemann, H., Willis, K. J., & Macias-Fauria, M. (2016). The devil is in the detail: unstable response functions in species distribution models challenge bulk ensemble modelling. *Global Ecology and Biogeography*, *25*(1), 26–35. https://doi.org/10.1111/geb.12381

Hirzel, A. H., & Le Lay, G. (2008). Habitat suitability modelling and niche theory. *Journal of Applied Ecology*, *45*(5), 1372–1381. https://doi.org/https://doi.org/10.1111/j.1365-2664.2008.01524.x

Hobbs, R. J., Higgs, E., & Harris, J. A. (2009). Novel ecosystems: implications for conservation and restoration. *Trends in Ecology & Evolution*, *24*(11), 599–605. https://doi.org/10.1016/j.tree.2009.05.012

Hodges, J. S., & Reich, B. J. (2010). Adding Spatially-Correlated Errors Can Mess Up the Fixed Effect You Love. *The American Statistician*, *64*(4), 325–334. https://doi.org/10.1198/tast.2010.10052

Hoffmann, S., Irl, S. D. H., & Beierkuhnlein, C. (2019). Predicted climate shifts within terrestrial protected areas worldwide. *Nature Communications*, *10*(1), 4787. https://doi.org/10.1038/s41467-019-12603-w

Jutfelt, F., Norin, T., Ern, R., Overgaard, J., Wang, T., McKenzie, D. J., Lefevre, S., Nilsson, G. E., Metcalfe, N. B., & Hickey, A. J. R. (2018). Oxygen-and capacity-limited thermal tolerance: blurring ecology and physiology. *Journal of Experimental Biology*, *221*(1), jeb169615. https://doi.org/10.1242/jeb.169615

Kearney, M., & Porter, W. (2009). Mechanistic niche modelling: combining physiological and spatial data to predict species' ranges. *Ecology Letters*, *12*(4), 334–350. https://doi.org/10.1111/j.1461-0248.2008.01277.x

Keller, A. A., Wallace, J. R., & Methot, R. D. (2017). *The northwest fisheries science center's west coast groundfish bottom trawl survey: history, design, and description*. http://doi.org/10.7289/V5/TM-NWFSC-136

Kramer-Schadt, S., Niedballa, J., Pilgrim, J. D., Schröder, B., Lindenborn, J., Reinfelder, V., Stillfried, M., Heckmann, I., Scharf, A. K., Augeri, D. M., Cheyne, S. M., Hearn, A. J., Ross, J., Macdonald, D. W., Mathai, J., Eaton, J., Marshall, A. J., Semiadi, G., Rustam, R., … Wilting, A. (2013). The importance of correcting for sampling bias in MaxEnt species distribution models. *Diversity and Distributions*, *19*(11), 1366–1379. https://doi.org/10.1111/ddi.12096

Kristensen, K., Nielsen, A., Berg, C. W., Skaug, H. and Bell, B. M. 2016. TMB: Automatic differentiation and Laplace approximation. *Journal of Statistical Software* 70: 1–21. https://doi.org/10.18637/jss.v070.i05

Laufkötter, C., Zscheischler, J., & Frölicher, T. L. (2020). High-impact marine heatwaves attributable to human-induced global warming. *Science*, *369*(6511), 1621–1625. https://doi.org/10.1126/science.aba0690

Lefevre, S., McKenzie, D. J., & Nilsson, G. E. (2018). In modelling effects of global warming, invalid assumptions lead to unrealistic projections. *Global Change Biology*, *24*(2), 553–556. https://doi.org/10.1111/gcb.13978

Leiva, F. P., Calosi, P., & Verberk, W. C. E. P. (2019). Scaling of thermal tolerance with body mass and genome size in ectotherms: a comparison between water-and air-breathers. *Philosophical Transactions of the Royal Society B*, *374*(1778), 20190035. https://doi.org/10.1098/rstb.2019.0035

Lenoir, J., Bertrand, R., Comte, L., Bourgeaud, L., Hattab, T., Murienne, J., & Grenouillet, G. (2020). Species better track climate warming in the oceans than on land. *Nature Ecology & Evolution*, *4*(8), 1044–1059. https://doi.org/10.1038/s41559-020-1198-2

Lindgren, F., Rue, H., & Lindström, J. (2011). An explicit link between Gaussian fields and Gaussian Markov random fields: the stochastic partial differential equation approach. *Journal of the Royal Statistical Society: Series B (Statistical Methodology)*, *73*(4), 423–498. https://doi.org/10.1111/j.1467-9868.2011.00777.x

Liu, X., Wall, M. M., & Hodges, J. S. (2005). Generalized spatial structural equation models. *Biostatistics*, *6*(4), 539–557. https://doi.org/10.1093/biostatistics/kxi026

Liu, O. R., Ward, E. J., Anderson, S. C., Andrews, K. S., Barnett, L. A. K., Brodie, S., Carroll, G., Fiechter, J., Haltuch, M. A., Harvey, C. J., Hazen, E. L., Hernvann, P. Y., Jacox, M., Kaplan, I. C., Matson, S., Norman, K., Buil, M. P., Selden, R. L., Shelton, A., & Samhouri, J. F. (2023). Species redistribution creates unequal outcomes for multispecies fisheries under projected climate change. *Science Advanc*es, 9(33). https://doi.org/10.1126/sciadv.adg5468

Mäkinen, J., Numminen, E., Niittynen, P., Luoto, M., & Vanhatalo, J. (2022). Spatial confounding in Bayesian species distribution modeling. *Ecography*, *2022*(11), e06183. https://doi.org/10.1111/ecog.06183

Marshall, K. N., Kaplan, I. C., Hodgson, E. E., Hermann, A., Busch, D. S., McElhany, P., Essington, T. E., Harvey, C. J., & Fulton, E. A. (2017). Risks of ocean acidification in the California Current food web and fisheries: ecosystem model projections. *Global Change Biology*, *23*(4), 1525–1539. https://doi.org/10.1111/gcb.13594

Martínez, B., Arenas, F., Trilla, A., Viejo, R. M., & Carreño, F. (2015). Combining physiological threshold knowledge to species distribution models is key to improving forecasts of the future niche for macroalgae. *Global Change Biology*, *21*(4), 1422–1433. https://doi.org/10.1111/gcb.12655

McClatchie, S., Goericke, R., Auad, G., & Hill, K. (2010). Re-assessment of the stock–recruit and temperature–recruit relationships for Pacific sardine (Sardinops sagax). *Canadian Journal of Fisheries and Aquatic Sciences*, *67*(11), 1782–1790. https://doi.org/10.1139/F10-101

Meineri, E., Deville, A.-S., Grémillet, D., Gauthier-Clerc, M., & Béchet, A. (2015). Combining correlative and mechanistic habitat suitability models to improve ecological compensation. *Biological Reviews*, *90*(1), 314–329. https://doi.org/10.1111/brv.12111

Melo-Merino, S. M., Reyes-Bonilla, H., & Lira-Noriega, A. (2020). Ecological niche models and species distribution models in marine environments: A literature review and spatial analysis of evidence. *Ecological Modelling*, *415*, 108837. https://doi.org/10.1016/j.ecolmodel.2019.108837

Methorst, J., Böhning-Gaese, K., Khaliq, I., & Hof, C. (2017). A framework integrating

physiology, dispersal and land-use to project species ranges under climate change. *Journal of Avian Biology*, *48*(12), 1532–1548. https://doi.org/10.1111/jav.01299

Monzón, J., Moyer-Horner, L., & Palamar, M. B. (2011). Climate Change and Species Range Dynamics in Protected Areas. *BioScience*, *61*(10), 752–761. https://doi.org/10.1525/bio.2011.61.10.5

Moore, C., Drazen, J.C., Radford, B, T.. Kelley, C., Newman, S. (2016). Improving essential fish habitat designation to support sustainable ecosystem-based fisheries management. Marine Policy, 69: 32-41. https://doi.org/10.1016/j.marpol.2016.03.021

Morée, A. L., Clarke, T. M., Cheung, W. W., & Frölicher, T. L. (2023). Impact of deoxygenation and warming on global marine species in the 21st century. *Biogeosciences*: 20(12), 2425-2454. https://doi.org/10.5194/bg-20-2425-2023

Morera-Pujol, V., Mostert, P. S., Murphy, K. J., Burkitt, T., Coad, B., McMahon, B. J., Nieuwenhuis, M., Morelle, K., Ward, A. I., & Ciuti, S. (2023). Bayesian species distribution models integrate presence-only and presence–absence data to predict deer distribution and relative abundance. *Ecography*, *2023*(2), e06451. https://doi.org/10.1111/ecog.06451

Muhling, B. A., Brodie, S., Smith, J. A., Tommasi, D., Gaitan, C. F., Hazen, E. L., Jacox, M. G., Auth, T. D., & Brodeur, R. D. (2020). Predictability of Species Distributions Deteriorates Under Novel Environmental Conditions in the California Current System. *Frontiers in Marine Science*, *7*. https://doi.org /10.3389/fmars.2020.00589

Myers, R. A. (1998). When Do Environment–recruitment Correlations Work? *Reviews in Fish Biology and Fisheries*, *8*(3), 285–305. https://doi.org/10.1023/A:100882873075

Oster, E. (2019). Unobservable Selection and Coefficient Stability: Theory and Evidence. *Journal of Business & Economic Statistics*, *37*(2), 187–204. https://doi.org/10.1080/07350015.2016.1227711

Parouffe, A., Garçon, V., Dewitte, B., Paulmier, A., Montes, I., Parada, C., Mecho, A., & Veliz, D. (2023). Evaluating future climate change exposure of marine habitat in the South East Pacific based on metabolic constraints. *Frontiers in Marine Science*, *9*. https://doi.org/articles/10.3389/fmars.2022.1055875

Penn, J. L., & Deutsch, C. (2022). Avoiding ocean mass extinction from climate warming. *Science*, *376*(6592), 524–526. https://doi.org/10.1126/science.abe9039

Penn, J. L., & Deutsch, C. (2024). Geographical and taxonomic patterns in aerobic traits of marine ectotherms. *Philosophical Transactions of the Royal Society of London. Series B, Biological Sciences*, *379*(1896), 20220487. https://doi.org/10.1098/rstb.2022.0487

Penone, C., Davidson, A. D., Shoemaker, K. T., Di Marco, M., Rondinini, C., Brooks, T. M., Young, B. E., Graham, C. H., & Costa, G. C. (2014). Imputation of missing data in life-history trait datasets: which approach performs the best? *Methods in Ecology and Evolution*, *5*(9), 961–970. https://doi.org/10.1111/2041-210X.12232

Peterson, A. T., Papeş, M., & Soberón, J. (2015). Mechanistic and Correlative Models of Ecological Niches. *European Journal of Ecology*, *1*(2), 28–38. https://doi.org/10.1515/eje-2015-0014

Phillips, S. J., Dudík, M., Elith, J., Graham, C. H., Lehmann, A., Leathwick, J., & Ferrier, S. (2009). Sample selection bias and presence-only distribution models: implications for background and pseudo-absence data. *Ecological Applications*, *19*(1), 181–197. https://doi.org/10.1890/07-2153.1

Polley, L., & Thompson, R. C. A. (2009). Parasite zoonoses and climate change: molecular tools for tracking shifting boundaries. *Trends in Parasitology*, *25*(6), 285–291. https://doi.org/ 10.1016/j.pt.2009.03.007

Pörtner, H. O., & Knust, R. (2007). Climate Change Affects Marine Fishes Through the Oxygen Limitation of Thermal Tolerance. *Science*, *315*(5808), 95–97. https://doi.org/10.1126/science.1135471

Pörtner, H. O. (2010). Oxygen- and capacity-limitation of thermal tolerance: a matrix for integrating climate-related stressor effects in marine ecosystems. *Journal of Experimental Biology*, 213(6): 881-893. https://doi.org/10.1242/jeb.037523

Pörtner, H.-O., Bock, C., & Mark, F. C. (2017). Oxygen- and capacity-limited thermal tolerance: bridging ecology and physiology. *Journal of Experimental Biology*, *220*(15), 2685–2696. https://doi.org/10.1242/jeb.134585

Rohr, J. R., & Cohen, J. M. (2020). Understanding how temperature shifts could impact infectious disease. *PLOS Biology*, *18*(11), e3000938-. https://doi.org/10.1371/journal.pbio.3000938

Rollinson, C. R., Finley, A. O., Alexander, M. R., Banerjee, S., Dixon Hamil, K.-A., Koenig, L. E., Locke, D. H., DeMarche, M. L., Tingley, M. W., Wheeler, K., Youngflesh, C., & Zipkin, E. F. (2021). Working across space and time: nonstationarity in ecological research and application. *Frontiers in Ecology and the Environment*, *19*(1), 66–72. https://doi.org/10.1002/fee.2298

Rosenberg, A., Bigford, T., Leathery, S., Hill, R., and Bickers, K. 2000. Ecosystem approaches to fishery management through essential fish habitat. *Bulletin of Marine Science* 66(3): 535-542.

Rubalcaba, J. G., Verberk, W. C., Hendriks, A. J., Saris, B., & Woods, H. A. (2020). Oxygen limitation may affect the temperature and size dependence of metabolism in aquatic ectotherms. *Proceedings of the National Academy of Sciences*, 117(50), 31963-31968. https://doi.org/10.1073/pnas.2003292117

Santika, T., & Hutchinson, M. F. (2009). The effect of species response form on species distribution model prediction and inference. *Ecological Modelling*, *220*(19), 2365–2379. https://doi.org/10.1016/j.ecolmodel.2009.06.004

Scheuffele, H., Jutfelt, F., & Clark, T. D. (2021). Investigating the gill-oxygen limitation hypothesis in fishes: intraspecific scaling relationships of metabolic rate and gill surface area. *Conservation Physiology*, *9*(1), coab040. https://doi.org/10.1093/conphys/coab040

Seibel, B. A., & Deutsch, C. (2020). Oxygen supply capacity in animals evolves to meet maximum demand at the current oxygen partial pressure regardless of size or temperature. *Journal of Experimental Biology*, *223*(12), jeb210492. https://doi.org/10.1242/jeb.210492

Shono, H. (2008). Application of the Tweedie distribution to zero-catch data in CPUE analysis. *Fisheries Research*, *93*(1), 154–162. https://doi.org/10.1016/j.fishres.2008.03.006

Smith, J. A., Pozo Buil, M., Fiechter, J., Tommasi, D., & Jacox, M. G. (2022). Projected novelty in the climate envelope of the California Current at multiple spatial-temporal scales. *PLOS Climate*, *1*(4), e0000022-. https://doi.org/10.1371/journal.pclm.0000022

Sogard, S. M., & Berkeley, S. A. (2017). Patterns of movement, growth, and survival of adult sablefish (Anoplopoma fimbria) at contrasting depths in slope waters off Oregon. *Fishery Bulletin*, *115*(2), 233–252. https://doi.org/10.7755/FB.115.2.10

Sunday, J. M., Howard, E., Siedlecki, S., Pilcher, D. J., Deutsch, C., MacCready, P., Newton, J., & Klinger, T. (2022). Biological sensitivities to high-resolution climate change projections in the California current marine ecosystem. *Global Change Biology*, *28*(19), 5726–5740. https://doi.org/10.1111/gcb.16317

Swanson, A. K., Dobrowski, S. Z., Finley, A. O., Thorne, J. H., & Schwartz, M. K. (2013). Spatial regression methods capture prediction uncertainty in species distribution model projections

through time. *Global Ecology and Biogeography*, *22*(2), 242–251. https://doi.org/10.1111/j.1466-8238.2012.00794.x

Talluto, M. V, Boulangeat, I., Ameztegui, A., Aubin, I., Berteaux, D., Butler, A., Doyon, F., Drever, C. R., Fortin, M.-J., Franceschini, T., Liénard, J., McKenney, D., Solarik, K. A., Strigul, N., Thuiller, W., & Gravel, D. (2016). Cross-scale integration of knowledge for predicting species ranges: a metamodelling framework. *Global Ecology and Biogeography*, *25*(2), 238–249. https://doi.org/10.1111/geb.12395

Thorson, J. T., Hermann, A. J., Siwicke, K., Zimmermann, M., & Grand, M. (2021a). Grand challenge for habitat science: stage-structured responses, nonlocal drivers, and mechanistic associations among habitat variables affecting fishery productivity. *ICES Journal of Marine Science*, *78*(6), 1956–1968. https://doi.org/10.1093/icesjms/fsa

Thorson, J., Salguero-Gómez, R., Jones, O. R., Childs, D. Z., & Beckerman, A. P. (2021b). Bridging gaps in demographic analysis with phylogenetic imputation. *Conservation Biology*, *35*(4), 1210–1221. https://doi.org/10.1111/cobi.13658

Thuiller, W., Brotons, L., Araújo, M. B., & Lavorel, S. (2004). Effects of restricting environmental range of data to project current and future species distributions. *Ecography*, *27*(2), 165–172. https://doi.org/10.1111/j.0906-7590.2004.03673.x

Tourinho, L., & Vale, M. M. (2023). Choosing among correlative, mechanistic, and hybrid models of species' niche and distribution. *Integrative Zoology*, *18*(1), 93–109. https://doi.org/10.1111/1749-4877.12618

Tweedie, M.C.K. 1984. An index which distinguishes between some important exponential families. In Statistics: Applications and New Directions. *Proceedings of the Indian Statistical Institute Golden Jubilee International Conference*. Edited by J.K. Gosh and J. Roy. Indian Statistical Institute, Calcutta. pp. 579–604.

Urban, M. C. (2019). Projecting biological impacts from climate change like a climate scientist. *WIREs Climate Change*, *10*(4), e585. https://doi.org/10.1002/wcc.585

Urban, M. C., Bocedi, G., Hendry, A. P., Mihoub, J.-B., Pe'er, G., Singer, A., Bridle, J. R., Crozier, L. G., De Meester, L., Godsoe, W., Gonzalez, A., Hellmann, J. J., Holt, R. D., Huth, A., Johst, K., Krug, C. B., Leadley, P. W., Palmer, S. C. F., Pantel, J. H., … Travis, J. M. J. (2016). Improving the forecast for biodiversity under climate change. *Science*, *353*(6304), aad8466. https://doi.org/10.1126/science.aad8466

Veloz, S. D., Williams, J. W., Blois, J. L., He, F., Otto-Bliesner, B., & Liu, Z. (2012). No-analog climates and shifting realized niches during the late quaternary: implications for 21st-century predictions by species distribution models. *Global Change Biology*, *18*(5), 1698–1713. https://doi.org/10.1111/j.1365-2486.2011.02635.x

Verberk, W. C. E. P., Atkinson, D., Hoefnagel, K. N., Hirst, A. G., Horne, C. R., & Siepel, H. (2021). Shrinking body sizes in response to warming: explanations for the temperature–size rule with special emphasis on the role of oxygen. *Biological Reviews*, *96*(1), 247–268. https://doi.org/10.1111/brv.12653

Verberk, W. C., Durance, I., Vaughan, I. P., & Ormerod, S. J. (2016a). Field and laboratory studies reveal interacting effects of stream oxygenation and warming on aquatic ectotherms. *Global Change Biology*, *22*(5), 1769–1778. https://doi.org/10.1111/gcb.13240

Verberk, W.C., Overgaard, J., Ern, R., Bayley, M., Wang, T., Boardman, L., & Terblanche, J. (2016b). Does oxygen limit thermal tolerance in arthropods? A critical review of evidence. *Comparative Biochemistry and Physiology* (192): 64-78. https://doi.org/10.1016/j.cbpa.2015.10.020

Waldock, C., Stuart-Smith, R. D., Albouy, C., Cheung, W. W. L., Edgar, G. J., Mouillot, D., Tjiputra, J., & Pellissier, L. (2022a). A quantitative review of abundance-based species distribution models. *Ecography*, *2022*(1). https://doi.org/10.1111/ecog.05694

Wang, J.-Y., Kuo, T.-C., & Hsieh, C. (2020). Causal effects of population dynamics and environmental changes on spatial variability of marine fishes. *Nature Communications*, *11*(1), 2635. https://doi.org/10.1038/s41467-020-16456-6

Warton, D. I., & Shepherd, L. C. (2010). Poisson point process models solve the" pseudo-absence problem" for presence-only data in ecology. *The Annals of Applied Statistics*, 1383–1402. https://doi.org/ 10.1214/10-AOAS331

Williams, J. W., & Jackson, S. T. (2007). Novel climates, no-analog communities, and ecological surprises. *Frontiers in Ecology and the Environment*, *5*(9), 475–482. https://doi.org/10.1890/070037

Whittaker, R. J., Willis, K. J., & Field, R. (2001). Scale and species richness: towards a general, hierarchical theory of species diversity. *Journal of Biogeography*, *28*(4), 453–470. https://doi.org/10.1046/j.1365-2699.2001.00563.x

Chapter 3. SKILL TESTING OXYGEN DATA FOR DISTRIBUTION MODELING OF MARINE SPECIES

Publication history: This study was co-authored with Sean Anderson, Lewis Barnett, John Pohl, Sean Rohan, Sam Siedlecki, Eric Ward and Timothy Essington. At the time this dissertation was submitted, a version of this chapter was accepted at *Fisheries Oceanography* (https://doi.org/10.1111/fog.70005).

3.1 ABSTRACT

Spatial models that identify statistical relationships between environmental conditions and species distributional data are commonly used in fisheries research to evaluate habitat suitability and predict distributional shifts, such as those driven by changing ocean temperature and oxygen. However, a lack of environmental data—particularly dissolved oxygen—at the same temporal and spatial resolution as biological data can limit these analyses. We evaluate the ability to predict bottom dissolved oxygen via imputation and extrapolation and with biophysical oceanographic models in the northeastern Pacific Ocean (Aleutian Islands, Eastern Bering Sea, Gulf of Alaska, British Columbia, and California Current). Specifically, we measure predictive skill compared to *in situ* observations (measured concurrently with bottom trawl data) for 1) predictions from an empirical statistical model fit to integrated dissolved oxygen observations; and 2) a commonly used dynamical oceanographic model estimate of oxygen, the Global Oceanographic Biogeochemistry Hindcast (GOBH). Lastly, we evaluate how estimation and interpretation of a species distribution model is impacted by use of different oxygen data sources. Using leave-one-year-out cross-validation, we find that the empirical statistical model predicts bottom dissolved oxygen for fish catch sampling events with relatively high accuracy in only certain regions (California Current and British Columbia) (root mean squared error [RMSE] ~16-30 μmol kg^{-1}). Prediction skill was more than 2x lower in Alaska regions that did not have extensive data (~<0.075 observations km^{-2}), and this approach would likely not provide sufficiently accurate oxygen values for SDMs in these regions. An oceanographic model (the Copernicus Global Oceanographic Biogeochemistry Hindcast) had substantially lower prediction skill than the integrated statistical predictions (RMSE ~30-90 μmol kg^{-1}). When applied to species distribution models, the estimated dissolved oxygen thresholds differed by 20-50 μmol kg^{-1} when fit to different dissolved oxygen data sources. We focus on oxygen in the northeastern Pacific, yet our approach is generalizable to other variables and systems. We recommend increased attention to validating oceanographic models when operationalized to fisheries applications, and evaluating the robustness of conclusions to environmental covariate data sources.

3.2 INTRODUCTION

To evaluate environmental drivers of ecological systems, researchers often use retrospective spatial models that identify statistical relationships between historical environmental conditions and biological data. In marine systems, seabed features (such as depth and substrate) and ocean

conditions (such as pH, temperature, and oxygen) are often included as covariates to assess their influence on habitat use and population dynamics, supporting sustainable fisheries management. For instance, spatial statistical models are used for designating essential habitat (Dambrine et al., 2021; Moore et al., 2016), identifying environmental impacts on individual traits (e.g., Lindmark et al., 2023; Oke et al., 2022), and for projecting population abundance and distribution under climate change (e.g. Grüss et al., 2021; Liu et al., 2023; Thompson, et al., 2023a). These models rely on temporal and spatial variation in observations across time and space to provide informative contrasts and estimate the responses of species to environmental conditions. Including data with a greater range of environmental conditions—such as including longer time series and greater spatial coverage—improves estimation of environmental sensitivities and projections of the impacts of climate change by increasing contrasts in the data and reducing extrapolation beyond the range of observations (Brodie et al., 2022; Davies et al., 2023; Indivero et al., 2024).

There has been particular focus on how declining ocean oxygen may impact fish distribution (Deutsch et al., 2023; Pörtner & Knust, 2007; Pörtner, 2010; Pörtner et al., 2017; Rubalcaba et al., 2020; Verberk et al., 2016). Dissolved oxygen in the ocean has decreased globally by approximately 2% since the pre-industrial period due to increased temperatures and various associated biological and physical changes (Schmidtko et al., 2017), expanding oxygen minima and hypoxic dead zones (Diaz & Rosenberg, 2008; Stramma et al., 2010). Globally, dissolved oxygen is projected to continue to decline over the next century by around 1-7% (Keeling et al., 2010; Kwiatkowski et al., 2020; Matear & Hirst, 2003). Organisms' sensitivity to dissolved oxygen depends on temperature (Deutsch et al., 2015; Pörtner & Knust 2007; Vaquer-Sunyer & Duarte, 2011), and empirical biogeographic studies have demonstrated that these interacting constraints can explain marine species distributions (Deutsch et al., 2015, 2020; Morée et al., 2023). In addition to lethal effects of low dissolved oxygen, such as those associated with large-scale mortality events in the Gulf of Mexico (Altieri et al., 2017; Joyce, 2000), moderate declines in oxygen can also impact fish behavior and influence habitable area (Deutsch et al., 2015; Gray et al., 2002; Kim et al., 2023; Kramer, 1987; Vaquer-Sunyer & Duarte, 2008). Fish response to low oxygen is expected to be non-linear (Fry, 1971; Farrell and Richards 2009). Behavioral and physiological plasticity (Kramer, 1987) can allow an organism to tolerate low oxygen up to a certain threshold, below which there are sublethal impacts on growth and other core metabolic functions (Fry, 1971; Pörtner and Knust, 2007; Farrell and Richards, 2009). Eventually oxygen becomes too low to support routine metabolism and fish must shift to habitat with sufficient oxygen to survive (Kramer, 1987). Quantifying these thresholds is therefore necessary for predicting how declining ocean oxygen will impact habitat availability and distributional shifts.
Scientists have long conducted laboratory experiments to measure thresholds of oxygen tolerance (e.g. Ultsch et al., 1978, Beamish 1964; and see Rogers et al., 2016 for meta-analysis of 96 published studies). Yet there can be high variability in such thresholds between species and taxa, and data are only available for a handful of species (Vaquer-Sunyer & Duarte, 2008; Rogers et al., 2016). Additionally, thresholds of oxygen tolerance from laboratory-derived physiological measures have sometimes failed to show improvement in predicting fish distribution at a fine spatial scale (Bandara et al., 2023; Essington et al., 2022).

Due to these limitations of laboratory studies, there is a need for statistical spatiotemporal models that can estimate dissolved oxygen effects from field observations of species density (Bandara et al., 2023; Essington et al., 2022; Franco et al., 2022; Liu et al., 2023; Thompson et al., 2023a;

Thompson et al., 2023b). However, these analyses are often hampered by limited availability of dissolved oxygen data at the same temporal and spatial resolution as the standardized catch data that are used to monitor fish distribution and abundance.

Fishery-independent surveys sometimes concurrently collect *in situ* dissolved oxygen data, though this is often limited to only a subset of years or locations (Figure 1A), often due to logistical and financial constraints. For instance, while the U.S. West Coast Bottom Trawl Survey has consistently collected annual data since 2003, concurrent oxygen data are publicly available only for a subset of years (2009-2015, 2022-2023). And while stationary profilers and buoys are useful for monitoring environmental conditions, coverage on the continental slopes and shelf habitat is often insufficient to characterize oxygen at a scale that matches catch data (e.g. in the GOBAI model, Sharp et al., 2022; Breitburg et al., 2018). Similarly, regional and global oceanographic circulation models are generally only available in a coarser spatial and temporal resolution than biological data. For instance, bottom trawl survey observations are located at multiple specific points within the ¼° grid of the Global Ocean Biogeochemistry Hindcast (GOBH, Mercator-Ocean, 2023) (Figure 1B). Bottom trawl observations are also collected at specific points of time within a day, while oceanographic outputs like GOBH are typically only available at broader daily or 3-day averages. (Figure 1B). This mismatch in resolution means that oceanographic models may not capture the oxygen dynamics at the particular time and location of a biological observation. Oceanographic models also have faced challenges reproducing historical ocean oxygen conditions (e.g. Oschlies et al., 2018). The predicted decline in dissolved oxygen over the next century is not uniform between or within ocean basins, and is caused by different processes in different areas and depths: reduced oxygen solubility in warmer waters (Diaz & Breitburg, 2009; Keeling et al., 2010), increased stratification causing reduced subsurface ventilation (Keeling et al., 2010; Schmidtko et al., 2017), increased eutrophication and aerobic decomposition (Diaz & Breitburg, 2009), changes in wind and upwelling patterns (Sydeman et al., 2014), and long-term natural variability (Broecker et al., 1999). Including oxygen as a covariate in species distribution modeling is overall challenging due to the limited data availability and complexity of dissolved oxygen dynamics.

There is a trade-off between spatial and temporal coverage and spatiotemporal resolution in the different approaches taken to address this lack of dissolved oxygen data. Some modelers have opted to limit analyses to subsets of biological data with concurrent dissolved oxygen data available (e.g. Essington et al., 2022; Franco et al., 2022). This provides a close observation to the time and location of the actual bottom conditions at each sampling event, capturing fine-scale spatial and temporal variation. However, it removes a large quantity of biological data from analysis, and consequently possibly removes important inter- and intra-annual environmental contrasts, especially when entire years lack environmental data. For instance, 2021 was a particularly strong hypoxic event in the U.S. Pacific Northwest coast (Barth et al., 2024). If this year of sampling data is removed from model fitting because it lacks concurrent oxygen data, unique information on fish response in extreme low oxygen conditions may be lost. Other studies instead use output from regional or global oceanographic models in place of any concurrent data, and extract the oceanographic output to sample locations via various methods, such as nearest neighbor matching or bilinear interpolation (e.g. Bandara et al., 2023; Liu et al., 2023). Such oceanographic models can cover a wider geographic area over a longer period of time, thereby providing a more complete time series to facilitate spatial coverage (Perruche et al., 2024).

However, oceanographic models may not resolve the fine-scale spatial and temporal variation in fluctuations (e.g. Verezemskaya et al., 2021, Arevalo-Martínez et al., 2015; Breitburg et al., 2018; McCarthy et al., 2015) to which fish can respond to oxygen conditions (Kim et al., 2023; Kramer, 1987). Typically oceanographic model outputs have been validated only at coarser spatial and temporal scales than biological sampling (such as climatological means and seasonal patterns, e.g. Kristiansen et al., 2024; Perruche et al., 2024), yet there have been increasing efforts to validate for the fine-scale dynamics relevant to ecological modeling, such as for temperature (Kearney, 2021; Kearney & Porter, 2009) and zooplankton (Sullaway et al., 2024). Overall, neither using *in situ* observations or oceanographic models fully uses the information available to identify links between species response and environmental conditions.

Here, we aim to improve the use of environmental covariates in spatial modeling of marine species in three main ways. First, we test an empirical statistical model to expand the fine-resolution bottom oxygen data available for spatiotemporal modeling of biological data, building off Thompson et al. (2023a). This method combines multiple sources of *in situ* bottom dissolved oxygen observations from concurrent surveys and various independent CTD casts, fits spatiotemporal statistical models to the data, and predicts oxygen levels at biological sampling events. When there are gaps in oxygen observations of biological data, this can provide a way to estimate oxygen at a fine spatial and temporal scale by interpolating to unsampled dates and locations in a robust statistical framework. We conduct skill testing of the empirical model to predict the *in situ* data. Second, we compare a commonly used oceanographic model of oxygen to *in situ* data collected by bottom trawl surveys. Third, we evaluate how use of the different oxygen data sources (concurrent only, empirical statistical predictions, and dynamical oceanographic model output) in species distribution models impacts estimation of a threshold effect of oxygen with case studies of two species (sablefish *Anoplopoma fimbria* and Dover sole *Microstomus pacificus*) in two regions (California Current and British Columbia). Overall, we provide guidance to species distribution modelers on trade-offs among different sources of dissolved oxygen data by comparing these three approaches.

In the context of improving oxygen data availability and guidance for using in marine species spatial modeling, we evaluate:

1. To what extent can *in situ* bottom dissolved oxygen observations accurately predict values at unsampled biological sampling events (i.e. those without concurrent measurements)?
2. How does accounting for different spatial and temporal variation structures in fitting models to the *in situ* oxygen data impact predictive skill?
3. How does this approach compare to bottom dissolved oxygen values from a dynamical oceanographic model output?
4. How does the choice of oxygen data source in species distribution modeling impact estimation and interpretation of effects of oxygen on species population density?

3.3 METHODS

We compared estimation of fish species distribution models when fit to three different sources of dissolved oxygen data: *in situ* concurrent observations, a dynamical oceanographic output, and predictions from an empirical statistical model. We used the northeastern Pacific Coast as a study system (from the Aleutian Islands and eastern Bering Sea through Gulf of Alaska, British Columbia, and California Current) (Figure 2). First, we validate the empirical statistical predictions compared to the concurrent *in situ* data to test an approach to expand the fine-scale bottom oxygen data available when fitting spatiotemporal models to fish catch data with environmental covariates. We then compare an oceanographic output to the *in situ* concurrent dissolved oxygen data. Lastly, we fit species distribution models from these three different oxygen data sources to case studies of two species in two regions.

Concurrent observations

Dissolved oxygen measurements collected at the time of bottom trawl sampling (i.e. concurrent) were obtained for the U.S. National Oceanic and Atmospheric Administration (NOAA) bottom trawl surveys in the Gulf of Alaska (Siple et al., 2023), eastern and northern Bering Sea continental shelf (Markowitz et al., 2024), eastern Bering Sea continental slope (Hoff, 2016), Aleutian Islands (Siple et al., 2025), and U.S. West Coast (Keller et al., 2017), and the Department of Fisheries and Oceans Canada (DFO) British Columbia Groundfish Concurrent Bottom Trawl Surveys in Queen Charlotte Sound, Hecate Strait, West Coast Vancouver Island, West Coast Haida Gwaii, and the Strait of Georgia (Anderson et al., 2019; DFO, 2024) (see Table 2). Measurements were similarly collected across all bottom trawl surveys, with dissolved oxygen sensors attached to the headline of trawls.

Predictions from empirical statistical model

We tested an empirical statistical approach to expand the fine-scale bottom oxygen data available when fitting spatiotemporal models to fish catch data with environmental covariates. This method is an extension of interpolation procedures to fill in missing data (see Li & Heap 2014, Nakagawa 2015, Little & Rubin 2020 for comprehensive reviews), expanding to integrate other data sources and rigorously skill test alternative model structures. In addition to the concurrent observations, we combined bottom dissolved oxygen observations from other scientific (i.e. fishery-independent) marine biological surveys (International Pacific Halibut Commission longline surveys, Joint U.S.-Canada Pacific Hake Acoustic Trawl Survey) and independent oxygen measurements from ocean monitoring programs (see Table 2 and Figure 1 for data included). Data were quality-controlled and standardized (see Appendix A and Appendix A Fig S1 for details). In total, 26,617 bottom dissolved oxygen observations were included in model fitting. For each region, we fit generalized linear mixed effects models (GLMMs) to the combined oxygen dataset that considered spatial and temporal structure in different configurations using the package sdmTMB (Anderson et al., 2025). Fitted models were then used to predict bottom dissolved oxygen to sampling events from fish catch surveys. To evaluate how including different spatial and temporal structures in the model might improve prediction skill, we compared models with increasing levels of complexity (Table 2). We describe these models below.

The simplest model was a GLMM that estimated bottom dissolved oxygen O of observation i in region r following a Gaussian distribution based on depth D in meters and day of year C

$$O_{i,r} = s(\log(\mathrm{D}_i)) + s(\mathrm{C}_i), \quad \text{Eq. 1}$$

where O_i is the oxygen measurement for sample i in μmol kg^{-1}, and $s(log(D))_i$ and $s(\mathrm{C})_i$ are smooth on log(D) and day-of-year (i.e. 1–365) (see Appendix A for additional model details). Specifically, we used penalized regression splines ("P-splines") for both smooths (Eilers & Marx, 2021). Depth and day-of-year were included to account for seasonal and depth-dependent variation in ocean dissolved oxygen. We then add a stationary spatial random effect ω_i to Eq. 1 that accounts for spatially structured Gaussian Markov random field (GMRF) latent variables that approximate a Gaussian random field with a Matérn correlation function (Eq. 4-6 in Table 1). We iteratively tested mesh size, and used a minimum allowed triangle edge length of 45 km to optimize number of knots in each region (~100-200) (see Appendix A for more details). The spatial field represents variation not explained by fixed effects, which includes both process variation (spatial patterning in oxygen levels shared across years) as well as sampling effects (slight differences in measurements from different surveys). We include temporal variability in two ways. One, we include a fixed effect of year t (as a factor) b_t to represent interannual variation in mean oxygen levels (Eq. 7-9). Second, we consider variation across space that evolves over time with a latent first-order autoregressive GMRF spatiotemporal processes ε_i (Eq. 10-12), which allows each year to have unique spatial patterning of oxygen levels.

For each of the four spatial and temporal structures described above (null, spatial only, annual+spatial, and spatial+spatiotemporal), we test three configurations of covariates—none, temperature only, and temperature and salinity—to determine the predictive ability of potential covariates that could be associated with oxygen concentration. Salinity (PSS-78, practical salinity units) was converted to potential density anomaly with a reference pressure of 0 dbar in kg m^{-3} (see Appendix A for more details). These covariates were considered because temperature and salinity are measured in trawl surveys more frequently than dissolved oxygen, and are likely to covary with dissolved oxygen due to shared physical drivers (e.g. upwelling, freshwater inputs). We also considered more complex model structures (e.g. spatially varying coefficients, interactions, bivariate splines, survey effects, and oxygen solubility) but found no improvement to predictive skill, so for brevity we do not include them here.

Table 1. Alternative models for fitting the empirical statistical model to combined dissolved oxygen data O_i, where i is used to index the observation. Four structures for accounting for latent spatial and temporal effects were considered (none, persistent spatial fields ω_i, annual effects in addition to persistent spatial fields $b_{t[i]}$, and persistent spatial fields in addition to latent spatiotemporal variation ε_i) for three covariate structures (no covariates, temperature only $s(T_i)$, and temperature and salinity $s(S_i)$ (potential density anomaly referenced to 0 dbar, kg m^{-3}). Components included in each model are marked with an X. Smoother functions were used on temperature and salinity. All models included smoothers on day-of-year $s(\mathrm{C}_i)$and depth $s(\log(D_i))$.

Equation Numbers	Spatial and Temporal Structure			Covariates		Equation
	Spatial	Annual	Spatiotemporal	Temp	Sal	

1						$O_i = s(\mathrm{C}_i) + s(log(\mathrm{D}_i))$
2				X		$+ s(T_i)$
3				X	X	$+s(T_i) + s(S_i)$
4	X					$+\omega_i$
5	X			X		$+\omega_i + s(T_i)$
6	X			X	X	$+\omega_i + s(T_i) + s(S_i)$
7	X	X				$+\omega_i + b_{year[i]}t_i$
8	X	X		X		$+\omega_i + b_{year[i]}t_i + s(T_i)$
9	X	X		X	X	$+\omega_i + b_{year[i]}t_i + s(T_i) + s(S_i)$
10	X		X			$+\omega_i + \varepsilon_i$
11	X		X	X		$+\omega_i + \varepsilon_i + s(T_i)$
12	X		X	X	X	$+\omega_i + \varepsilon_i + s(T_i) + s(S_i)$

To evaluate prediction skill of all models, we used a cross-validation procedure that iteratively removed one year of bottom trawl oxygen observations from the integrated oxygen dataset (i.e. "test year"), trained the model on the remaining years of data (which included data from non-concurrent sources in the test year, i.e. "training years"), used the fitted model to predict to concurrent sampling events from the test year, and compared the model predictions of dissolved oxygen to the observed concurrent oxygen in the test year. We are assessing whether we can accurately predict oxygen for an entire missing sample year, given concurrent data (i.e. the measurements collected with fish sampling) from the same survey available in other years and non-concurrent data from other sources in that missing year. Only years with more than 50 concurrent observations and independent data within that year were included as test years. For the California Current, this allowed nine test years (2009-2015, 2022-2023), six years for British Columbia (2017-2019, 2021-2023), but only two years for the Gulf of Alaska (2013, 2015), Eastern Bering Sea (2012, 2016), and Aleutian Islands (2014, 2016). The number of observations in each test year for each region ranged from 50—1314, and in training data from 680—10,592 (see Table S1df). We calculated root mean squared error (RMSE) of model predictions to observations in each excluded test year as a metric of predictive skill.

Table 2. Bottom dissolved oxygen data included in model fitting. "Concurrent" refers to oxygen observations measured *in situ* in the same survey protocol as bottom trawl sampling (either trawl-mounted or concurrent CTD cast). "Independent" refers to oxygen observations measured as part of surveys or research separate from bottom trawl surveys.

Name	Type	Region	Years	Number of observations	Source
West Coast Bottom Trawl	Concurrent	California Current	2009-2015, 2022-2023	5233	Keller et al., 2017
Alaska Bottom Trawl Survey	Concurrent	Gulf of Alaska	2013, 2015, 2023-2024	1316	Rohan et al., 2024; Siple et al., 2023
Alaska Bottom Trawl Survey	Concurrent	Aleutian Islands	2014, 2016, 2024	551	Rohan et al., 2024; Siple et al., 2025

Alaska Bottom Trawl Survey	Concurrent	Eastern Bering Sea	2012, 2016, 2023-2024	300	Rohan et al., 2024; Markowitz et al., 2023
DFO West Coast	Concurrent	British Columbia	2017-2023	1802	Anderson et al., 2019; DFO Canada, 2024
International Pacific Halibut Commission Long-Line Survey	Independent	California Current, British Columbia, Eastern Bering Sea (2 years), Gulf of Alaska, Aleutian Islands	2009-2022; Bering Sea 2006, 2015	7598	IPHC, 2022, 2024
Pacific Hake Acoustic Trawl Survey	Independent	California Current	2011-2013, 2015	368	NOAA, 2020
Newport Line	Independent	California Current	1998-2021	2425	Risien et al., 2022, 2023
CalCOFI	Independent	California Current	1949-2021	1176	CalCOFI, 2024
Line P	Independent	British Columbia, California Current	1990-2019	3	Franco et al., 2021
WCOA (NOAA West Coast Ocean Acidification) and Harmful Algal Bloom surveys	Independent	California Current	2007, 2011-2013, 2016-2017, 2021	964	NOAA, 2021b
CODAP	Independent	West Coast, Gulf of Alaska, Eastern Bering Sea	2007-2013, 2015-2017	1347	NOAA, 2021a
OCNMS (Olympic Coast National Marine Sanctuaries)	Independent	West Coast	2005-2023 2004-2015	2692	Risien et al., 2024b, 2024a

Oceanographic output

We also compared how a widely used dynamical oceanographic model product—the Copernicus Global Ocean Biogeochemistry Hindcast (GOBH)—compared to *in situ* bottom dissolved oxygen

observations from concurrent fish surveys versus predictions from our approach. GOBH provides 3D dissolved oxygen values at a ¼ degree resolution and with 75 vertical levels (fixed levels for all points, except for the last level, where thickness is adapted to the bathymetry) from December 1992 through March 2024 at a daily resolution (Mercator-Ocean, 2024; Perruche et al., 2024). We selected GOBH because it provided comprehensive and consistent coverage of our entire study region and time period.

We extracted the bottom dissolved oxygen for each fish catch event from GOBH by using a statistically robust method to interpolate between the grid points and depths in GOBH. For each region in each year of fish catch data, we subset the GOBH model for the geographic domain of the region (including all depths) for the time period of the survey (May 1st-October 30th). We then fit the dissolved oxygen output for this entire GOBH subset to a generalized linear mixed effects model (GLMM) using sdmTMB, including smoother effects on depth and day-of-year, spatial random fields, and following a Gaussian distribution (Eq. 13). We then extracted dissolved oxygen as predictions to the specific day, depth, and location (coordinates) of each fish catch observation. We calculated RMSE of *in situ* oxygen observations as a metric of accuracy.

$$O_{i,year,region} = s(log(\text{depth}_i)) + s(\text{doy}_i) + \omega_i \quad \text{Eq. 13}$$

Species distribution modeling comparison

We fit case studies of fish distribution models using each of the three dissolved oxygen data sources and compared estimated effects of oxygen on fish density. We chose two benthic-associated species with commercial importance—one that has a deeper habitat preference, sablefish (*Anoplopoma fimbria*), and one shallower, Dover sole (*Microstomus pacificus*)—in the California Current and British Columbia. To estimate the response of fish density to dissolved oxygen, we implemented GLMMs in sdmTMB (Anderson et al, 2025) using total catch rate as a Tweedie distributed response (Appendix A Eqs S1-S2). The model formula included fixed effects of quadratic logged depth, year, and dissolved oxygen, and a random spatial field (Appendix A Eqs S1). Dissolved oxygen was modeled as a breakpoint function (Eq. S3). We focus on a breakpoint model of oxygen (see Appendix A for more details) because fish response to dissolved oxygen is expected to be saturating (Kramer, 1987) and we are primarily interested in how different oxygen data sources could impact detection and estimation of an oxygen limitation on fish distribution. For the test of concurrent data only, we restricted model fitting to include data only where concurrent dissolved oxygen was available. For dissolved oxygen from empirical statistical predictions, we used the model that included spatiotemporal variation and temperature, which was the model with the highest predictive skill and would maximize the number of additional trawls (as salinity data was missing in many trawls).

3.4 RESULTS

Empirical statistical predictions

The skill in predicting oxygen from the empirical statistical model varied between regions. Dissolved oxygen at bottom trawl sampling events in the California Current and British Columbia could be predicted with relatively high accuracy, while predictions were less skilled in all Alaska regions. For the model with the highest predictive skill in each region, the overall RMSE (across all test years) for the California Current was 16.2 μmol kg^{-1} and 25.1 μmol kg^{-1} for British

Columbia (relative to observed range of 1-400 μmol kg^{-1} and 2-370 μmol $kg^{-1,}$ respectively), but was 36.7 μmol kg^{-1} for the eastern Bering Sea (relative to observations ranging from 16-450 μmol kg^{-1}), 55.1 μmol kg^{-1} for the Gulf of Alaska (relative observations ranging from 15-690 μmol kg^{-1}), and 55.2 μmol kg^{-1} for the Aleutian Islands (relative to observations ranging from 14-560 μmol kg^{-1}) (Table 3). At the resolution of sampling events, across all regions combined, 92% of test observations (n=13,581) were within 50 μmol kg^{-1} and 78% within 25 μmol kg^{-1} (Figure 3). Within each region, predictions from the model of bottom dissolved oxygen that included all covariates were more accurate and unbiased for the California Current, British Columbia, and Eastern Bering Sea, while predicted oxygen in the Gulf of Alaska and Aleutian Islands were consistently underestimated by the model (Figure 3).

In all regions, the model with the highest predictive skill in each region included both temperature and salinity, and a spatial and/or spatiotemporal random fields (Table 3). Including only temperature increased accuracy (i.e. reduced RMSE) over models with no covariates by ~2-8 μmol kg^{-1}, while including both temperature and salinity improved predictive skill by ~5-11 μmol kg^{-1} (Table 3). For models with both temperature and salinity, including latent spatial, temporal, or spatiotemporal structures usually improved predictive skill, but with smaller improvements than from adding temperature and salinity to the null model and by varying amounts across regions (Table 3). The strongest improvement was seen in the Eastern Bering Sea where RMSE decreased by 3.9 μmol kg^{-1} when spatial and spatiotemporal structures were added. However, in some cases, certain temporal and spatial structures increased RMSE compared to the temperature and salinity only models (e.g., Gulf of Alaska S+T vs. S+T+spatiotemporal in Table 3). For models with no observable covariates, including spatial, temporal, or spatiotemporal structure only improved predictive skill over a null model by up to ~4 μmol kg^{-1}, except for in British Columbia where it improved accuracy by ~7 μmol kg^{-1}. The spatial or temporal structure that provided the most accurate predictions differed between regions. For the full covariate model (which was consistently more accurate than a model with no observable covariate regardless of spatial or temporal structure), the spatial and temporal structure with the highest predictive skill was spatial variation in the California Current, Gulf of Alaska, and Aleutian Islands, and both spatial and spatiotemporal variation in British Columbia and the Eastern Bering Sea. Overall, all the most accurate models included spatial and/or spatiotemporal structures, but these structures alone could not achieve the same predictive skill as including observable covariates.

Differences in accuracy between regions were likely driven by the amount and coverage of training data available. Accuracy was notably improved with increased density of observations (Appendix B Figure S2). The densities of observations in the Gulf of Alaska and Aleutian Islands were only a quarter the density of observations in the California Current, and RMSE was three times higher. In the Aleutian Islands, for instance, there were fewer than 1,000 (ranging from 685—745 for each test year) bottom dissolved oxygen observations for fitting models in a survey area of over 70,000 km^2, while in the California Current there was an order of magnitude more—over 12,000 observations—for an area around 100,000 km^2 (Appendix B Figure S2). British Columbia had ~5,000 observations and an area of 53,580 km^2, while the Gulf of Alaska had ~5,000 observations for an area of 320,202 km^2. Data coverage in some regions was patchier and more spatially unbalanced between years than other regions; for instance, the Eastern Bering Sea had highly varied spatial coverage between years (Appendix B Figure S3C), while the California Current was more consistently covered (Appendix B Figure S3A). The concurrent bottom trawl dissolved

oxygen data in Gulf of Alaska and the Aleutian Islands also had overall higher oxygen values than the training datasets, but no bias was observed in any other region (Appendix B Figure S4). Since only two years of concurrent bottom trawl data were available in each Alaska region for predictive skills testing, there were fewer years for comparison than the California Current and British Columbia. As dynamic oceanographic variables (such as temperature, oxygen, and salinity used here) and depth are highly correlated (Appendix B Figure S6), distinct bathymetric and oceanographic features of each region likely contributed to regional differences in predictive skill and the best spatial and temporal structures. Yet overall there were not evident patterns in bias of predictions within each region across space (Appendix B Figure S3), salinity, temperature, year, or day-of-year (Appendix B Figure S5A). However, oxygen was generally over-predicted at shallower depths with higher predicted oxygen in the Alaska regions, while in British Columbia and the California Current there was underestimation of oxygen at shallow depths and low predicted oxygen (Figure 4).

Oceanographic model

Accuracy of the oceanographic output, Copernicus Global Ocean Biogeochemistry Hindcast (GOBH), compared to the observed bottom dissolved oxygen at fish catch points also differed between regions. The overall error (i.e. RMSE) was 38.2 μmol kg^{-1} in the California Current and 43.7 μmol kg^{-1} in British Columbia, but almost doubled in Alaskan regions, with an RMSE of 66.5 μmol kg^{-1} in the Gulf of Alaska, 65.8 μmol kg^{-1} in the Eastern Bering Sea, and 89.4 μmol kg^{-1} in the Aleutian Islands. There was both a consistent bias in predictions underestimating observed oxygen and a high imprecision in estimates, as evident at the scale of individual fish catch sampling events (Figure 5). This inaccuracy in predicting oxygen at fish sampling events was similar when comparing GOBH to independent CTD cast observations (Appendix B Figure S7). Overall the GOBH oxygen values were less accurate (i.e. a higher RMSE) than empirical statistical predictions in each region, with an RMSE ~15-30 μmol kg^{-1} higher than the integrated predictions in each region (Table 3).

Table 3. Overall root mean squared error (RMSE) of predictions empirical statistical predictions of bottom dissolved oxygen predictions for fish catch survey events withheld from training data for each region. Models with different spatial and temporal structures—none, persistent spatial fields ("Spatial") and plus annual fixed effects of year ("Annual") or plus spatiotemporal latent effects ("Spatiotemporal"— and including either no covariates ("None"), temperature ("T") or temperature and salinity ("T+S") (with salinity as sigma0) were fit to *in situ* dissolved bottom oxygen observations. Units are μmol kg^{-1}. RMSE is also shown for the Copernicus Global Ocean Biogeochemistry Hindcast (GOBH). an interpolation method that uses a spatial model to predict bottom dissolved oxygen from GOBH given depth, day-of-year, and latent spatial fields. Blue cells indicate models with the lowest out-of-sample RMSE.

		California Current			**British Columbia**			**Gulf of Alaska**			**Eastern Bering Sea**			**Aleutian Islands**		
		None	*T*	*S+T*	*None*	*T*	*S+T*	*None*	*T*	*S+T*	*None*	*T*	*S+T*	*None*	*T*	*S+T*
Empirical Statistical	*None*	23.4	20.7	17.4	36.9	33.3	25.5	64.4	65.0	57.9	47.2	40.1	40.6	68.6	63.6	56.6
	Spatial	21.1	19.1	16.2	28.3	27.7	25.6	56.9	59.5	55.1	47.8	40.3	40.6	69.1	57.9	55.2
	Annual	22.2	19.9	16.9	29.0	28.3	25.2	59.9	61.1	56.7	46.6	55.6	44.8	83.6	71.7	76.4
	Spatiotemporal	21.6	19.7	16.8	29.5	27.7	25.1	60.2	61.8	59.4	45.6	43.9	36.7	71.5	62.4	65.6
	GOBH	38.2			43.7			66.5			65.8			89.4		

Application to fish distribution model

In the case studies, the detection of a threshold—the biologically expected model—did not depend on the oxygen data used; however, if there was a threshold effect, the oxygen value at which fish densities were limited was sensitive to the type of oxygen data. For Dover sole in the California Current and sablefish in British Columbia, there was no threshold effect of oxygen detected (i.e. a flat line in the conditional effects plots) when fish density was fit to any of the oxygen data types (Figure 6). Similarly, for Dover sole in British Columbia and sablefish in the California Current, a threshold effect was detected regardless of the oxygen data type (Figure 6). However, the estimated threshold of this effect depended on data type. For instance, for sablefish in the California Current, when fit to only the concurrent *in situ* data, the estimated breakpoint (maximum likelihood estimate ± standard error) was 20.7 ± 60.8 μmol kg^{-1}, but 56.14 ± 69 μmol kg^{-1} when using empirical statistical predictions, and 73.6 ± 60.9 μmol kg^{-1} from the oceanographic model (Appendix B Table S2). For Dover sole in British Columbia, the estimated threshold was 22.7 ± 111.9 μmol kg^{-1} for the *in situ* data, 38.6 ± 114 μmol kg^{-1} for empirical statistical predictions, and 54.9 ± 130.8 μmol kg^{-1} for the oceanographic model. When these estimated dissolved oxygen thresholds are subsequently used to estimate habitat with dissolved oxygen concentrations higher than or less than the threshold, a much wider range (essentially all trawls across the California Current) would be identified as having insufficient oxygen (i.e. unsuitable) using the integrated predictions of oxygen (Figure 7). However, the model fit to concurrent data identifies only a narrow band at the (deeper) western edge of the range with unsuitable conditions (Figure 7).

The distribution of fish catch across depth and oxygen conditions in the different data types likely contributed to differences in estimated thresholds. For instance, in the California Current the concurrent data shows a much tighter range of oxygen conditions than predicted by the integrated model or in the oceanographic output at deeper depths (Figure 8). The difference in estimated effects are primarily due to differences in the oxygen predictions, rather than just the amount of data available. Here we showed the most realistic scenario, in which we used the integrated predictions or oceanographic model to predict at all trawl samples when concurrent *in situ* data was not available, which greatly expanded the number of years of fish data that were used in model fitting. When data used in model fitting is instead restricted to only the years where concurrent data is available, there are even greater differences in estimated effects. For British Columbia Dover sole (Appendix B Figure S8), no threshold effect was detected when using the predictions from the integrated statistical model or the oceanographic output. In the California Current, no threshold is detected when using the oceanographic output (but is still detected from the integrated statistical predictions) (Appendix B Figure S8). The differences in the oxygen values between data sources is therefore impacting threshold estimation.

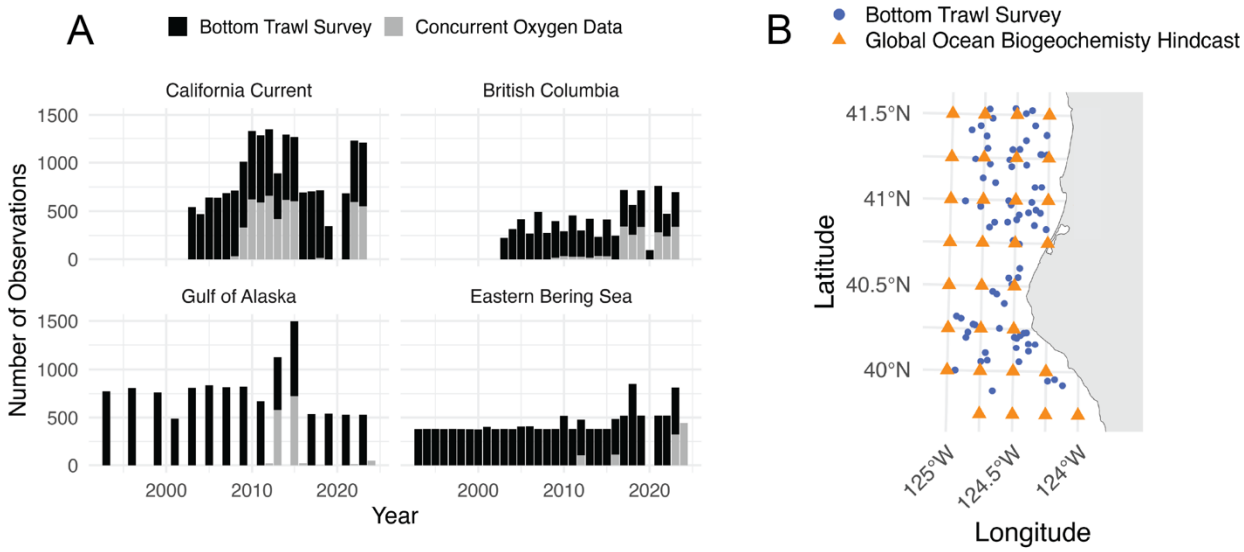

Figure 1. The trade-off between spatiotemporal coverage and resolution in oxygen data options for species distribution modeling. A) There are inter- and intra-annual gaps in oxygen data coverage of fish catch surveys. Number of observations from bottom trawl surveys (black) in the California Current (the NOAA Northwest Fisheries Science Center West Coast Bottom Trawl Survey), British Columbia (the Department of Fisheries and Oceans Canada West Coast Concurrent Trawl Surveys), the Gulf of Alaska and Eastern Bering Sea (NOAA Alaska Fisheries Science Center Gulf of Alaska and Eastern Bering Sea Bottom Trawl Surveys), and the number of trawls with *in situ* oxygen observations available (grey). B) The spatiotemporal resolution mismatch between oceanographic model output and fish catch surveys. Example of fish catch survey locations for a section of the West Coast Bottom Trawl Survey in the California Current in 2012) (blue points) and the Global Ocean Biogeochemistry Hindcast grid points (orange stars).

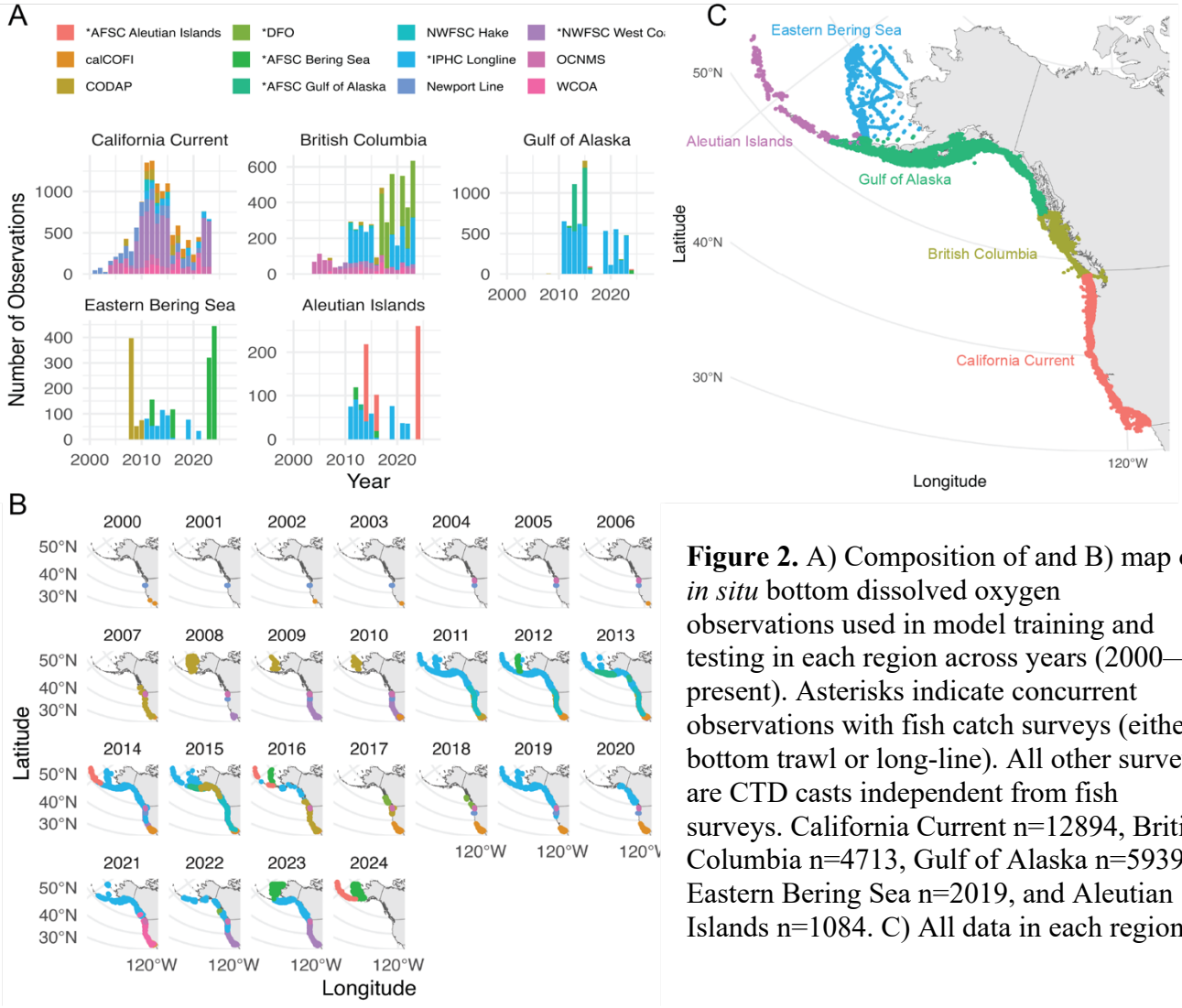

Figure 2. A) Composition of and B) map of *in situ* bottom dissolved oxygen observations used in model training and testing in each region across years (2000—present). Asterisks indicate concurrent observations with fish catch surveys (either bottom trawl or long-line). All other surveys are CTD casts independent from fish surveys. California Current n=12894, British Columbia n=4713, Gulf of Alaska n=5939, Eastern Bering Sea n=2019, and Aleutian Islands n=1084. C) All data in each region.

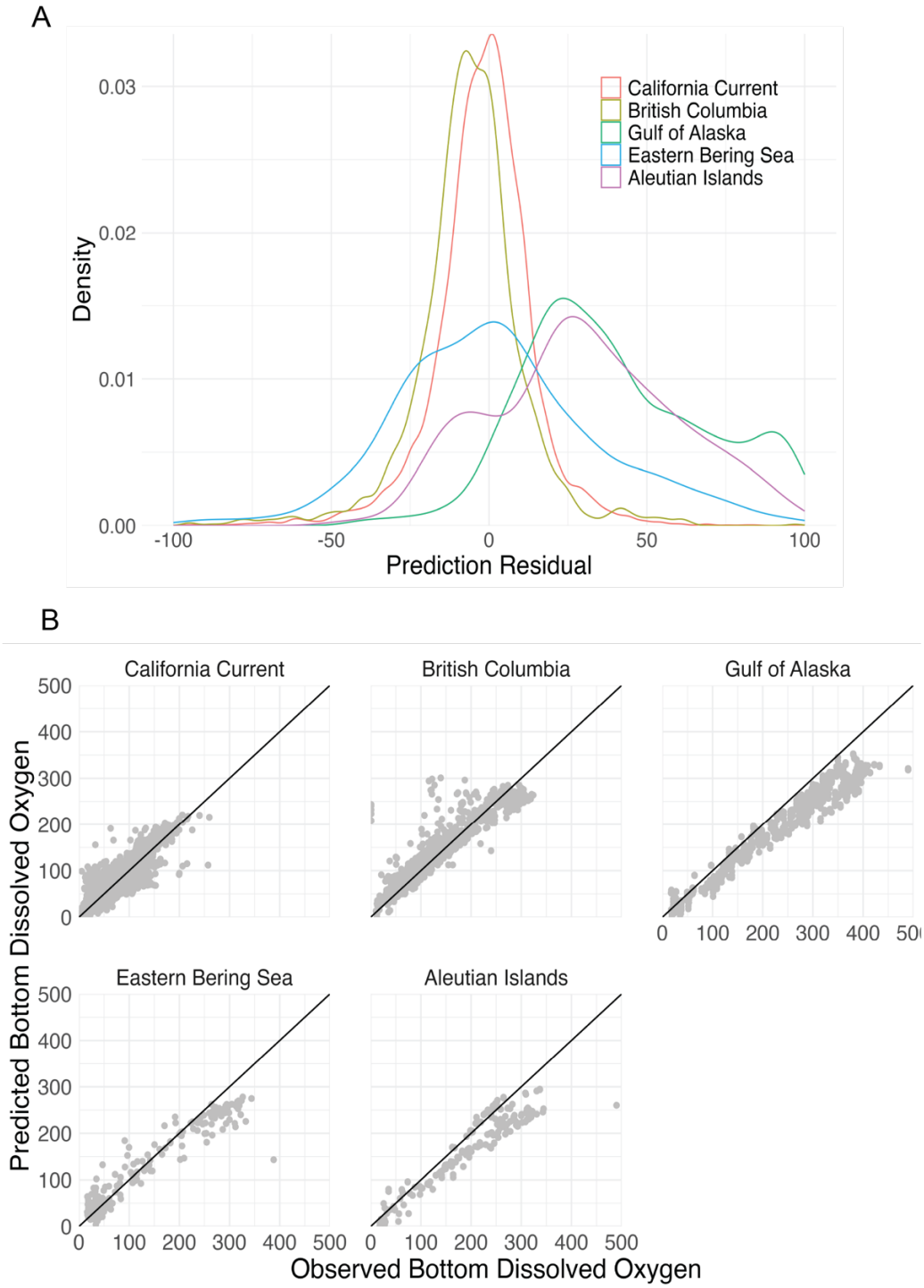

Figure 3. A) Distribution of residuals (observations minus predictions) (μmol kg^{-1}) for predictions of bottom dissolved oxygen for fish catch surveys (observations withheld from model fitting) from the highest-skill model of *in situ* bottom dissolved oxygen observations for each region. B) Predicted bottom dissolved oxygen and observed bottom dissolved oxygen in μmol kg^{-1} (*in situ* observations withheld from training data) for each region. Black line indicates a 1:1 relationship (i.e. perfect accuracy).

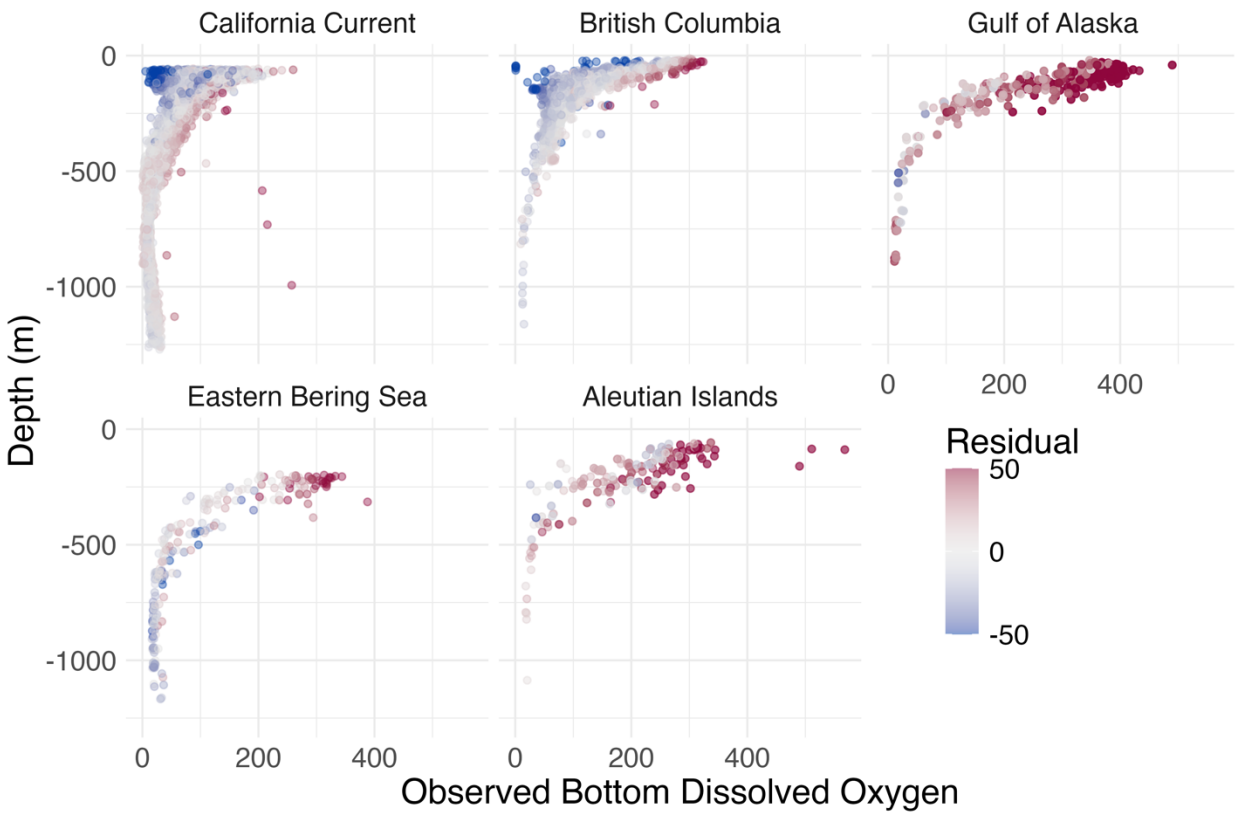

Figure 4. Residuals of predictions (observation—prediction) from all years of leave-one-year-out skills testing by observed bottom dissolved oxygen (µmol kg^{-1}) and depth of observation (m).

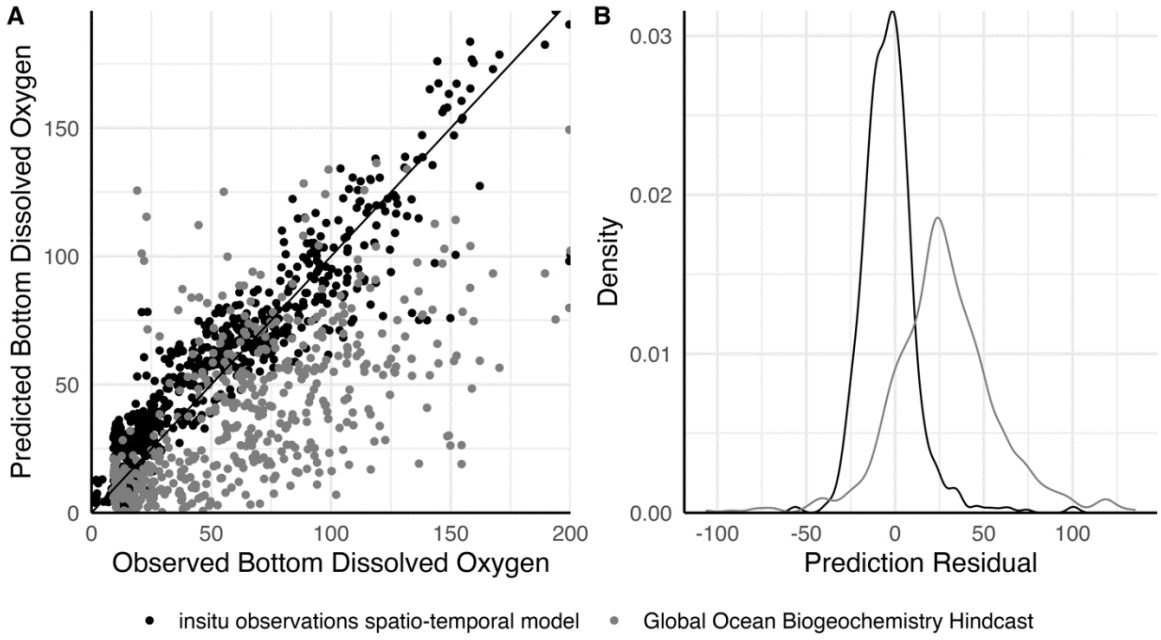

Figure 5. A) Predicted bottom dissolved oxygen and observed bottom dissolved oxygen in μmol kg^{-1} (*in situ* observations withheld from training data) for an example year and region, the

California Current in 2012, for the spatiotemporal model with both temperature and salinity covariates fit to in situ data (black) and the Global Ocean Biogeochemistry Hindcast model interpolated to depth, day-of-year, and coordinates (grey). Black line indicates a 1:1 relationship (i.e. perfect accuracy). B) Distribution of residuals (μmol kg^{-1}) for the predictions versus observations from each.

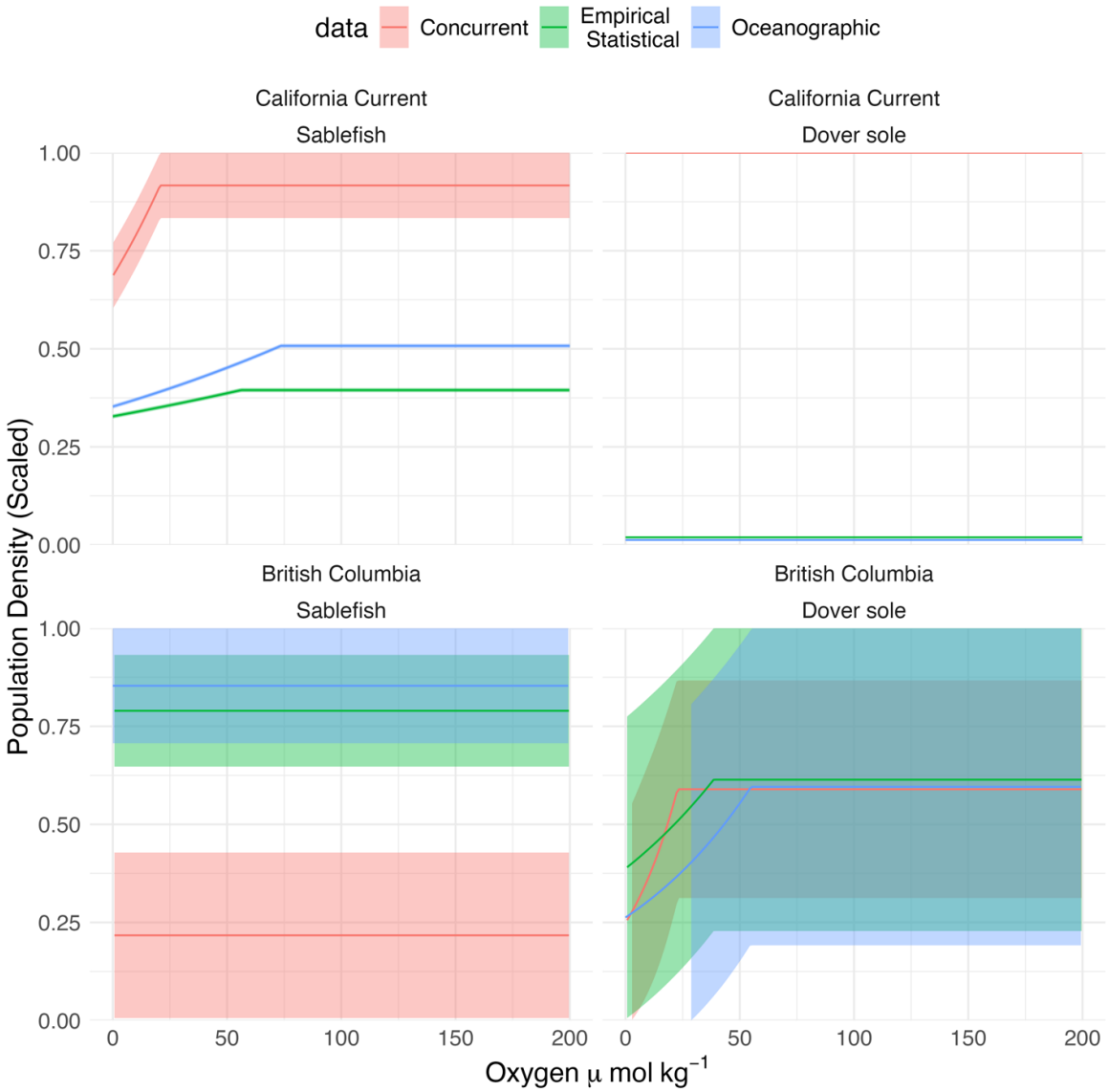

Figure 6. The response of fish density to dissolved oxygen for each species and region estimated from the three different sources of dissolved oxygen data (concurrent *in situ* measurements from the bottom trawl surveys, predictions from the empirical statistical model, and output from a global oceanographic model, the Global Oceanographic Biogeochemistry Hindcast). Response is shown as the conditional effect (maximum likelihood estimate ± standard error) of the dissolved oxygen breakpoint model. Conditional effects without standard errors are due to inherent computational challenges in maximum likelihood estimation when the second derivative of the log-likelihood is near zero or undefined, making the curvature-based (inverse

Hessian) calculation of standard errors not reliably approximated. Dover sole in British Columbia and sablefish in the California Current show a threshold effect, but the specific breakpoint differs when estimated from different data sources. Dover sole in the California Current and sablefish in British Columbia show no effect of dissolved oxygen on fish density regardless of data source. Conditional effects were calculated with depth effects set to 0 m, year at a reference year (2012 in California Current and 2019 in British Columbia), and no random effects. Population density (unscaled units of biomass kg km^{-2}) is shown scaled to the maximum value of the conditional effect on biomass density (i.e. 1) in each species and region.

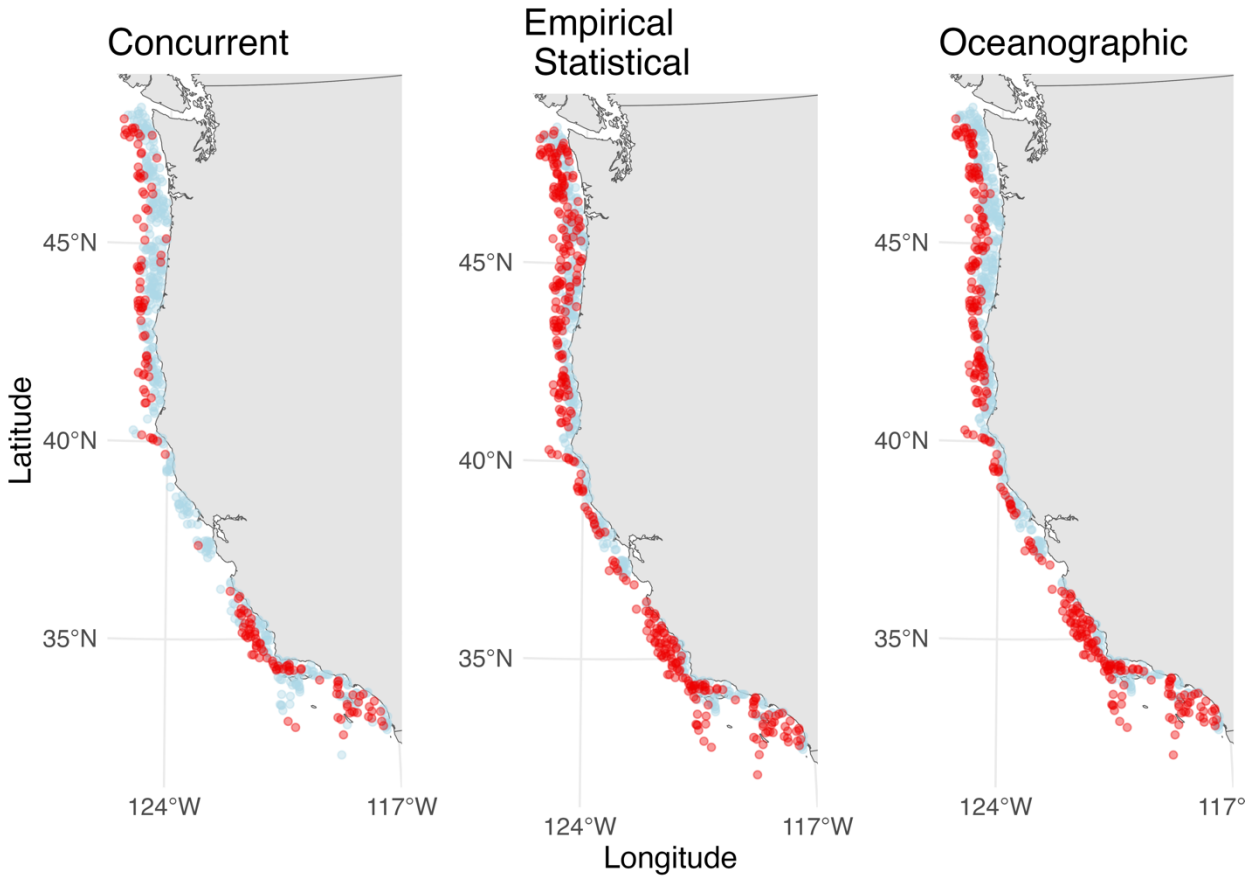

Figure 7. Trawl locations where dissolved oxygen conditions were estimated to be suitable (blue, no effect on fish density) and unsuitable (red, a reducing effect on fish density) for one example year (2023) for a case study species and region, sablefish in the California Current, using the estimated threshold from the dissolved oxygen breakpoint model fit to dissolved oxygen data from the different data sources: (left) concurrent *in situ* observations only, (center) predictions from the empirical statistical model, and (right) oceanographic model output, from the Global Oceanographic Biogeochemistry Hindcast.

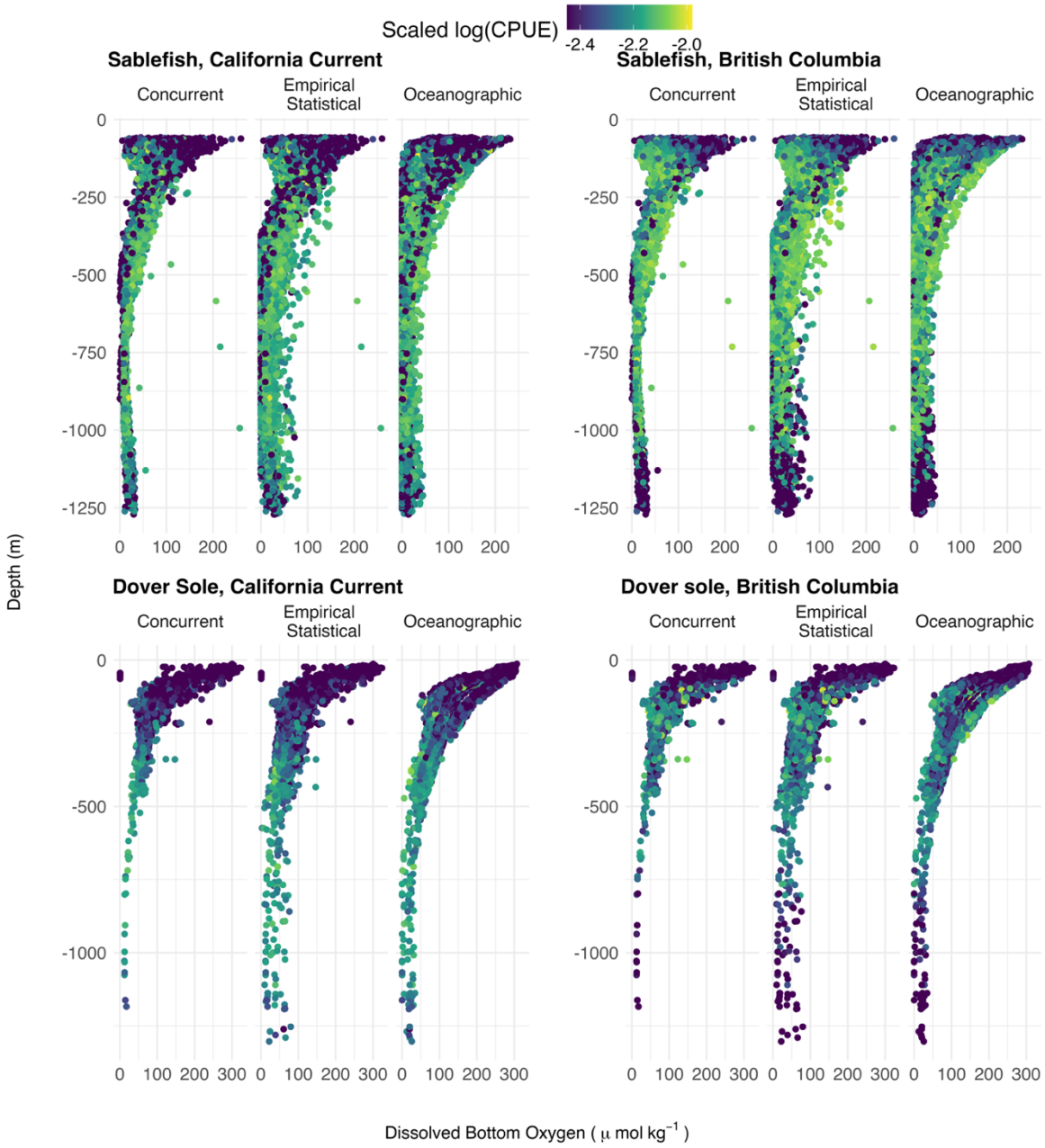

Figure 8. Dissolved oxygen (μmol kg^{-1}) and depth (m) for each of the three dissolved oxygen data sources (concurrent *in situ* observations measured at each bottom trawl survey, empirical statistical predictions, and the dynamical oceanographic output, Global Ocean Biogeochemistry Hindcast) at each haul for each case study species and region. Color indicates the fish catch per unit effort (CPUE) (kg km^{-2}) of each bottom trawl survey, scaled by the mean and standard deviation of log(CPUE) (i.e. the geometric mean and standard deviation). *In situ* observations have a narrower range of estimated dissolved oxygen concentrations across depth, especially at deeper locations, while there is much greater variation in dissolved oxygen in predictions from the empirical statistical model or oceanographic output.

3.5 DISCUSSION

Here we demonstrate the necessity of carefully considering the source of covariate environmental data in species distribution modeling, focusing on dissolved oxygen in the northeastern Pacific. We found possible benefits and drawbacks to expanding the amount of data through empirical statistical predictions or with dynamical oceanographic model output. Using a relatively simple structure of the empirical statistical model to predict dissolved oxygen by integrating multiple existing datasets, we could reasonably predict oxygen conditions at the resolution of marine biological surveys in two of the five regions (only British Columbia and California Current) over the required duration. Yet achieving reasonably accurate predictions required an extensive amount of oxygen data. The Alaska regions, with limited data, produced large errors in predictions. In all regions, the dynamical oceanographic model output (GOBH) had even lower predictive skill at specific sampling events. The level of accuracy in both approaches still introduced sufficient variation in oxygen values to affect the outcome of estimated oxygen thresholds when used in species distributions models.

We found that empirical statistical predictions could be a viable option for expanding coverage of environmental data in only some cases. Leave-one-year-out cross-validation skill testing showed that the model could reliably predict dissolved oxygen at bottom trawl events in the California Current and British Columbia (with an RMSE ~16 μmol kg^{-1} and 22 μmol kg^{-1} respectively). And in all regions, this approach could fill in gaps in *in situ* concurrent observations with greater accuracy than using the oceanographic model output for the period of time it was trained to reproduce. In all regions here, the most accurate predictions could be generated from simple regression models of other covariates (temperature and salinity) that are driven by similar oceanographic processes as oxygen, plus spatial and sometimes spatiotemporal random fields. Since temperature has historically been more frequently available in trawl datasets than dissolved oxygen, this method may be readily applicable to other biological datasets. It can also be useful to fill in missing oxygen observations if measured simultaneously with temperature and salinity and sensors fail. If temperature and salinity are not available, accounting for latent spatial and temporal structure with random fields could still reasonably predict dissolved oxygen but with more error (an additional ~5-10 μmol kg^{-1}).

Despite the utility of empirical statistical approaches for resolving oxygen at appropriate scales, this method should only be used if data can provide sufficient spatial and temporal coverage. We find that regions with lower density of observations data available (<0.075 observations per km^2) had less accurate predictions. In Alaska regions, error was especially large (~35-50 μmol kg^{-1}), and ~2x greater than British Columbia and California Current. In the Gulf of Alaska, around four times more data than available (~20,000 observations; only ~5,000 available here) would be needed to achieve the same observational density as the California Current. Regions with fewer observations had both reduced years of coverage (e.g. less than 10 years of data with annual gaps in the Aleutian Islands vs. over 20 years of continuous annual data in the California Current) and were more spatially patchy data relative to the area of the survey region, and fewer independent sources of oxygen data (e.g. three sources of oxygen data in the Aleutian Islands versus eight in the California Current). The amount of data available relative to capturing the unique oceanographic characteristics within each region (such as particular bathymetry, river outflows,

wind mixing, upwelling dynamics, and biogeochemical processes) may also impact predictive skill and needs to be considered specifically for each system.

Interpolating to fill in missing covariate data is commonly used in distribution modeling (e.g. Li & Heap, 2014; Thompson et al., 2023), yet we recommend considering empirical statistical predictions only after validating for the specific region of analysis with cross-validation techniques (Roberts et al., 2017) and using only if accuracy (e.g. RMSE) is within a tolerable range for the purpose of the analysis. For instance, in our case studies of groundfish distribution modeling, we would consider using this approach only for British Columbia and California Current, as the errors in the Alaska regions are too large relative to the low oxygen values that define hypoxic conditions. There are additional limitations to consider when applying this empirical statistical method. We did not intend for this approach to mechanistically evaluate drivers of dissolved oxygen dynamics, but rather to maximize predictive skill for obtaining point oxygen value at biological sampling events to use as a covariate in species distribution models. In our case, simpler models with salinity and temperature produced more skillful predictions than models with only latent random fields. Combining both provided the highest accuracy. Testing alternative models of increasing levels of complexity—from simple models to highly parameterized models and with complex error structures—can help identify the most skillful model for the unique oceanographic conditions in other systems. In addition, we only evaluated skill for predicting entirely unsampled years. For using this method to fill in gaps in spatial coverage within a sampled year, one could conduct skill testing with spatial blocking (Roberts et al., 2017). Lastly, not unlike statistical predictions for ocean acidification (Carter et al. 2021; Alin et al. 2023) this statistical method does not include possible long-term change (i.e. deoxygenation signals) because of the short temporal duration (< 20 years) of observations in the training period. For ocean acidification reconstructions without time-varying anthropogenic effects, usage is often limited to 10 years around the training period (McGarry et al. 2021; Alin et al. 2020). Some regions may do well to predict contemporaneous oxygen, but it is likely that biases will emerge over the future years, particularly in regions with high uptake of anthropogenic CO_2 such as the North Atlantic (Gruber et al. 2019; Carter et al. 2021).

We validate that oceanographic model outputs for dissolved bottom oxygen can be a suitable alternative if sufficient *in situ* observations are not available, but a greater amount of error in dissolved oxygen should be expected. While the oceanographic model output used here (the Global Oceanographic Biogeochemical Hindcast) has been validated for capturing climatological and seasonal dynamics across space and depth (Perruche et al., 2024), it could not precisely describe fluctuations at the resolution of fish catch surveys. This inaccuracy was due in part to bias but also due to greater variation; adjusting with a simple constant (i.e. a delta-correction method) therefore would not sufficiently correct the discrepancy.

Overall, we recommend validating oceanographic model outputs for specific applications to species distribution modeling. Oceanographic model outputs are often validated at coarser spatial and temporal scales than biological sampling (such as climatological means and seasonal patterns, e.g. Kristiansen et al., 2024; Perruche et al., 2024; though see Kearney, 2021 and Kearney & Porter, 2009 for fine-scale temperature validation and Sullaway et al., 2024 for zooplankton). Our approach compares output to *in situ* observations for the specific biological survey being analyzed, and can therefore help quantify uncertainty in oceanographic models at the scale of biological

observations. We did not intend to be a comprehensive survey of oceanographic data options. Rather, we aimed to validate the model most suitable for our purposes and provide a demonstration and framework that could be generalized for any oceanographic output when applying to species distribution models. Here, we used GOBH because it provided the most comprehensive spatial and temporal coverage for our study system. However, because of the resolution it does not capture some local processes at smaller scales. In other studies, such as for a more constrained geographic area, oceanographic model outputs such as regionally downscaled models that have higher resolution of bathymetry and coastal dynamics (e.g. upwelling and eddies) may be available and could be validated using our approach. For instance, there are hindcasts from Regional Ocean Modeling System (ROMS) models (e.g. in the northeastern Pacific, Hauri et al., 2020; Pozo Buil et al., 2021), upcoming MOM6 models (Ross et al., 2023), GOBAI-O2 (Sharp et al., 2022), and ESPER-NN (Carter et al., 2021). In addition to validating oceanographic models, we also recommend to fit a spatial model to oceanographic output to interpolate values at specific location, depth, and day of each biological sampling event, rather than using the nearest oceanographic output grid location. Error of the oceanographic output was significantly greater when using nearest neighbor matching (~200% greater RMSE in the California Current and British Columbia, and 33% in the Alaskan regions). The interpolation method used here can greatly improve the accuracy of dissolved oxygen values by reducing the coarseness of the oceanographic model and better capturing the spatial resolution of biological data.

Our analysis spotlights that the level of error in both empirical statistical predictions and dynamical oceanographic output can be enough to impact the outcomes of species distributions models of demersal fishes. In our case studies, the detection of an effect of oxygen on fish distribution did not differ between oxygen data types. Yet if a threshold effect was detected (sablefish in the California Current and Dover sole in British Columbia), the estimated breakpoint—the oxygen value below which fish density is reduced—was sensitive to data type. Our results suggest that this is due to bias and variation in empirical statistical predictions and dynamical oceanographic values compared to *in situ* data. In estimating and projecting biological responses to the environment, there are multiple sources of uncertainty (e.g. Brodie et al., 2022; Davies et al., 2023) and decision points throughout the data and modeling process (e.g. Commander et al., 2023). Here we aim to highlight that the decisions of which environmental data source to use and how to account for uncertainty in this data are two other key decision points that needs to be carefully considered.

First, in deciding the input for an environmental covariate, modelers need to evaluate the tradeoff between coverage and resolution given the options available for the specific region and time period and the purpose of the model. There is no single "best" choice. Spatial models of biological data are used for various purposes, including projecting distributions of changing climate (e.g. Liu et al., 2023), designating essential fish habitat designation (e.g. Moore et al., 2016), and evaluating environmental drivers of characteristic such as growth (e.g. Lindmark et al., 2022a; Lindmark et al., 2022b). If the primary goal is historical ecological inference and precise empirical estimates, then prioritizing resolution over coverage and using *in situ* observations collected at the time of biological sampling would likely provide the most specific measure of conditions at the location and time of biological data. For instance in our case studies, we considered our baseline as expected oxygen based on the database of oxygen measurements. Using empirical statistical predictions or GOBH to fill in missing observations and expand the amount of data for distribution modeling did

not provide enough benefit to outweigh information lost by introducing greater error in oxygen values. However for studies that need wider temporal or geographic coverage than that available from *in situ* data, empirical statistical predictions or a dynamical oceanographic model output would be more suitable. If using an oceanographic output, we recommend using the option available with the highest resolution possible that still covers the geographic extent of the study region, and following the validation and interpolation methods discussed above. Combining multiple downscaled oceanographic outputs to patch together across multiple regions (rather than using one more global model, as done with GOBH here) would require validating in each region and evaluating biases between regions to be able to compare biological models fit to different oceanographic outputs. For many species (such as Dover sole here), there are not laboratory estimates on oxygen sensitivity available. However considering the ecology and physiology of the species when available can provide context and biological realism when evaluating the sensitivity of the estimated biological response to possible error from the environmental data. For instance, the low end of hypoxia definitions (10 μmol kg^{-1}) and estimated loss-of-equilibrium for sablefish of 16 μmol kg^{-1} (at 12 C; $pO_{2,\,crit}$ of 44 μmol kg^{-1}) (Leeuwis et al., 2019) is within the RMSE of the empirical statistical and oceanographic models here even for regions with the highest predictive skill. It therefore may not be precise enough for studies evaluating precise empirical responses these low thresholds. Yet using these methods (for only the regions with higher predictive skill) may be more robust for species expected to have a higher threshold, such as Atlantic cod (52-58 μmol kg^{-1}·Claireaux et al., 2000) or Doryteuthis squid (51-68 μmol kg^{-1},Birk 2018).

There are other situations where an oceanographic model or empirical predictions may be more suitable. Oceanographic model outputs are a powerful tool for capturing biogeochemical and physical dynamics (Di Biagio et al., 2023; Li et al., 2024; Siedlecki et al. 2015; Pena et al., 2010) and are crucial for projecting impacts of future oxygen and temperature conditions (e.g. Liu et al., 2023; Thompson et al., 2023; Sunday et al. 2022). We did find that different data sources in our case studies were robust to overall categorical classification of whether a species did or did not have any response to oxygen conditions. Similarly, oceanographic model outputs would be useful for studies needing to summarize monthly, season, and annual indices and across broader geographic regions because they are often accurate at recreating trends and dynamics at these broader scales (e.g. Perruche et al., 2024). This includes annual recruitment models (e.g. Ward et al., 2024), characterizing marine heatwaves (e.g. Fredston et al., 2024), or evaluating spatially varying responses to global or regional conditions (e.g. Thorson 2019). Lastly, oceanographic model output, even if biased, is still effective for forecasting biological responses if they are used consistently. For instance, using the historical reconstruction and climate projections from the same oceanographic model will keep biases consistent between the data used to estimate the environmental effects and the projected environmental conditions.

A second decision point to consider, regardless of data source, is accounting for uncertainty in the environmental covariate data. Our framework—comparing species models fit to different environmental input data (e.g. oceanographic output versus *in situ* model) to quantify differences in estimated threshold due to data uncertainty—is one option. These range of thresholds could subsequently classify vulnerability of a species to low oxygen in a particular region by comparing the threshold range to predicted future changes in dissolved oxygen. Similar methods are already common for projecting ecological responses to climate forecasts from multiple different Earth System Models (e.g. Liu et al., 2023; Townhill et al., 2023). If only an oceanographic model

hindcast and no *in situ* data are available in the region for comparison, using standard sensitivity analysis techniques (Cariboni et al., 2007; Steel et al., 2009), such as by simulating error in the oceanographic output, could quantify the robustness of estimated effects to error in the oceanographic output. Models could be combined via ensemble methods with equal or non-equal weights (e.g. Anderson et al., 2017; Harris et al., 2024). State-space models could explicitly build observation error in the environmental covariate into the model (Correa et al., 2023; Lindén & Knape, 2009; Thorson et al., 2021). Oceanographic output could be included in models as a separate covariate (Sullaway et al., 2024), or as joint models with observations as responses using shared latent variables (Thorson et al., 2021), to generate spatially resolved corrections (Hay et al., 2000). In some cases, it may be suitable to aggregate species density data into coarser scales, such as pooling data into the resolution of oceanographic output (Chen et al., 2023; Commander et al., 2022). Conversely, local biological response to regionally or globally scaled environmental variables (such as an oceanographic index) could be evaluated via spatially varying coefficients (e.g. Thorson 2019). Here, we focused on GLMMs for species distribution, but other approaches for estimating effects of oxygen on species populations, such as structural equation models (Thorson et al., 2024), simulating ecosystem dynamics in Ecopath and Ecosim (e.g. de Mutsert et al., 2016) or reconstructing environmental histories with otoliths (e.g. Valenza et al., 2023) may provide additional insights. Overall, considering uncertainty stemming from the environmental data will ensure more robust estimates of environmental drivers on ecological systems and projections of impacts under future climate change.

Our findings indicate that prioritizing measuring environmental data concurrently with biological sampling can reduce uncertainty in estimating environmental effects on marine species. We found that a global hindcast could produce greater uncertainty than concurrent data when using retrospective models to estimate environmental drivers of marine species distributions. Oceanographic models that have performed well at finer scales are not available at the large scales of time and space required for analyses like the one we performed here, due primarily to computational limitations. Concurrent observations are similarly prioritized in carbon cycling research (termed co-locating observations, e.g. Newman et al., 2019). Prioritizing environmental data can also improve oceanographic models. Dissolved oxygen is particularly challenging to capture at a fine scale in oceanographic models (Stramma et al., 2012). Yet dissolved oxygen observations at bottom depths are less widely available (Wang et al., 2024); for instance, satellites do not detect bottom oxygen, and only a subset of Argo floats measure dissolved oxygen (Argo, 2024). Expanding advanced ocean observing instrumentation to regions with limited coverage, such as the Bering Sea and Aleutian Islands, and generating high-quality and long-term, historical reconstructions of subsurface environmental conditions will improve oceanographic modeling outputs (Breitburg et al., 2018). Collecting dissolved oxygen data concurrently requires time and financial resources that may be limited with possible declining budgets (NOAA, 2024b) and upcoming survey changes (NOAA, 2024a; NOAA Fisheries, 2024). Here, we demonstrate that these data are highly valuable for capturing fine-resolution environmental conditions at an ecologically relevant resolution, validating oceanographic outputs, and expanding coverage with predictions from empirical statistical approaches.

There is a growing need to bridge the gap between the methods and priorities of oceanographic and fisheries research communities to advance fisheries management (Berx et al., 2011, Drenkard et al., 2021). Here, we identify an opportunity for increasing alignment by validating

oceanographic outputs for the resolution of biological sampling. We provide guidance on operationalizing *in situ* and oceanographic model outputs to be applicable to fisheries data and methods. In our case studies, relying on only *in situ* data or only an oceanographic output would have led to different interpretations of the vulnerability of species to decreased oxygen. The most suitable data source will depend on a study's purpose and the options available for the region and time period. We suggest greater attention to evaluating model sensitivity, quantifying uncertainty, and testing robustness of conclusions to environmental data inputs. We focused on bottom dissolved oxygen because it is less available in marine biological surveys and more difficult to capture in oceanographic models. Yet our approach and guidance can be similarly applied to other environmental characteristics often included in species modeling, such as temperature and phytoplankton. We also encourage the fisheries research community to develop standardized techniques for how environmental data (whether *in situ* or from oceanographic output) are processed in spatial models to facilitate comparison across systems.

3.6 ACKNOWLEDGEMENTS

We thank all survey participants of the NOAA West Coast, Gulf of Alaska, Bering Sea, and Aleutian Islands Bottom Trawl Surveys and the Department of Fisheries and Oceans Canada British Columbia Synoptic Bottom Trawl Surveys. We also thank Ole Shelton for helpful comments on an earlier review. This publication was partially funded by Washington Sea Grant grant no. R/SFA-12, and from the Lowell E. Wakefield Professorship.

3.7 REFERENCES

Akaike, H. (1974). A new look at the statistical model identification. *IEEE Transactions on Automatic Control*, *19*(6), 716–723. https://doi.org/10.1109/TAC.1974.1100705

Altieri, A. H., Harrison, S. B., Seemann, J., Collin, R., Diaz, R. J., & Knowlton, N. (2017). Tropical dead zones and mass mortalities on coral reefs. *Proceedings of the National Academy of Sciences*, *114*(14), 3660–3665. https://doi.org/10.1073/pnas.1621517114

Anderson, S. C., Cooper, A. B., Jensen, O. P., Minto, C., Thorson, J. T., Walsh, J. C., Afflerbach, J., Dickey-Collas, M., Kleisner, K. M., & Longo, C. (2017). Improving estimates of population status and trend with superensemble models. *Fish and Fisheries*, *18*(4), 732–741.

Anderson, S. C., Keppel, E. A., & Edwards, A. M. (2019). *A reproducible data synopsis for over 100 species of British Columbia groundfish*. https://www.dfo-mpo.gc.ca/csas-sccs/Publications/ResDocs-DocRech/2019/2019_041-eng.html

Anderson, S. C., Ward, E. J., English, P. A., Barnett, L. A. K., & Thorson, J.T. (2025). sdmTMB: an R package for fast, flexible, and user-friendly generalized linear mixed effects models with spatial and spatiotemporal random fields. In press at *Journal of Statistical Software*. *BioRxiv* preprint: 2022.03.24.485545. https://doi.org/10.1101/2022.03.24.485545

Anderson, Sean. A., Keppel, E. A., & Edwards, A. M. (2019). *A reproducible data synopsis for over 100 species of British Columbia groundfish*. publications.gc.ca/pub?id=9.884045&sl=0

Araújo, M. B., & New, M. (2007). Ensemble forecasting of species distributions. *Trends in Ecology & Evolution*, *22*(1), 42–47.

Arevalo-Martínez, D. L., Kock, A., Löscher, C. R., Schmitz, R. A., & Bange, H. W. (2015). Massive nitrous oxide emissions from the tropical South Pacific Ocean. *Nature Geoscience*, *8*(7), 530–533.

Argo. (2024). *Argo float data and metadata from Global Data Assembly Centre (Argo GDAC)*. https://doi.org/10.17882/42182

Bandara, R. M. W. J., Curchitser, E., & Pinsky, M. L. (2023). The importance of oxygen for explaining rapid shifts in a marine fish. *Global Change Biology*, *n/a*(n/a), e17008. https://doi.org/https://doi.org/10.1111/gcb.17008

Barth, J. A., Pierce, S. D., Carter, B. R., Chan, F., Erofeev, A. Y., Fisher, J. L., Feely, R. A., Jacobson, K. C., Keller, A. A., & Morgan, C. A. (2024). Widespread and increasing near-bottom hypoxia in the coastal ocean off the United States Pacific Northwest. *Scientific Reports*, *14*(1), 3798.

Beamish, F.W.H. 1964. Respiration of fishes with special emphasis on standard oxygen consumption: II. Influence of weight and temperature on respiration of several species. *Canadian Journal of Zoology,* 42(2): 177-188. https://doi.org/10.1139/z64-016

Berx, B., Dickey-Collas, M., Skogen, M. D., De Roeck, Y.-H., Klein, H., Barciela, R., Forster, R. M., Dombrowsky, E., Huret, M., & Payne, M. (2011). Does operational oceanography address the needs of fisheries and applied environmental scientists? *Oceanography*, *24*(1), 166–171.

Birk, M.A. 2018. Ecophysiology of Oxygen Supply in Cephalopods. Dissertation. University of South Florida. https://digitalcommons.usf.edu/etd/7265

Breitburg, D., Levin, L. A., Oschlies, A., Grégoire, M., Chavez, F. P., Conley, D. J., Garçon, V., Gilbert, D., Gutiérrez, D., Isensee, K., Jacinto, G. S., Limburg, K. E., Montes, I., Naqvi, S. W. A., Pitcher, G. C., Rabalais, N. N., Roman, M. R., Rose, K. A., Seibel, B. A., & Zhang, J. (2018). Declining oxygen in the global ocean and coastal waters. *Science*, *359*(6371), eaam7240. https://doi.org/10.1126/science.aam7240

Brodie, S., Smith, J. A., Muhling, B. A., Barnett, L. A. K., Carroll, G., Fiedler, P., Bograd, S. J., Hazen, E. L., Jacox, M. G., Andrews, K. S., Barnes, C. L., Crozier, L. G., Fiechter, J., Fredston, A., Haltuch, M. A., Harvey, C. J., Holmes, E., Karp, M. A., Liu, O. R., … Kaplan, I. C. (2022). Recommendations for quantifying and reducing uncertainty in climate projections of species distributions. *Global Change Biology*, *28*(22), 6586–6601. https://doi.org/10.1111/gcb.16371

Broecker, W. S., Sutherland, S., & Peng, T.-H. (1999). A possible 20th-century slowdown of Southern Ocean deep water formation. *Science*, *286*(5442), 1132–1135.

Brown, J. H., Gillooly, J. F., Allen, A. P., Savage, V. M., & West, G. B. (2004). Toward a metabolic theory of ecology. *Ecology*, *85*(7), 1771–1789. https://doi.org/10.1890/03-9000

CalCOFI. (2024). *CTD Cast Files, California Cooperative Ocean Fisheries Investigations2*. https://calcofi.org/data/oceanographic-data/ctd-cast-files/

Cariboni, J., Gatelli, D., Liska, R., & Saltelli, A. (2007). The role of sensitivity analysis in ecological modelling. *Ecological Modelling*, *203*(1), 167–182. https://doi.org/https://doi.org/10.1016/j.ecolmodel.2005.10.045

Carter, B. R., Bittig, H. C., Fassbender, A. J., Sharp, J. D., Takeshita, Y., Xu, Y.-Y., Álvarez, M., Wanninkhof, R., Feely, R. A., & Barbero, L. (2021). New and updated global empirical seawater property estimation routines. *Limnology and Oceanography: Methods*, *19*(12), 785–809. https://doi.org/https://doi.org/10.1002/lom3.10461Chen, Y., Shan, X., Gorfine, H., Dai, F., Wu, Q., Yang, T., Shi, Y., & Jin, X. (2023). Ensemble projections of fish distribution in response to climate changes in the Yellow and Bohai Seas, China. *Ecological Indicators*, *146*, 109759. https://doi.org/https://doi.org/10.1016/j.ecolind.2022.109759

Claireaux, G., Webber, D.M., Lagardère, J.P., and Kerr, S.R. 2000. Influence of water temperature and oxygenation on the aerobic metabolic scope of Atlantic cod (Gadus morhua). *Journal of Sea Research* 44(3-4): 257-265. https://doi.org/10.1016/S1385-1101(00)00053-8

Commander, C. J. C., Barnett, L. A. K., Ward, E. J., Anderson, S. C., & Essington, T. E. (2022). The shadow model: how and why small choices in spatially explicit species distribution models affect predictions. *PeerJ*, *10*, e12783. https://doi.org/10.7717/peerj.12783

Correa, G. M., Monnahan, C. C., Sullivan, J. Y., Thorson, J. T., & Punt, A. E. (2023). Modelling time-varying growth in state-space stock assessments. *ICES Journal of Marine Science*, *80*(7), 2036–2049. https://doi.org/10.1093/icesjms/fsad133

Dambrine, C., Woillez, M., Huret, M., & de Pontual, H. (2021). Characterising Essential Fish Habitat using spatio-temporal analysis of fishery data: A case study of the European seabass spawning areas. *Fisheries Oceanography*, *30*(4), 413–428.

Davies, S. C., Thompson, P. L., Gomez, C., Nephin, J., Knudby, A., Park, A. E., Friesen, S. K., Pollock, L. J., Rubidge, E. M., Anderson, S. C., Iacarella, J. C., Lyons, D. A., MacDonald, A., McMillan, A., Ward, E. J., Holdsworth, A. M., Swart, N., Price, J., & Hunter, K. L. (2023). Addressing uncertainty when projecting marine species' distributions under climate change. *Ecography*, *2023*(11), e06731. https://doi.org/https://doi.org/10.1111/ecog.06731

de Mutsert, K., Steenbeek, J., Lewis, K., Buszowski, J., Cowan Jr, J. H., & Christensen, V. (2016). Exploring effects of hypoxia on fish and fisheries in the northern Gulf of Mexico using a dynamic spatially explicit ecosystem model. *Ecological Modelling*, *331*, 142–150.

Deutsch, C., Ferrel, A., Seibel, B., Pörtner, H.-O., & Huey, R. B. (2015). Climate change tightens a metabolic constraint on marine habitats. *Science*, *348*(6239), 1132–1135.

Deutsch, C., Penn, J. L., & Lucey, N. (2023). Climate, Oxygen, and the Future of Marine Biodiversity. *Annual Review of Marine Science*. https://doi.org/10.1146/annurev-marine-040323-095231

Deutsch, C., Penn, J. L., & Seibel, B. (2020). Metabolic trait diversity shapes marine biogeography. *Nature*, *585*(7826), 557–562. https://doi.org/10.1038/s41586-020-2721-y

DFO Canada. (2024). *Groundfish Concurrent Bottom Trawl Surveys*. https://open.canada.ca/data/en/dataset/a278d1af-d567-4964-a109-ae1e84cbd24a

Di Biagio, V., Martellucci, R., Menna, M., Teruzzi, A., Amadio, C., Mauri, E., & Cossarini, G. (2023). Dissolved oxygen as an indicator of multiple drivers of the marine ecosystem: the southern Adriatic Sea case study. *State of the Planet*, *1*, 1–13.

Diaz, R. J., & Breitburg, D. L. (2009). Chapter 1 The Hypoxic Environment. In J. G. Richards, A. P. Farrell, & C. J. Brauner (Eds.), *Fish Physiology* (Vol. 27, pp. 1–23). Academic Press. https://doi.org/https://doi.org/10.1016/S1546-5098(08)00001-0

Diaz, R. J., & Rosenberg, R. (2008). Spreading Dead Zones and Consequences for Marine Ecosystems. *Science*, *321*(5891), 926–929. https://doi.org/10.1126/science.1156401

Drenkard, E.J., Stock, C., Ross, A.C., Dixon, K.W., Adcroft, A., Alexander, M., Balaji, V., Bograd, S.J., Butenschön, M., Cheng, W. & Curchitser, E. (2021). Next-generation regional ocean projections for living marine resource management in a changing climate. *ICES Journal of Marine Science,* 78(6), 1969-1987.

Eilers, P.H.C. & Marx, B.D. (2021) *Practical Smoothing: The Joys of P-splines.* Cambridge University Press.

Essington, T. E., Anderson, S. C., Barnett, L. A. K., Berger, H. M., Siedlecki, S. A., & Ward, E. J. (2022). Advancing statistical models to reveal the effect of dissolved oxygen on the spatial

distribution of marine taxa using thresholds and a physiologically based index. *Ecography*, *2022*(8), e06249.
Farrell, A. P., & Richards, J. G. (2009). Defining hypoxia: an integrative synthesis of the responses of fish to hypoxia. In *Fish physiology* (Vol. 27, pp. 487-503). Academic Press.
Franco, A. C., Ianson, D., Ross, T., Hamme, R., Monahan, A., Christian, J., Davelaar, M., William, J., Miller, L., Robert, M., & Tortell, P. D. (2021). *A compilation of inorganic carbon system and other hydrographic and chemical discrete profile measurements obtained during the fifty five Line P cruises in the Northeast Pacific Ocean over the period from 1990 to 2019 (NCEI Accession 0234342)*. NOAA National Centers for Environmental Information. https://doi.org/10.25921/zrw8-kn24
Franco, A. C., Kim, H., Frenzel, H., Deutsch, C., Ianson, D., Sumaila, U. R., & Tortell, P. D. (2022). Impact of warming and deoxygenation on the habitat distribution of Pacific halibut in the Northeast Pacific. *Fisheries Oceanography*, *31*(6), 601–614. https://doi.org/10.1111/fog.12610
Fredston, A.L., Cheung, W.W., Frölicher, T.L., Kitchel, Z.J., Maureaud, A.A., Thorson, J.T., Auber, A., Mérigot, B., Palacios-Abrantes, J., Palomares, M.L.D. and Pecuchet, L., 2023. Marine heatwaves are not a dominant driver of change in demersal fishes. *Nature*, *621*(7978): 324-329. https://doi.org/10.1038/s41586-023-06449-y
Fry, F.E.J. 1971. The effect of environmental factors on the physiology of fish. *Fish Physiology* 6: 1-98.
Gillooly, J.F., Brown, J., West, G., Savage, V.M, & Charnov, E.L. (2001). Effects of size and temperature on metabolic rate. *Science,* 293(5538): 2248-2251. https:doi.org/10.1126/science.1061967
Gray, J. S., Wu, R. S., & Or, Y. Y. (2002). Effects of hypoxia and organic enrichment on the coastal marine environment. *Marine Ecology Progress Series*, *238*, 249–279.
Gruber, N., Clement, D., Carter, B., Feely, R., Van Heuven, S., Hoppema, M., Ishii, M., Key, R., Kozyr, A., Lauvset, S., Monaco, C., Mathis, J., Murata, A., Olsen, A., Perez, F., Sabine, C., and Wanninkhof, R. 2019. The oceanic sink for anthropogenic CO_2 from 1994 to 2007. Science, *363*(6432): 1193-1199. https://doi.org/ 10.1126/science.aau5153
Grüss, A., Thorson, J. T., Stawitz, C. C., Reum, J. C. P., Rohan, S. K., & Barnes, C. L. (2021). Synthesis of interannual variability in spatial demographic processes supports the strong influence of cold-pool extent on eastern Bering Sea walleye pollock (Gadus chalcogrammus). *Progress in Oceanography*, *194*. https://doi.org/10.1016/j.pocean.2021.102569
Hao, T., Elith, J., Lahoz-Monfort, J. J., & Guillera-Arroita, G. (2020). Testing whether ensemble modelling is advantageous for maximising predictive performance of species distribution models. *Ecography*, *43*(4), 549–558.
Harris, J., Pirtle, J. L., Laman, E. A., Siple, M. C., & Thorson, J. T. (2024). An ensemble approach to species distribution modelling reconciles systematic differences in estimates of habitat utilization and range area. *Journal of Applied Ecology*, *61*(2), 351–364. https://doi.org/https://doi.org/10.1111/1365-2664.14559
Hauri, C., Schultz, C., Hedstrom, K., Danielson, S., Irving, B., Doney, S. C., Dussin, R., Curchitser, E. N., Hill, D. F., & Stock, C. A. (2020). A regional hindcast model simulating ecosystem dynamics, inorganic carbon chemistry, and ocean acidification in the Gulf of Alaska. *Biogeosciences*, *17*(14), 3837–3857.
Hay, L. E., Wilby, R. L., & Leavesley, G. H. (2000). A comparison of delta change and downscaled GCM scenarios for three mountainous basins in the United States. *Journal of the American*

Water Resources Association, 36(2), 387-397. https://doi.org/10.1111/j.1752-1688.2000.tb04276.x
Hoff, G. R. 2016. Results of the 2016 eastern Bering Sea upper continental slope survey of groundfish and invertebrate resources. U.S. Department of Commerce, NOAA Tech. Memo. NMFS-AFSC-339. http://doi.org/10.7289/V5/TM-AFSC-339
Indivero, J., Anderson, S., Barnett, L., Essington, T. E., & Ward, E. (2024). Estimating a physiological threshold to oxygen and temperature from marine monitoring data reveals challenges and opportunities for forecasting distribution shifts. Ecography, 2025(4): e07413https://doi.org/10.22541/au.172446072.20202938/v1
IPHC. (2022). *IPHC Water Column Profiler Deployment Procedures and Maintenance Guide*. https://www.iphc.int/uploads/pdf/manuals/2022/iphc-2022-wcpm-001.pdf
IPHC. (2024). *Water Column Profiler Data*. https://www.iphc.int/data/water-column-profiler-data/
Joyce, S. (2000). The dead zones: oxygen-starved coastal waters. *Environmental Health Perspectives*, *108*(3), A120–A125. https://doi.org/10.1289/ehp.108-a120
Kearney, K., Hermann, A., Cheng, W., Ortiz, I., & Aydin, K (2020). A coupled pelagic-benthic-sympagic biogeochemical model for the Bering Sea: documentation and validation of the BESTNPZ model (v2019.08.23) within a high-resolution regional ocean model. Geosci Model Dev 13:597–650. https://doi.org/10.5194/gmd-13-597-2020
Kearney, K. (2021). *Temperature Data from the Eastern Bering Sea Continental Shelf Bottom Trawl Survey as Used for Hydrodynamic Model Validation and Comparison*. https://doi.org/10.25923/e77k-gg40
Kearney, M., & Porter, W. (2009). Mechanistic niche modelling: combining physiological and spatial data to predict species' ranges. *Ecology Letters*, *12*(4), 334–350. https://doi.org/https://doi.org/10.1111/j.1461-0248.2008.01277.x
Keeling, R. F., Körtzinger, A., & Gruber, N. (2010). Ocean deoxygenation in a warming world. *Annual Review of Marine Science*, *2*(1), 199–229.
Keller, A. A., Wallace, J. R., & Methot, R. D. (2017). *The northwest fisheries science center's west coast groundfish bottom trawl survey: history, design, and description*.
Kim, H., Franco, A. C., & Sumaila, U. R. (2023). A selected review of impacts of ocean deoxygenation on fish and fisheries. *Fishes*, *8*(6), 316.
Kramer, D. L. (1987). Dissolved oxygen and fish behavior. *Environmental Biology of Fishes*, *18*(2), 81–92. https://doi.org/10.1007/BF00002597
Kristiansen, T., Butenschön, M., & Peck, M. A. (2024). Statistically downscaled CMIP6 ocean variables for European waters. *Scientific Reports*, *14*(1), 1209. https://doi.org/10.1038/s41598-024-51160-1
Kwiatkowski, L., Torres, O., Bopp, L., Aumont, O., Chamberlain, M., Christian, J. R., Dunne, J. P., Gehlen, M., Ilyina, T., & John, J. G. (2020). Twenty-first century ocean warming, acidification, deoxygenation, and upper-ocean nutrient and primary production decline from CMIP6 model projections. *Biogeosciences*, *17*(13), 3439–3470.
Leeuwis, R.H., Nash, G.W., Sandrelli, R. M., Zanuzzo F.S., and Gamperl, A.K. (2019). The environmental tolerances and metabolic physiology of sablefish (*Anoplopoma fimbria*). *Comparative Biochemistry and Physiology, Part A, 231:* 140-148. https://doi.org/10.1016/j.cbpa.2019.02.004.
Li, C., Huang, J., Liu, X., Ding, L., He, Y., & Xie, Y. (2024). The ocean losing its breath under the heatwaves. *Nature Communications*, *15*(1), 6840. https://doi.org/10.1038/s41467-024-51323-8

Li, J., & Heap, A. D. (2014). Spatial interpolation methods applied in the environmental sciences: A review. *Environmental Modelling & Software*, *53*, 173–189. https://doi.org/10.1016/j.envsoft.2013.12.008

Lindén, A., & Knape, J. (2009). Estimating environmental effects on population dynamics: consequences of observation error. *Oikos*, *118*(5), 675–680. https://doi.org/https://doi.org/10.1111/j.1600-0706.2008.17250.x

Lindmark, M., Anderson, S. C., Gogina, M., & Casini, M. (2023). Evaluating drivers of spatiotemporal variability in individual condition of a bottom-associated marine fish, Atlantic cod (Gadus morhua). *ICES Journal of Marine Science*, *80*(5), 1539–1550. https://doi.org/10.1093/icesjms/fsad084

Lindmark, M., Audzijonyte, A., Blanchard, J. L., & Gårdmark, A. (2022a). Temperature impacts on fish physiology and resource abundance lead to faster growth but smaller fish sizes and yields under warming. *Global Change Biology*, *28*(21), 6239–6253. https://doi.org/10.1111/gcb.16341

Lindmark, M., Ohlberger, J., & Gårdmark, A. (2022b). Optimum growth temperature declines with body size within fish species. *Global Change Biology*, *28*(7), 2259–2271.Little, R. J. A., & Rubin, D. B. (2020). *Statistical analysis with missing data* (Third edition). Wiley.

Liu, O. R., Ward, E. J., Anderson, S. C., Andrews, K. S., Barnett, L. A. K., Brodie, S., Carroll, G., Fiechter, J., Haltuch, M. A., Harvey, C. J., Hazen, E. L., Hernvann, P. Y., Jacox, M., Kaplan, I. C., Matson, S., Norman, K., Buil, M. P., Selden, R. L., Shelton, A., & Samhouri, J. F. (2023). Species redistribution creates unequal outcomes for multispecies fisheries under projected climate change. *Science Advances*, *9*(33). https://doi.org/10.1126/sciadv.adg5468

Markowitz, E. H., Dawson, E. J., Wassermann, S. N., Anderson, C. B., Rohan, S. K., Charriere, N. E., & Stevenson, D. E. (2024). Results of the 2023 eastern and northern Bering Sea continental shelf bottom trawl survey of groundfish and invertebrate fauna. U.S. Department of Commerce, NOAA Technical Memorandum NMFS-AFSC-487. https://doi.org/10.25923/2mry-yx09

Matear, R. J., & Hirst, A. C. (2003). Long-term changes in dissolved oxygen concentrations in the ocean caused by protracted global warming. *Global Biogeochemical Cycles*, *17*(4). https://doi.org/https://doi.org/10.1029/2002GB001997

McCarthy, M. J., Newell, S. E., Carini, S. A., & Gardner, W. S. (2015). Denitrification dominates sediment nitrogen removal and is enhanced by bottom-water hypoxia in the Northern Gulf of Mexico. *Estuaries and Coasts*, *38*, 2279–2294.

McGarry, K., Siedlecki, S., Salisbury, J., and Alin, S. 2020. Multiple linear regression models for reconstructing and exploring processes controlling the carbonate system of the Northeast UW from basic hydrographic data. *Journal of Geophysical Research: Oceans, 126*(2): e2020JC016480. https://doi.org/10.1029/2020JC016480

Mercator-Ocean. (2024). *Global Ocean Biogeochemistry Hindcast (v3.6_STABLE)*. Https://Doi.Org/10.48670/Moi-00019.

Mignot, A., D'Ortenzio, F., Taillandier, V., Cossarini, G., & Salon, S. (2019). Quantifying Observational Errors in Biogeochemical-Argo Oxygen, Nitrate, and Chlorophyll a Concentrations. *Geophysical Research Letters*, *46*(8), 4330–4337. https://doi.org/https://doi.org/10.1029/2018GL080541

Moore, C., Drazen, J. C., Radford, B. T., Kelley, C., & Newman, S. J. (2016). Improving essential fish habitat designation to support sustainable ecosystem-based fisheries management. *Marine Policy*, *69*, 32–41.

Morée, A. L., Clarke, T. M., Cheung, W. W. L., & Frölicher, T. L. (2023). Impact of deoxygenation and warming on global marine species in the 21st century. *Biogeosciences*, *20*(12), 2425–2454.

Nakagawa, S. 2015. Chapter 4 Missing data: mechanisms, methods, and messages, in Gordon A. Fox, Simoneta Negrete-Yankelevich, and Vinicio J. Sosa (eds), *Ecological Statistics: Contemporary theory and application*: 81-105. https://doi-org.offcampus.lib.washington.edu/10.1093/acprof:oso/9780199672547.003.0005, accessed 6 June 2025.

Newman, L., Heil, P., Trebilco, R., Katsumata, K., Constable, A., Van Wijk, E., Assmann, K., Beja, J., Bricher, P., Coleman, R. and Costa, D. (2019). Delivering sustained, coordinated, and integrated observations of the Southern Ocean for global impact. *Frontiers in Marine Science*, *6*. https://doi.org/10.3389/fmars.2019.00433

NOAA. (2020). *Oceanographic and Ecosystem Sampling During the Pacific Hake Survey*. https://www.fisheries.noaa.gov/west-coast/science-data/oceanographic-and-ecosystem-sampling-during-pacific-hake-survey#measuring-conductivity-temperature-and-depth

NOAA. (2021a). *Coastal Ocean Data Analysis Product in North America (CODAP-NA, Version 2021) (NCEI Accession 0219960)*. Coastal Ocean Data Analysis Product in North America (CODAP-NA, Version 2021) (NCEI Accession 0219960)

NOAA. (2021b). *NOAA West Coast Ocean Acidification Cruises (WCOA) and Harmful Algal Blooms cruise (NOAA HABs)*. https://www.ncei.noaa.gov/access/ocean-carbon-acidification-data-system/oceans/Coastal/WCOA.html

NOAA. (2024a). *Integrated West Coast Pelagics Survey*. https://www.fisheries.noaa.gov/west-coast/science-data/integrated-west-coast-pelagics-survey

NOAA. (2024b). *National Oceanic and Atmospheric Administration Budget Estimates Fiscal Year 2025*. https://www.noaa.gov/sites/default/files/2024-03/NOAA_FY25_Congressional_Justification.pdf

NOAA Fisheries. (2024). *NOAA Fisheries Announces Changes in its Alaska Survey Portfolio*. https://www.fisheries.noaa.gov/feature-story/noaa-fisheries-announces-changes-its-alaska-survey-portfolio

Oke, K. B., Mueter, F., & Litzow, M. A. (2022). Warming leads to opposite patterns in weight-at-age for young versus old age classes of Bering Sea walleye pollock. *Canadian Journal of Fisheries and Aquatic Sciences*, *79*(10), 1655–1666. https://doi.org/10.1139/cjfas-2021-0315

Oschlies, A., Brandt, P., Stramma, L., & Schmidtko, S. (2018). Drivers and mechanisms of ocean deoxygenation. *Nature Geoscience*, *11*(7), 467–473. https://doi.org/10.1038/s41561-018-0152-2

Pena, M. A., Katsev, S., Oguz, T., & Gilbert, D. (2010). Modeling dissolved oxygen dynamics and hypoxia. *Biogeosciences*, *7*(3), 933–957.

Perruche, C., Szczypta, C., Paul, J., & Drévillon, M. (2024). *Quality Information Document Global Production Centre GLOBAL_MULTIYEAR_BGC_001_029 Issue 1.2*. https://catalogue.marine.copernicus.eu/documents/QUID/CMEMS-GLO-QUID-001-029.pdf

Pörtner, H. O., & Knust, R. (2007). Climate Change Affects Marine Fishes Through the Oxygen Limitation of Thermal Tolerance. *Science*, *315*(5808), 95–97. https://doi.org/10.1126/science.1135471

Pörtner, H.-O. (2010). Oxygen-and capacity-limitation of thermal tolerance: a matrix for integrating climate-related stressor effects in marine ecosystems. *Journal of Experimental Biology*, *213*(6), 881–893.

Pörtner, H.-O., Bock, C., & Mark, F. C. (2017). Oxygen- and capacity-limited thermal tolerance: bridging ecology and physiology. *Journal of Experimental Biology*, *220*(15), 2685–2696. https://doi.org/10.1242/jeb.134585

Pozo Buil, M., Jacox, M. G., Fiechter, J., Alexander, M. A., Bograd, S. J., Curchitser, E. N., Edwards, C. A., Rykaczewski, R. R., & Stock, C. A. (2021). A dynamically downscaled ensemble of future projections for the California current system. *Frontiers in Marine Science*, *8*, 612874. https://doi.org/10.3389/fmars.2021.612874

Risien, C., Hough, K., Waddell, J., Fewings, M., & Cervantes, B. (2024a). *Conductivity–Temperature–Depth (CTD) and dissolved oxygen profile data from shipboard surveys collected within Olympic Coast National Marine Sanctuary, 2005-2023 (v1.0)*. [Data Set]. Zenodo. https://doi.org/10.5281/zenodo.10466124

Risien, C., Hough, K., Waddell, J., Fewings, M., & Cervantes, B. (2024b). *Shipboard Conductivity–Temperature–Depth (CTD) and dissolved oxygen profile data collected during hypoxia surveys along six hydrographic sampling lines within Olympic Coast National Marine Sanctuary, 2004–2015 (v1.0)*. [Data Set]. Zenodo. https://doi.org/10.5281/zenodo.11167853

Risien, C. M., Cervantes, B. T., Fewings, M. R., Barth, J. A., & Kosro, P. M. (2023). A stitch in time: Combining more than two decades of mooring data from the central Oregon shelf. *Data in Brief*, *48*, 109041. https://doi.org/https://doi.org/10.1016/j.dib.2023.109041

Risien, C. M., Fewings, M. R., Fisher, J. L., Peterson, J. O., & Morgan, C. A. (2022). Spatially gridded cross-shelf hydrographic sections and monthly climatologies from shipboard survey data collected along the Newport Hydrographic Line, 1997–2021. *Data in Brief*, *41*, 107922. https://doi.org/https://doi.org/10.1016/j.dib.2022.107922

Roberts, D. R., Bahn, V., Ciuti, S., Boyce, M. S., Elith, J., Guillera-Arroita, G., Hauenstein, S., Lahoz-Monfort, J. J., Schröder, B., Thuiller, W., Warton, D. I., Wintle, B. A., Hartig, F., & Dormann, C. F. (2017). Cross-validation strategies for data with temporal, spatial, hierarchical, or phylogenetic structure. *Ecography*, *40*(8), 913–929. https://doi.org/https://doi.org/10.1111/ecog.02881

Rohan, S. K., Charriere, N. E., Riggle, B., O'Leary, C. A., & Raring, N. W. (2024). *A Flexible approach for processing data collected using trawl-mounted CTDs during Alaska bottom-trawl surveys*. https://repository.library.noaa.gov/view/noaa/55614

Ross, A. C., Stock, C. A., Adcroft, A., Curchitser, E., Hallberg, R., Harrison, M. J., Hedstrom, K., Zadeh, N., Alexander, M., & Chen, W. (2023). A high-resolution physical-biogeochemical model for marine resource applications in the Northwest Atlantic (MOM6-COBALT-NWA12 v1. 0). *Geoscientific Model Development Discussions*, *2023*, 1–65. https://doi.org/10.5194/gmd-16-6943-2023

Rubalcaba, J. G., Verberk, W. C. E. P., Hendriks, A. J., Saris, B., & Woods, H. A. (2020). Oxygen limitation may affect the temperature and size dependence of metabolism in aquatic ectotherms. *Proceedings of the National Academy of Sciences*, *117*(50), 31963–31968. https://doi.org/10.1073/pnas.2003292117

Schmidtko, S., Stramma, L., & Visbeck, M. (2017). Decline in global oceanic oxygen content during the past five decades. *Nature*, *542*(7641), 335–339. https://doi.org/10.1038/nature21399

Sharp, J. D., Fassbender, A. J., Carter, B. R., Johnson, G. C., Schultz, C., & Dunne, J. P. (2022). GOBAI-O 2: temporally and spatially resolved fields of ocean interior dissolved oxygen over nearly two decades. *Earth System Science Data Discussions*, *2022*, 1–46. https://doi.org/10.5194/essd-15-4481-2023

Siple, M. C., von Szalay, P. G., Raring, N. W., Dowlin, A. N., and Riggle, B. C. (2024). Data Report: 2023 Gulf of Alaska bottom trawl survey. AFSC Processed Rep. 2024-09. Alaska Fisheries Science Center, NOAA, National Marine Fisheries Service. https://doi.org/10.25923/gbb1-x748

Steel, E. A., McElhany, P., Yoder, N. J., Purser, M. D., Malone, K., Thompson, B. E., Avery, K. A., Jensen, D., Blair, G., Busack, C., Bowen, M. D., Hubble, J., & Kantz, T. (2009). Making the Best Use of Modeled Data: Multiple Approaches to Sensitivity Analysis of a Fish-Habitat Model. *Fisheries*, *34*(7), 330–339. https://doi.org/https://doi.org/10.1577/1548-8446-34.7.330

Stramma, L., Oschlies, A., & Schmidtko, S. (2012). Mismatch between observed and modeled trends in dissolved upper-ocean oxygen over the last 50 yr. *Biogeosciences*, *9*(10), 4045–4057. https://doi.org/10.5194/bg-9-4045-2012

Stramma, L., Schmidtko, S., Levin, L. A., & Johnson, G. C. (2010). Ocean oxygen minima expansions and their biological impacts. *Deep Sea Research Part I: Oceanographic Research Papers*, *57*(4), 587–595. https://doi.org/https://doi.org/10.1016/j.dsr.2010.01.005

Sullaway, G., Cunningham, C. J., Kimmel, D., Pilcher, D. J., & Thorson, J. T. (2025). Evaluating the performance of a system model in predicting zooplankton dynamics: Insights from the Bering Sea ecosystem. *Fisheries Oceanography*, 34(1), e12691. https://doi.org/10.1111/fog.12691

Sydeman, W. J., García-Reyes, M., Schoeman, D. S., Rykaczewski, R. R., Thompson, S. A., Black, B. A., & Bograd, S. J. (2014). Climate change and wind intensification in coastal upwelling ecosystems. *Science*, *345*(6192), 77–80. http://www.jstor.org.offcampus.lib.washington.edu/stable/24744817

Thompson, P. L., Nephin, J., Davies, S. C., Park, A. E., Lyons, D. A., Rooper, C. N., Angelica Peña, M., Christian, J. R., Hunter, K. L., & Rubidge, E. (2023a). Groundfish biodiversity change in northeastern Pacific waters under projected warming and deoxygenation. *Philosophical Transactions of the Royal Society B*, *378*(1881), 20220191. https://doi.org/10.1098/rstb.2022.0191

Thompson, P. L., Rooper, C. N., Nephin, J., Park, A. E., Christian, J. R., Davies, S. C., Hunter, K., Lyons, D. A., Peña, M. A., Proudfoot, B., Rubidge, E. M., & Holdsworth, A. M. (2023b). Response of Pacific halibut (Hippoglossus stenolepis) to future climate scenarios in the Northeast Pacific Ocean. *Fisheries Research*, *258*, 106540. https://doi.org/https://doi.org/10.1016/j.fishres.2022.106540

Thorson, J.T. (2019). Measuring the impact of oceanographic indices on species distribution shifts: The spatially varying effect of cold-pool extent in the eastern Bering Sea. *Limnology and Oceanography, 64*(6): 2632-2645. https://doi.org/10.1002/lno.11238

Thorson, J.T., Arimitsu, M.L., Barnett, L.A.K., Cheng, W., Eisner, L.B., Haynie, A. C., Hermann, A.J., Holsman, K., Kimmel, D. G., Lomas, M. W., Richar, J., & Siddon, E. (2021). Forecasting community reassemblage using climate-linked spatio-temporal ecosystem models. *Ecography, 44*(4): 612-625. https://doi.org/10.1111/ecog.05471

Thorson, J. T., Andrews, A. G. III, Essington, T. E., & Large, S. I. (2024). Dynamic structural equation models synthesize ecosystem dynamics constrained by ecological mechanisms. *Methods in Ecology and Evolution* 15: 744–755. https://doi.org/10.1111/2041-210X.14289

Townhill, B. L., Couce, E., Tinker, J., Kay, S., & Pinnegar, J. K. (2023). Climate change projections of commercial fish distribution and suitable habitat around north western Europe. *Fish and Fisheries*, *24*(5), 848–862. https://doi.org/https://doi.org/10.1111/faf.12773

Ultsch, G.R., Boschung, H., and Ross, M. 1978. Metabolism, critical oxygen tension, and habitat selection in Darters (Etheostoma). *Ecology*, 59(1):99-107. https://doi.org/10.2307/1936635

Valenza, A. N., Altenritter, M. E., & Walther, B. D. (2023). Reconstructing consequences of lifetime hypoxia exposure on metabolism of demersal fish in the northern Gulf of Mexico using otolith

chemistry. *Environmental Biology of Fishes*, *106*(11), 2045–2057. https://doi.org/10.1007/s10641-023-01483-1

Vaquer-Sunyer, R., & Duarte, C. M. (2008). Thresholds of hypoxia for marine biodiversity. *Proceedings of the National Academy of Sciences*, *105*(40), 15452–15457. https://doi.org/10.1073/pnas.0803833105

Vaquer-Sunyer, R., & Duarte, C. M. (2011). Temperature effects on oxygen thresholds for hypoxia in marine benthic organisms. *Global Change Biology*, *17*(5), 1788–1797. https://doi.org/https://doi.org/10.1111/j.1365-2486.2010.02343.x

Verberk, W. C. E. P., Overgaard, J., Ern, R., Bayley, M., Wang, T., Boardman, L., & Terblanche, J. S. (2016). Does oxygen limit thermal tolerance in arthropods? A critical review of current evidence. *Comparative Biochemistry and Physiology Part A: Molecular & Integrative Physiology*, *192*, 64–78.

Verezemskaya, P., Barnier, B., Gulev, S. K., Gladyshev, S., Molines, J., Gladyshev, V., Lellouche, J., & Gavrikov, A. (2021). Assessing Eddying (1/12) ocean reanalysis GLORYS12 using the 14-yr instrumental record from 59.5 N section in the Atlantic. *Journal of Geophysical Research: Oceans*, *126*(6), e2020JC016317.

Wang, Z., Xue, C., & Ping, B. (2024). A Reconstructing Model Based on Time–Space–Depth Partitioning for Global Ocean Dissolved Oxygen Concentration. *Remote Sensing*, *16*(2), 228. https://doi.org/10.3390/rs16020228

Ward, E. J., Hunsicker, M. E., Marshall, K. N., Oken, K. L., Semmens, B. X., Field, J. C., Haltuch, M. A., Johnson, K. F., Taylor, I. G., Thompson, A. R., & Tolimieri, N. (2024). Leveraging ecological indicators to improve short term forecasts of fish recruitment. *Fish and Fisheries*, 25, 895–909. https://doi.org/10.1111/faf.12850

Chapter 4. OXYGEN CONSTRAINS LOCAL DENSITIES ACROSS DIVERSE BOTTOM-ASSOCIATED MARINE FISHES

Publication history: This study was co-authored with Sean C. Anderson, Lewis A.K. Barnett, Samantha Siedlecki, James T. Thorson, Eric J. Ward and Timothy E. Essington. At the time this dissertation was submitted, a version of this chapter was in prep for journal submission.

4.1 ABSTRACT

Dissolved oxygen has often been used to explain the distributions of marine species. However, much of this research has focused on broad-scale biogeographic patterns in species' distributions, rather than how oxygen may constrain densities at local scales, where other ecological processes operate. As ocean oxygen is expected to decline under climate change, understanding possible thresholds to low oxygen at fine spatial scales is vital for fisheries management. Here we evaluate whether and to what extent there is evidence for oxygen limitation on local density in 32 demersal (i.e. bottom-associated) species in the northeastern Pacific Ocean, by combining observational data from five fishery-independent surveys from 2008-–2024 in robust statistical models. We find that more than one-half of fish species showed a threshold relationship between local density and oxygen. Local densities were consistently more reduced by low-oxygen conditions in southern regions (California Current and British Columbia) compared to northern regions (Gulf of Alaska and Eastern Bering Sea). Species with an oxygen threshold spanned a diverse range of taxonomies and ecologies, and estimated thresholds ranged widely across species from ~2—25 kPa. These estimates of the sensitivity of local density to oxygen can help anticipate effects of future deoxygenated oceans on marine ecosystems.

4.2 INTRODUCTION

Understanding the drivers of species' spatial patterns has long been a focus of research in both terrestrial and marine systems[1]. In marine species, oxygen limitation has often been identified as a key determinant of range limits[2,3], past extinctions[4], biodiversity[5], thermal tolerance[6–9], and growth and size[10–12]. There are various metrics for quantifying species' oxygen requirements [7,13,14], but the impacts of oxygen on these dynamics in marine species are generally rooted in fundamental physiological constraints on how temperature and size govern metabolic rate and therefore oxygen demand[15,16]. Given that ocean oxygen is projected to decline over the next century by approximately 1—7%[17–19] , and has already decreased by ~2% globally since 1960[20], the extent to which oxygen requirements can determine species' range limits holds particular importance for projecting the impacts of changing environmental conditions on marine habitats and populations[21].

However, these global assessments of macroecological patterns in oxygen limitation have often overlooked nuances in species' ecology and other environmental processes that can drive

distributional patterns at smaller scales. At a local level, ecological dynamics such as predator-prey interactions[22], food availability[23], and competition[24], as well as other environmental preferences such as temperature[25–27], depth[28], and substrate[29], can also dictate species' local densities and mediate physiological constraints. Species also have a wide potential for local acclimations[30] and adaptations to tolerate environmental conditions. And even above levels that would be physiologically lethal, decreased oxygen can still impact marine species' growth[31,32], behavior [33,34], and avoidance of areas[35]. Fine scale changes in local distributions can have cascading impacts on ecosystem dynamics[36,37], fishing opportunities[38], critical habitat[39], and transboundary fisheries governance[40]. While distributional shifts associated with temperature have been more widely investigated [41–43], deoxygenation may effect distributions even more than temperature and acidification[44] and can profoundly shape ecological systems[45–47]. Yet there is relatively less evidence of the extent to which oxygen shapes local fish distributions.

This limited evidence is partly due to lack of data at scales relevant for these small-scale processes. For example, oxygen thresholds have been measured in laboratory settings with well-defined procedures[48–50]. The physiological complexity of oxygen tolerance means that it is often parameterized with other terms, such as temperature-dependence[7]. There is extensive variability in oxygen tolerance and associated physiological traits between species[51,52], and laboratory data is only available for ~80 of the hundreds of thousands of marine fish species. Additionally, laboratory-derived oxygen thresholds have in some cases not adequately described effects of oxygen on species at local scales[53,54]. For the majority of species, laboratory data therefore often does not provide sufficient information to determine low oxygen tolerances or how oxygen may impact habitat use within their ranges.

Observational data can instead reveal information on associations of fish densities to oxygen in real environmental contexts. However, observational data also does not provide unambiguous information concerning oxygen thresholds that prompt ecological responses. Depth, temperature, and oxygen in particular strongly covary in many ocean systems (Fig 1). This covariance makes it particularly challenging to identify the specific distributional responses associated with oxygen versus depth preferences[55]. Reliable estimates from observational data depend on properly accounting for other measured and unmeasured environmental variables, though these are often not included in analyses[2]. Additionally, empirical estimation requires observational datasets large enough to provide sufficient variation in density and environmental conditions to allow statistical inferences. Yet *in situ* oxygen measurements collected at the time of biological sampling are less frequently available in species' density data, and oceanographic model hindcasts and interpolation techniques that are sometimes used[56] do not adequately capture oxygen dynamics to estimate unbiased and precise oxygen thresholds at local scales[57]. Lastly, the functional form of oxygen should approximate physiological and ecological responses. As described above, oxygen requirements are often temperature-dependent through metabolic constraints, and these parameters are species-specific. Limited laboratory data, as described above, poses difficulties for parameterizing the response. The effect of oxygen on fish is also expected to be non-linear, with a saturating threshold effect[58,59]. Yet research often does not consider these physiological or non-linear structures [38,56,60]. To date, there have been few analyses of observational data of local densities associated with oxygen that fully address these challenges for a wide number of species.

Here, we evaluate whether and to what extent there is evidence for oxygen limitation on local distributions in 32 demersal (i.e. bottom-associated) species in the northeastern Pacific Ocean (eastern Bering Sea through southern California Current, Fig S1) by combining insight from physiological trait and observational data in statistical models. This area is especially relevant as continental shelf ecosystems like this coast contain some of the most valuable fisheries in the world[61] and include a diverse array of fishes and oxygen regimes. We compile data from five fishery-independent surveys from 2008-2024, with over 8,000 observations for each species of density and *in situ* temperature, oxygen, and depth. Fishery-independent data are uniquely useful for statistical inference because they follow standardized grids and protocols and report zero (i.e. absent) catches. Compiling data from multiple surveys provides both high spatial and temporal resolution and wide geographic coverage that spans a range of habitats and climates. While there are not physiological data for the majority of species we evaluate, we take advantage of a recent phylogenetic imputation of oxygen-tolerance traits[51] to correct oxygen for temperature-dependence (i.e. pO_2'). We use correlative species distribution models [51] to fit these data in coastwide and region-specific models. This approach is flexible to address the challenges outlined above, by estimating oxygen effects on local density where statistical robustness is strengthened by accounting for survey catchability effects, measured confounding environmental effects (depth and temperature) and unmeasured (i.e. latent) spatial and spatio-temporal variation. It additionally can consider oxygen as temperature-dependent and in a biologically-informed saturating threshold function. We use fitted models to first identify species with local distributional responses to oxygen, either coastwide or in specific regions. We then use these estimated oxygen thresholds to retrospectively identify spatial and annual patterns in local biomass density (i.e. shifts in distribution, not total population biomass).

4.3 RESULTS

More than one half of fish species (18 out of 32) showed a positive threshold association between local density and oxygen, either coastwide or in at least one region (Fig 1, Table S2). For these species, models with an additional threshold effect of a temperature-corrected oxygen term (pO_2') improved explanation of local densities compared to alternative models that included only baseline effects (catchability terms, latent fields, and depth) or temperature. Most of the species with evidence for an effect of oxygen use shallower habitat (<500 m deep), and only one species, shortspine thornyhead (*Sebastolobus alascanus*), commonly inhabits deeper than 1000 m (Table S1). Species influenced by oxygen spanned different families (e.g. Gadidae, Pleuronectidae, Scorpaenidae), occupied different parts of the water column (benthic, demersal, and semi-pelagic), and included commercially and culturally important species.

To evaluate the threshold below which local fish density is reduced due to pO_2', we calculated ensemble conditional effects from estimated oxygen coefficients in the fitted models. Only species that included pO_2' as a best-fitting model were evaluated. Each species' conditional effect comprises five fitted alternative SDMs: the base and temperature models, and three configurations of pO_2' thresholds. These configurations were fit with pO_2' calculated from three taxon-specific temperature-sensitivity parameters spanning the 95% confidence interval expected from phylogenetic imputation[51]. Temperature-sensitivity terms from laboratory measurements were not available for these species, and a threshold and temperature-sensitivity cannot be uniquely estimated directly from observational data[55]. Rather than selecting a single best-fitting model or

single temperature-sensitivity value for each species, we used ensembling to combine estimated effects and incorporate uncertainty[62] in fish response and in species' temperature sensitivity to oxygen. Ensembled effects were calculated for 100 Monte Carlo simulations drawn from Maximum Likelihood Estimation and averaged by weighting with marginal Akaike Information Criteria (AIC).

There was high variation among species in the ensembled threshold of pO_2' below which local fish density was reduced, ranging from ~2 kPa to as high as 25 kPa (Fig 2). Oxygen thresholds in some species were estimated with relatively low uncertainty (e.g. coastwide yellowtail rockfish, *Sebastes flavidus* and shortspine thornyhead, *Sebastolobus alascanus*), yet with higher uncertainty in others (e.g. coastwide sandpaper skate and pacific cod) (Fig 2). There was generally alignment of estimated thresholds between species' coastwide and region-specific models (Fig S2). More species had evidence for an oxygen threshold in the southern extent of the coast (British Columbia and California Current) than northern (Gulf of Alaska and eastern Bering Sea). In regional models, for instance, oxygen improved models of local fish density for only three species in the Gulf of Alaska (walleye pollock, Pacific cod, and Pacific halibut) and only two species in the eastern Bering Sea (Pacific cod and Pacific halibut) (Table S2). There were also regional differences in spatial variability of oxygen. Oxygen observations were more variable in the California Current and British Columbia (spatial SD=2.8 and 2.3, and spatiotemporal SD=0.8 and 1.4, respectively), than in the Gulf of Alaska and Eastern Bering Sea (spatial SD=1.9 and 0.9, and spatiotemporal SD= 1.4 and 1.2, respectively).

To evaluate retrospective spatial and annual patterns in local fish densities associated with oxygen, we calculated ensembled conditional effects, following the approach above, for coastwide models at all oxygen observations in a compiled database (Indivero et al., in review) from the study period (2008-2024). There were consistent regional differences in oxygen effects (Fig 3), with little evidence for oxygen influencing local fish densities in the Eastern Bering Sea and Gulf of Alaska. Most oxygen observations in the Gulf of Alaska and Eastern Bering Sea were above the oxygen threshold, while most of oxygen observations in the California Current and British Columbia were below (Fig S3). Consequently, there were greater local reductions in fish density associated with oxygen in southern areas compared to northern sections of the coast (Fig 3). And while the proportion of oxygen observations below species' thresholds in each region varied across years, there has not been a consistent temporal trend (Fig S4), and spatial patterns were generally stable over time (e.g. Fig S5). This aligns with patterns in the oxygen data, which had greater persistent spatial variation (SD= ~2.5) than spatio-temporal variation (SD= ~1) (Fig S6). While regional differences in oxygen effects were generally similar, the magnitude of density reduction due to oxygen varied across species. Lingcod and Pacific halibut, for instance, have historically experienced less strong reductions in fish density from oxygen compared to big skate and canary rockfish (Fig 3).

We focused on regions with greater oxygen effects (British Columbia and the California Current) in higher spatial resolution by interpolating oxygen across regional grids (Indivero et al., in review; see Materials and Methods) and similarly calculating ensembled conditional effects of oxygen on local fish density. There were species, spatial, and annual differences in oxygen effects. Big skate, canary rockfish, shortspine thornyhead, silvergray rockfish, and Pacific cod had the greatest estimated reductions in local fish density due to oxygen in these regions (Fig 4). The portion of

the California Current off the coasts of Washington and Oregon experienced particularly strong limiting effects of oxygen on fish density compared to further north in British Columbia, and this was generally consistent across all species (Fig 4). Some species (e.g. shortspine thornyhead and big skate) also showed strong effects in the southernmost area of California (Fig 4). As expected, greater effects of oxygen on fish density were seen further offshore throughout the coast (Fig 4). The amount of area with limited oxygen (i.e. below estimated thresholds) generally increased with increasing depth (Figure S7). For instance, the Washington state coast showed relatively consistent effects latitudinally, but reductions in local density from oxygen increased further offshore (Figure S8).

While oxygen (Fig S9) and the magnitude of reduction in local densities associated with oxygen varied among years in these regions over the study period (2008-2024), there was no clear trend that would signal improving or worsening conditions (Fig S10). However, there were certain years with distinctly increased reductions in local fish density associated with oxygen, such as 2021 (Fig S10, S11). These reductions were most pronounced off the coasts of Oregon and Washington (Fig S12). In 2021, for instance, off the Washington coast fish density reductions due to oxygen were higher and more widespread, and particularly apparent offshore (Fig 5), compared to 2010. For canary rockfish, for example, though in a typical year local fish densities are not strongly reduced by oxygen, in a low oxygen year there is a wide band of limiting oxygen conditions at the deeper edge of their typical depth (Fig 5).

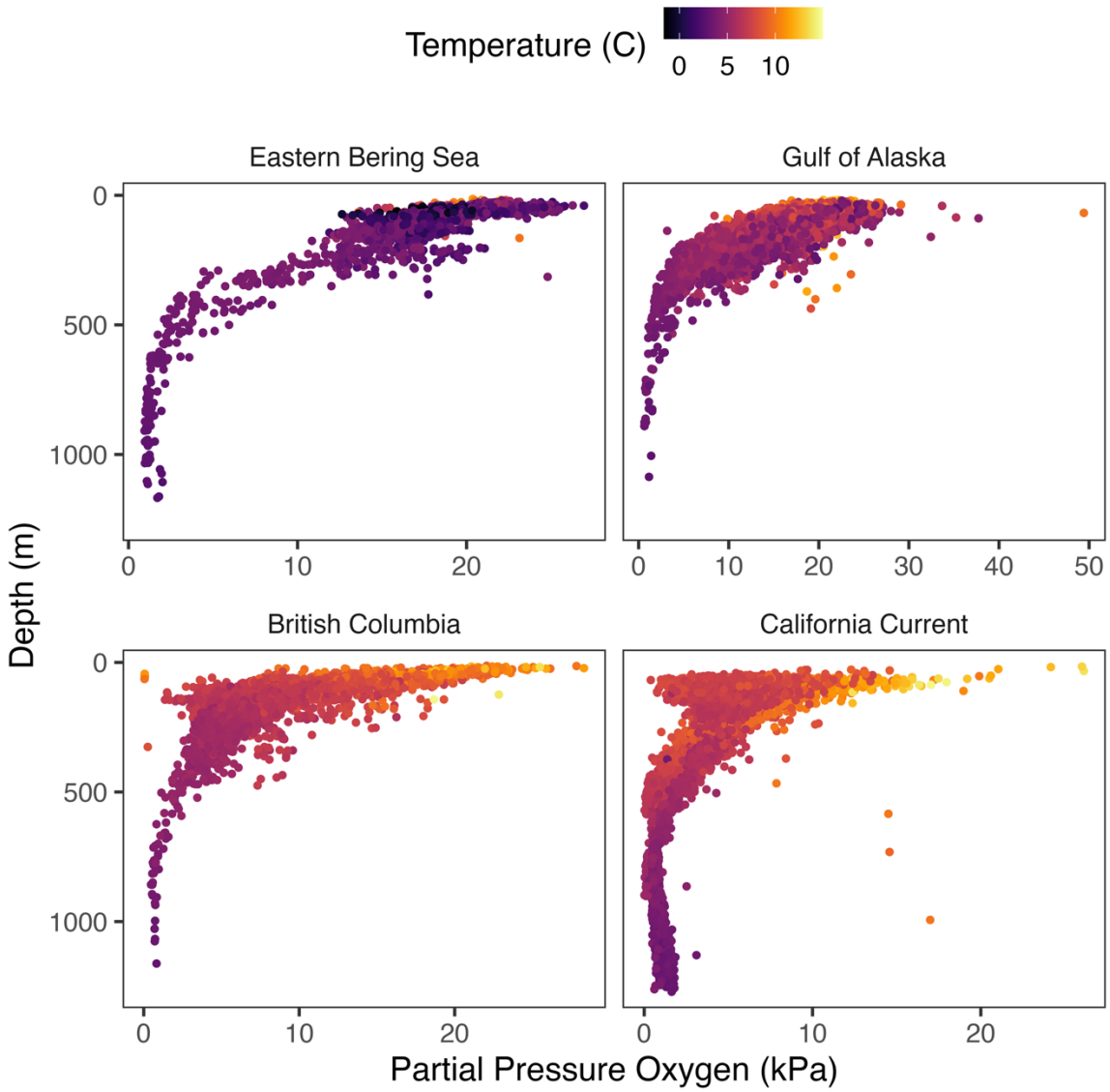

Figure 1. Observations of oxygen and temperature measured *in situ* at the time of fish survey sampling across depths in each region.

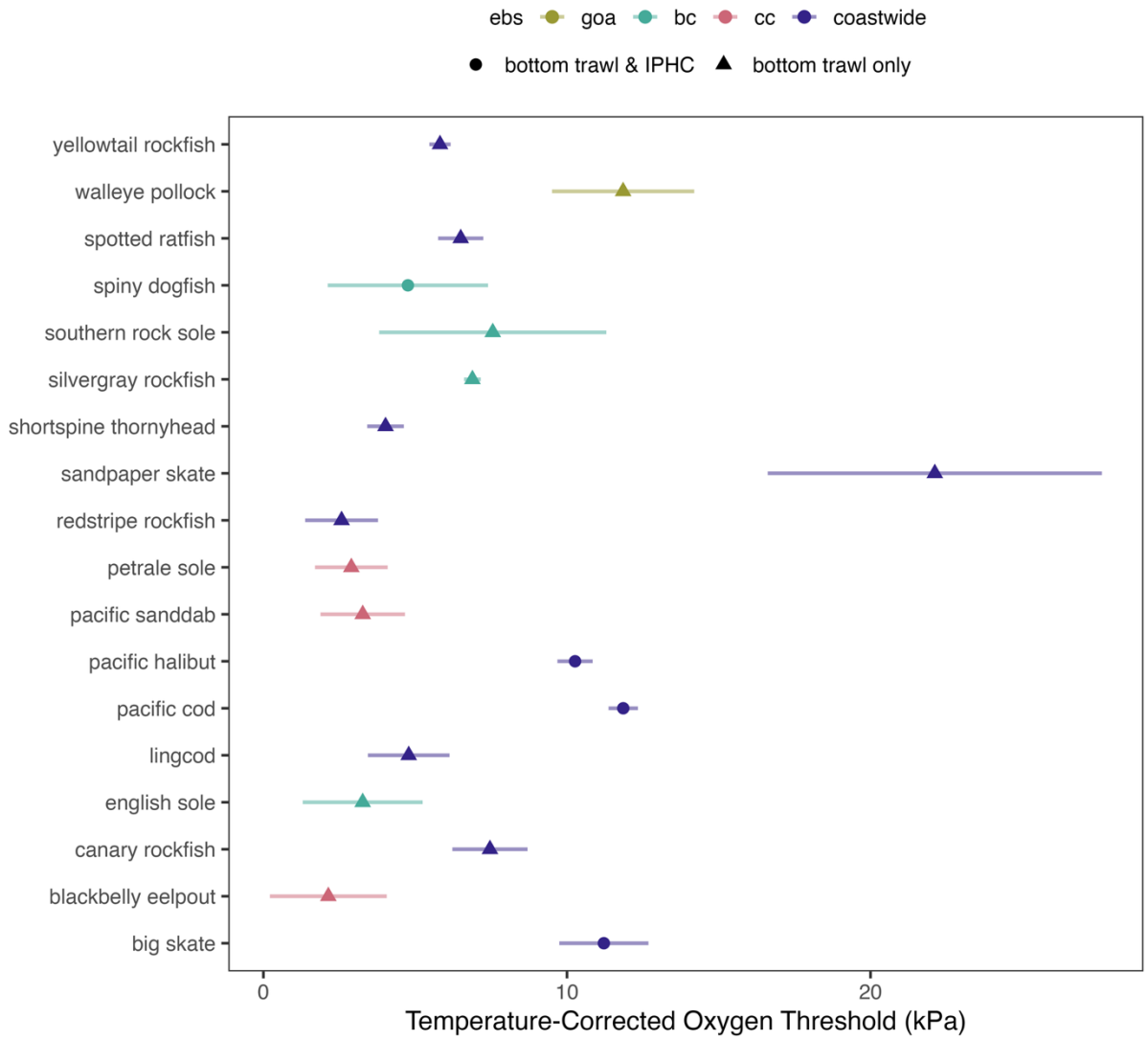

Figure 2. Threshold (± standard error) of the temperature-corrected pO_2 (i.e. pO_2'). Color indicates the geographic extent of the model (region-specific or coastwide). Circles are models fit with both IPHC and bottom trawl data, and triangles are models fit to bottom trawl data only. Thresholds estimates are calculated as the mean ensemble ± standard deviation from the three pO_2' models (low, median, and high E_0) weighted by marginal Akaike Information Criteria (ΔAIC) across 100 Monte Carlo simulations drawn from the mean and standard deviation of the maximum likelihood estimate of the threshold parameter.

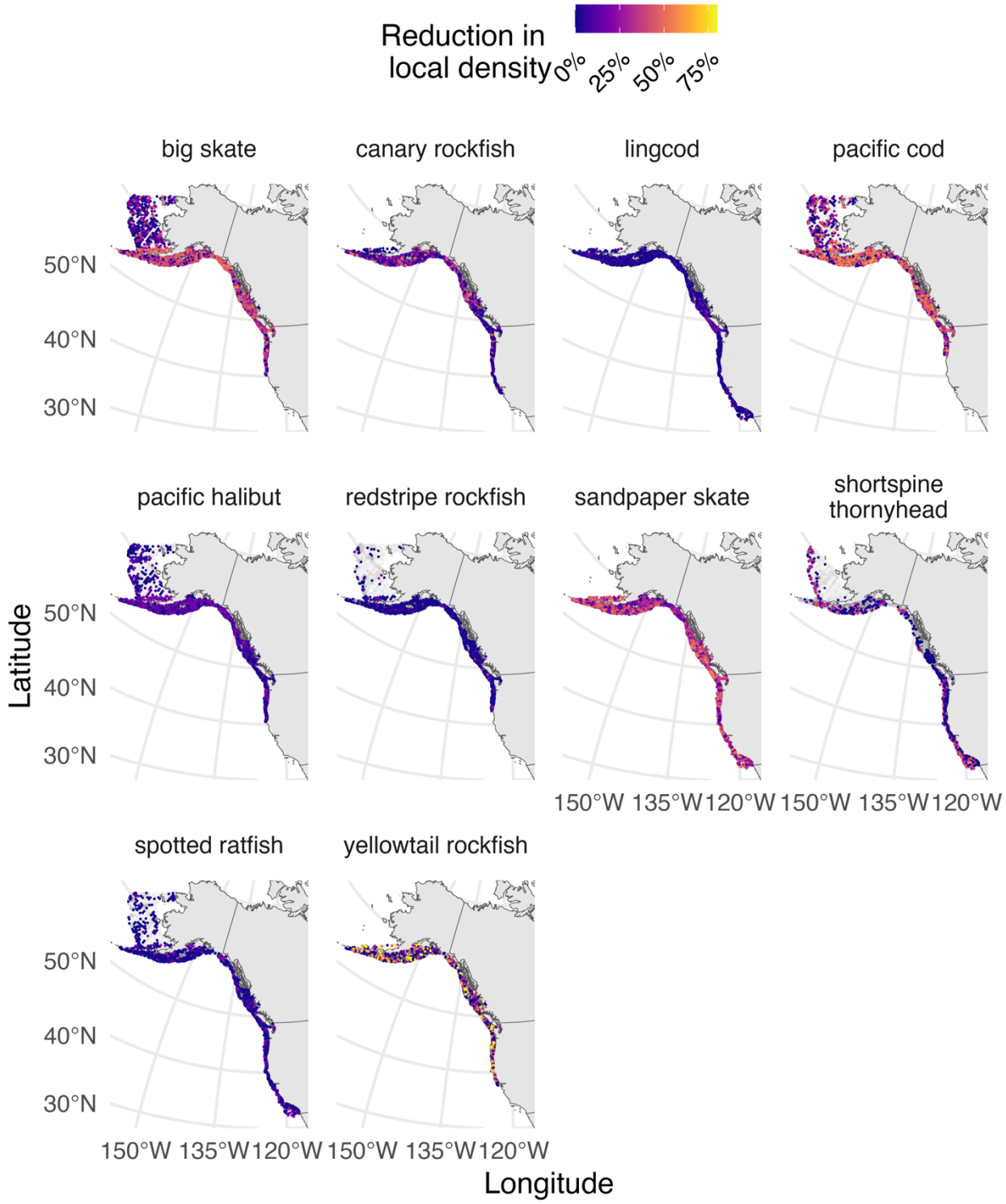

Figure 3. Impact of oxygen on local fish density, expressed as predicted % reduction in local density, at oxygen observations compiled coastwide. Observations across all years of study period (2008-2024) are included. Reductions in density were calculated as the mean conditional effects

ensembled across the five models–base, temperature, and the three breakpoint(pO_2')–with conditional effects weighted by conditional Akaike Information Criteria (AIC) across 100 Monte Carlo simulations of the maximum likelihood estimation of the breakpoint and slope parameters. Only species with a coastwide pO_2' model are included. All other fixed (year, survey, region) and random fields (spatial and spatio-temporal variation) are set to zero. Observations are constrained to the latitudinal range and typical depth habitat (200m buffer deeper than 99% cumulative catch) of each species. Pacific halibut and Pacific cod models were fit to combined bottom trawl and IPHC longline survey, and the remainder of species were fit to only bottom trawl data (NOAA and DFO). Pacific cod was fit to abundance (numbers of fish ha^{-1}) data, and the remainder of species were fit to biomass data (kg ha^{-1}). Grey points indicate there was no estimated density reduction from oxygen at that oxygen observation.

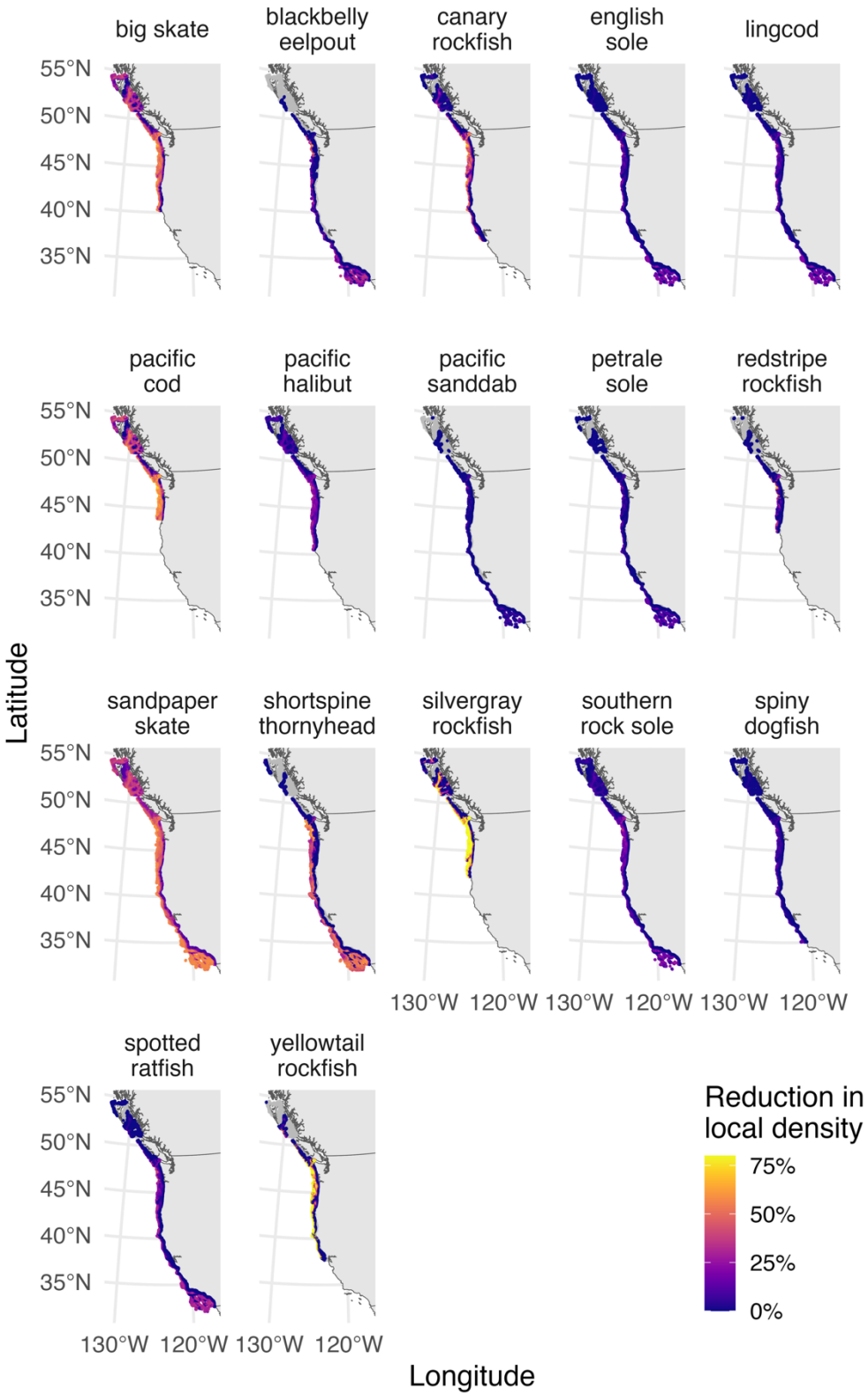

Figure 4. Impact of oxygen on local fish density, expressed as predicted % reduction in local density, at oxygen observations compiled coastwide. in 2021 (a year with hypoxic conditions[63]). Reductions in biomass were calculated as the mean conditional effects ensembled across the five

models–null, temperature, and the three breakpoint(pO_2')–with conditional effects weighted by conditional Akaike Information Criteria (AIC) across 100 Monte Carlo simulations of the maximum likelihood estimation of the breakpoint and slope parameters. All other fixed (year, survey, region) and random (spatial and spatio-temporal variation) effects were set to zero. Observations are constrained to the latitudinal range and typical depth habitat (200m buffer deeper than 99% cumulative catch) of each species. For each species, the model fit to coastwide data and including IPHC data were used if available, otherwise region-specific models were used. Pacific halibut and Pacific cod models were fit to combined bottom trawl and IPHC longline survey, and the remainder of species were fit to only bottom trawl data (NOAA and DFO). Pacific cod was fit to abundance (numbers of fish) data, and the remainder of species were fit to biomass data (kg ha^{-1}). Grey indicates there was no estimated density reduction from oxygen. Oxygen was statistically interpolated across the grid from compiled *in situ* oxygen observations (Indivero et al, in review).

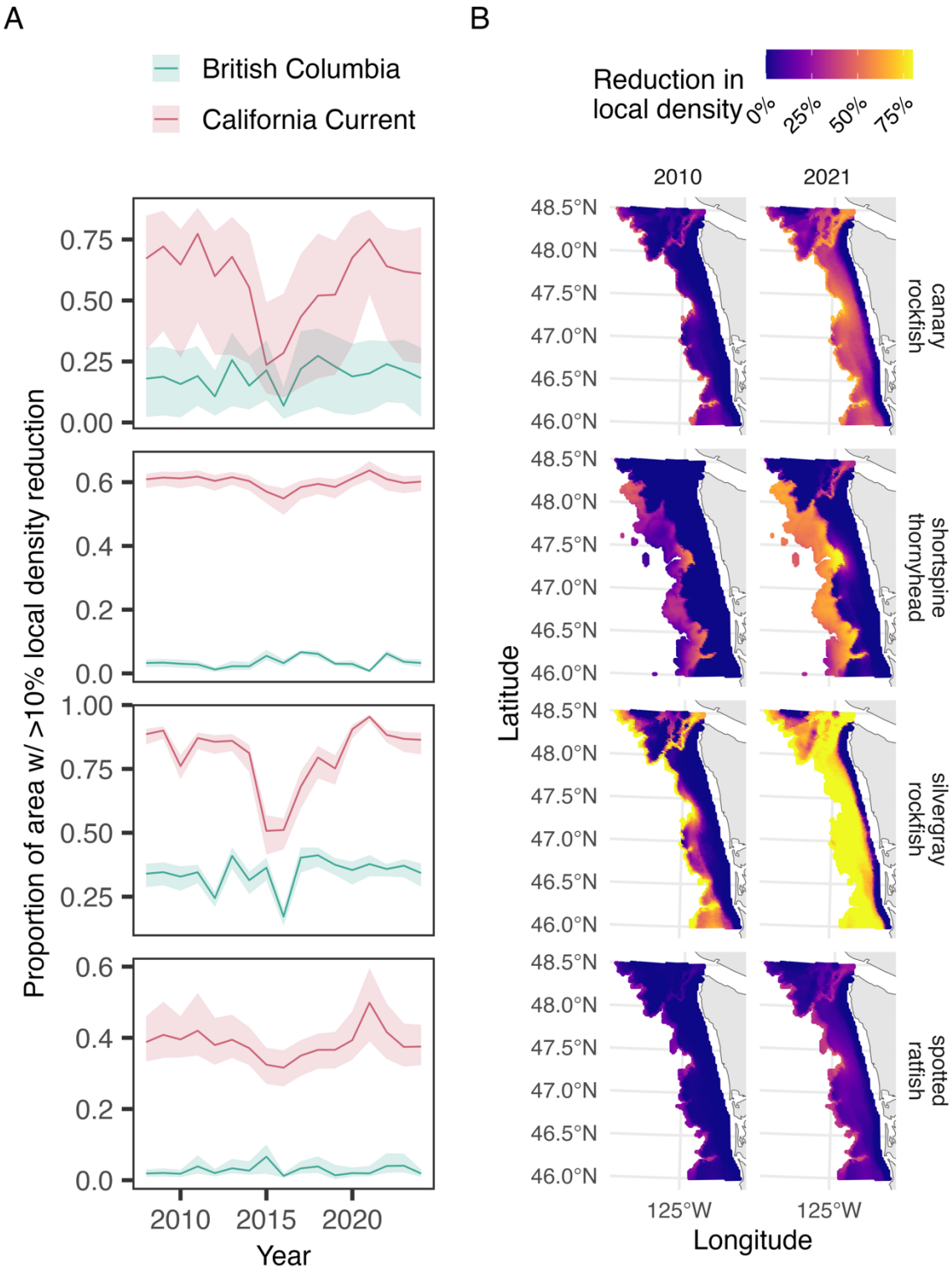
A
British Columbia
California Current
Proportion of area w/ >10% local density reduction
0.75
0.50
0.25
0.00
0.6
0.4
0.2
0.0
1.00
0.75
0.50
0.25
0.6
0.4
0.2
0.0
2010
2015
2020
Year
B
Reduction in local density
0%
25%
50%
75%
2010
2021
48.5°N
48.0°N
47.5°N
47.0°N
46.5°N
46.0°N
canary rockfish
shortspine thornyhead
silvergray rockfish
spotted ratfish
Latitude
125°W
125°W
Longitude

Figure 5. A) Proportion of area ± standard deviation across California Current and British Columbia survey grids that historical oxygen is estimated to be associated with greater than 10% reduction in local fish density, and B) Comparison of impact of oxygen on local fish density, expressed as predicted % reduction in local density, at in a recent year with hypoxic conditions (2021) versus less hypoxic year (2010) for four example species along the Washington state coast. Grid cells are constrained to the latitudinal range and typical depth habitat (200m buffer deeper than 99% cumulative catch) of each species. Reductions in density were calculated as the mean conditional effects ensembled across the five models–null, temperature, and the three breakpoint(pO2')–with conditional effects weighted by marginal Akaike Information Criteria (AIC) across 100 Monte Carlo simulations of the maximum likelihood estimation of the breakpoint and slope parameters. All other fixed (year, survey, region) and random fields (spatial and spatio-temporal variation) are set to zero.

4.4 DISCUSSION

We found evidence for oxygen limitation on local densities across a wide variety of demersal fish species evaluated in the northeastern Pacific Ocean from 2008-2024. Oxygen limitation has often been used to explain biogeographic patterns in species' range edges[2,3,7], but this work has often failed to account for local ecological and environmental processes that may also shape species' densities at finer scales. Our study expanded on existing research in several ways. We conducted a comprehensive treatment of oxygen sensitivity for a diverse suite of demersal species, combining standardized data from multiple fishery-independent surveys with high spatial and temporal resolution of fish densities and oxygen conditions across a wide geographic area. These data were analyzed in statistical models that considered the high dimensionality of species' habitat and environmental preferences and the physiological temperature-dependence of oxygen tolerance. By providing ways for variability in species density to be explained by other drivers and processes, we conservatively estimate the extent to which local fish density could be associated with oxygen. Some, but not all, groundfish species evaluated in the northeastern Pacific Ocean showed evidence for an effect of oxygen on local distributions.

Fishes in our study widely differed in the magnitude of their response to oxygen conditions. Species that showed evidence for an oxygen threshold spanned a variety of taxonomies and ecologies. Those with limiting effects included rockfishes, flatfishes, and gadids, and across ecological niches. One relatively consistent pattern is that species that commonly live in deeper water (below 1000m) were less likely to have evidence for a limiting effect of oxygen on abundance, as only one deeper-living species (shortspine thornyhead) had support for an oxygen threshold. It is likely that species adapted to deep habitat, with naturally limited oxygen, are able to tolerate these low oxygen conditions[64] or rapidly acclimate[30].

Among species with evidence for an association of oxygen and density, there was a wide range of oxygen thresholds below which species' local densities were reduced, ranging from 3-25 kPa (~4-32 μmol kg^{-1}). Laboratory studies have similarly found high heterogeneity in hypoxia tolerance across taxonomies[50–52]. Sablefish, for instance, were measured to have a loss of equilibrium at 6 μmol kg^{-1} (at 12 C; $pO_{2,\,crit}$ of 44 μmol kg^{-1})[65], while Atlantic cod at 52-58 μmol kg^{-1}[66]. Hypoxia is

typically defined at a level (<60 μmol kg^{-1}, or ~47 kPa at 500m and 12° C) higher than the distributional thresholds we estimated from observational data. Yet here we are evaluating oxygen thresholds as the level of oxygen below which are reductions in local densities, i.e. a distributional response, rather than physiological limits. As there are no laboratory data on oxygen tolerance for the majority of the species in our study, we cannot compare these distributional thresholds directly to laboratory-measured physiological limits. Because there appear to be idiosyncratic oxygen tolerances across taxa, there was no straightforward way to flag species that may be oxygen-limited. While biogeographic theories of oxygen limitation tend to assume it is universally applicable to species, we find a wide variety of realized responses to oxygen at local scales.

There were also distinct regional differences in exposure to potentially limiting oxygen in the last few decades that may indicate areas with higher vulnerability to low oxygen. In more poleward regions (eastern Bering Sea and Gulf of Alaska), oxygen levels in our dataset have been consistently high compared to more southly sites. The Arctic is warming faster than average[67] and has experienced heatwaves[68] that are likely to increase in frequency[69]. Increased temperatures may increase fishes' oxygen demand. Yet in our dataset, we observed that oxygen levels were generally well above estimated thresholds associated with constraints on local densities, even accounting for the temperature-dependence of oxygen demand. Conversely further south, the California Current naturally experiences depleted oxygen conditions due to upwelling processes[70] and higher variability[71], such as the 2021 hypoxic event in the California Current[63] during our study period. Oxygen is expected to decline in the California Current[72] and British Columbia [73] under future climate scenarios. Considering the effect of oxygen on local densities—not just temperature—may more accurately project species' responses to climate change. Prioritizing the evaluation of species' association with oxygen in regions known to experience low oxygen conditions, such as the eastern tropical Pacific and Atlantic[74] and tropical reefs[75], can help target research efforts to anticipate effects of hypoxia in the regions where it may be of particular concern.

These regional differences additionally highlight the challenge of detecting associations between species' densities and environmental conditions when limiting thresholds are rarely experienced. For species that did not show evidence for association between oxygen and local density, oxygen conditions may not have dropped below their tolerances, at least during the spatial and seasonal extent of the bottom trawl and longline surveys and in the time period of our study. The fish surveys are also conducted in the summer, when oxygen conditions have likely already seasonally deteriorated and fish may have already re-distributed to suitable oxygen habitats. Together these circumstances may have made it more difficult to detect effects by reducing contrast in the fish and oxygen data. Our approach spatially expanded the data available for estimation, by combining standardized data from multiple independent surveys and accounting for catchability differences in statistical models. While there was patchy regional coverage between years, oxygen data varied more in persistent spatial patterns than annually. For instance, oxygen conditions were consistently high in the eastern Bering Sea, and region-specific oxygen thresholds were not detected for most species in this region. However by combining data coastwide to encompass more of a species' range, we were able to estimate a distributional threshold with oxygen for more species than would models fit to regional data only. Predicting future ecological responses can be particularly challenging when ecosystems experience novel conditions that are unprecedented and non-analogous to existing historical datasets [76,77]. In smaller datasets, it is more likely that critical information on limitation are missing or are present in only a portion of the full time series.

Combining sources to expand datasets may encompass more environmental extremes and reduce extrapolation to novel environmental conditions.

Changes in species' spatial distributions are a commonly documented outcome of climate change in both terrestrial and aquatic environments[78]. Research tracking species' shifts has primarily focused on rising temperatures as the driver[79,80]. Yet oxygen dynamics in the ocean are also expected to be profoundly altered[17–19]. Here we add to the growing body of research[53,54,56,60,81] that for some marine species, sensitivity to low oxygen may be an additional trait that shapes some species' responses to climate change. Changes in species' densities at small scales can disrupt ecosystem dynamics[36]. For instance, diverging species' responses to low oxygen may alter community interactions[82] such as predator—prey , competition, and host—parasite[83] dynamics, following habitat compression[84,85] or spatial mismatch[38,86]. These local density changes may also have implications for fisheries management, as they can reduce or redistribute fishing opportunities[38], increase bycatch risk[87], and challenge transboundary governance[40,88].

Using robust statistical frameworks can disentangle the environmental associations of densities at small scales. While there is a rich body of theory and laboratory research on physiological constraints on oxygen limitation in marine species, researchers have often failed to consider the context of local conditions when using observational data to evaluate the effect of oxygen on local density. Yet distributions are determined by various ecological factors, not just physiological limits, and oxygen is highly correlated with other environmental processes, such as temperature and depth. Failing to include these dynamics in analysis can result in spuriously attributing distribution to oxygen rather than other factors. By considering species densities in a robust statistical framework as we used here, we can directly account for certain effects and to include latent fields for other unobserved ecological or ecosystem processes. This approach is flexible to include the specific processes and biases in other systems and datasets. Researchers can therefore take advantage of publicly available and large datasets to better understand the patterns of oxygen limitation and other environmental drivers at the finer scales that matter for ecological processes and management decisions.

4.5 Materials and Methods

Data

We selected 32 species of demersal (bottom-associated) fishes that were well-sampled and wide-ranging, with at least 50 positive catches in at least two regions in the northeastern Pacific Ocean. Species represent a range of depth preferences, latitudinal distributions, ecological niches, commercial target and bycatch species, and cultural significance (See Table S1 for full species list).

We combined data from scientific bottom trawl surveys from the Eastern Bering Sea through southern California: the U.S. National Oceanic and Atmospheric Administration Gulf of Alaska[89], eastern and northern Bering Sea continental shelf[90], eastern Bering Sea continental slope[91], and U.S. West Coast[92] surveys; and the Department of Fisheries and Oceans Canada (DFO) British Columbia Groundfish Concurrent Bottom Trawl Surveys in Queen Charlotte Sound, Hecate Strait, West Coast Vancouver Island, West Coast Haida Gwaii, and the Strait of Georgia[93,94]. We also

included the International Pacific Halibut Commission fishery-independent set survey (FISS)[95] (Fig S1, Fig S13). The bottom trawl survey catch data is reported as catch-per-unit effort in biomass (kg ha^{-1}) and abundance (numbers ha^{-1}). More detailed explanations of survey protocols and data harmonization of bottom trawl surveys can be found in Ward et al. [96].

While the IPHC FISS is designed to survey Pacific halibut, it collects catch data on additional species. Typically the first 20 hooks of each 100-hook skate are observed, and data are then extrapolated to all hooks observed from this subsample. We included IPHC FISS data for only eight species that are considered well-sampled by the FISS survey: *Anoplopoma fimbria* (sablefish), *Gadus macrocephalus* (pacific cod), *Sebastes ruberrimus* (yelloweye rockfish), *Caliraja rhina* (longnose skate), *Caliraja binoculata* (big skate), *Squalus suckleyi* (spiny dogfish), and *Sebastes aleutianus* (rougheye rockfish). Catch-per-unit-effort for Pacific halibut is reported in biomass (kg $hook^{-1}$) and all other species in abundance (numbers $hook^{-1}$). All data are corrected with site-specific hook competition adjustment factors[97].

For each species, data were included for model fitting only in the species typical depth habitat (up to the depth at 99% cumulative biomass in the complete coastwide data, Fig S14, Table S1) and latitudinal range (up to the northern latitude at the 99% cumulative biomass in the eastern Bering Sea, and down to the southern latitude at the 99% cumulative biomass within the California Current; Fig S15, Table S1). Data were constrained to species' typical depth and range limits because we were interested in evaluating the thresholds below which local density is reduced within a species' range, and it is assumed that factors beyond the scope of this modeling effort contribute to depth and latitudinal range edges.

We used temperature and oxygen *in situ* observations measured concurrently with sampling events during fish surveys. Only fish catch observations with concurrent temperature and oxygen observations were included in model fitting. There are not oxygen data for all years of fish catch surveys, and this consequently limited years of data available for model fitting. However, we use *in situ* data, rather than interpolating missing values or using oceanographic model hindcasts, to prioritize the precision of the oxygen conditions at the time of bottom trawl sampling for ecological inference, as other methods introduce sufficient variation to bias threshold estimates[57].

We transformed oxygen to account for the interactive effect of oxygen and temperature as described by the metabolic index[7]. The critical oxygen partial pressure below which an organism's metabolic rate is unsustainable (P_{crit}) is a widely used measure of hypoxia tolerance[98]. In log space, P_{crit} is linear with inverse temperature[53]. Additional terms that scale the metabolic index (A_o and B^n) are inseparable when estimated in a threshold function[55]. We therefore instead transform each oxygen observation $pO_{2,i}$ with the terms of the metabolic index that depend on pO_2 and temperature to calculate a temperature-dependent pO_2 (i.e. $pO_2{}'$) following an Arrhenius equation:

$$pO_{2,i}{}' = pO_{2,i} \exp\left[\frac{E_0}{k_b}\left(\frac{1}{T_i} - \frac{1}{T_{ref}}\right)\right] \quad \text{Eq. 1}$$

where E_0 is an estimated parameter that describes the temperature dependence of the ratio of oxygen supply to demand, k_b is Boltzmann's constant, and T_{ref} is a reference temperature (here chosen as 12 C). Both T and T_{ref} are in Kelvin units in Eq. 1. Previous work has shown that the

temperature-sensitivity and hypoxia thresholds cannot be uniquely estimated from distribution data[55], and there is not experimental laboratory data on the E_0 parameter for the 32 species in this study. We instead draw the E_0 parameter for each species from a phylogenetic imputation of metabolic index traits[51]. For each species, pO_2' was calculated with three E_0 values. We used the median, low 90th percentile, and high 90th percentile for the lowest taxonomic group available, usually family (see Table S1). We calculate $pO_{2,i}{}'$ for each of the three E_0 values.

Model Fitting

For each species, data were fit to five spatial statistical models using sdmTMB[99] for each region separately (Eastern Bering Sea, Gulf of Alaska, British Columbia, and California Current) and combined coastwide data. The five models are a base model, temperature, and three configurations of temperature+oxygen. The details are described below. The base SDM model is a generalized linear mixed effects model (Eq. 2 for coastwide and Eq. 3 for region-species) that estimates the expected density μ of observation i with a log link,

$$\text{Coastwide: } \log(\mu_i) = b_{y[i]}y_i + b_2 d_i + b_3 d_i^2 + b_4 d_i^3 + b_{r[i]}r_i + \omega_i \quad \text{Eq. 2}$$

$$\text{Region: } \log(\mu_i) = b_{y[i]}y_i + b_2 d_i + b_3 d_i^2 + b_4 d_i^3 + \omega_i + \varepsilon_i \quad \text{Eq. 3}$$

$$C_i \sim \text{Tweedie}(\mu_i, \phi, p) \quad \text{Eq. 4}$$

where b_y are independent year effects for each year y_i; b_2, b_3, and b_4 are the estimated effects of scaled log(depth) (d_i), its square (d_i^2), and its cube. By scaled, we mean we subtracted by the mean and divided by one standard deviation. Depth is included because fish have depth preferences separate from other environmental conditions[100]. Coastwide models also include fixed effect b_r of region. Species whose datasets include IPHC data in addition to bottom trawl data have an additional fixed effect for survey type included in both coastwide and region models, essentially calculating a fishing-power correction (i.e. catchability ratio) for each survey relative to the base level of the fixed effect term. Both region and coastwide models include ω_i, a spatial random effect that accounts for spatially structured latent variables. Region-specific models also include spatio-temporal random effect ε_i to account for annual changes in spatially structured latent fields, that treat effects in each year as independent and identically distributed. Spatial and spatio-temporal random effects are modeled with the stochastic partial differential equation (SPDE) approximation to Gaussian random fields via Gaussian Markov random fields (GMRFs)[101] and implemented in TMB[102]. The GMRF estimates spatial covariance with a Matern covariance function and anisotropy at a set of vertices (i.e. knots) and projects to the locations of data observations via bilinear interpolation. Because initial testing showed computational challenges estimating spatio-temporal random fields with very patchy data for many species (Fig S16), spatio-temporal fields were included in region-specific models but not coastwide models. We model the observed catch rate C_i to follow a Tweedie distribution [103,104], with power parameter p ($1 < p < 2$) and scale parameter ϕ (Eq. 4). The Tweedie distribution is flexible to account for the large number of zeroes in catch rate data without requiring a delta or hurdle two-part model.

To test if including temperature and oxygen improve estimation of fish density, we add temperature and oxygen terms to the base model described above. We add temperature as a scaled quadratic effect[105]. We consider oxygen as the temperature-dependent oxygen pO_2' as a "breakpoint" function, and test three separate models with pO_2' calculate from the low, median, and high expected temperature-sensitivity. The breakpoint function relates a slope β on the

predictor variable, x, (i.e. pO_2') up until the breakpoint of the predictor variable x_{bp}, on the expected value of the response variable:

$$g(x) = \begin{cases} x\beta & if\ x < x_{bp} \\ x_{bp}\beta & otherwise \end{cases} \quad \text{Eq. 5}$$

Slope was constrained to be positive, and breakpoint estimates that were outside the range of oxygen values in the data and with 0 slope estimate (i.e. no effect of oxygen on fish density) were assumed to have no breakpoint effect of oxygen.

Within each dataset (coastwide and each of the region-specific models) for each species, we evaluated the suite of five models with conditional Akaike Information Criteria[106] (ΔAIC). Only models that passed convergence and diagnostics checks were included in model comparison.

Evaluation of oxygen effects

If a pO_2' model improved fitting species density (i.e. ΔAIC=0 for that model) over the base and temperature-only models, we evaluated the conditional effects of pO_2' on fish density. For each species, we show results for the coastwide model if available, or region-specific if oxygen was only included in best-fitting model in a particular region. For species with IPHC data available, we show results for the model that included both bottom trawl and IPHC data. See Table S2 and Supplemental Fig S6 and S7 for comparisons of coastwide and regional models and data types. Conditional effects were calculated with model ensembles of the five model (base, temperature, and three breakpoint pO_2' models), weighted by ΔAIC. To account for uncertainty in model estimation, we used Monte Carlo simulation with 100 iterations. For each iteration, we generated a draw of the pO_2' parameters (the slope and threshold values of the breakpoint function) from the multivariate normal approximation to the distribution for the threshold and slope parameters (i.e. the mean and standard error of the maximum likelihood estimation). All other fixed and random effects in the model were set to zero. We then calculated the ΔAIC-weighted ensemble conditional effect for each iteration. Across all 100 iterations, we then calculate the average and standard deviation of ensembled conditional effects. We use this approach to calculate the ensembled estimates of the threshold term (Fig S5) and conditional effects across oxygen from 0-30 kPa at 12 C (Fig 2, Fig S6).

To compare historical oxygen conditions between regions, we evaluate to what extent fish density was estimated to be reduced due to oxygen from compiled coastwide oxygen observations from 2008-2024. We calculated pO_2' (Eq. 1) from observed dissolved oxygen and temperature in an integrated coastwide oxygen dataset that includes all bottom trawl data, IPHC data, and independent oxygen observations (such as the Newport Line, CODAP, calCOFI, etc.)[57]. Oxygen observations were limited to the species' latitudinal range and typical depth habitat (200m deeper than observed depth limit). The estimated reduction in fish density due to observed pO_2' was then calculated as the mean ensemble conditional effect following the Monte Carlo model-weighting described above.

To evaluate historical spatial and annual patterns in effects of oxygen on fish density at a finer spatial scale in focus regions (the California Current and British Columbia), we used integrated statistical predictions of oxygen observations[57] to interpolate oxygen and temperature to a grid of

each region for each year of the study period (2008-2024) for the middle of the survey period (mid-July). Temperature and oxygen were each interpolated across the grid from observations using a spatial statistical model with a smoother on depth and day-of-year, and spatial and spatio-temporal (IID) random fields, following Indivero et al[57]. We evaluated the conditional effect of oxygen on density at each grid cell in each year, with the same protocol as for coastwide observations above.

4.6 ACKNOWLEDGEMENTS

We thank all survey participants of the NOAA West Coast, Gulf of Alaska, and Bering Sea bottom trawl surveys; Department of Fisheries and Oceans Canada British Columbia Synoptic Bottom Trawl Surveys; and International Pacific Halibut Commission fishery-independent setline survey. This publication was partially funded by Washington Sea Grant grant no. R/SFA-12, and from the Lowell E. Wakefield Professorship. We also thank Jenny Bigman and Chelsea Wood for suggestions on an earlier version of this manuscript.

4.7 REFERENCES

1. Grinnell, J. Field tests of theories concerning distributional control. *Am Nat* **51**, 115–128 (1917).
2. Deutsch, C., Penn, J. L. & Seibel, B. Metabolic trait diversity shapes marine biogeography. *Nature* **585**, 557–562 (2020).
3. Penn, J. L. & Deutsch, C. Geographical and taxonomic patterns in aerobic traits of marine ectotherms. *Philos Trans R Soc Lond B Biol Sci* **379**, 20220487 (2024).
4. Penn, J. L., Deutsch, C., Payne, J. L. & Sperling, E. A. Temperature-dependent hypoxia explains biogeography and severity of end-Permian marine mass extinction. *Science (1979)* **362**, eaat1327 (2018).
5. Sperling, E. A., Frieder, C. A. & Levin, L. A. Biodiversity response to natural gradients of multiple stressors on continental margins. *Proceedings of the Royal Society B: Biological Sciences* **283**, 20160637 (2016).
6. Pörtner, H.-O. Oxygen-and capacity-limitation of thermal tolerance: a matrix for integrating climate-related stressor effects in marine ecosystems. *Journal of Experimental Biology* **213**, 881–893 (2010).
7. Deutsch, C., Ferrel, A., Seibel, B., Pörtner, H.-O. & Huey, R. B. Climate change tightens a metabolic constraint on marine habitats. *Science (1979)* **348**, 1132–1135 (2015).
8. Verberk, W. C. E. P. *et al.* Does oxygen limit thermal tolerance in arthropods? A critical review of current evidence. *Comp Biochem Physiol A Mol Integr Physiol* **192**, 64–78 (2016).
9. Rubalcaba, J. G., Verberk, W. C. E. P., Hendriks, A. J., Saris, B. & Woods, H. A. Oxygen limitation may affect the temperature and size dependence of metabolism in aquatic ectotherms. *Proceedings of the National Academy of Sciences* **117**, 31963–31968 (2020).
10. Verberk, W. C. E. P. *et al.* Shrinking body sizes in response to warming: explanations for the temperature–size rule with special emphasis on the role of oxygen. *Biological Reviews* **96**, 247–268 (2021).
11. Cheung, W. W. L. *et al.* Shrinking of fishes exacerbates impacts of global ocean changes on marine ecosystems. *Nat Clim Chang* **3**, 254–258 (2013).

12. Deutsch, C. *et al.* Impact of warming on aquatic body sizes explained by metabolic scaling from microbes to macrofauna. *Proceedings of the National Academy of Sciences* **119**, e2201345119 (2022).
13. Clarke, T. M. *et al.* Aerobic growth index (AGI): An index to understand the impacts of ocean warming and deoxygenation on global marine fisheries resources. *Prog Oceanogr* **195**, 102588 (2021).
14. Pörtner, H.-O., Bock, C. & Mark, F. C. Oxygen- and capacity-limited thermal tolerance: bridging ecology and physiology. *Journal of Experimental Biology* **220**, 2685–2696 (2017).
15. Gillooly, J., Brown, J., West, G., Savage, V. & Charnov, E. *Effects of Size and Temperature on Metabolic Rate*. https://digitalrepository.unm.edu/biol_fsp (2001).
16. Brown, J. H., Gillooly, J. F., Allen, A. P., Savage, V. M. & West, G. B. Toward a metabolic theory of ecology. in *Ecology* vol. 85 1771–1789 (Ecological Society of America, 2004).
17. Keeling, R. F., Körtzinger, A. & Gruber, N. Ocean deoxygenation in a warming world. *Ann Rev Mar Sci* **2**, 199–229 (2010).
18. Kwiatkowski, L. *et al.* Twenty-first century ocean warming, acidification, deoxygenation, and upper-ocean nutrient and primary production decline from CMIP6 model projections. *Biogeosciences* **17**, 3439–3470 (2020).
19. Matear, R. J. & Hirst, A. C. Long-term changes in dissolved oxygen concentrations in the ocean caused by protracted global warming. *Global Biogeochem Cycles* **17**, (2003).
20. Schmidtko, S., Stramma, L. & Visbeck, M. Decline in global oceanic oxygen content during the past five decades. *Nature* **542**, 335–339 (2017).
21. Cheung, W. W. L., Close, C., Lam, V., Watson, R. & Pauly, D. Application of macroecological theory to predict effects of climate change on global fisheries potential. *Mar Ecol Prog Ser* **365**, 187–197 (2008).
22. Swain, D. P., Benoît, H. P. & Hammill, M. O. Spatial distribution of fishes in a Northwest Atlantic ecosystem in relation to risk of predation by a marine mammal. *Journal of Animal Ecology* **84**, 1286–1298 (2015).
23. Cominassi, L. *et al.* Food availability modulates the combined effects of ocean acidification and warming on fish growth. *Sci Rep* **10**, 2338 (2020).
24. Hansson, S. Competition as a Factor Regulating the Geographical Distribution of Fish Species in a Baltic Archipelago: A Neutral Model Analysis. *J Biogeogr* **11**, 367–381 (1984).
25. Freitas, C., Olsen, E. M., Knutsen, H., Albretsen, J. & Moland, E. Temperature-associated habitat selection in a cold-water marine fish. *Journal of Animal Ecology* **85**, 628–637 (2016).
26. Thorson, J. Forecasting distribution shifts using oceanographic indices: the spatially varying effect of cold-pool extent in the. (2019).
27. Grüss, A. *et al.* Synthesis of interannual variability in spatial demographic processes supports the strong influence of cold-pool extent on eastern Bering Sea walleye pollock (Gadus chalcogrammus). *Prog Oceanogr* **194**, (2021).
28. Freitas, C., Villegas-Ríos, D., Moland, E. & Olsen, E. M. Sea temperature effects on depth use and habitat selection in a marine fish community. *Journal of Animal Ecology* **90**, 1787–1800 (2021).
29. Webster, M. M. & Hart, P. J. B. Substrate discrimination and preference in foraging fish. *Anim Behav* **68**, 1071–1077 (2004).
30. Donelson, J. M., Munday, P. L., McCormick, M. I. & Pitcher, C. R. Rapid transgenerational acclimation of a tropical reef fish to climate change. *Nat Clim Chang* **2**, 30–32 (2012).
31. CHABOT, D. & DUTIL, J.-D. Reduced growth of Atlantic cod in non-lethal hypoxic conditions. *J Fish Biol* **55**, 472–491 (1999).

32. Farrell, A. P. & Richards, J. G. Chapter 11 Defining Hypoxia: An Integrative Synthesis of the Responses of Fish to Hypoxia. in *Fish Physiology* (eds. Richards, J. G., Farrell, A. P. & Brauner, C. J.) vol. 27 487–503 (Academic Press, 2009).
33. Moss, S. A. & McFarland, W. N. The influence of dissolved oxygen and carbon dioxide on fish schooling behavior. *Mar Biol* **5**, 100–107 (1970).
34. Hansson, S. Competition as a Factor Regulating the Geographical Distribution of Fish Species in a Baltic Archipelago: A Neutral Model Analysis. *J Biogeogr* **11**, 367–381 (1984).
35. McKenzie, D. J. & Farrell, A. P. Encyclopedia of fish physiology. (2011).
36. Goodman, M. C. *et al.* Shifting fish distributions impact predation intensity in a sub-Arctic ecosystem. *Ecography* **2022**, e06084 (2022).
37. Stuart-Smith, R. D., Mellin, C., Bates, A. E. & Edgar, G. J. Habitat loss and range shifts contribute to ecological generalization among reef fishes. *Nat Ecol Evol* **5**, 656–662 (2021).
38. Liu, O. R. *et al.* Species redistribution creates unequal outcomes for multispecies fisheries under projected climate change. *Sci Adv* **9**, (2023).
39. Champagnat, J., Brown, E. J., Rivot, E. & Le Pape, O. Modelling the impact of hypoxia on critical essential fish habitats throughout the life cycle of exploited marine species. *ICES Journal of Marine Science* **82**, fsae178 (2025).
40. Pinsky, M. L. *et al.* Preparing ocean governance for species on the move. *Science* vol. 360 1189–1191 Preprint at https://doi.org/10.1126/science.aat2360 (2018).
41. Lawlor, J. A. *et al.* Mechanisms, detection and impacts of species redistributions under climate change. *Nat Rev Earth Environ* **5**, 351–368 (2024).
42. Sunday, J. M., Bates, A. E. & Dulvy, N. K. Thermal tolerance and the global redistribution of animals. *Nat Clim Chang* **2**, 686–690 (2012).
43. Fredston, A. *et al.* Range edges of North American marine species are tracking temperature over decades. *Glob Chang Biol* **27**, 3145–3156 (2021).
44. Sampaio, E. *et al.* Impacts of hypoxic events surpass those of future ocean warming and acidification. *Nat Ecol Evol* **5**, 311–321 (2021).
45. Wu, R. S. S. Hypoxia: from molecular responses to ecosystem responses. *Mar Pollut Bull* **45**, 35–45 (2002).
46. Diaz, R. J. & Rosenberg, R. Spreading Dead Zones and Consequences for Marine Ecosystems. *Science (1979)* **321**, 926–929 (2008).
47. Deutsch, C., Penn, J. L. & Lucey, N. Climate, oxygen, and the future of marine biodiversity. *Ann Rev Mar Sci* **16**, 217–245 (2024).
48. Ultsch, G. R., Boschung, H. & Ross, M. J. Metabolism, Critical Oxygen Tension, and Habitat Selection in Darters (Etheostoma). *Ecology* **59**, 99–107 (1978).
49. Beamish, F. W. H. Standard oxygen consumption: Influence of weight and temperature on respiration of several species. *Can. J. Zool* **42**, 177–188 (1964).
50. Rogers, N. J., Urbina, M. A., Reardon, E. E., McKenzie, D. J. & Wilson, R. W. A new analysis of hypoxia tolerance in fishes using a database of critical oxygen level (P crit). *Conserv Physiol* **4**, cow012 (2016).
51. Essington, T. E., Thorson, J. T. & Deutsch, C. Remarkable similarity in oxygen tolerance among taxonomically diverse marine taxa revealed through hierarchical analysis. *bioRxiv* 2024.08.23.606857 (2024) doi:10.1101/2024.08.23.606857.
52. Vaquer-Sunyer, R. & Duarte, C. M. Thresholds of hypoxia for marine biodiversity. *Proceedings of the National Academy of Sciences* **105**, 15452–15457 (2008).

53. Essington, T. E. *et al.* Advancing statistical models to reveal the effect of dissolved oxygen on the spatial distribution of marine taxa using thresholds and a physiologically based index. *Ecography* **2022**, (2022).
54. Bandara, R. M. W. J., Curchitser, E. & Pinsky, M. L. The importance of oxygen for explaining rapid shifts in a marine fish. *Glob Chang Biol* **n/a**, e17008 (2023).
55. Indivero, J., Anderson, S., Barnett, L., Essington, T. E. & Ward, E. Estimating physiological mechanisms from monitoring data reveals challenges and opportunities for forecasting distribution shifts. (2024) doi:10.22541/au.172446072.20202938/v1.
56. Thompson, P. L. *et al.* Groundfish biodiversity change in northeastern Pacific waters under projected warming and deoxygenation. *Philosophical Transactions of the Royal Society B* **378**, 20220191 (2023).
57. Indivero, J. *et al.* Skill testing oxygen data for distribution modeling of marine species. *Fish Oceanogr* (2025) doi:10.1111/fog.70005.
58. Kramer, D. L. Dissolved oxygen and fish behavior. *Environ Biol Fishes* **18**, 81–92 (1987).
59. FRY, F. E. J. 1 - The Effect of Environmental Factors on the Physiology of Fish. in *Fish Physiology* (eds. Hoar, W. S. & Randall, D. J.) vol. 6 1–98 (Academic Press, 1971).
60. Keller, A. A. *et al.* Species-specific responses of demersal fishes to near-bottom oxygen levels within the California Current large marine ecosystem. *Mar Ecol Prog Ser* **568**, 151–173 (2017).
61. FAO. *The State of World Fisheries and Aquaculture 2020: Sustainability in Action*. (Food and Agriculture Organization of the United Nations, 2020).
62. Brodie, S. *et al.* Recommendations for quantifying and reducing uncertainty in climate projections of species distributions. *Glob Chang Biol* **28**, 6586–6601 (2022).
63. Barth, J. A. *et al.* Widespread and increasing near-bottom hypoxia in the coastal ocean off the United States Pacific Northwest. *Sci Rep* **14**, 3798 (2024).
64. Childress, J. J. & Seibel, B. A. Life at Stable low Oxygen Levels: Adaptations of Animals to Oceanic Oxygen Minimum Layers. *Journal of Experimental Biology* **201**, 1223–1232 (1998).
65. Leeuwis, R. H. J., Zanuzzo, F. S., Peroni, E. F. C. & Gamperl, A. K. Research on sablefish (Anoplopoma fimbria) suggests that limited capacity to increase heart function leaves hypoxic fish susceptible to heat waves. *Proceedings of the Royal Society B: Biological Sciences* **288**, 20202340 (2021).
66. Claireaux, G., Webber, D. M., Lagardère, J.-P. & Kerr, S. R. Influence of water temperature and oxygenation on the aerobic metabolic scope of Atlantic cod (Gadus morhua). *J Sea Res* **44**, 257–265 (2000).
67. Rantanen, M. *et al.* The Arctic has warmed nearly four times faster than the globe since 1979. *Commun Earth Environ* **3**, 168 (2022).
68. Hauri, C. *et al.* More Than Marine Heatwaves: A New Regime of Heat, Acidity, and Low Oxygen Compound Extreme Events in the Gulf of Alaska. *AGU Advances* **5**, e2023AV001039 (2024).
69. Gou, R., Wolf, K. K. E., Hoppe, C. J. M., Wu, L. & Lohmann, G. The changing nature of future Arctic marine heatwaves and its potential impacts on the ecosystem. *Nat Clim Chang* **15**, 162–170 (2025).
70. Harvey, C. *et al.* Ecosystem status report of the california current for 2019-20: a summary of ecosystem indicators compiled by the california current integrated ecosystem assessment team (CCIEA). (2020).
71. Di Lorenzo, E. *et al.* Synthesis of Pacific Ocean climate and ecosystem dynamics. *Oceanography* **26**, 68–81 (2013).

72. Long, M. C., Deutsch, C. & Ito, T. Finding forced trends in oceanic oxygen. *Global Biogeochem Cycles* **30**, 381–397 (2016).
73. Crawford, W. R. & and Peña, M. A. Declining Oxygen on the British Columbia Continental Shelf. *Atmosphere-Ocean* **51**, 88–103 (2013).
74. PRINCE, E. D. & GOODYEAR, C. P. Hypoxia-based habitat compression of tropical pelagic fishes. *Fish Oceanogr* **15**, 451–464 (2006).
75. Lucey, N. M. *et al.* Climate warming erodes tropical reef habitat through frequency and intensity of episodic hypoxia. *PLOS Climate* **2**, e0000095- (2023).
76. Fitzpatrick, M. C. & Hargrove, W. W. The projection of species distribution models and the problem of non-analog climate. *Biodivers Conserv* **18**, 2255–2261 (2009).
77. Muhling, B. A. *et al.* Predictability of Species Distributions Deteriorates Under Novel Environmental Conditions in the California Current System. *Front Mar Sci* **7**, (2020).
78. Parmesan, C. & Yohe, G. A globally coherent fingerprint of climate change impacts across natural systems. *Nature* **421**, 37–42 (2003).
79. Dulvy, N. K. *et al.* Climate change and deepening of the North Sea fish assemblage: a biotic indicator of warming seas. *Journal of Applied Ecology* **45**, 1029–1039 (2008).
80. Cheung, W. W. L., Watson, R. & Pauly, D. Signature of ocean warming in global fisheries catch. *Nature* **497**, 365–368 (2013).
81. Duncan, M. I., James, N. C., Potts, W. M. & Bates, A. E. Different drivers, common mechanism; the distribution of a reef fish is restricted by local-scale oxygen and temperature constraints on aerobic metabolism. *Conserv Physiol* **8**, coaa090 (2020).
82. Chu, J. W. F. & Tunnicliffe, V. Oxygen limitations on marine animal distributions and the collapse of epibenthic community structure during shoaling hypoxia. *Glob Chang Biol* **21**, 2989–3004 (2015).
83. Byers, J. E. Marine parasites and disease in the era of global climate change. *Ann Rev Mar Sci* **13**, 397–420 (2021).
84. Köhn, E. E., Münnich, M., Vogt, M., Desmet, F. & Gruber, N. Strong Habitat Compression by Extreme Shoaling Events of Hypoxic Waters in the Eastern Pacific. *J Geophys Res Oceans* **127**, e2022JC018429 (2022).
85. Craig, J. K. Aggregation on the edge: effects of hypoxia avoidance on the spatial distribution of brown shrimp and demersal fishes in the Northern Gulf of Mexico. *Mar Ecol Prog Ser* **445**, 75–95 (2012).
86. Neuenfeldt, S. The influence of oxygen saturation on the distributional overlap of predator (cod, Gadus morhua) and prey (herring, Clupea harengus) in the Bornholm Basin of the Baltic Sea. *Fish Oceanogr* **11**, 11–17 (2002).
87. Santora, J. A. *et al.* Habitat compression and ecosystem shifts as potential links between marine heatwave and record whale entanglements. *Nat Commun* **11**, 536 (2020).
88. Pinsky, M. L. *et al.* Preparing ocean governance for species on the move. *Science (1979)* **360**, 1189–1191 (2018).
89. Siple, M. C., von Szalay, P. G., Raring, N. W., Dowlin, A. N. & Riggle, B. C. *Data Report: 2023 Gulf of Alaska Bottom Trawl Survey. AFSC Processed Rep. 2024-09*. (2024).
90. Markowitz, E. H. *et al.* Results of the 2022 eastern and northern Bering Sea continental shelf bottom trawl survey of groundfish and invertebrate fauna. (2023).
91. Hoff, G. R. *Results of the 2016 Eastern Bering Sea Upper Continental Slope Survey of Groundfish and Invertebrate Resources.* . (2016).

92. Keller, A. A., Wallace, J. R. & Methot, R. D. The northwest fisheries science Center's West coast Groundfish bottom trawl survey: History, design, and description. (2017).
93. Anderson, S. C., Keppel, E. A. & Edwards, A. M. *A Reproducible Data Synopsis for over 100 Species of British Columbia Groundfish*. https://www.dfo-mpo.gc.ca/csas-sccs/Publications/ResDocs-DocRech/2019/2019_041-eng.html (2019).
94. DFO Canada. Groundfish Synoptic Bottom Trawl Surveys. https://open.canada.ca/data/en/dataset/a278d1af-d567-4964-a109-ae1e84cbd24a (2024).
95. IPHC. *International Pacific Halibut Commission Fishery-Independent Setline Survey Sampling Manual (2024)*. (2024).
96. Ward, E. J. *et al.* surveyjoin: A Standardized Database of Fisheries Bottom Trawl Surveys in the Northeast Pacific Ocean. *bioRxiv* 2025.03.14.643022 (2025) doi:10.1101/2025.03.14.643022.
97. IPHC. *IPHC Fishery-Independent Setline Survey (FISS) and Commercial Data Modelling*. https://www.iphc.int/uploads/pdf/srb/srb019/iphc-2021-srb019-05.pdf (2021).
98. Beamish, F. W. H. Respiration of fishes with special emphasis on standard oxygen consumption: III. Influence of oxygen. *Can J Zool* **42**, 355–366 (1964).
99. Anderson, S. C., Ward, E. J., English, P. A. & Barnett, L. A. K. sdmTMB: an R package for fast, flexible, and user-friendly generalized linear mixed effects models with spatial and spatiotemporal random fields. *bioRxiv* 2022.03.24.485545 (2022) doi:10.1101/2022.03.24.485545.
100. Sogard, S. M. & Berkeley, S. A. Patterns of movement, growth, and survival of adult sablefish (Anoplopoma fimbria) at contrasting depths in slope waters off Oregon. *Fishery Bulletin* **115**, 233–252 (2017).
101. Lindgren, F., Rue, H. & Lindström, J. An explicit link between Gaussian fields and Gaussian Markov random fields: the stochastic partial differential equation approach. *J R Stat Soc Series B Stat Methodol* **73**, 423–498 (2011).
102. Kristensen, K., Nielsen, A., Berg, C. W., Skaug, H. & Bell, B. M. TMB: automatic differentiation and Laplace approximation. *J Stat Softw* **70**, 1–21 (2016).
103. Shono, H. Application of the Tweedie distribution to zero-catch data in CPUE analysis. *Fish Res* **93**, 154–162 (2008).
104. Tweedie, M. C. K. An index which distinguishes between some important exponential families. in *Statistics: Applications and new directions: Proc. Indian statistical institute golden Jubilee International conference* vol. 579 579–604 (1984).
105. Ward, E. J. *et al.* Win, lose, or draw: Evaluating dynamic thermal niches of northeast Pacific groundfish. *PLOS Climate* **3**, e0000454- (2024).
106. Akaike, H. A new look at the statistical model identification. *IEEE Trans Automat Contr* **19**, 716–723 (1974).

SYNTHESIS

The ocean is rapidly changing. Understanding how fish population dynamics are linked to the environment over space and time can allow fisheries managers, scientists, and communities to anticipate effects of these changes. Yet estimating links between the environment and ecological responses can be challenging due to mismatches in scale, confounding processes, and nonlinear relationships. This dissertation adds to our understanding of the spatial and temporal dynamics of fish demographics and distributions, particularly those associated with temperature and oxygen, and improves statistical methods for estimating these relationships. I applied fundamental metabolic principles to provide a theoretical basis for how we might expect fish to respond and advanced statistical methods for using field data to disentangle realized effects. Together, these ecological insights and statistical advancements can be readily applied to sustainable fisheries management.

The impacts of environmental conditions on fish growth, abundance, and other demographic characteristics have long been a focus of research (Ekman, 1953), such as biogeographic patterns in range edges (Grinnell, 1917), fish size and temperature (Bergmann, 1847), and annual fluctuations in population size (Hjort, 1914). This dissertation contributes to this body of work in evaluating environmental effects on two attributes of fish population—individual size and distribution—applied to groundfish in the northeast Pacific Ocean. For one, I find extensive variation in weight-at-age over space and time in walleye pollock, a highly commercially important species (Chapter 1). While links to environmental conditions were not directly evaluated, this research captured how variation in weight-at-age over space and time was associated with unmeasured spatial and spatio-temporal environmental processes. I found extensive spatial fine-scale heterogeneity in size-at-age within a species' range that may be driven by environmental features, and the framework of this analysis was used in subsequent work to evaluate temperature drivers of weight-at-age (Bigman et al., in review). My research also contributed additional evidence of declines in size in older age classes over the last few decades, which has been similarly observed in other species (Baudron et al., 2014). This may be due to long-term increases in temperature in the region, aligning with the temperature-size rule (Atkinson, 1994). This dissertation additionally contributes evidence of oxygen-limiting effects on distribution in some groundfish species across diverse marine fishes (Chapter 4). As almost all of the 32 species evaluated in this study had never been measured for oxygen tolerance in laboratory settings, this provided the first assessment of oxygen limitations for many of these species through field observations. Oxygen limitation from physiological constraints (Vaquer-Sunyer & Duarte, 2008) has been used to explain broad biogeographic edges to marine species' ranges (Deutsch et al., 2020), prehistoric species extinction (Penn et al., 2018), and community assembling (Brandl et al., 2023). I added to these broad-scale patterns by identifying species and regional differences in how oxygen may constrain species' densities on smaller, local scales. I find that species' distributions within their range may be associated with oxygen for some, but not all, species, and find wide variation in species' sensitivities to oxygen and differences in regional exposure to low oxygen conditions.

This dissertation developed novel approaches to estimate these environment-population relationships by applying ecological principles and advancing statistical methods. Correlative

species distributions—the backbone of the analytical approaches in this dissertation—are an increasingly used approach for estimating associations between populations and the environment (Liu et al., 2023; Ward et al., 2024). Using these models, this dissertation developed a modeling framework for weight-at-age that accounts for spatial and spatio-temporal variation in size and changes in abundance, which can better capture species' movement year-to-year or when there are spatial patterns in growth (Chapter 1). Additionally, this dissertation developed an approach to apply concepts from fundamental metabolic theory (Brown et al., 2004) to spatial statistical models by including a functional response of the effect of temperature on oxygen tolerance (Chapter 2). This allows estimation of fish response to the environmental to more realistically reflect fish physiology. Other functional mechanisms (Kearney & Porter, 2009) could be used in spatial statistical analysis to estimate responses from observational data following a similar template. This dissertation also applied insights about the spatial and temporal resolution of fish response compared to environmental conditions to evaluate impacts of different data sources on the robustness of environmental relationships estimated from distribution models (Chapter 3). It identified a key need to validate climate projections for ecological modeling and provided a framework for validating and evaluating uncertainty, a main consideration in forecasting climate-driven ecological dynamics (Brodie et al., 2022; Davies et al., 2023).

The ecological findings and statistical advancements of this dissertation have practical applications for sustainable fisheries management. The spatio-temporal model of weight-at-age (Chapter 1) in Bering Sea walleye pollock has been operationalized and presented to the North Pacific Fishery Management Council. Because of the dynamic variation in weight-at-age found across space and time, this work will provide a more accurate estimate of population-level size-at-age than previous methods and can address issues of unbalanced survey designs. National Oceanic and Atmospheric Administration (NOAA) regional offices could also use the weight-at-age model to identify areas that support larger fish for additional habitat protections by designating as Essential Fish Habitat (EFH). This makes a step towards addressing the challenge of considering spatial demographic processes in designating EFH (Thorson et al., 2021).

Temperature-adjusted oxygen thresholds for groundfish species (Chapter 4) can similarly inform fisheries management policies that are strongly dependent on where fish are located (Pinsky et al., 2018), and therefore might be vulnerable to shifts in distribution due to future declines in oxygen in a warming ocean. Research on fish distributions and environmental change is a key concern of fisheries worldwide and to management agencies responsible for the region studied in this dissertation, such as the Pacific Fisheries Management Council and North Pacific Fisheries Management Council (Dorn et al., 2017). There is still much uncertatiny in how oxygen drives fish distributions, due to difficulty in estimating the physiological thresholds of oxygen tolerance (Chapter 2) and limited ocean oxygen data (Chapter 3). Additionally, other factors such as temperature, predator avoidance, prey and food availability, and depth preferences add complexity, where oxygen thresholds alone will not fully explain or predict fish distributions. The thresholds estimated here (Chapter 4) therefore can provide general bounds for what oxygen and temperature conditions may be limiting, but likely would not allow precise quantitative predictions of future distributions. For instance, at decadel and century time scales, using projected climate scenarios to evaluate against estimated oxygen thresholds may help generally identify regions likely to experience oxygen-limiting conditions. To account for these at-risk areas and align with expected future distributions, regional Councils and state and Tribal fisheries agencies could change fishing quota boundaries (Baudron et al., 2020). Local governments and the fishing industry could also

strategically locate and invest in new infrastructure, such as ports and processing facilities. In the near-term, temperature-adjusted oxygen thresholds may be considered in a general risk management approach, with temperature and oxygen conditions one possible indicator for adaptive management, which are of recent interest to state managers (Watson et al., 2023a). For instance, certain sections of the coast could be automatically closed to fishing of specific species, or bycatch limits reduced, when temperature and oxygen conditions jointly reach thresholds. With further refining of estimated temperature-adjusted oxygen thresholds, these could also be the basis for parametric insurance, triggering payments to fishers when there are extreme environmental events that limit fishing opportunities (Hobday et al., 2025; Watson et al., 2023b). Overall, identifying the species and areas vulnerable to low oxygen (Chapter 4) can guide development of effective strategies to adequately plan for a warming and deoxygenating ocean.

The research of this dissertation highlights several ongoing challenges and possible solutions in analyzing the effect of the environment on fish population dynamics using observational data. For one, the classic problem of scale in ecology (Levin 1992) needs continued deliberate consideration in spatio-temporal analysis of fish populations. Marine systems have overlapping processes operating across a range of spatial and temporal scales. Local-scale variation can broadcast out to large-scale changes, and at the same time global forces can have localized effects (Levin, 1992). Spatially, there are processes down from a centimeter (e.g. the relationship of zooxanthellae and a single piece of symbiotic coral), to meters (e.g. the species assemblage of micropatches of a coral reef or single schools of fish), up through kilometers (a whole coral reef), regional, (the Gulf of Mexico, Bering Sea, to entire current and upwelling systems), and global (Levin, 1992). Similarly, across temporal scales, there are processes occurring on time scales of less than a day (e.g. diel migrations, predator-prey interactions), seasonal cycles, and annual and decadal, and longer cycles (e.g. ENSO, PDO, NAO), and even longer time scales (e.g. how much temperatures will rise over the next two centuries, evolution). It is necessary to properly consider how variation at one scale may broadcast out to larger scales, such as when fine-scale spatial and temporal differences are aggregated into population-level metrics (Chapter 1). It is also important to consider possible mismatches in scale in analysis, such as oceanographic models at coarser spatial scale than the data relevant to ecological research (Chapter 3). Spatially- and temporally-varying coefficients (Gelfand et al., 2003), for instance, are an emerging method that may bridge scales of analysis, such as by capturing local responses to oceanographic regional and global metrics (J. Thorson, 2019).

Isolating the effect of a particular environmental driver amongst complex, overlapping spatial and temporal processes is also a persistent problem. In a classic case of regime shift of Atlantic cod, for instance, high inter-annual natural variation masked a trend of response to climate change (Wooster & Zhang, 2004). At smaller spatial and temporal scales, there are numerous co-occurring dynamics that complicate detecting environmental links, such as the confounding effects of depth, temperature, and oxygen (Chapters 2 & 4). The work in this dissertation primarily focused on physical drivers of local fish densities; ecological dynamics, such as food availability or species interactions, were not formally considered in model structure and were considered only as unmeasured latent effects. Future research could explicitly include these, such as in joint species distribution models that assume joint responses of species to the environment and each other (e.g. Pichler & Hartig, 2021). Structural equation modeling (Grace et al., 2015; Pearl, 2012) may also better delineate and isolate complex spatial and temporal processes in population dynamics by capturing confounding, indirect, and reciprocal effects. This can also help move estimation

towards causal inference (Cox & Wermuth, 2004), improving projections of how species may respond when extrapolating to future novel environmental conditions.

Continuing to explore non-linear effects of environmental conditions will also aid more realistic estimates of fish response to environmental change. For instance, ecological theory expects "pulse" events such as marine heatwaves to be more impactful than the long-term average "press" changes (Harris et al., 2018) that this dissertation focused on (Chapter 4). Marine heatwaves are forecasted to increase in frequency, magnitude, intensity, and duration due to anthropogenic climate change (Frölicher et al., 2018). Mass coral bleaching events, for example, are a highly visible example of abrupt ecosystem responses to extreme climate conditions (Eakin et al., 2019). Tipping points and regime shifts are widely expected under climate change (Berx et al., 2011; Selkoe et al., 2015). Advancing techniques to identify these ecosystem thresholds (Detmer et al., 2025) from observational data will refine how we can estimate and anticipate a wider range of possible ecological responses to the environment.

Expanding data availability will also help address these various analytic challenges. For instance, a focus on collecting observational data of environmental covariates at the same time as biological sampling will help expand the spatio-temporally precise data that provides enough information for inference from pointwise correlative distribution modeling (Chapter 3). International and cross-agency data sharing and collaboration was crucial for this work (Chapter 4). Combining data from multiple surveys allowed evaluation of species' response to oxygen across a wide geographic region. Efforts to compile, standardize, and make data publicly available will be a powerful tool for detecting other ecological patterns at broader spatial and temporal scales (A. Maureaud et al., 2021; Comte et al., 2020; Lawlor et al., 2024; Maureaud et al., 2024). This can provide coverage across a wider range of environmental conditions, such as including more temperature extremes or both a species' warm and cool range edges, which reduces extrapolation (Brodie et al., 2022). Additionally, there are geographic biases in data availability (Parker et al., 2024; White et al., 2021). Emphasis on capacity building in less developed regions can fill these global gaps in coverage and cover more species and environmental conditions.

Lastly, combining insights from theory with statistical analysis of observational data, as done in this dissertation, can refine identification and projection of fish responses to environmental change. This dissertation focused on metabolic constraints and oxygen limitation (Chapters 2 & 4). Yet fishery-independent survey data, such as the bottom trawl and longline data used here (Chapters 1-4), can be a rich source of observational data for testing other predictions from theoretical and fundamental theory. These datasets are particularly useful because they have long time series in regions around the world, each collected with standardized protocols (A. Maureaud et al., 2021). For instance, there is a strong theoretical basis for how temperature and oxygen impact size and growth of fish (Rubalcaba et al., 2020), yet empirical support for the mechanisms behind these patterns and how they manifest in natural populations is unresolved (Audzijonyte et al., 2019). Observational specimen and abundance data from bottom trawl surveys could be applied to test empirical support for these theories and evaluate whether and the extent to which there is evidence for consistent patterns in environmental drivers of size.

The analytical challenges of assessing variation in fish population dynamics discussed above are important to consider when applying to management and conservation. For instance, it is crucial

to ensure the scale and resolution of analysis is useful to the needs of management or stakeholders. In some cases, the spatial scale of analysis can impact conclusions on outcome. A global-level analysis may show no large total decline in fisheries catch (Gaines et al., 2018), yet at a regional level there may be some gains and other losses (Oremus et al., 2020). Similarly, there may be port-level differences in climate impacts even within the same region (Santora et al., 2020; Selden et al., 2020). Individual fishers care about the response at the local level of their fishing grounds, while managers may be interested in the abundance and distribution changes at the level of management unit. Temporally, there may be management decisions that need to be informed by short-, medium-, or long-term understandings of how the marine system will respond (Holsman et al., 2019). The timescale of a species distribution shift is also important for determining when governance structures and fishing agreements need to be in place (Palacios-Abrantes et al., 2022). Interdisciplinary research that can align on spatial and temporal scales—such as rapid access to output from numerical ocean models for use in within-season "dynamic ocean management" — will enable providing more effective information to decisionmakers.

This dissertation's analysis of the links between population dynamics and the environment is particularly relevant for fisheries management in the context of climate change. Currently, climate change is often not directly factored into the information used in decision-making by fisheries management councils (Bryndum-Buchholz et al., 2021). However, recent initiatives (e.g. Changing Ecosystems Fisheries Initiative [CEFI] in the United States, , Saba, 2023) are transitioning to climate-ready fisheries management. The joint effects of temperature and oxygen on fish estimated here (Chapter 4) could be incorporated into CEFI initatives to operationalize climate (i.e. temperature and oxygen effects) into the quantitative analyses that inform decisions by the Fishery Management Councils in myriad ways: including impacts of annual environmental conditions in age structures (Chavez et al., 2017), reference points (Morrison et al., 2024), abundance indices and vital rates (Link et al., 2011), and harvest control rules (Free et al., 2023); developing environmental indicators (ICCAT, 2013; Selkoe et al., 2015); evaluating seasonal time scales and correcting for phenological changes (Olmos et al., 2023) and correctly accounting for climate-driven distribution shifts in survey indices (O'Leary et al., 2020). Additionally, Ecosystem Status Reports could include temperature and oxygen conditions in a region in the current year and projected for future years shown visualized against species' temperature-adjusted oxygen thresholds. This would identify risks of the environment nearing species' limits and inform Council decisions on allowed catches. These technical changes can provide more comprehensive and accurate assessments of the status of fish populations that incorporate climate and are directly embedded within the scientific information that Council decisions rely on.

Analytical challenges in isolating ecological responses to environmental conditions and uncertainties in predictions of environmental conditions (Chapter 3) compound into unresolved uncertainty in projecting effects of climate change that fisheries management also needs to consider. Approaches that promote flexibility across different climate outcomes will therefore likely be most effective (Golden et al., 2024). While technical advice and statistical modeling can provide some actionable information, often the range of uncertainty in projected effects are too large for specific management recommendations. Rather, scenario evaluation (Moore et al., 2013) can be an effective management approach for climate change by providing bracketed exploration of plausible future conditions. Decisionmakers can then aim to select approaches that do the best under a range of possible scenarios (Kaplan et al., 2012; Lim-Camacho et al., 2015). Establishing

policies—such as bilateral/multilateral agreements, harvest control rules, and quota allocation schemes—that can adapt to different climate outcomes will promote resiliency of ecological and social systems.

Because of heterogeneity in environmental conditions in marine systems around the world, fisheries management approaches will also need to be tailored for specific climate vulnerabilities, ecological dynamics, and economic, socio-political, and cultural values. For instance, this dissertation focused on a region of the world that is particularly data-rich and economically advantaged, and there are inherent differences between fisheries such as these versus small-scale artisanal subsistence fisheries (Cochrane et al. 2009). Engaging with local communities is crucial to address the management needs, governance structures, and values of the specific community (Mason et al. 2023). Likewise, it is important to note scientists' role in pushing for co-production of knowledge that prioritizes Indigenous Peoples' values and knowledge systems, in order to ensure ecosystem management is not only resilient but also more equitable and just (Yua et al., 2022).

Identifying environmental drivers of spatial and temporal patterns in the natural environment is a rich source of future ecological research. This dissertation focused primarily on two direct impacts of climate change, increasing temperature and decreasing oxygen in the ocean, and on population outcomes of fish size and distribution. Yet there are numerous environmental stressors that are similarly important to explore. The ocean habitat will continue to be shaped by natural environmental variability, pollution, climate change, and emerging marine spatial uses such as seabed mining and renewable energy. These complex stressors similarly pose questions about how they will impact marine populations, communities, and ecosystems. The tools to answer these questions will need to continue to be refined and advanced to take advantage of new technologies, expanding datasets, and increasingly complex natural dynamics. The aim of this dissertation, and of future work, is to apply these tools, rooted in our understanding of ecological theories, to provide information with enough lead time to develop, evaluate, and apply the policy actions that allow marine systems to thrive for future generations.

References

Maureaud, A., Frelat, R., Pécuchet, L., Shackell, N., Mérigot, B., Pinsky, M. L., Amador, K., Anderson, S. C., Arkhipkin, A., Auber, A., Barri, I., Bell, R. J., Belmaker, J., Beukhof, E., Camara, M. L., Guevara-Carrasco, R., Choi, J., Christensen, H. T., Conner, J., … T. Thorson, J. (2021). Are we ready to track climate-driven shifts in marine species across international boundaries? - A global survey of scientific bottom trawl data. *Global Change Biology*, *27*(2), 220–236. https://doi.org/https://doi.org/10.1111/gcb.15404

Arkema, K. K., Abramson, S. C., & Dewsbury, B. M. (2006). Marine ecosystem-based management: from characterization to implementation. *Frontiers in Ecology and the Environment*, *4*(10), 525–532.

Atkinson, D. (1994). Temperature and Organism Size—A Biological Law for Ectotherms? In M. Begon & A. H. Fitter (Eds.), *Advances in Ecological Research* (Vol. 25, pp. 1–58). Academic Press. https://doi.org/https://doi.org/10.1016/S0065-2504(08)60212-3

Audzijonyte, A., Barneche, D. R., Baudron, A. R., Belmaker, J., Clark, T. D., Marshall, C. T., Morrongiello, J. R., & van Rijn, I. (2019). Is oxygen limitation in warming waters a valid mechanism to explain decreased body sizes in aquatic ectotherms? *Global Ecology and Biogeography*, *28*(2), 64–77. https://doi.org/https://doi.org/10.1111/geb.12847

Baudron, A. R., Brunel, T., Blanchet, M., Hidalgo, M., Chust, G., Brown, E. J., Kleisner, K. M., Millar, C., MacKenzie, B. R., & Nikolioudakis, N. (2020). Changing fish distributions challenge the effective management of European fisheries. *Ecography*, *43*(4), 494–505.

Baudron, A. R., Needle, C. L., Rijnsdorp, A. D., & Tara Marshall, C. (2014). Warming temperatures and smaller body sizes: synchronous changes in growth of North Sea fishes. *Global Change Biology*, *20*(4), 1023–1031.

Bergmann, C. (1847). Ueber die verhäitnisseder wärmeökonomie der thiere zu ihrer grösse. *Gottinger Studien*.

Berx, B., Dickey-Collas, M., Skogen, M. D., De Roeck, Y.-H., Klein, H., Barciela, R., Forster, R. M., Dombrowsky, E., Huret, M., & Payne, M. (2011). Does operational oceanography address the needs of fisheries and applied environmental scientists? *Oceanography*, *24*(1), 166–171.

Brandl, S. J., Lefcheck, J. S., Bates, A. E., Rasher, D. B., & Norin, T. (2023). Can metabolic traits explain animal community assembly and functioning? *Biological Reviews*, *98*(1), 1–18. https://doi.org/https://doi.org/10.1111/brv.12892

Brodie, S., Smith, J. A., Muhling, B. A., Barnett, L. A. K., Carroll, G., Fiedler, P., Bograd, S. J., Hazen, E. L., Jacox, M. G., Andrews, K. S., Barnes, C. L., Crozier, L. G., Fiechter, J., Fredston, A., Haltuch, M. A., Harvey, C. J., Holmes, E., Karp, M. A., Liu, O. R., … Kaplan, I. C. (2022). Recommendations for quantifying and reducing uncertainty in climate projections of species distributions. *Global Change Biology*, *28*(22), 6586–6601. https://doi.org/10.1111/gcb.16371

Brown, J. H., Gillooly, J. F., Allen, A. P., Savage, V. M., & West, G. B. (2004). Toward a metabolic theory of ecology. *Ecology*, *85*(7), 1771–1789. https://doi.org/10.1890/03-9000

Chavez, F. P., Costello, C., Aseltine-Neilson, D., Doremus, D., Field, J. C., Gaines, S. D., Hall-Arber, M., Mantua, N. J., McCovey, B., & Pomeroy, C. (2017). *Readying California fisheries for climate change*.

Comte, L., Grenouillet, G., Bertrand, R., Murienne, J., Bourgeaud, L., Hattab, T., & Lenoir, J. (2020). *BioShifts: a global geodatabase of climate-induced species redistribution over land and sea*.

Cox, D. R., & Wermuth, N. (2004). Causality: A statistical view. *International Statistical Review*, *72*(3), 285–305.

Davies, S. C., Thompson, P. L., Gomez, C., Nephin, J., Knudby, A., Park, A. E., Friesen, S. K., Pollock, L. J., Rubidge, E. M., Anderson, S. C., Iacarella, J. C., Lyons, D. A., MacDonald, A., McMillan, A., Ward, E. J., Holdsworth, A. M., Swart, N., Price, J., & Hunter, K. L. (2023). Addressing uncertainty when projecting marine species' distributions under climate change. *Ecography*, *2023*(11), e06731. https://doi.org/https://doi.org/10.1111/ecog.06731

Detmer, A. R., Ward, E. J., Hunsicker, M. E., Andrews, K. S., Conrad, M., Ferriss, B. E., Hazen, E. L., Holsman, K. K., Indivero, J., Large, S. I., Malick, M., Marshall, K. N., Munsch, S. H., Oken, K. L., Satterthwaite, W. H., Shotwell, S. K., Thompson, A. R., & Samhouri, J. F. (2025). Evaluating the robustness of generalized additive models as a tool for threshold detection in variable environments. *Ecosphere*, *16*(3), e70117. https://doi.org/https://doi.org/10.1002/ecs2.70117

Deutsch, C., Penn, J. L., & Seibel, B. (2020). Metabolic trait diversity shapes marine biogeography. *Nature*, *585*(7826), 557–562.

Dorn, M. W., Cunningham, C. J., Dalton, M., Fadely, B. S., Gerke, B. L., Hollowed, A. B., Holsman, K. K., Moss, J. H. H., Ormseth, O. A., & Palsson, W. A. (2017). *A climate science: regional action plan for the Gulf of Alaska*.

Eakin, C. M., Sweatman, H. P. A., & Brainard, R. E. (2019). The 2014–2017 global-scale coral bleaching event: insights and impacts. *Coral Reefs*, *38*(4), 539–545.

Ekman, S. (1953). Zoogeography of the sea. *(No Title)*.

Free, C. M., Mangin, T., Wiedenmann, J., Smith, C., McVeigh, H., & Gaines, S. D. (2023). Harvest control rules used in US federal fisheries management and implications for climate resilience. *Fish and Fisheries*, *24*(2), 248–262. https://doi.org/10.1111/faf.12724

Frölicher, T. L., Fischer, E. M., & Gruber, N. (2018). Marine heatwaves under global warming. *Nature*, *560*(7718), 360–364. https://doi.org/10.1038/s41586-018-0383-9

Gaines, S. D., Costello, C., Owashi, B., Mangin, T., Bone, J., García Molinos, J., Burden, M., Dennis, H., Halpern, B. S., Kappel, C. V, Kleisner, K. M., & Ovando, D. (2018). Improved fisheries management could offset many negative effects of climate change. In *Sci. Adv* (Vol. 4). https://www.science.org

Gelfand, A. E., Kim, H.-J., Sirmans, C. F., & Banerjee, S. (2003). Spatial modeling with spatially varying coefficient processes. *Journal of the American Statistical Association*, *98*(462), 387–396.

Golden, A. S., Baskett, M. L., Holland, D., Levine, A., Mills, K., & Essington, T. (2024). Climate adaptation depends on rebalancing flexibility and rigidity in US fisheries management. *ICES Journal of Marine Science*, *81*(2), 252–259. https://doi.org/10.1093/icesjms/fsad189

Grinnell, J. (1917). Field tests of theories concerning distributional control. *The American Naturalist*, *51*(602), 115–128.

Harris, R. M. B., Beaumont, L. J., Vance, T. R., Tozer, C. R., Remenyi, T. A., Perkins-Kirkpatrick, S. E., Mitchell, P. J., Nicotra, A. B., McGregor, S., Andrew, N. R., Letnic, M., Kearney, M. R., Wernberg, T., Hutley, L. B., Chambers, L. E., Fletcher, M.-S., Keatley, M. R., Woodward, C. A., Williamson, G., … Bowman, D. M. J. S. (2018). Biological responses to the press and pulse of climate trends and extreme events. *Nature Climate Change*, *8*(7), 579–587. https://doi.org/10.1038/s41558-018-0187-9

Hjort, J. (1914). *Fluctuations in the great fisheries of northern Europe viewed in the light of biological research*.

Hollowed, A. B., Barange, M., Beamish, R. J., Brander, K., Cochrane, K., Drinkwater, K., Foreman, M. G. G., Hare, J. A., Holt, J., Ito, S., Kim, S., King, J. R., Loeng, H., MacKenzie, B. R., Mueter, F. J., Okey, T. A., Peck, M. A., Radchenko, V. I., Rice, J. C., … Yamanaka, Y. (2013). Projected

impacts of climate change on marine fish and fisheries. *ICES Journal of Marine Science*, *70*(5), 1023–1037. https://doi.org/10.1093/icesjms/fst081

Holsman, K. K., Hazen, E. L., Haynie, A., Gourguet, S., Hollowed, A., Bograd, S. J., Samhouri, J. F., & Aydin, K. (2019). Towards climate resiliency in fisheries management. *ICES Journal of Marine Science*, *76*(5), 1368–1378. https://doi.org/10.1093/icesjms/fsz031

ICCAT. (2013). Report of the 2013 Atlantic Swordfish Stock Assessment Session. *International Commission for the Conservation of Atlantic Tunas*, *Doc. No SCI-036/2013*.

Kaplan, I. C., Horne, P. J., & Levin, P. S. (2012). Screening California Current fishery management scenarios using the Atlantis end-to-end ecosystem model. *Progress in Oceanography*, *102*, 5–18.

Kearney, M., & Porter, W. (2009). Mechanistic niche modelling: combining physiological and spatial data to predict species' ranges. *Ecology Letters*, *12*(4), 334–350. https://doi.org/https://doi.org/10.1111/j.1461-0248.2008.01277.x

Keyl, F., & Wolff, M. (2008). Environmental variability and fisheries: what can models do? *Reviews in Fish Biology and Fisheries*, *18*, 273–299.

Lawlor, J. A., Comte, L., Grenouillet, G., Lenoir, J., Baecher, J. A., Bandara, R. M. W. J., Bertrand, R., Chen, I.-C., Diamond, S. E., Lancaster, L. T., Moore, N., Murienne, J., Oliveira, B. F., Pecl, G. T., Pinsky, M. L., Rolland, J., Rubenstein, M., Scheffers, B. R., Thompson, L. M., … Sunday, J. (2024). Mechanisms, detection and impacts of species redistributions under climate change. *Nature Reviews Earth & Environment*, *5*(5), 351–368. https://doi.org/10.1038/s43017-024-00527-z

Levin, S. A. (1992). The problem of pattern and scale in ecology. *Ecology*, *73*(6), 1943–1967. https://doi.org/10.2307/1941447

Link, J. S., Nye, J. A., & Hare, J. A. (2011). Guidelines for incorporating fish distribution shifts into a fisheries management context. *Fish and Fisheries*, *12*(4), 461–469. https://doi.org/10.1111/j.1467-2979.2010.00398.x

Liu, O. R., Ward, E. J., Anderson, S. C., Andrews, K. S., Barnett, L. A. K., Brodie, S., Carroll, G., Fiechter, J., Haltuch, M. A., Harvey, C. J., Hazen, E. L., Hernvann, P. Y., Jacox, M., Kaplan, I. C., Matson, S., Norman, K., Buil, M. P., Selden, R. L., Shelton, A., & Samhouri, J. F. (2023). Species redistribution creates unequal outcomes for multispecies fisheries under projected climate change. *Science Advances*, *9*(33). https://doi.org/10.1126/sciadv.adg5468

Maureaud, A. A., Palacios-Abrantes, J., Kitchel, Z., Mannocci, L., Pinsky, M. L., Fredston, A., Beukhof, E., Forrest, D. L., Frelat, R., Palomares, M. L. D., Pecuchet, L., Thorson, J. T., van Denderen, P. D., & Mérigot, B. (2024). FISHGLOB_data: an integrated dataset of fish biodiversity sampled with scientific bottom-trawl surveys. *Scientific Data*, *11*(1), 24. https://doi.org/10.1038/s41597-023-02866-w

Moore, S. S., Seavy, N. E., & Gerhart, M. (2013). Scenario planning for climate change adaptation. *A Guidance for Resource Managers. Point Blue Conservation Science and the California Coastal Conservancy, Oakland, USA*.

Morrison, W. E., Oakes, S. A., Karp, M. A., Appelman, M. H., & Link, J. S. (2024). Ecosystem-level reference points: Moving toward ecosystem-based fisheries management. *Marine and Coastal Fisheries*, *16*(2), e210285. https://doi.org/10.1002/mcf2.10285

O'Leary, C. A., Thorson, J. T., Ianelli, J. N., & Kotwicki, S. (2020). Adapting to climate-driven distribution shifts using model-based indices and age composition from multiple surveys in the walleye pollock (Gadus chalcogrammus) stock assessment. *Fisheries Oceanography*, *29*(6), 541–557.

Oremus, K. L., Bone, J., Costello, C., García Molinos, J., Lee, A., Mangin, T., & Salzman, J. (2020). Governance challenges for tropical nations losing fish species due to climate change. *Nature Sustainability*, *3*(4), 277–280. https://doi.org/10.1038/s41893-020-0476-y

Palacios-Abrantes, J., Frölicher, T. L., Reygondeau, G., Sumaila, U. R., Tagliabue, A., Wabnitz, C. C. C., & Cheung, W. W. L. (2022). Timing and magnitude of climate-driven range shifts in transboundary fish stocks challenge their management. *Global Change Biology*, *28*(7), 2312–2326. https://doi.org/10.1111/gcb.16058

Parker, E. J., Weiskopf, S. R., Oliver, R. Y., Rubenstein, M. A., & Jetz, W. (2024). Insufficient and biased representation of species geographic responses to climate change. *Global Change Biology*, *30*(7), e17408. https://doi.org/https://doi.org/10.1111/gcb.17408

Pearl, J. (2012). The causal foundations of structural equation modeling. *Handbook of Structural Equation Modeling*, 68–91.

Penn, J. L., Deutsch, C., Payne, J. L., & Sperling, E. A. (2018). Temperature-dependent hypoxia explains biogeography and severity of end-Permian marine mass extinction. *Science*, *362*(6419), eaat1327.

Pichler, M., & Hartig, F. (2021). A new joint species distribution model for faster and more accurate inference of species associations from big community data. *Methods in Ecology and Evolution*, *12*(11), 2159–2173.

Pinsky, M. L., & Mantua, N. J. (2014). Emerging adaptation approaches for climate-ready fisheries management. *Oceanography*, *27*(4), 147–159. https://doi.org/10.5670/oceanog.2014.93

Pinsky, M. L., Reygondeau, G., Caddell, R., Palacios-Abrantes, J., Spijkers, J., & Cheung, W. W. L. (2018). Preparing ocean governance for species on the move. In *Science* (Vol. 360, Issue 6394, pp. 1189–1191). American Association for the Advancement of Science. https://doi.org/10.1126/science.aat2360

Rubalcaba, J. G., Verberk, W. C. E. P., Hendriks, A. J., Saris, B., & Woods, H. A. (2020). Oxygen limitation may affect the temperature and size dependence of metabolism in aquatic ectotherms. *Proceedings of the National Academy of Sciences*, *117*(50), 31963–31968. https://doi.org/10.1073/pnas.2003292117

Saba, V., Borggaard, D., Caracappa, J. C., Chambers, R. C., Clay, P. M., Colburn, L. L., Deroba, J., DePiper, G., du Pontavice, H., Fratantoni, P., Ferguson, M., Gaichas, S., Hayes, S., Hyde, K., Johnson, M., Kocik, J., Keane, E., Kircheis, D., Large, S., … Wikfors, G. (2023). NOAA fisheries research geared towards climate-ready living marine resource management in the northeast United States. *PLOS Climate*, *2*(12), e0000323-. https://doi.org/10.1371/journal.pclm.0000323

Selkoe, K. A., Blenckner, T., Caldwell, M. R., Crowder, L. B., Erickson, A. L., Essington, T. E., Estes, J. A., Fujita, R. M., Halpern, B. S., Hunsicker, M. E., Kappel, C. V, Kelly, R. P., Kittinger, J. N., Levin, P. S., Lynham, J. M., Mach, M. E., Martone, R. G., Mease, L. A., Salomon, A. K., … Zedler, J. (2015). Principles for managing marine ecosystems prone to tipping points. *Ecosystem Health and Sustainability*, *1*(5), 1–18. https://doi.org/https://doi.org/10.1890/EHS14-0024.1

Thorson, J. (2019). *Forecasting distribution shifts using oceanographic indices: the spatially varying effect of cold-pool extent in the*.

Thorson, J. T., Hermann, A. J., Siwicke, K., Zimmermann, M., & Grand, M. (2021). Grand challenge for habitat science: stage-structured responses, nonlocal drivers, and mechanistic associations among habitat variables affecting fishery productivity. *ICES Journal of Marine Science*, *78*(6), 1956–1968. https://doi.org/10.1093/icesjms/fsa

Vaquer-Sunyer, R., & Duarte, C. M. (2008). Thresholds of hypoxia for marine biodiversity. *Proceedings of the National Academy of Sciences*, *105*(40), 15452–15457. https://doi.org/10.1073/pnas.0803833105

Ward, E. J., Anderson, S. C., Barnett, L. A. K., English, P. A., Berger, H. M., Commander, C. J. C., Essington, T. E., Harvey, C. J., Hunsicker, M. E., Jacox, M. G., Johnson, K. F., Large, S., Liu, O. R., Richerson, K. E., Samhouri, J. F., Siedlecki, S. A., Shelton, A. O., Somers, K. A., & Watson, J. T. (2024). Win, lose, or draw: Evaluating dynamic thermal niches of northeast Pacific groundfish. *PLOS Climate*, *3*(11), e0000454-. https://doi.org/10.1371/journal.pclm.0000454

White, C. R., Marshall, D. J., Chown, S. L., Clusella-Trullas, S., Portugal, S. J., Franklin, C. E., & Seebacher, F. (2021). Geographical bias in physiological data limits predictions of global change impacts. *Functional Ecology*, *35*(7), 1572–1578. https://doi.org/https://doi.org/10.1111/1365-2435.13807

Wooster, W. S., & Zhang, C. I. (2004). Regime shifts in the North Pacific: early indications of the 1976–1977 event. *Progress in Oceanography*, *60*(2), 183–200. https://doi.org/https://doi.org/10.1016/j.pocean.2004.02.005

Yua, E., Raymond-Yakoubian, J., Daniel, R. A., & Behe, C. (2022). A framework for co-production of knowledge in the context of Arctic research. *Ecology and Society*, *27*(1). https://doi.org/10.5751/ES-12960-270134

CHAPTER 1 APPENDIX

Appendix A. Weight-length relationships

Appendix Table 1. Values of parameters used for length-weight relationship $w=aL^b$ in walleye pollock stock assessment (Ianelli *et al*. 2020)		
Sex	*a (kg x cm^b)*	*b*
Male	0.000004919	3.038
Female	0.000006681	2.986
Unknown	0.0000063611	2.9954

Appendix B. Data availability

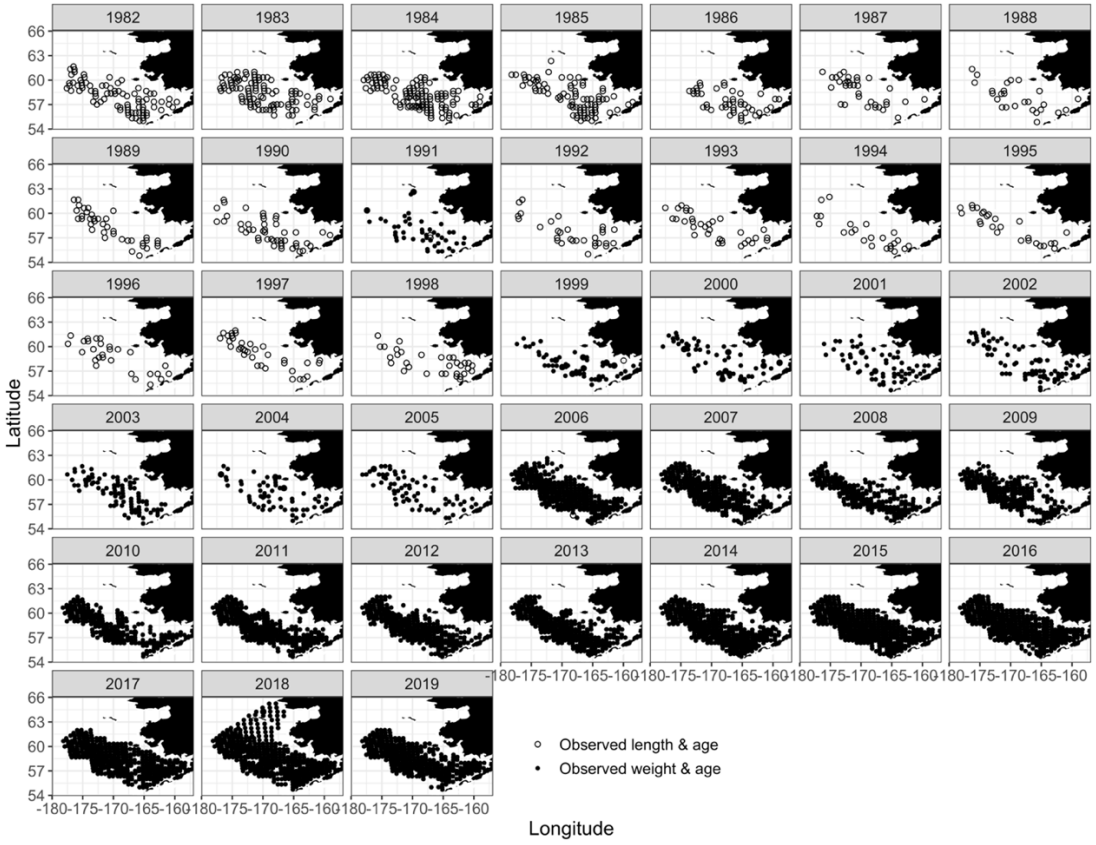

Appendix Figure 1. Locations of walleye pollock (*Gadus chalcogrammus*) specimen measurements used for size (i.e. weight) data. For 1982—1999 (except for 1991), length and age data was used to calculate weight using the weight-length relationship. For 2000—2019 (and 1991), direct weight measurements were used (N=59,576 individual fish)

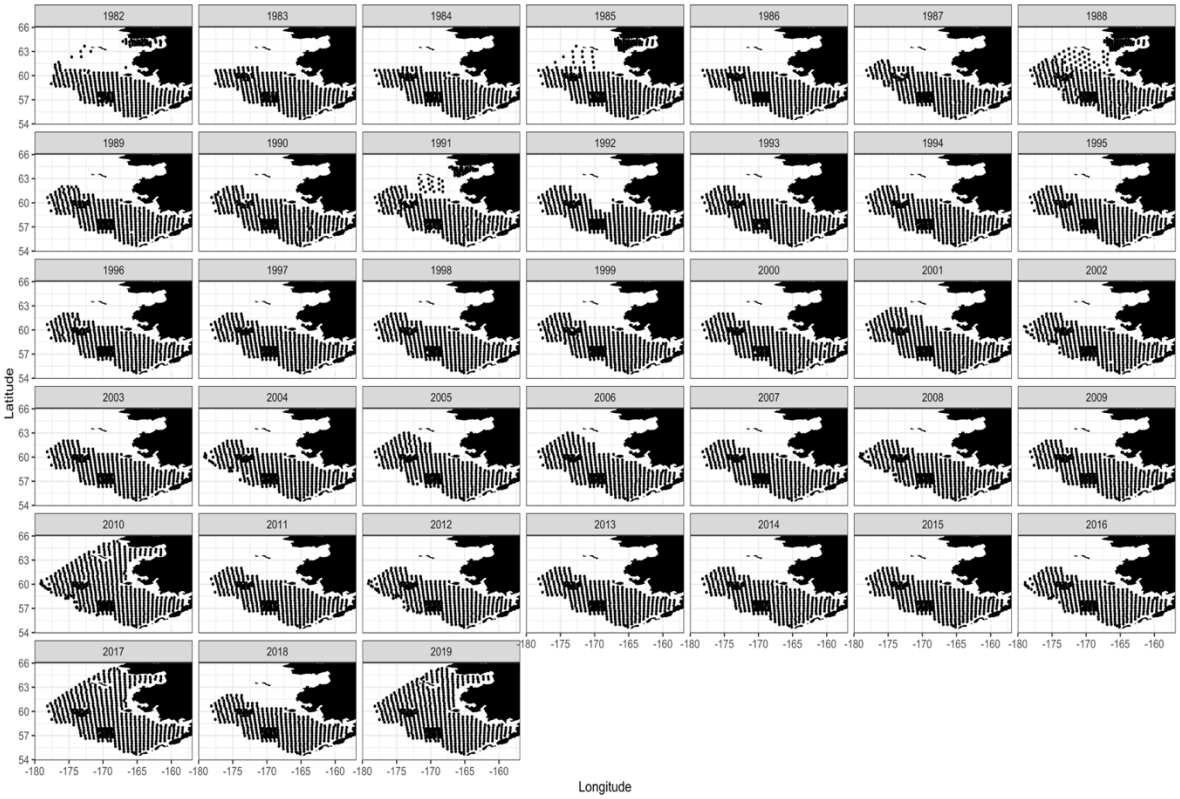

Appendix Figure 2. Locations of density-corrected catch-per-unit-effort per haul for years 1982—2019 (N=14,500 distinct hauls)

Appendix C. Calculation of simple empirical mean (i.e. non-spatial estimate)

For the simple empirical estimate (i.e. a non-spatial estimate), we calculated a non-spatially explicit weighted average of observations. We calculated the weighted average of size-at-age $\bar{v}_{\mathrm{a,y}}$ per age a and year y from the observed size data v_i, weighting mean size-at-age $v_{a,h}$ per haul h by catch-at-age in density-corrected-numbers-of-fish in that haul from the survey data. First, we took the average size $\bar{v}_{\mathrm{a,h}}$ in each haul for each age class present in the haul:

$$\bar{v}_{\mathrm{a,h}} = \begin{cases} Null & \text{if } c_{a,h} = 0 \\ \frac{1}{N}\sum_i^N v_i & \text{if } c_{a,h} > 0 \end{cases} \qquad \text{[Equation S1]}$$

Then, total catch-per-unit-effort $c_{a,y}$ of age a per year y was calculated as the sum of catch $c_{a,h}$ of each age class across all hauls within each year.

$$c_{a,y} = \sum_h^h c_{a,h} \qquad \text{[Equation S2]}$$

Catch of each age in each haul $c_{a,h}$ was then weighted by total catch $c_{a,y}$ for each age in each year, if individual specimens of that age class were present, to obtain the weighted catch-per-unit-effort for each age in each haul, $\hat{c}_{a,h}$.

$$\hat{c}_{a,h} = \begin{cases} Null & \text{if } \bar{v}_{a,h} = Null \\ \frac{c_{a,y,h}}{c_{a,y}} & \text{if } \bar{v}_{a,h} > 0 \end{cases} \quad \text{[Equation S3]}$$

For each haul and age, the average size was corrected by $\hat{c}_{a,h}$ to calculate the weighted-average size per haul per age $\hat{v}_{\mathrm{a,h}}$.

$$\hat{v}_{\mathrm{a,h}} = \begin{cases} Null & \text{if } \bar{v}_{\mathrm{a,h}} = 0 \\ \bar{\mathrm{v}}_{\mathrm{a,h}} \times \dot{c}_{\mathrm{a,h}} & \text{if } v_{\mathrm{a,h}} > 0 \end{cases} \quad \text{[Equation S4]}$$

For each age and year, $\hat{v}_{\mathrm{a,h}}$ were then summed to obtain the annual simple empirical estimate of size-at-age $\bar{v}_{\mathrm{a,y}}$

$$\bar{v}_{\mathrm{a,y}} = \sum_h \hat{v}_{\mathrm{a,h}} \quad \text{[Equation S5]}$$

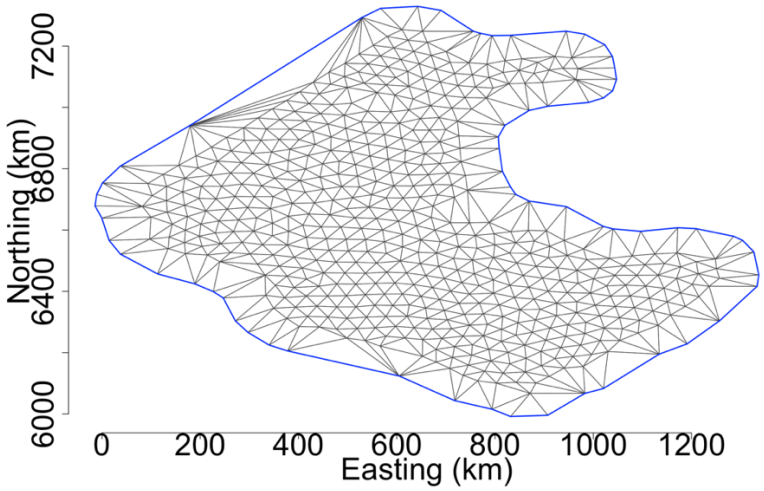

Appendix Figure 3. Plot of SPDE mesh

Appendix D. Guidance for implementing models in VAST

In order to jointly estimate abundance-at-age $n_{g,a,y}$ and size-at-age $w_{g,a,a}$, we needed to implement a model that could accommodate two different assumptions and structures of each response variable. Given these constraints, we implemented the joint model using the Poisson-link delta approach. Each size- and density-at-age category is specified with its probability distributions and link function (i.e. by setting the ObsModel in VAST terminology), and separate spatial (i.e. omega term) and spatio-temporal (i.e. epsilon term) variation are estimated for each size- and density-at-age. Spatial and spatio-temporal terms are not correlated across ages (i.e. they are "IID" in VAST input terminology). Abundance followed the same structure as the univariate model of abundance above [Eqs. 5-9]. However, modeling encounter probability $r_{1,i}$ is

unnecessary for size-at-age because there are no zero-measurements in the size-at-age data set. If there was any size measurement from an age class in a year, the temporal variation term β_{1,a_i,y_i} was set at an arbitrarily high value. This essentially fixed the encounter probability $r_{1,i}$ at 1 (i.e. 100% encountered). This subsequently sets the probability of encounter, $w = 0$ (a meaningless measure for size) to 0. As the final estimated metric in the Poisson-link model is the product of $r_{1,i}$ and $r_{2,i}$, the estimated size $w_{g,a,y}$ is ultimately determined by $r_{2,i}$. Additionally, to handle any possible missing observations from the size data, if for a certain age class in a year there was not any size measurement from the survey, β_{1,a_i,y_i} was set to an arbitrarily low value so that the encounter probability was 0, and the final estimated size was 0 and could be considered null. The linear predictors for size included the same terms for spatial, spatio-temporal, and temporal variation as for abundance [Eq. 7-8]. Estimated size (i.e. $w > 0$) was then assumed to follow a lognormal distribution. For additional details on how we coded this model in VAST, see https://github.com/jindivero/BS_pollock_size.

Appendix E. Results

Appendix Table 2. Estimated parameters from model fit

Age	Type	log (σ_ω)	log (σ_ε)	log (σ_v)	log (σ_r)	log (κ)	ρ_ε
1-15+	Abundance & Size	--	--	--	--	-4.06394897	0.362476913
1	Abundance	0.97807	1.557673	--	0.115971		
2	Abundance	1.223764	1.762706	--	0.269778		
3	Abundance	1.946981	1.927802	--	0.206826		
4	Abundance	1.940865	1.842483	--	0.212377		
5	Abundance	2.298627	2.106406	--	0.214086		
6	Abundance	2.120513	1.959273	--	0.156079		
7	Abundance	1.992946	1.840066	--	0.088229		
8	Abundance	1.763281	1.592529	--	0.06348		
9	Abundance	1.523168	1.431957	--	-0.01098		
10	Abundance	1.428176	1.349939	--	-0.00129		
11	Abundance	1.188955	1.17892	--	-0.03362		
12	Abundance	1.054299	1.154933	--	-0.03973		
13	Abundance	0.949679	1.081978	--	-0.03917		
14	Abundance	0.832815	1.065698	--	-0.061		
15+	Abundance	0.932644	1.03676	--	-0.00944		
1	Size	0.220492	0.262857	-1.03459			
2	Size	0.267444	0.339945	-1.12323			
3	Size	0.165468	0.273865	-1.14332			
4	Size	0.096283	0.176453	-1.48536			
5	Size	0.085841	0.146942	-1.54024			

6	Size	0.066936	0.147395	-1.56107			
7	Size	0.073079	0.142947	-1.57347			
8	Size	-0.07264	0.139977	-1.53177			
9	Size	0.09113	0.14984	-1.50034			
10	Size	0.094674	0.147367	-1.47795			
11	Size	0.097925	0.141009	-1.43676			
12	Size	0.111473	0.124506	-1.39966			
13	Size	0.109395	0.123049	-1.38787			
14	Size	0.121948	0.136685	-1.4969			
15+	Size	0.107769	0.115632	-1.46591			

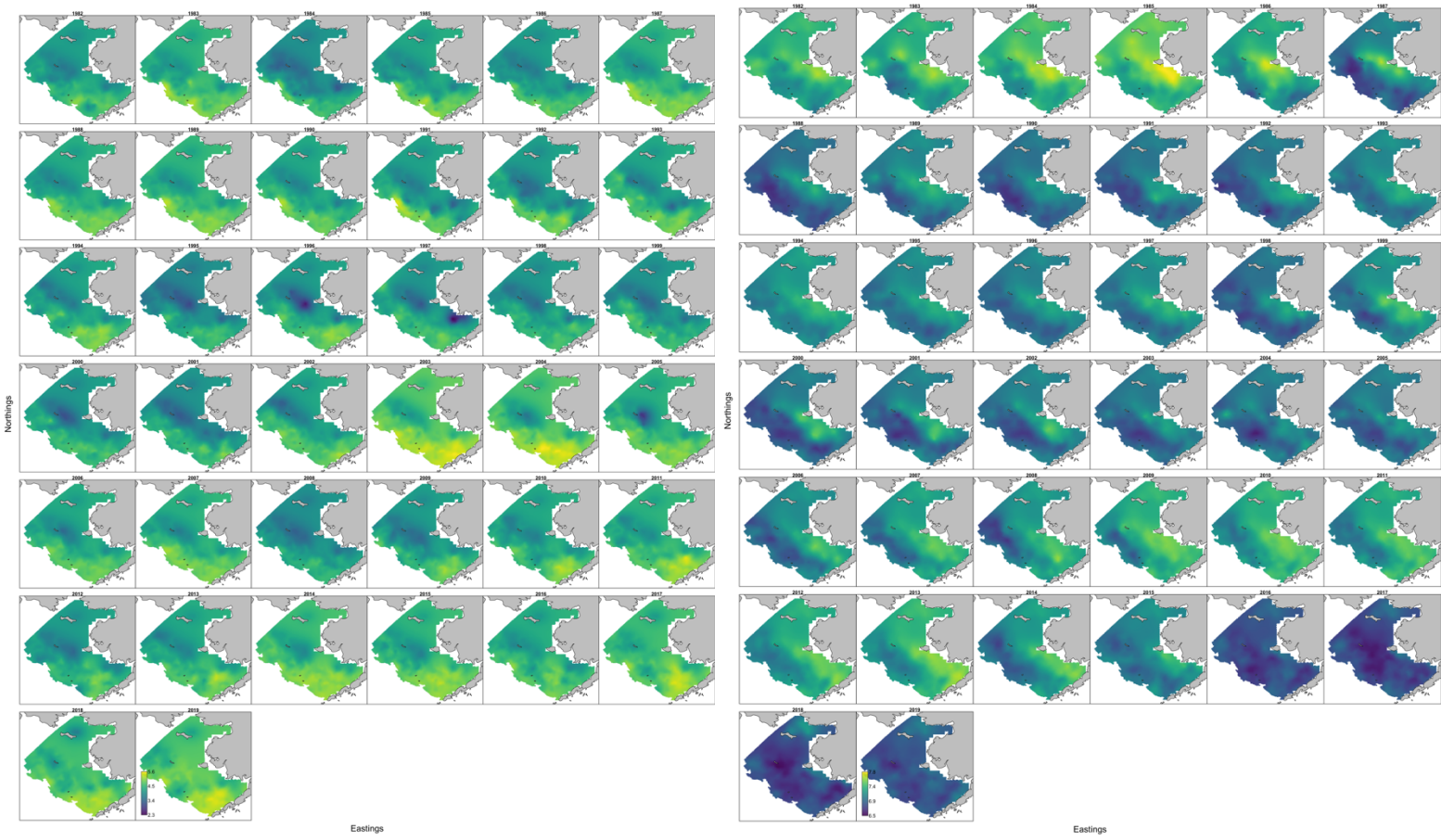

Appendix Figure 4. Log(weight, grams) for age-1 (left) and age-9 (right) pollock in 1982—2019.

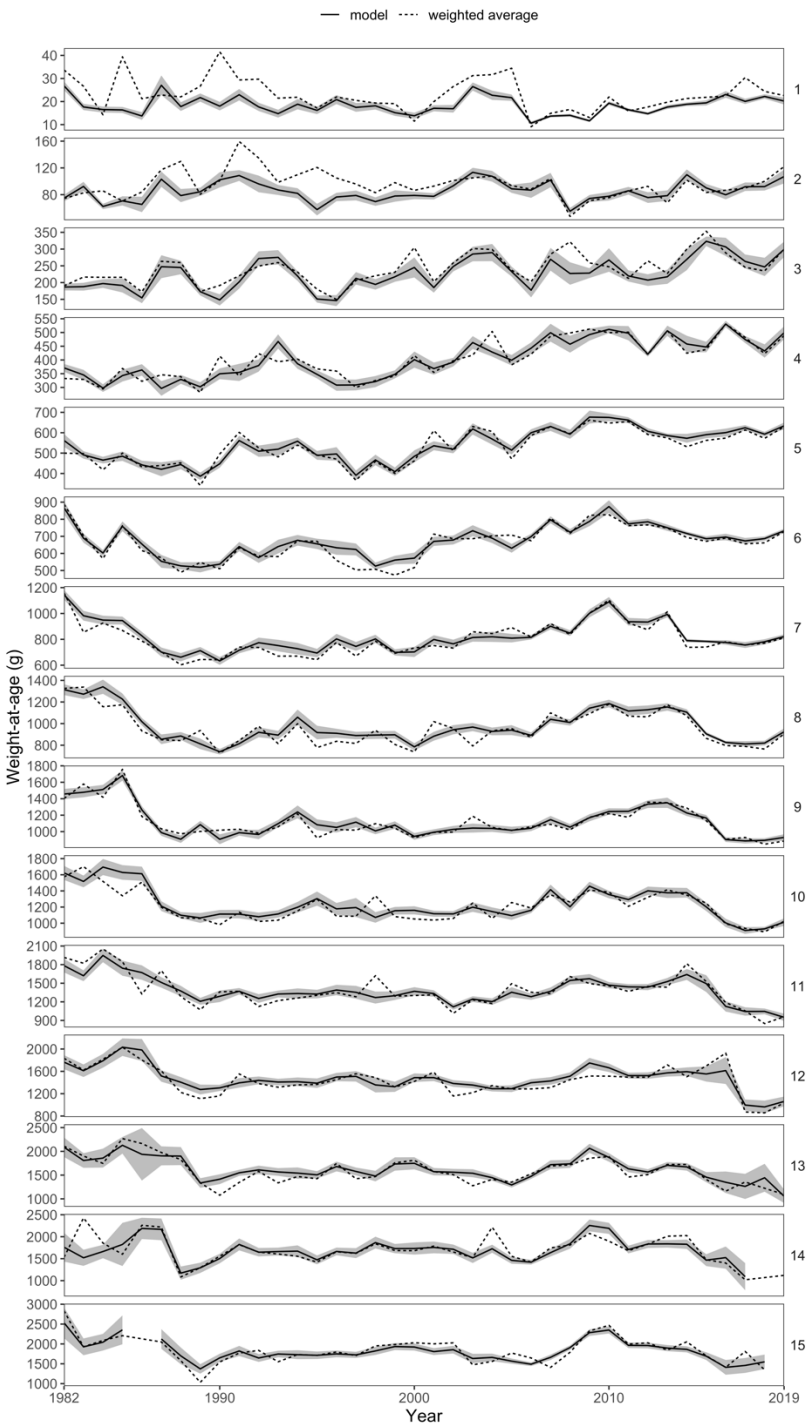

Appendix Figure 5. Annual abundance-weighted size-at-age (i.e. size-at-age matrix) from model estimates (solid black line) and standard error (grey shaded) compared to the non-spatially explicit weighted average of observations (dashed line).

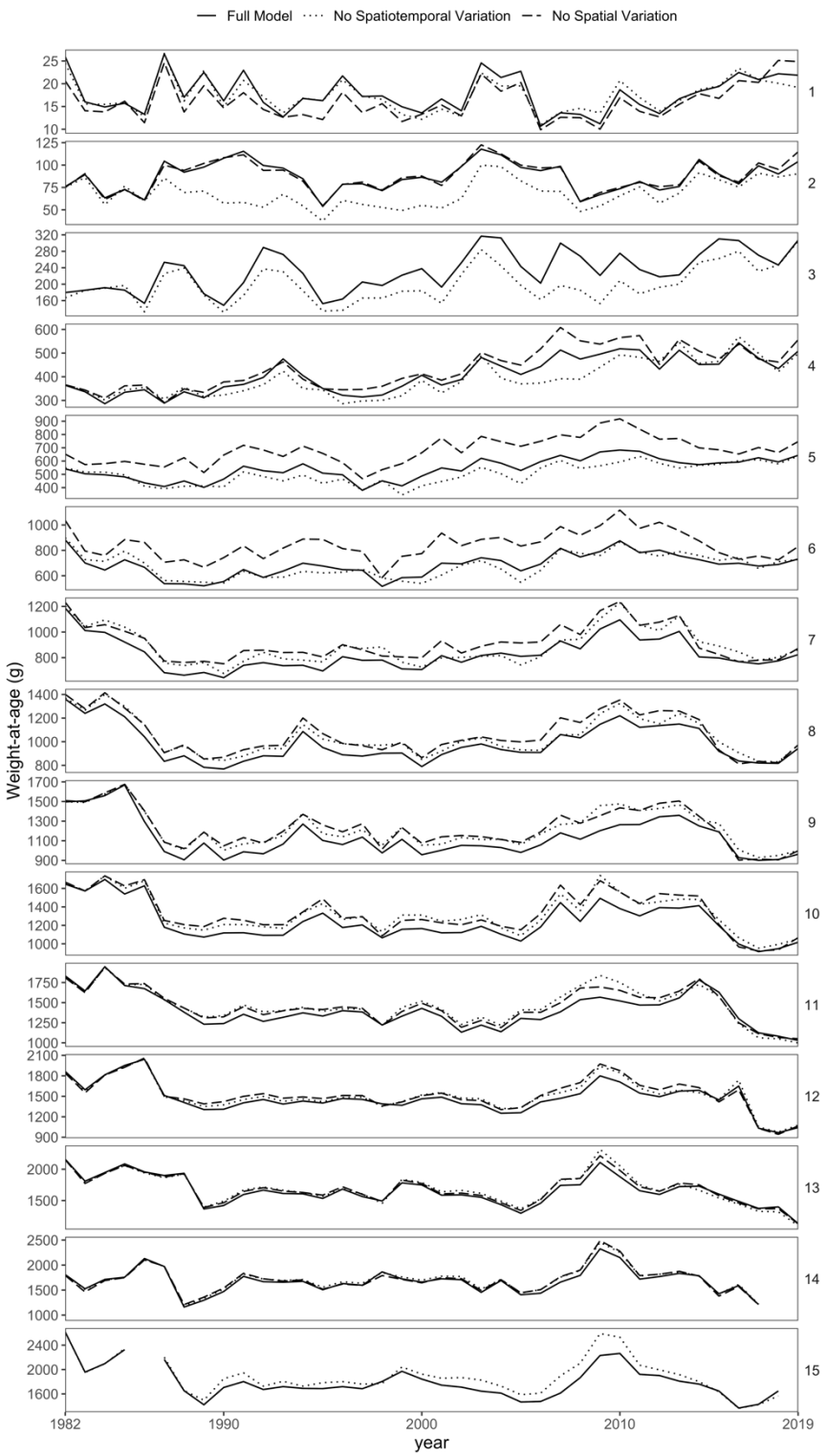

Appendix Figure 6. Contribution of spatial (dashed line) and spatio-temporal (dotted line) variation to the population size-at-age matrix compared to the full model (black line).

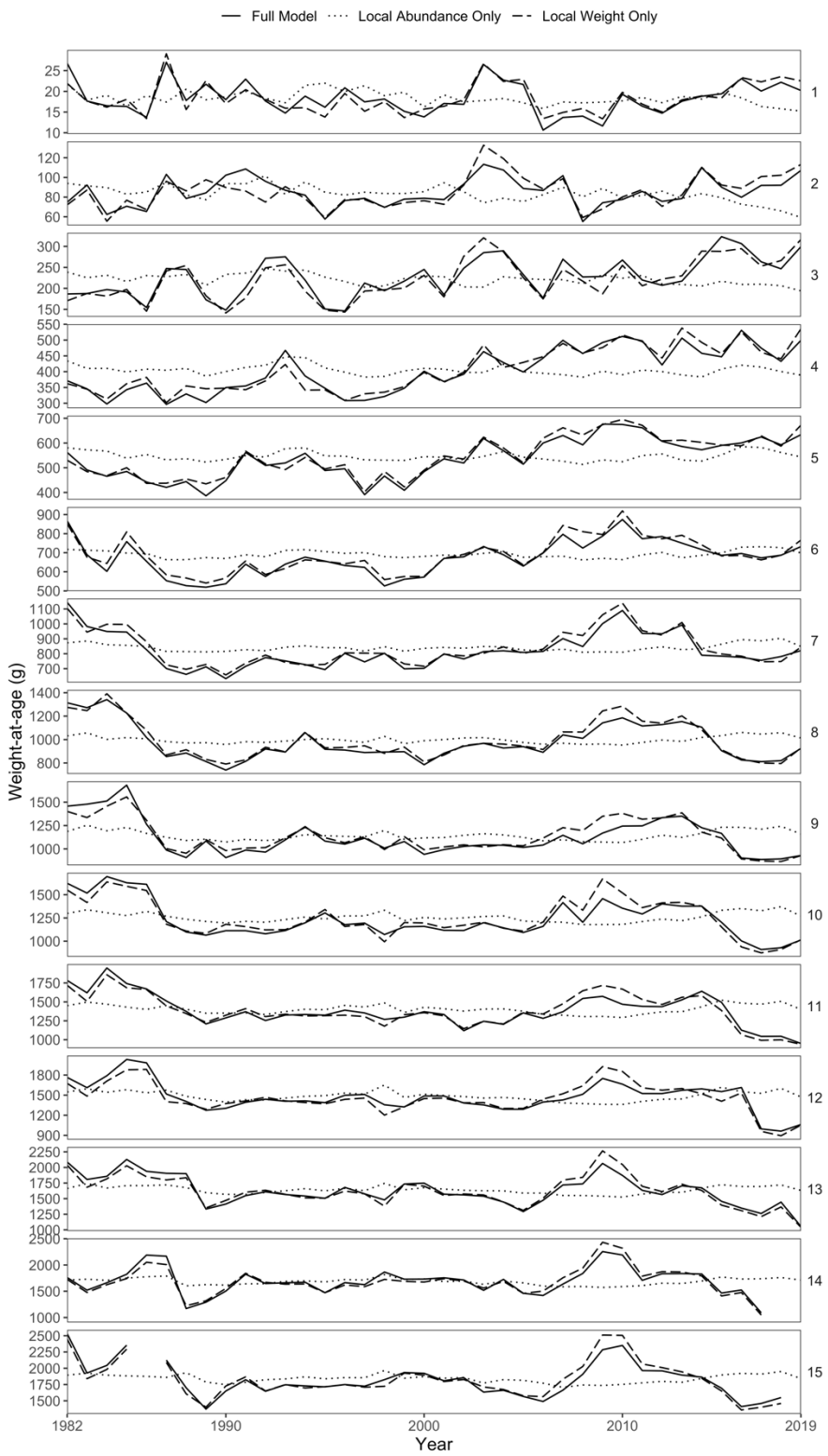

Appendix Figure 7. Contribution of local abundance (dotted line) versus local size-at-age (dashed line) to the population size-at-age matrix (solid black line) compared to the full model.

CHAPTER 2 APPENDIX

Appendix A. Re-parameterization of logistic function

We re-parameterized the threshold function (Eq. 3), since α_0 and α_1 are not readily interpretable and their estimates covary. We therefore applied a common reparameterization of the logistic function by replacing these two terms with two location parameters, one describing the value of $f(\Phi_{eco})$ at which $e^{f(\Phi_{eco})}$ equals 0.5 ($s50$) and another describing the value of $f(\Phi_{eco})$ at which $e^{f(\Phi_{eco})}$ equals 0.95 ($s95$).

Given those parameters, the two parameters α_o and α_1 equal:

$$\alpha_0 = \left(\frac{b-a}{s_{95}-s_{50}}\right) \quad \text{Eq. S1}$$

$$\alpha_1 = \left(\frac{a-b}{s_{95}-s_{50}}\right) \quad \text{Eq. S2}$$

Where,

$$a = \left(\frac{\psi}{log\,(0.5)+\psi} - 1\right) \quad \text{Eq. S3}$$

$$b = \left(\frac{\psi}{log\,(0.95)+\psi} - 1\right) \quad \text{Eq. S4}$$

Linking estimation model to the metabolic index

The metabolic index is a ratio of Arrhenius equations expressing the ratio of oxygen supply to oxygen demand:

$$\Phi = A_o B^n\, pO_2\, exp\left[\frac{E_0}{k_b}\left(\frac{1}{T} - \frac{1}{T_{ref}}\right)\right] \quad \text{Eq. S5}$$

Where Φ is the metabolic index, A_o is the ratio of resting metabolic oxygen supply to oxygen demand at a reference temperature (T_{ref}), B is body mass, n is an allometric scaling factor, T is temperature in degrees Kelvin, k_b is Boltzmann's constant, and E_0 is the effect of temperature on the ratio of oxygen supply to demand.

We wish to use the metabolic index as the basis of Eq. 2, i.e. we want the model to relate local abundance to the metabolic index. Substituting Eq. S4 for Φ_{eco}:

$$f(\Phi_{eco}) = \psi\left(\frac{1}{1+exp\left(-\alpha_0-\alpha_1 A_o B^n\, pO_{2,i}\, exp\left[\frac{E_0}{k_b}\left(\frac{1}{T_i}-\frac{1}{T_{ref}}\right)\right]\right)} - 1\right) \quad \text{Eq. S6}$$

However, this expression includes three non-separable terms: α_1, A_o and B^n. The estimated parameter α_1 (Eq. 3) is a combination of terms that includes A_o and B^n, and we therefore instead express Φ_{eco} as only those terms of the metabolic index that depend on pO_2 and temperature:

$$\Phi_{eco,i} = pO_{2,i}\, e^{\frac{E_o}{k_b}\left(\frac{1}{T_i}-\frac{1}{T_{ref}}\right)} \quad \text{Eq. S7}$$

Appendix B. Supplemental Methods

Table S1. Summary of variable names, symbols, values, and units used in data simulation and model fitting

Name	Source	Symbol	Value in Simulated data	Units
Dissolved oxygen	Data	pO_2	NOAA bottom trawl data	Partial pressure
Temperature	Data	T	NOAA bottom trawl data	Celsius (converted to Kelvin)
Depth	Data	d	NOAA bottom trawl data	Meters (logged and scaled)
Observation	Data, model	i	NOAA bottom trawl data	Year and latitude and longitude of catch
Year	Data, model	t	NOAA bottom trawl data	--
Fish density	Data, model	y	Eq. 2	Kilograms kilometer^{-2}
Year effects (2011, 2012, 2013, 2014, 2015)	Parameter (model)	b_{year}	N(4,1)	--
Depth effect	Parameter (model)	b_2	1.5	--
Depth^2 effect	Parameter (model)	b_3	-1.0	--
Spatial variation	Model	ω	--	--
Spatial range	Parameter	r	85	--
Spatial standard deviation	Parameter	σ	1.77	--
Mean fish density	Tweedie distribution (model)	μ	--	--
Tweedie scale parameter	Parameter (Tweedie distribution)	σ	10	--
Tweedie power parameter	Parameter (Tweedie distribution)	p	1.5	--
$f(\Phi_{eco})$	Synergistic temperature-oxygen effect term (Model)		Eq. 3; (Eqs. S1—4)	
Scaling parameter	Parameter (logistic function)	ψ	50	--
95% threshold	Parameter (logistic function)	$s95$	4	--
50% threshold	Parameter (logistic function)	$s50$	2	--

Logistic coefficient	Re-parameterized coefficient (logistic function)	α_0	1.119	--
Logistic coefficient	Re-parameterized coefficient (logistic function)	α_1	1.313	--
Logistic coefficient	Re-parameterized coefficient (logistic function)	a	-3.744	--
Logistic coefficient	Re-parameterized coefficient (logistic function)	b	-6.369	--
Metabolic Index	Adapted metabolic index (Model)	Φ_{eco}	Eq. 4; (Eqs. S5—S7)	
Boltzmann's constant	Constant (Derived metabolic index)	k_b	8.6173324×10^5	eV K^{-1}
Reference temperature	Constant (Derived metabolic index)	T_{ref}	12	Celsius (converted to Kelvin)
Temperature-sensitivity of oxygen dependence	Parameter (Derived metabolic index)	E_0	0.3 (Typical Case) 0.7 (Unusual Case)	--

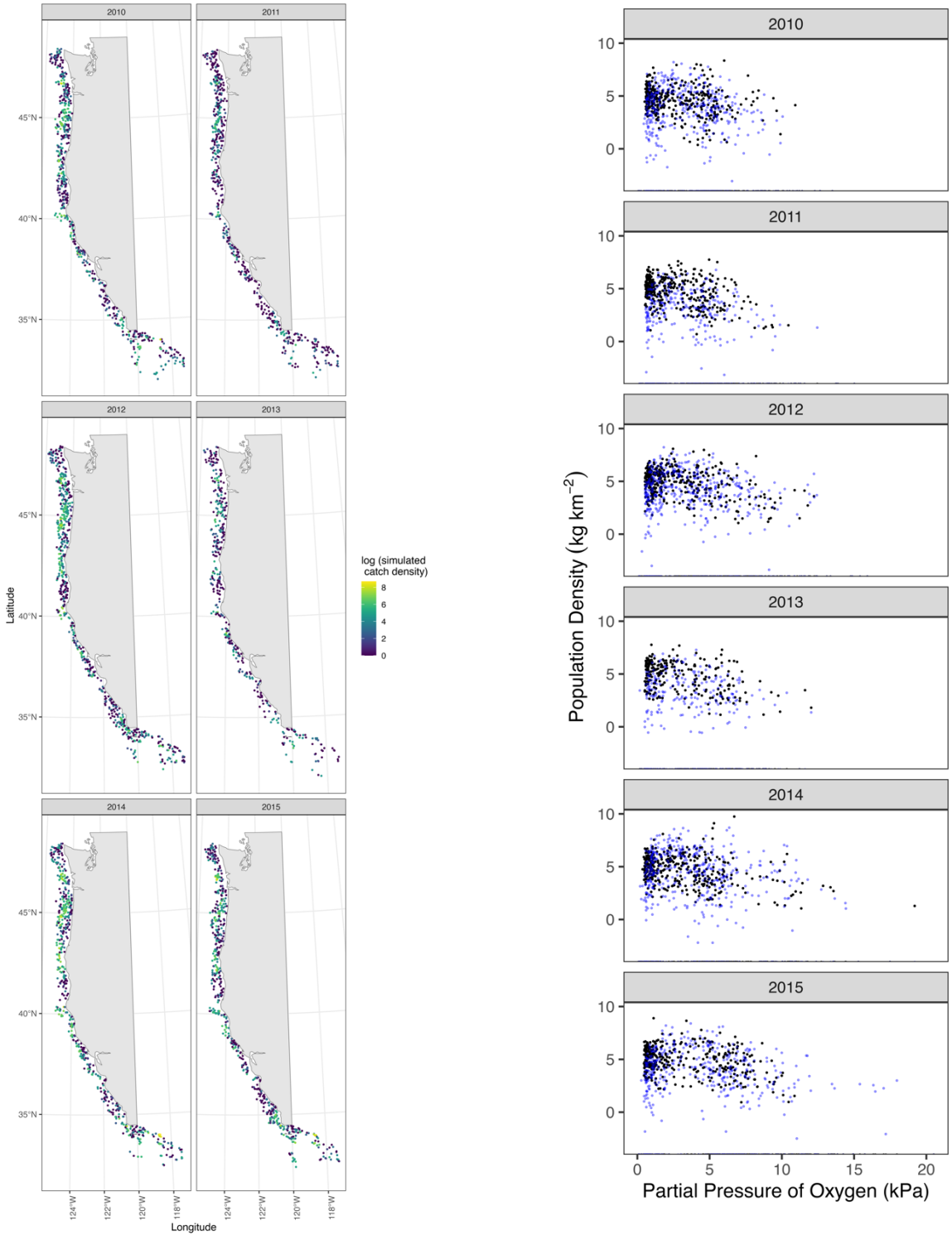

Figure S1. Example of one simulated dataset of catches across years and space (left), and across oxygen compared to the real data (right).

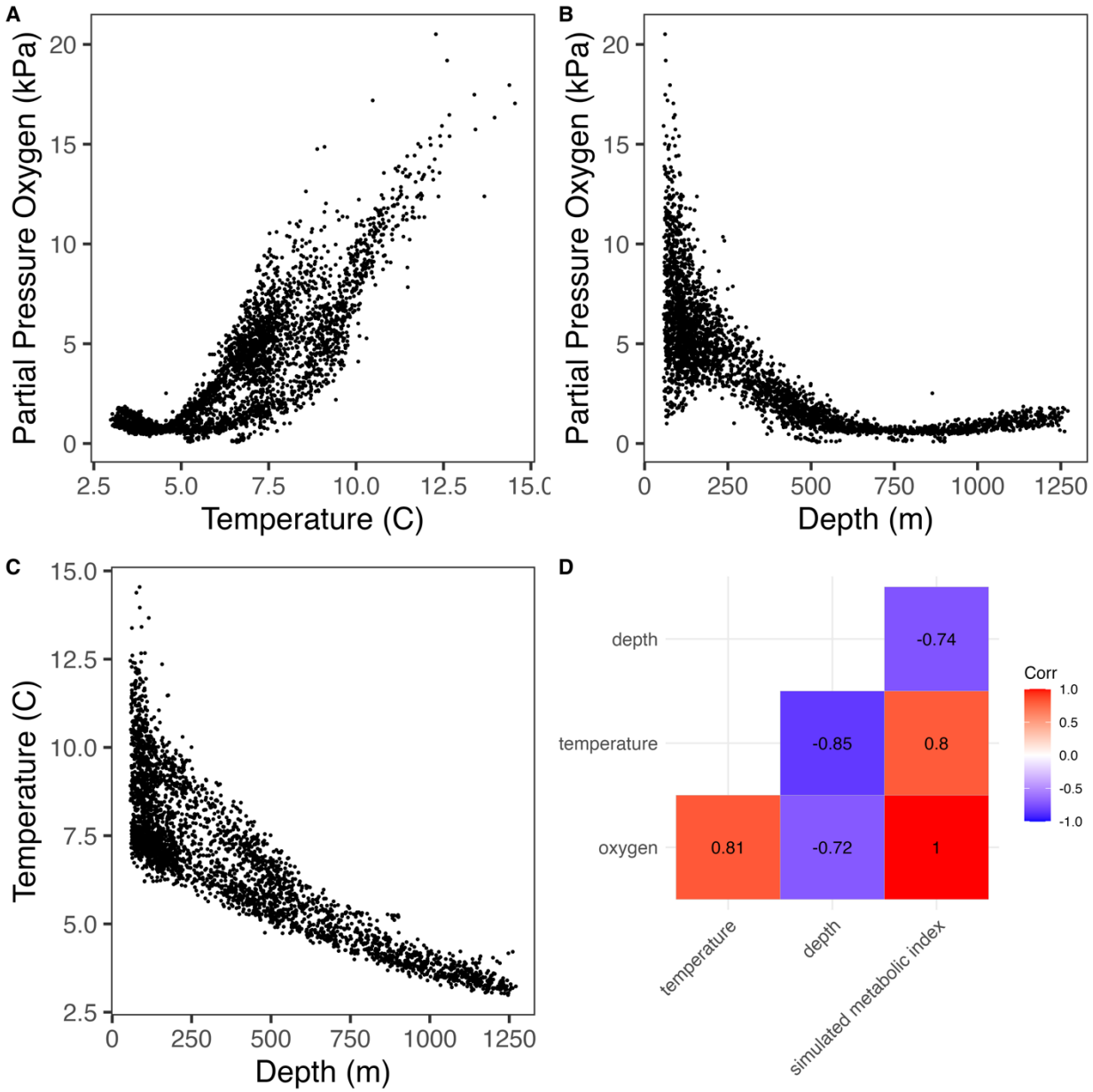

Figure S2. (A-C) Temperature (C), depth (m), and partial pressure oxygen (kPa) from the West Coast Bottom Trawl Survey data 2010-2015 (see Keller et al., 2017) used for the data simulations, (D) correlation matrix of depth, temperature, oxygen, and the simulated metabolic index

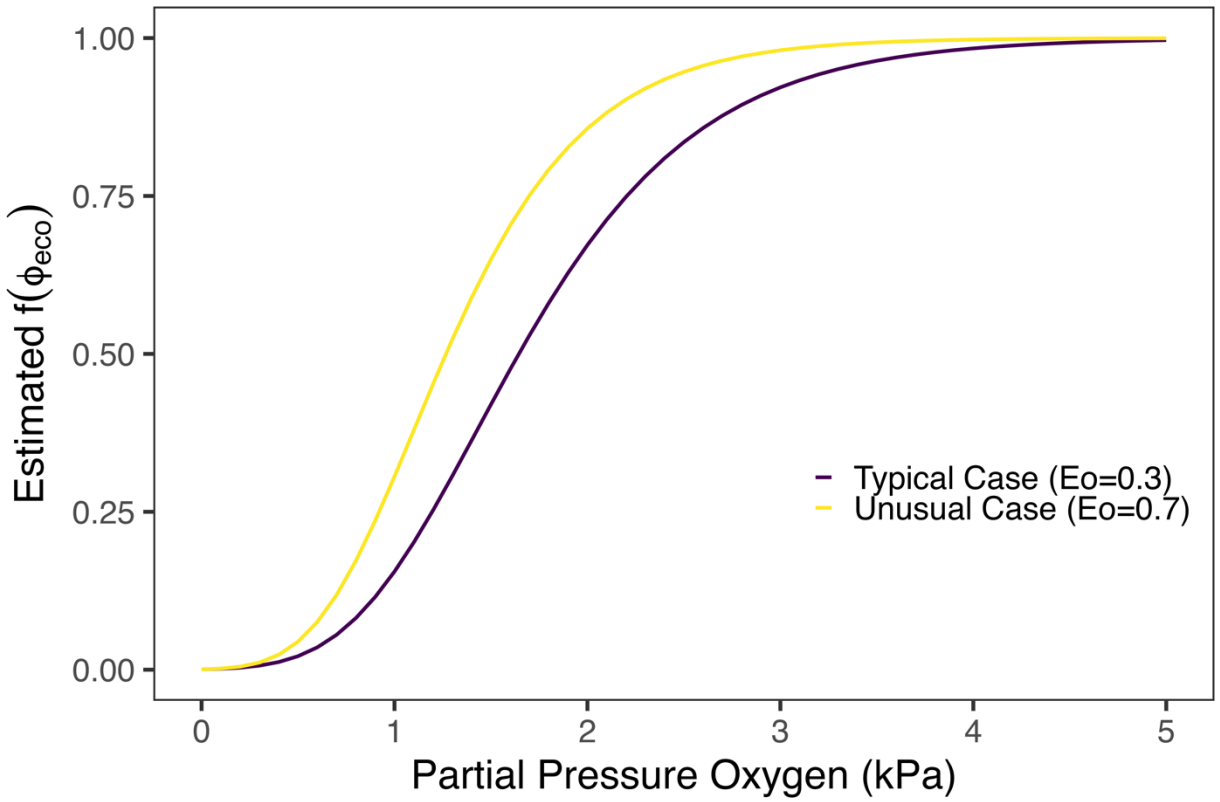

Figure S3. The sigmoidal response to the adapted metabolic index $f(\Phi_{eco})$ simulated for the typical case (E_o=0.3) and the unusual case (E_o=0.7) across a range of oxygen at an example temperature (6 C). The typical case represents a simulated species' temperature-dependence of oxygen tolerance that is close to the median value from the empirical meta-analysis for a generic teleost (E_0=0.3), and the unusual case where a simulated species' temperature-dependence of oxygen sensitivity deviates greatly from the expected value (i.e. the median of the meta-analysis) and is roughly equal to the upper 90% of the meta-analysis distribution (E_0=0.7).

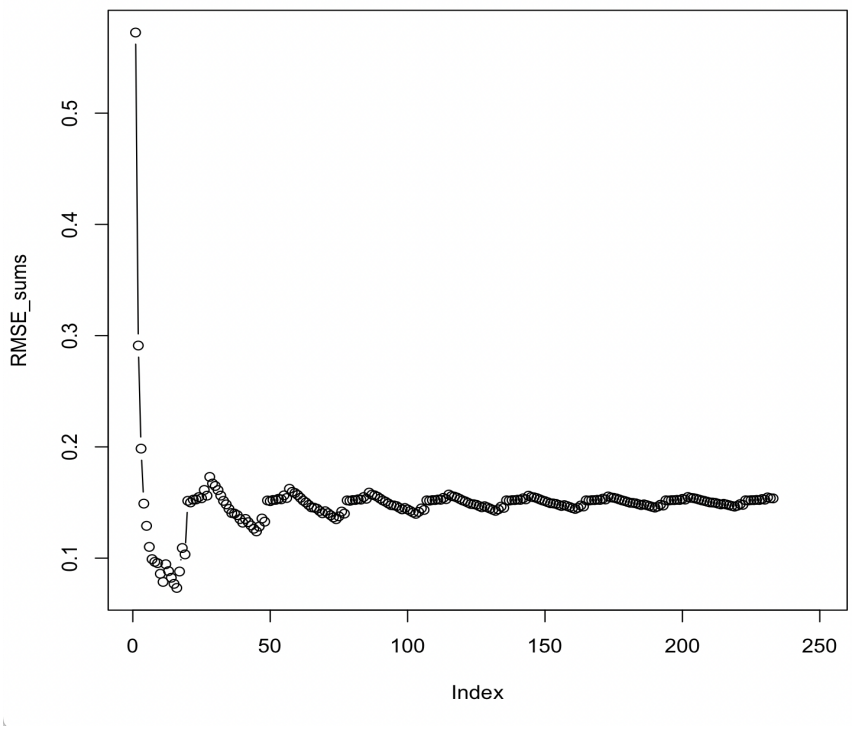

Figure S4. Cumulative root mean squared error (RMSE) for increasing number of iterations of generated data, with 250 total simulated datasets.

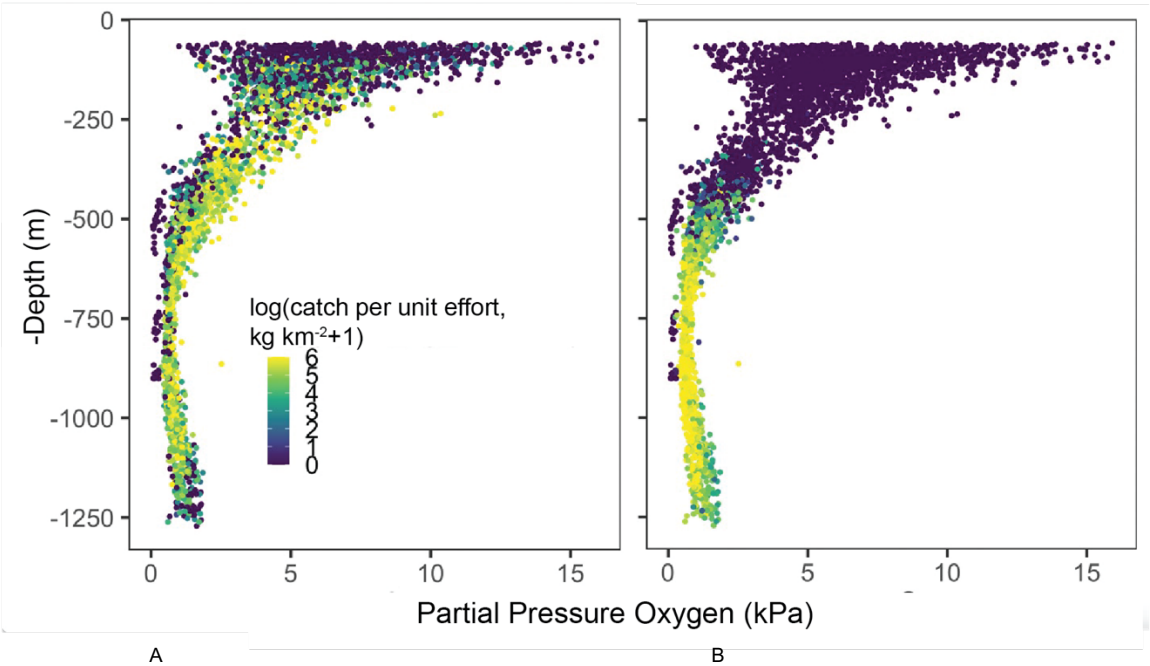

Figure S5. (A) Catch for sablefish and (B) longspine thornyhead across depth (meters) and oxygen (kPa)

Appendix C. Supplemental Results

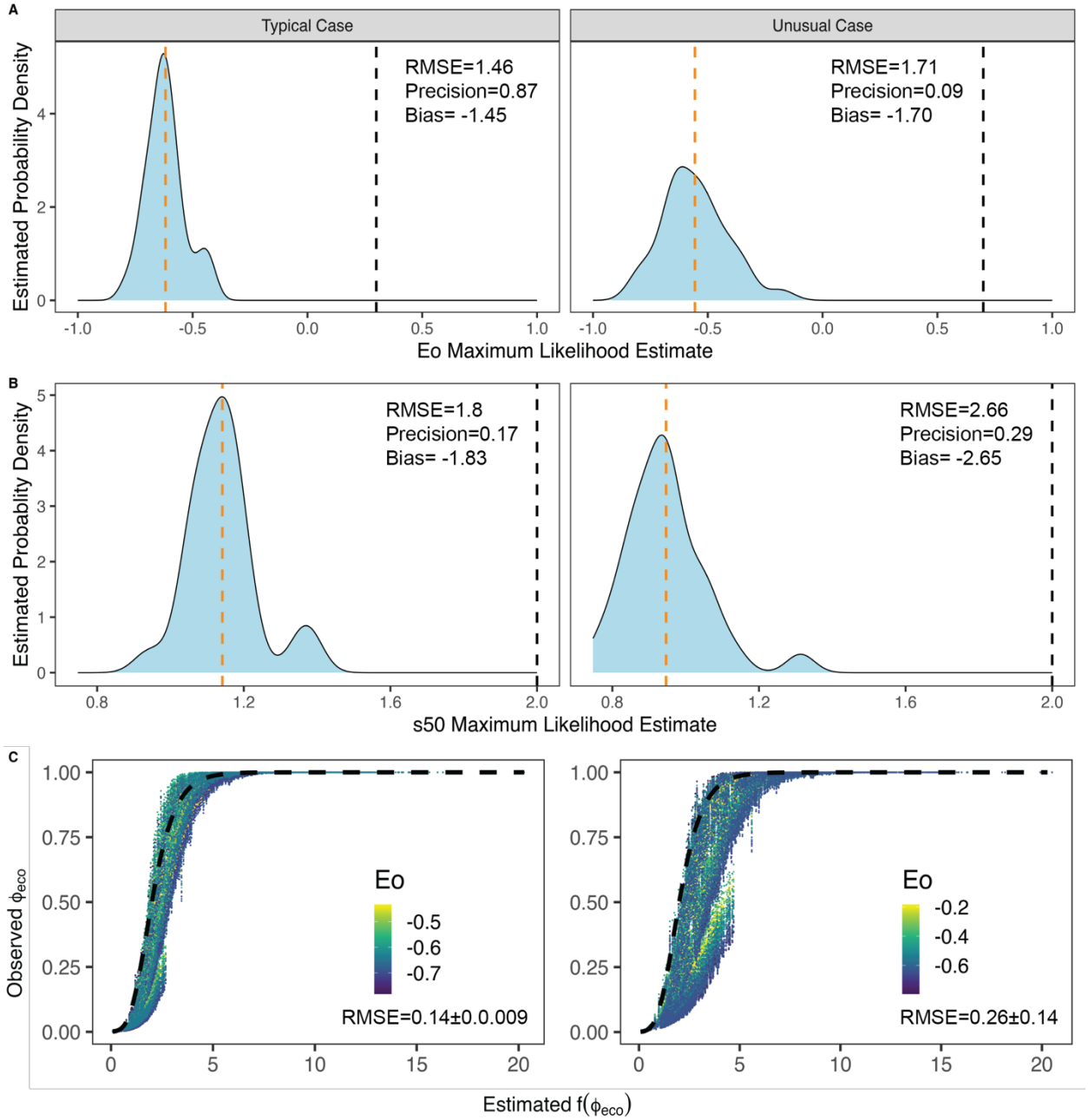

Figure S6. (A-B) Predicted parameter estimates and (C) $f(\Phi_{eco})$ marginal effect for the mis-specific model for the simulated typical and unusual cases with maximum likelihood estimates. The dashed black line indicates the true value across all panels, and dashed orange line the average maximum likelihood estimate.

Table S2. Alternative models for simulated data of species with typical and unusual temperature-dependences of oxygen. Δ AIC was calculated for alternative models within each data simulation compared to the best-supported model, + $f(\Phi_{eco})$, and then averaged across

the 250 data simulations. Average Δ AIC ± standard deviation across the 250 data simulations is reported.		
Model	Δ AIC typical species	ΔAIC unusual species
+breakpoint(pO_2)	294±53	265±72
+ $f(\Phi_{eco})$	0	0
+logistic(pO_2)	2.75±4	20±62
+ temperature	494±74	394±92
+ pO_2	483±73	386±92
+Temperature + pO_2	483±73	387±92
+Temperature * pO_2	425±69	347±85
Null	506±77	400±93

Table S3. Parameter estimates of threshold parameters for alternative models fit to sablefish and longspine thornyhead. Parameter estimated reported as maximum likelihood estimate ± standard error. (*NA* indicates standard error was not calculated because of NA values returned in estimation procedure.)		
Model	Sablefish	Longspine thornyhead
+Breakpoint(pO_2)	Slope= 41.84±13.7 Breakpoint= -1.0± 0.01	Slope=21.7±2.63 Breakpoint= -1.12±0.0
+$f(\Phi_{eco})$	s50=0.88±0.08 s95 =0.57±0.13 ψ =3365±62201 E_0=1.53±0.28	s50=0.26±0.05 s95=0.06±0.04 ψ=100±*NA* E_0=-0.79±0.56
+Logistic(pO_2)	s50=-1.11±0.01 s95=-2.42±0.21 ψ =200±1066	s50= -1.18 ±0.01 s95=-3.34±0.43 ψ =64.62±769.35

CHAPTER 3 APPENDIX

Appendix A Methods

Study Region Descriptions

The California Current system extends approximately 3,000 km from southern British Columbia to the Baja California, Mexico and ~500-800 km offshore into deeper water off the continental shelf. It is characterized by strong wind-driven upwelling in the spring and summer (overlapping with the bottom trawl sampling period), and outflows of large freshwater rivers (Checkley and Barth, 2009). The British Columbia region encompasses the continental shelf and upper slope of most of the British Columbia coast (Queen Charlotte Sound, Hecate Strait, West Coast Vancouver Island, West Coast Haida Gwaii, and the Strait of Georgia). It has an intricate coastline of islands, deep fjords, and networks of inlets and straits with seasonal upwelling (Crawford and Thomson, 1991). The Eastern Bering Sea is a broad (>500 km wide) and flat continental shelf terminating with a steep continental slope and large marine canyons. It is characterized by high seasonal dynamics and oceanographic conditions influenced strongly by variation in the extent of seasonal sea ice that can extend across the continental shelf and northern slope during winter and spring (Coachman 1986; Stabeno et al., 2016a). The Gulf of Alaska is a semi-enclosed basin that is influenced by variation in the timing and magnitude of river discharge and eddy transport (Stabeno et al., 2004; Stabeno et al., 2016b. The bottom trawl survey samples across ranging from glacial fjords with a freshwater lens to marine-influenced continental slope regions with glacial troughs and submarine canyons that facilitate on-shelf flow (Mordy et al., 2019). The Aleutian Islands are an ice-free archipelago over 2000 km long with a narrow (25-100 km) continental shelf divided by ocean passes. Its oceanography is coastally influenced in the east because of coastal currents (warmer and fresher; salinity < 33) and oceanic currents further west (colder and saltier; salinity > 33) (Hunt Jr. & Stabeno, 2005).

Oxygen data quality control and standardization

Dissolved oxygen data flagged with quality issues were removed. CTD cast data were filtered to the bottom depth of the cast. Reported depth was compared to NOAA bathymetry depth (ETOPO 2022 NOAA bathymetry database, NOAA 2022). Observations with reported depth more than twice the RMSE of the NOAA bathymetry data were removed. Oxygen values were standardized to units of μmol kg^{-1}. Salinity S was converted to potential density anomaly with a reference pressure of 0 dbar, i.e. sigma0, ($\rho(S_A, \theta, p) - 1000$ kg m^{-3}), with potential density ρ , absolute salinity S_A, potential temperature θ, and pressure p following the TEOS-10 polynomial expressions (Roquet et al., 2015) implemented using the R package *gsw* (Kelley et al., 2024). Salinity values less than 28 were replaced with 24 to improve computation of estimation, as marginal effects showed little effect of salinity lower than 24 (Appendix A Figure S1). Oxygen outliers (greater than 1500 μmol kg^{-1}) were removed from training data.

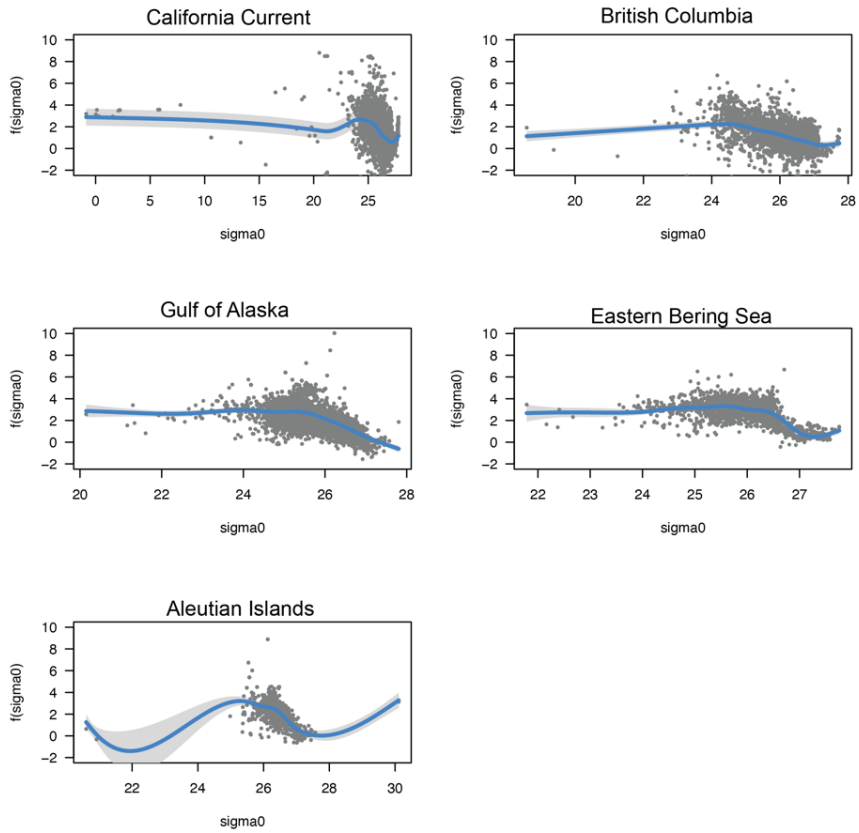

Figure S1. Marginal effect of smoother on salinity, converted to sigma0, fit to all the combined oxygen data.

Application to fish distributions

Distribution models were fit to two species in two regions for each of the three oxygen data sources using a widely used framework and following the methods of Essington et al. (2022). The base species distribution model (SDM) is a generalized linear mixed effects model (GLMM) that estimates the expected density μ of observation i at location s at year t with a log link,

$$\log(\mu_i) = b_{t[i]}t_i + b_2 d_i + b_3 d_i^2 + \omega_i \quad \text{Eq.S1}$$

$$y_i \sim \text{Tweedie}(\mu_i, \phi, p) \quad \text{Eq. S2}$$

where b_t are independent year effects for each year t_i, b_2 and b_3 are the estimated effects of scaled *log*(depth) (d_i) and its square (d_i^2), and ω_i is a spatial random effect that accounts for spatially structured latent variables. By "scaled", we mean we subtracted the mean and divided by one standard deviation. Observed catch rate y_i is assumed to follow a Tweedie distribution with power parameter p ($1 < p < 2$) and scale parameter ϕ (Shono, 2008, Tweedie 1984), because it is flexible to account for the large number of zeroes in catch rate data without requiring a delta or hurdle two-part model. Spatial effects are modeled as the stochastic partial differential equation (SPDE) approximation to Gaussian random fields via Gaussian Markov random fields (GMRFs) (Lindgren et al., 2011) as implemented in TMB (Kristensen et al.,

2016). The random effects describing the spatial field are estimated at a set of vertices or knots and then projected to the locations of observed data with bilinear interpolation, assuming spatial covariance is modeled using a GMRF that approximates a Matérn covariance function with anisotropy (directionally dependent correlation) (Lindgren et al., 2011, Thorson et al. 2015). We iteratively tested mesh size, and used a cutoff of 45 to optimize the number of knots in regions of different sizes: 150 knots in California Current, 100 in British Columbia, 250 in Gulf of Alaska, and 150 in Aleutian Islands. The approach allows modelling a sparse precision matrix of a GMRF, which is considerably more efficient than modelling the covariance matrix of a Gaussian random field directly (Lindgren et al., 2011).

We consider oxygen as a "breakpoint" function that relates a slope β on a predictor variable, x, up until the breakpoint of the predictor variable x_{bp}, on the expected value of the response variable:

$$g(x) = \begin{cases} x\beta & if\ x < x_{bp} \\ x_{bp}\beta & otherwise \end{cases} \quad \text{Eq. S3}$$

Slope was constrained to be positive, breakpoint estimates that were outside the range of oxygen values in the data and with 0 slope estimate (i.e. no effect of oxygen on fish density) were assumed to have no breakpoint effect of oxygen.

Appendix B Results

Figure S2. Root mean squared error (RMSE) for each test year in each region for the empirical *in situ* statistical predictions, and the oceanographic output Global Oceanographic Biogeochemistry Hindcast (GOBH). Models with different spatial and temporal structures—none, persistent spatial fields ("Spatial") and plus annual fixed effects of year ("Annual") or plus spatio-temporal latent effects ("Spatiotemporal")— and including either no covariates ("None"), temperature ("T") or temperature and salinity, as sigma0 ("T+S") were fit to *in situ* dissolved bottom oxygen observations. Units are μmol kg^{-1}.

Region	Year	N training data	N testing data	Empirical Statistical Predictions												GOBH
				None			Spatial			Annual			Spatiotemporal			
				N	T	S+T	N	T	S+T	N	T	S+T	N	T	S+T	
California Current	2009	12452	331	22	19.2	14.9	18.1	16.9	13.5	18	23.9	17.1	18.6	21.7	16.9	43.4
California Current	2010	12161	622	18.5	19.6	15.1	19.6	16.7	13.7	24.6	21.4	17.3	17.9	17	13.4	30.9
California Current	2011	12192	591	21.5	20.1	15.9	19.9	16.9	13.9	19.6	16.6	13.6	17.9	16.2	13.1	33.2
California Current	2012	12124	659	22.6	21	18.1	18.8	19.3	16.6	18.9	20.3	17.5	22	19.8	17	40.6
California Current	2013	12362	421	19.5	20.5	16	18.3	20.5	15.8	18.5	20.1	15.7	22.8	21.1	16.5	31.8
California Current	2014	12167	616	24.6	18.9	17.9	21.7	16.8	16.4	21.7	16.6	16	24.4	17.5	17	32
California Current	2015	12181	602	28	21.2	18	26.5	19	16.9	22.9	17.9	17	26.1	17.7	16.7	33
California Current	2022	12190	593	27	24.2	19.8	23.5	22	18.8	25.1	21.6	18.8	22.9	22.4	20	36.3
California Current	2023	12231	552	23.8	20.7	19	19.9	22.1	18.8	25.6	21.4	18.3	19.2	22.8	19.3	57.5
British Columbia	2017	4644	343	37	34.2	33.2	38.7	36.5	37.5	37.8	38	35.4	37.1	32	33.5	46.8
British Columbia	2018	4730	257	33.5	36.1	15.9	16.7	15.7	10.7	15.7	19.9	12.8	22.5	23.9	19.3	17.3
British Columbia	2019	4648	339	34.1	34.7	33.1	33.9	34.8	33.1	34.4	34.5	33.7	33.4	32.3	33.2	38.5
British Columbia	2021	4704	283	28.6	22.7	13.1	20.7	15.8	13	20.7	14.2	12.6	25.9	15.5	14.4	18.9
British Columbia	2022	4746	241	33.9	30.9	18.2	21.8	20.8	16.7	23	20.2	13.2	24.2	22.2	17.4	20.9

British Columbia	2023	4647	340	48.4	39.1	25.1	27.9	28.4	23	35	32.2	23.6	50.3	41.7	25.8	74.9
Gulf of Alaska	2013	5704	579	82.8	78.5	73.8	73.9	77.1	72.8	72.5	75.8	69.5	72.6	76.9	70.2	86.6
Gulf of Alaska	2015	5559	724	46.5	54.3	42.1	39	42	35.9	47.9	47.9	46.6	48.4	48.6	51.5	61.2
Eastern Bering Sea	2012	1913	103	54.6	43	36.9	53.4	43.8	39.9	45.9	45.4	44.6	46.9	46.8	41.6	97.7
Eastern Bering Sea	2016	1905	111	39	37.2	43.8	42	36.8	41.3	47.1	63.7	45.1	44.3	41	31.4	79.4
Aleutian Islands	2014	885	177	63.9	59	52.4	64.6	54.7	48.6	71.1	70.7	80.4	65.2	58.3	62.1	99.5
Aleutian Islands	2016	964	98	76.4	71.3	63.5	76.5	63.2	65.5	102.3	73.4	68.7	81.8	69.3	71.5	118.2

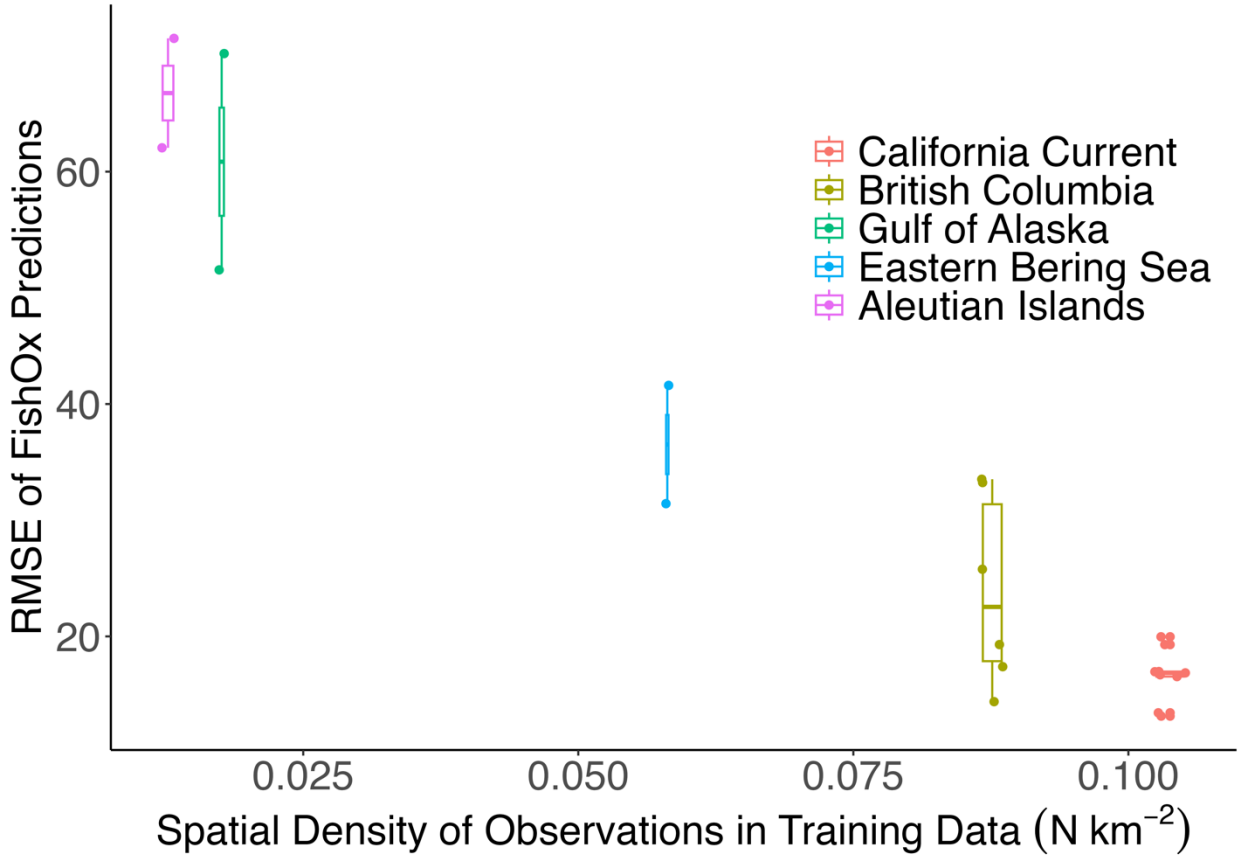

Figure S2. Root mean squared error of each test year (*in situ* bottom dissolved oxygen observations withheld from model fitting, units in μmol kg^{-1}) for each region and the density of observations in the training data (number of observations in training data per area (in km^2) of the testing region (i.e. bottom trawl survey footprint). The California Current had ~12,000 observations per year and an area of 118,391 km^2. British Columbia had ~5,000 observations and an area of 53,580 km^2. The Gulf of Alaska had ~5,000 observations and an area of 320,202 km^2. The Eastern Bering Sea had ~2,000 observations and an area of 32,861 km^2. The Aleutian Islands had <1,000 observations per year and an area of 72,741 km^2.

A

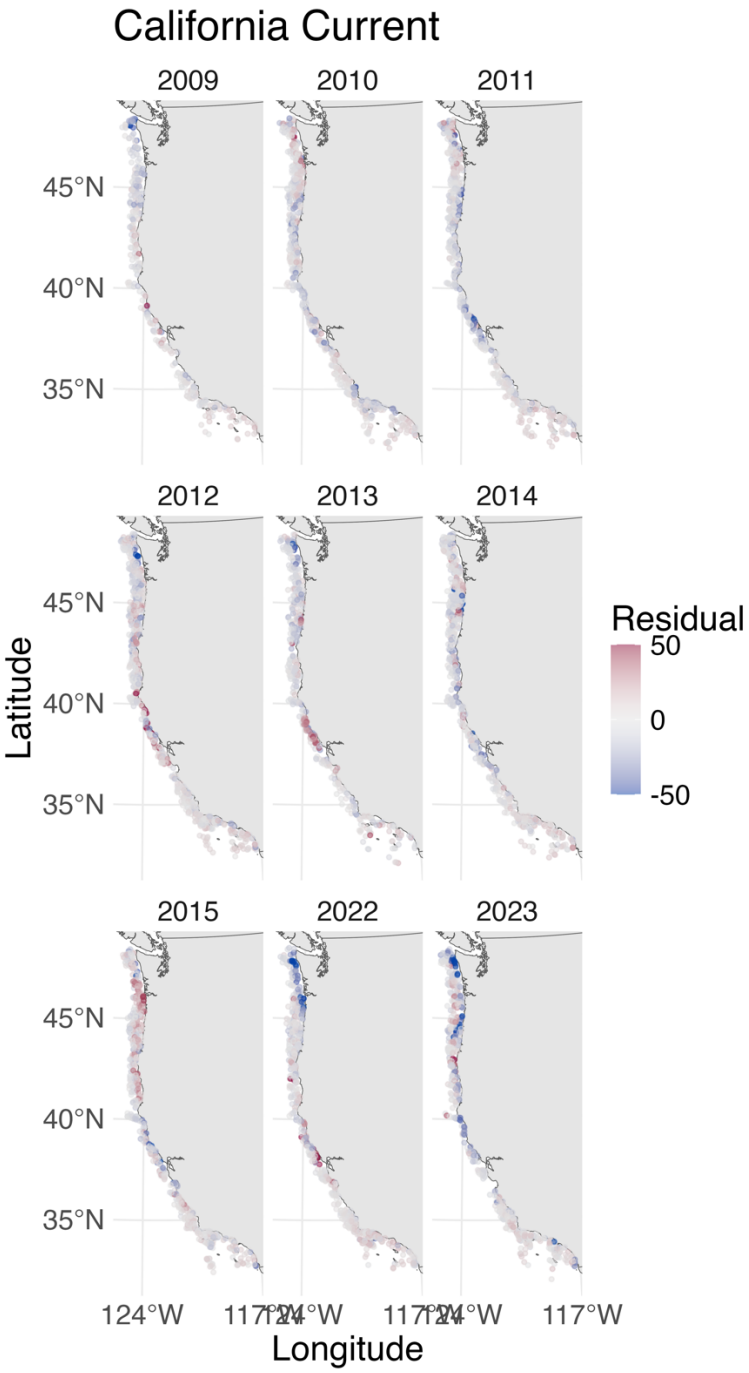
California Current
2009
2010
2011
2012
2013
2014
2015
2022
2023
45°N
40°N
35°N
Latitude
Residual
50
0
-50
124°W
117°W
Longitude

B

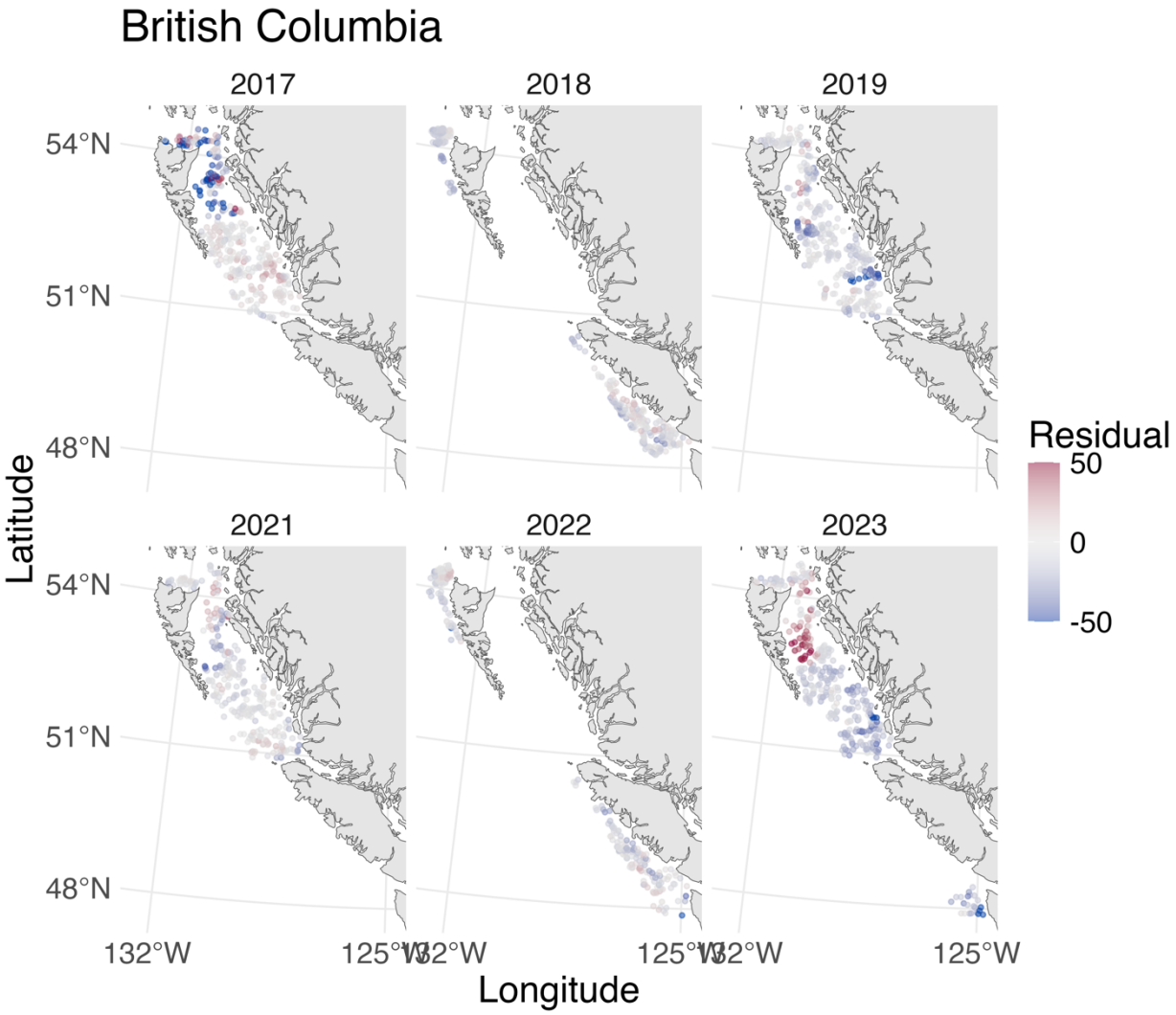
British Columbia
2017
2018
2019
2021
2022
2023
54°N
51°N
48°N
132°W
125°W
Latitude
Longitude
Residual
50
0
-50

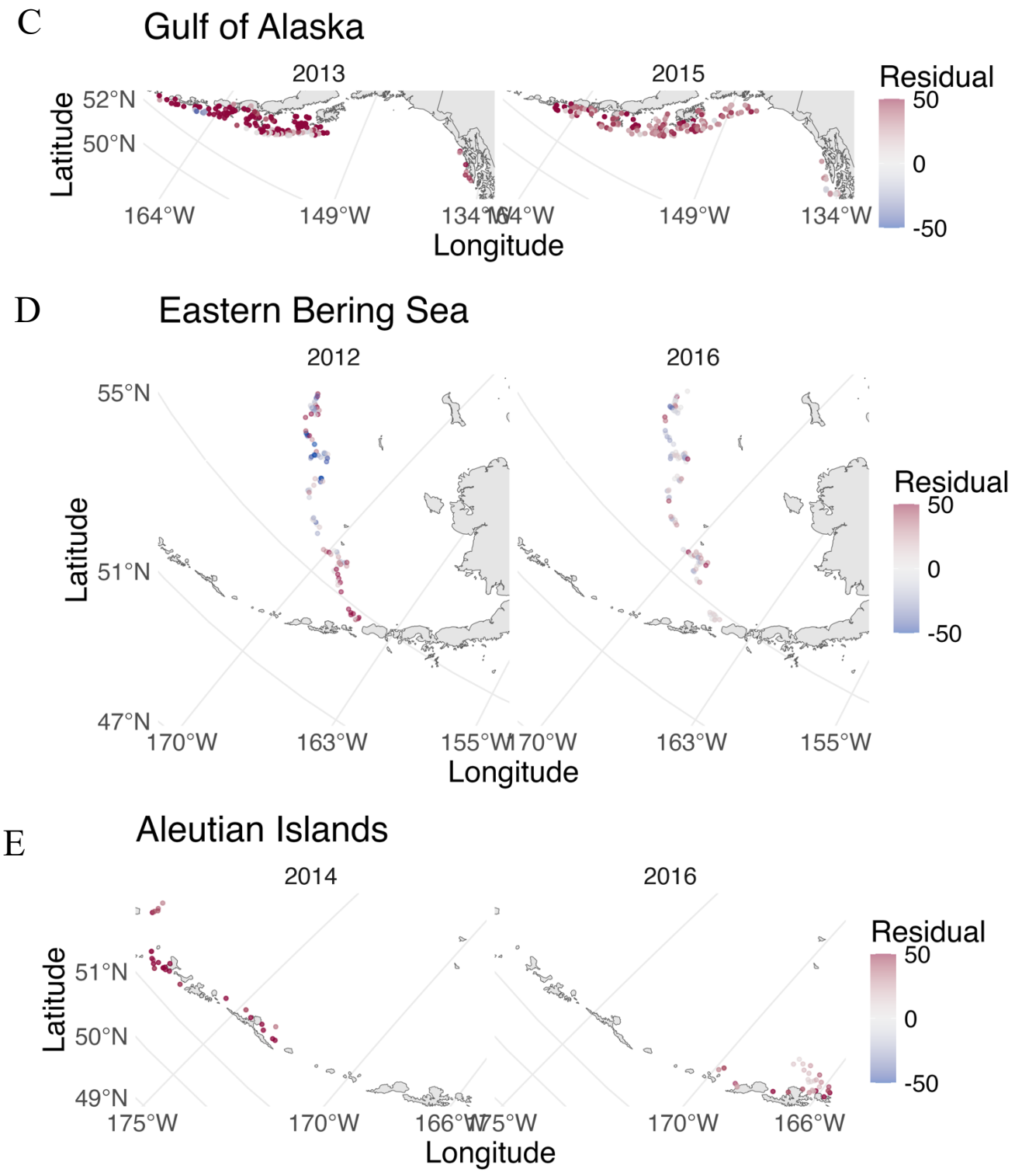

Figure S3. Residual (observation—prediction) of the spatio-temporal model with both covariates (temperature and salinity) for California Current, B) British Columbia, C) Gulf of Alaska, D) Eastern Bering Sea, and E) Aleutian Islands.

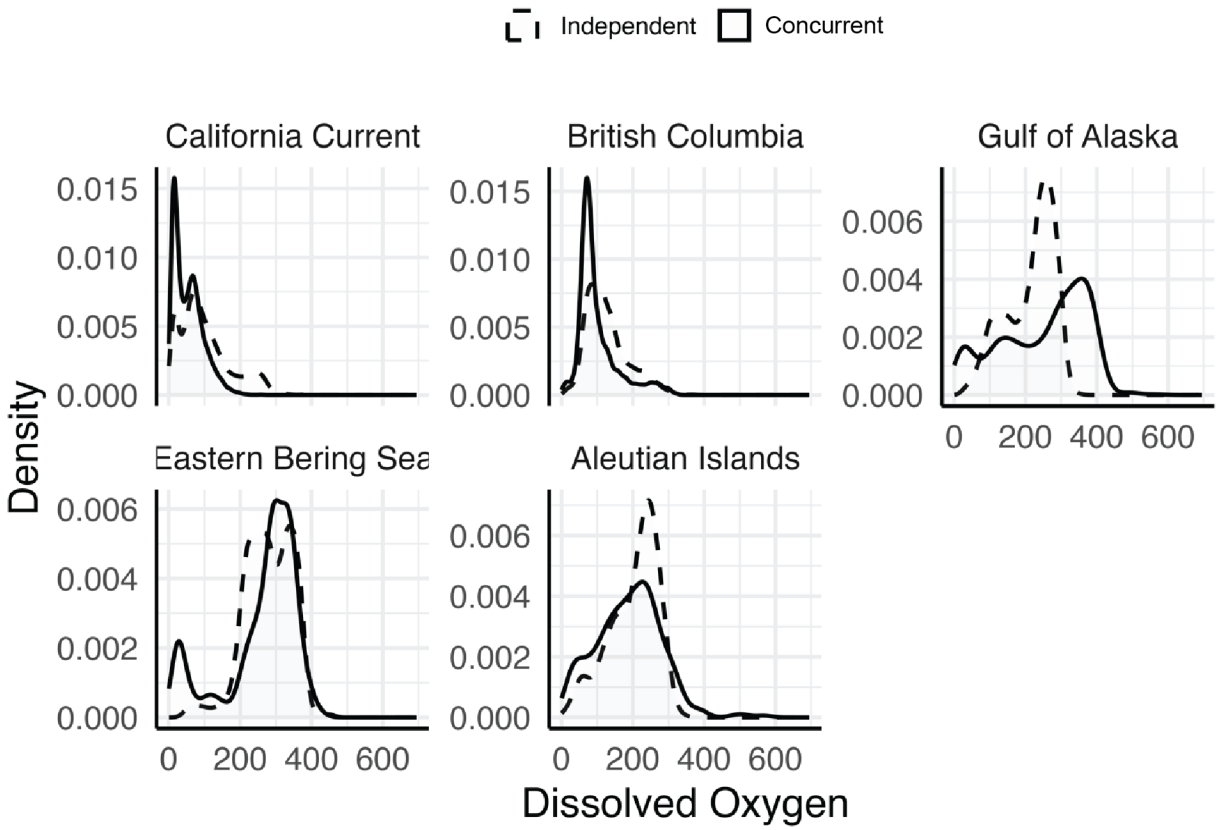

Figure S4. Distribution of oxygen values in observations from concurrent (bottom trawl surveys) sources and CTD casts independent from fish surveys.

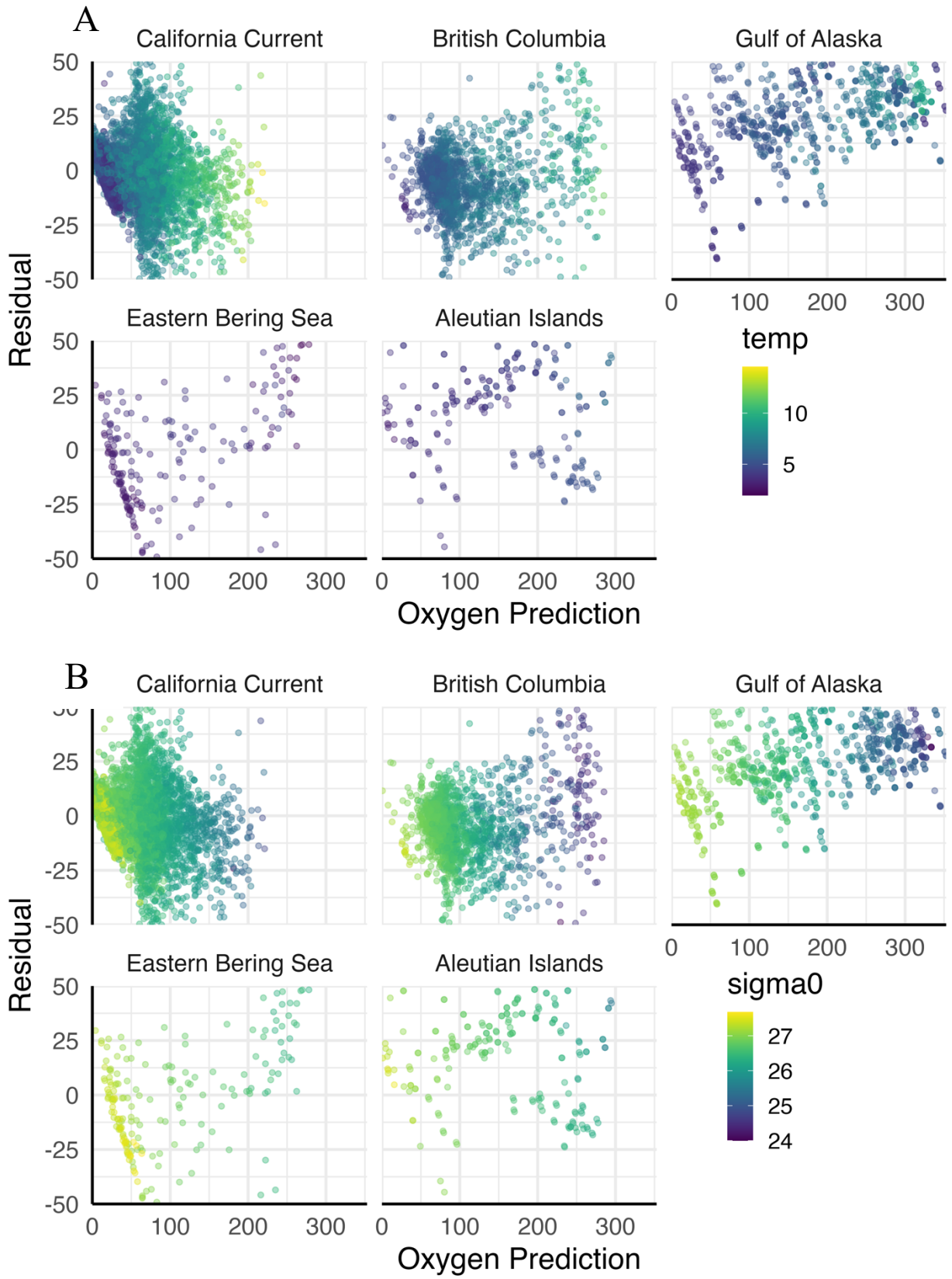
A
California Current
British Columbia
Gulf of Alaska
Eastern Bering Sea
Aleutian Islands
Residual
Oxygen Prediction
temp
10
5
B
California Current
British Columbia
Gulf of Alaska
Eastern Bering Sea
Aleutian Islands
Residual
Oxygen Prediction
sigma0
27
26
25
24

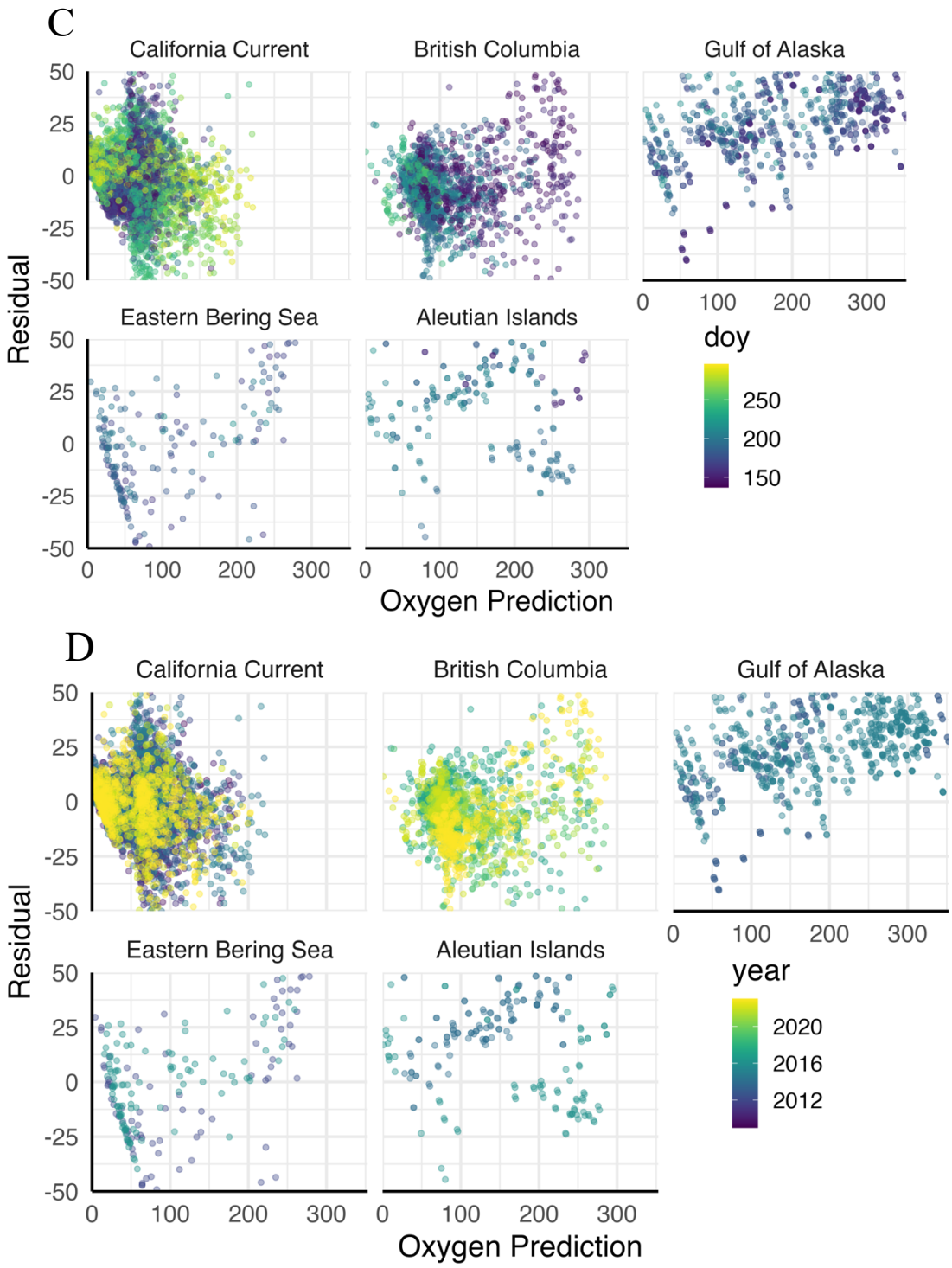

Figure S5. Residual (observation—prediction) for each oxygen predicted from the empirical statistical model in each region with color indicating observed A) temperature, B) salinity (in sigma0), C) day-of-year, and D) year

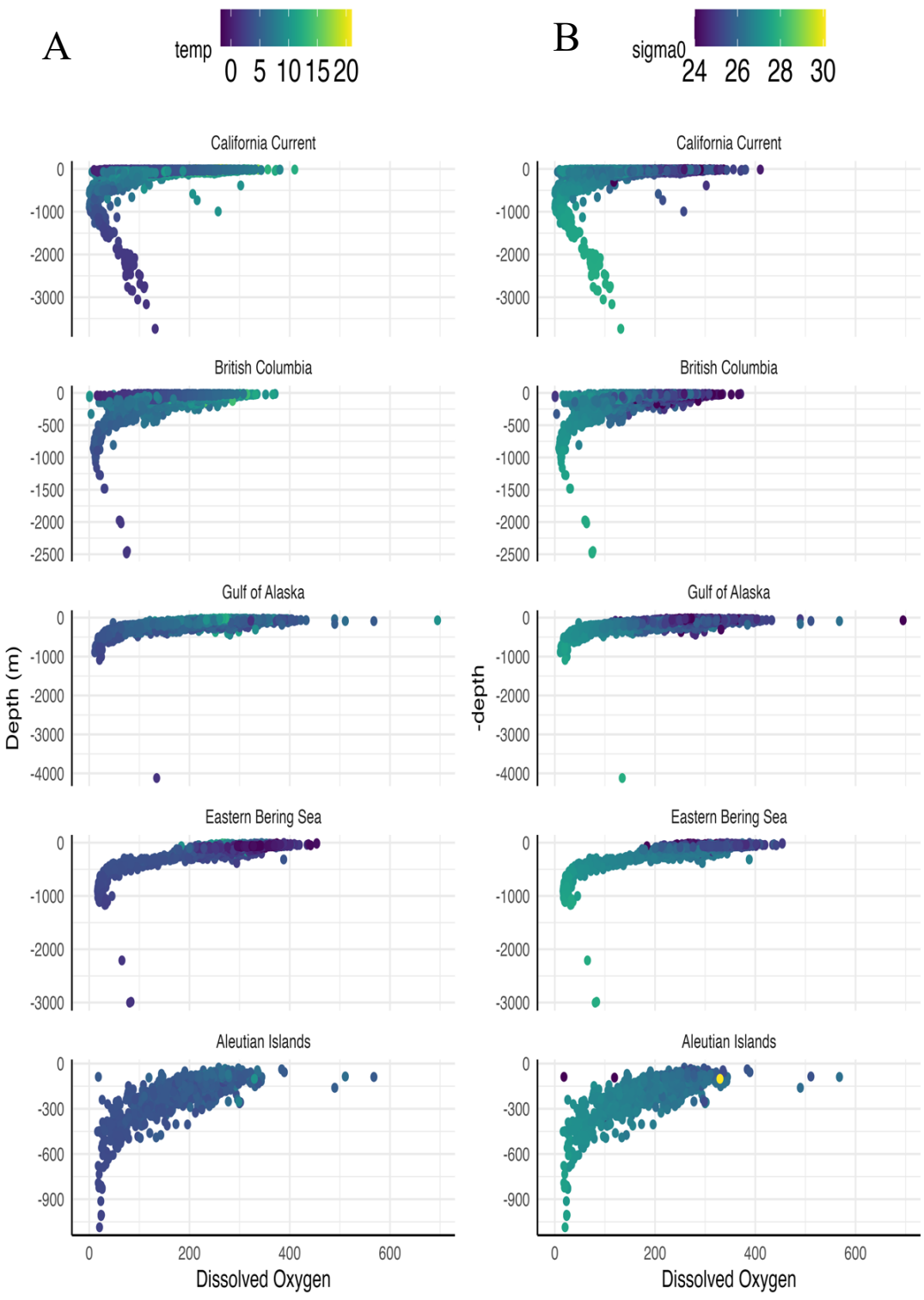

Figure S6. Observations of concurrent *in situ* data A) temperature (Celsius) and B) salinity (as sigma0) by depth (m) and dissolved oxygen (μmol kg^{-1}).

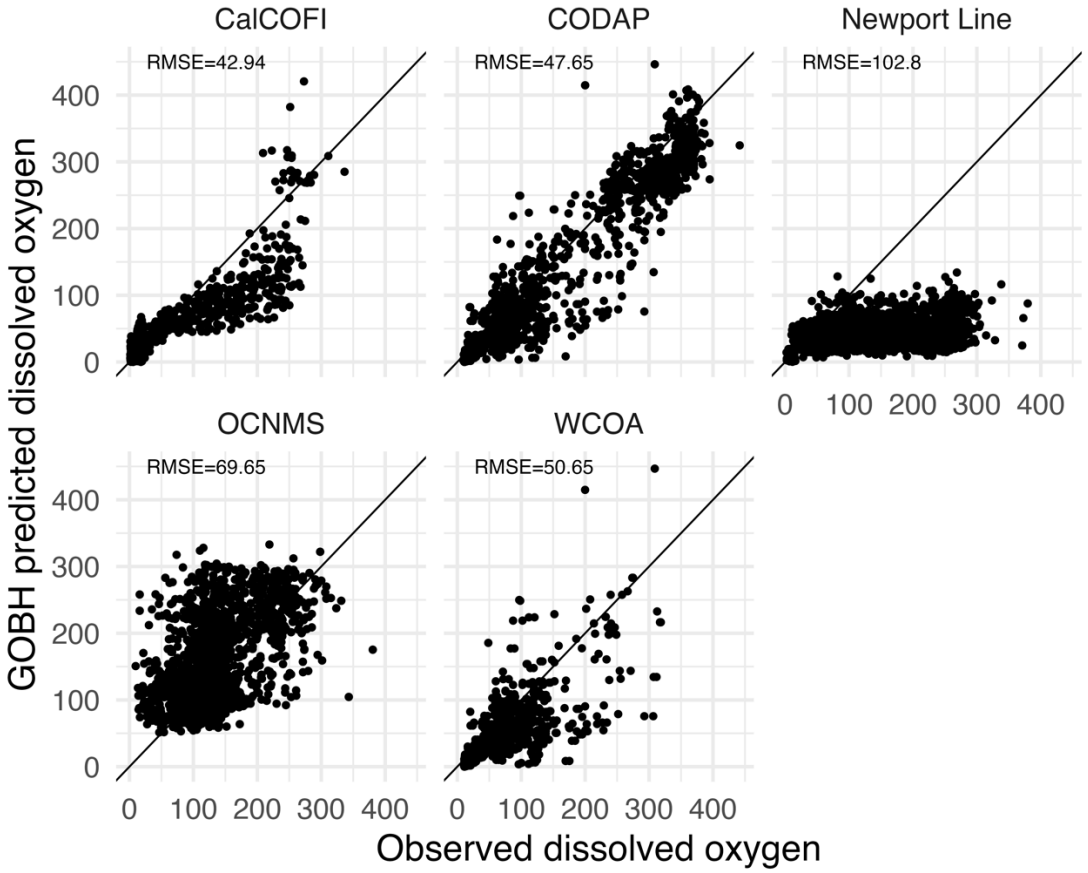

Figure S7. Predicted dissolved oxygen from Global Ocean Biogeochemistry Hindcast output compared to observed dissolved oxygen observations from independent CTD casts from different sources (see Table 1), and root mean squared error (RMSE) for each data source. Black line indicates 1:1 relationship.

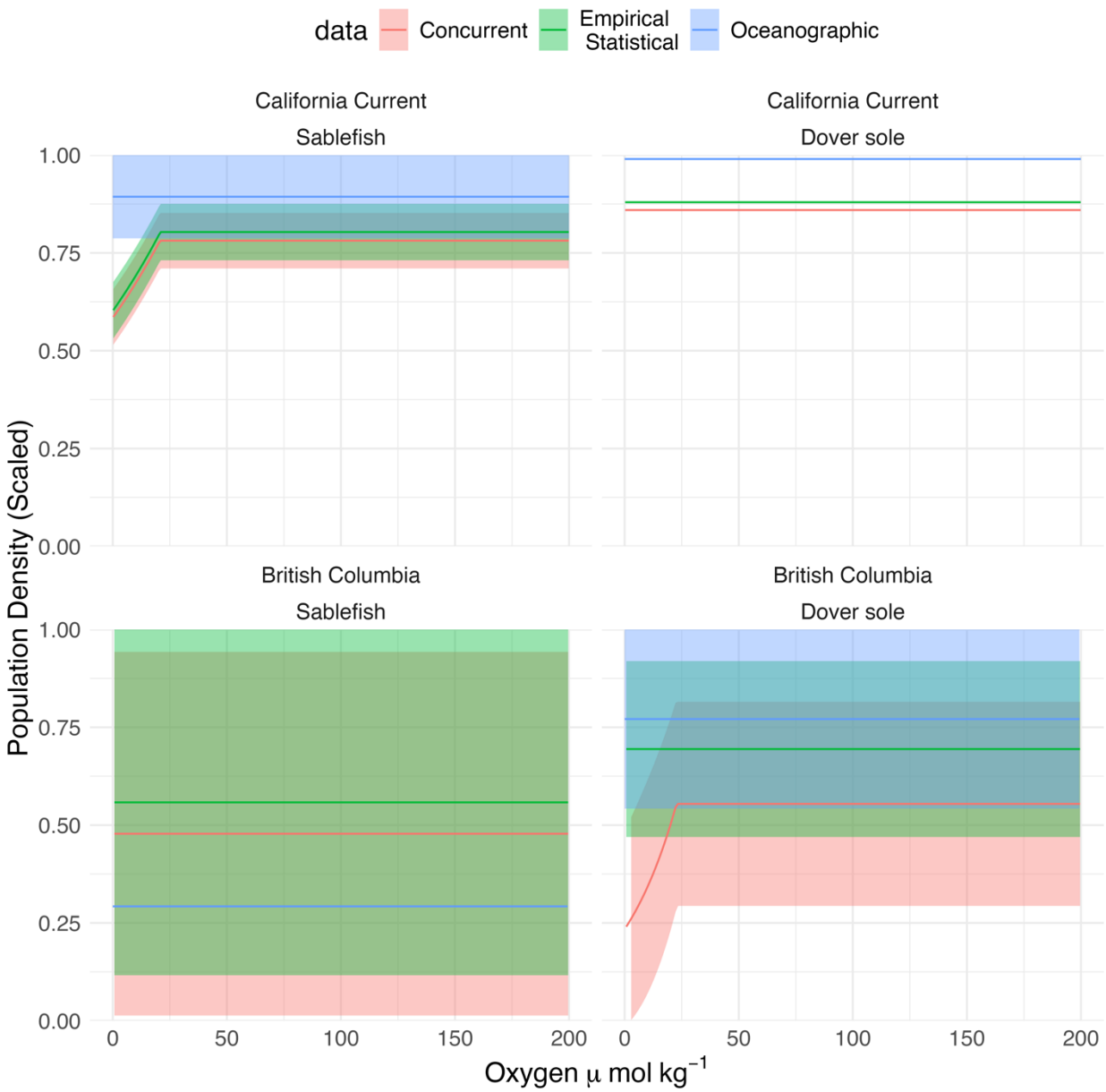

Figure S8. Conditional effect (maximum likelihood estimate ± standard error) of the dissolved oxygen breakpoint model for each dissolved oxygen data source for the case study species and regions for the test of limited years to only the subset where concurrent *in situ* data was available. Conditional effects were calculated with depth effects set to 0, year at a reference year (2012 in California Current and 2019 in British Columbia), and no random effects. Population density in biomass kg km^{-2} is shown scaled to maximum density for each species and region.

Table S2. Maximum likelihood estimate and standard error for the oxygen slope and breakpoint terms in the four case study applications of the three different oxygen data types (concurrent *in situ* data only, predicted values from empirical statistical models, and values from the dynamical oceanographic model the Global Oceanographic Biogeochemistry Hindcast [GOBH]) to sablefish and dover sole in the California Current and British Columbia regions. Breakpoint estimates that

were outside the range of oxygen values in the data and with 0 slope estimate were assumed to have no breakpoint effect of oxygen.

Data Type	Region	Species	Parameter	Estimate	Standard Error
Concurrent	California Current	Sablefish	Slope	0.566	1.235
Concurrent	California Current	Sablefish	Breakpoint	20.715	60.883
Predicted	California Current	Sablefish	Slope	0.137	1.585
Predicted	California Current	Sablefish	Breakpoint	56.144	69.536
GOBH	California Current	Sablefish	Slope	0.2	1.513
GOBH	California Current	Sablefish	Breakpoint	73.56	60.909
Concurrent	British Columbia	Sablefish	Slope	0	4651.98
Concurrent	British Columbia	Sablefish	Breakpoint	--	--
Predicted	British Columbia	Sablefish	Slope	0	72.557
Predicted	British Columbia	Sablefish	Breakpoint	--	--
GOBH	British Columbia	Sablefish	Slope	0	87.915
GOBH	British Columbia	Sablefish	Breakpoint	-	--
Concurrent	California Current	Dover sole	Slope	0	222.1
Concurrent	California Current	Dover sole	Breakpoint	--	--
Predicted	California Current	Dover sole	Slope	0	6.164
Predicted	California Current	Dover sole	Breakpoint	--	--
GOBH	California Current	Dover sole	Slope	0	17.101
GOBH	California Current	Dover sole	Breakpoint	--	--
Concurrent	British Columbia	Dover sole	Slope	2.267	1.566
Concurrent	British Columbia	Dover sole	Breakpoint	22.729	111.907
Predicted	British Columbia	Dover sole	Slope	0.661	1.646
Predicted	British Columbia	Dover sole	Breakpoint	38.576	114.329
GOBH	British Columbia	Dover sole	Slope	0.854	1.28
GOBH	British Columbia	Dover sole	Breakpoint	54.894	130.822

Appendix References

Checkley Jr, D.M. and Barth, J.A. (2009). Patterns and processes in the California Current System. *Progress in Oceanography*, *83*(1-4): 49-64. https://doi.org/10.1016/j.pocean.2009.07.028

Coachman, L.K., 1986. Circulation, water masses, and fluxes on the southeastern Bering Sea shelf. *Continental Shelf Research*, *5*(1-2), pp.23-108. https://www.sciencedirect.com/science/article/abs/pii/0278434386900117

Crawford, W.R. and Thomson, R.E., 1991. Physical oceanography of the western Canadian continental shelf. *Continental Shelf Research*, *11*(8-10), pp.669-683. https://doi.org/10.1016/0278-4343(91)90073-F

Essington, T. E., Anderson, S. C., Barnett, L. A. K., Berger, H. M., Siedlecki, S. A., & Ward, E. J. (2022). Advancing statistical models to reveal the effect of dissolved oxygen on the spatial distribution of marine taxa using thresholds and a physiologically based index. *Ecography*, *2022*(8), e06249. https://doi.org/10.1111/ecog.06249

Hunt Jr, G.L. & Stabeno, P.J. (2005.) Oceanography and ecology of the Aleutian Archipelago: spatial and temporal variation. *Fisheries oceanography*, *14*: 292-306. https://doi.org/10.1111/j.1365-2419.2005.00378.x

Lindgren, F., Rue, H., & Lindström, J. (2011). An explicit link between Gaussian fields and Gaussian Markov random fields: the stochastic partial differential equation approach. *Journal of the Royal Statistical Society: Series B (Statistical Methodology)*, *73*(4), 423–498. https://doi.org/https://doi.org/10.1111/j.1467-9868.2011.00777.x

Kelley D, Richards C, SCOR/IAPSO W (2024). gsw: Gibbs Sea Water Functions. R package version 1.2-0, http://teos-10.github.io/GSW-R/.

Kristensen, K., Nielsen, A., Berg, C. W., Skaug, H. and Bell, B. M. 2016. TMB: Automatic differentiation and Laplace approximation. *Journal of Statistical Software* 70: 1–21. https://doi.org/10.18637/jss.v070.i05

Mordy, C.W., Stabeno, P.J., Kachel, N.B., Kachel, D., Ladd, C., Zimmermann, M., Hermann, A.J., Coyle, K.O. and Doyle, M.J. (2019). Patterns of flow in the canyons of the northern Gulf of Alaska. Deep Sea Research Part II: Topical Studies in Oceanography, 165: 203-220. https://doi.org/10.1016/j.dsr2.2019.03.009

NOAA. (2022). 2022: ETOPO 2022 15 Arc-Second Global Relief Model. NOAA National Centers for Environmental Information.https://doi.org/10.25921/fd45-gt74

Thorson, J.T., Shelton, A.O, Ward, E.J., & Skaug, H.J. (2015) Geostatistical delta-generalized linear mixed models improve precision for estimated abundance indices for West Coast groundfishes. *ICES Journal of Marine Science*, 72(5): 1297-1310. https://doi.org/10.1093/icesjms/fsu243

Tweedie, M.C.K. 1984. An index which distinguishes between some important exponential families. In Statistics: Applications and New Directions. *Proceedings of the Indian Statistical Institute Golden Jubilee International Conference*. Edited by J.K. Gosh and J. Roy. Indian Statistical Institute, Calcutta. pp. 579–604

Shono, H. (2008). Application of the Tweedie distribution to zero-catch data in CPUE analysis. *Fisheries Research*, *93*(1), 154–162. H ttps://doi.org/https://doi.org/10.1016/j.fishres.2008.03.006

Stabeno, P.J., Danielson, S.L., Kachel, D.G., Kachel, N.B. and Mordy, C.W. (2016a.) Currents

and transport on the Eastern Bering Sea shelf: An integration of over 20 years of data. *Deep Sea Research Part II: Topical Studies in Oceanography*, *134*: 13-29. https://doi.org/10.1016/j.dsr2.2016.05.010

Stabeno, P.J., Bell, S., Cheng, W., Danielson, S., Kachel, N.B. and Mordy, C.W. (2016b). Long-term observations of Alaska Coastal Current in the northern Gulf of Alaska. *Deep Sea Research Part II: Topical Studies in Oceanography*, *132*: 24-40. https://doi.org/10.1016/j.dsr2.2015.12.016

Stabeno, P.J., Bond, N.A., Hermann, A.J., Kachel, N.B., Mordy, C.W. and Overland, J.E. (2004). Meteorology and oceanography of the Northern Gulf of Alaska. *Continental Shelf Research*, *24*(7-8): 859-897. https://doi.org/10.1016/j.csr.2004.02.007

CHAPTER 4 APPENDIX

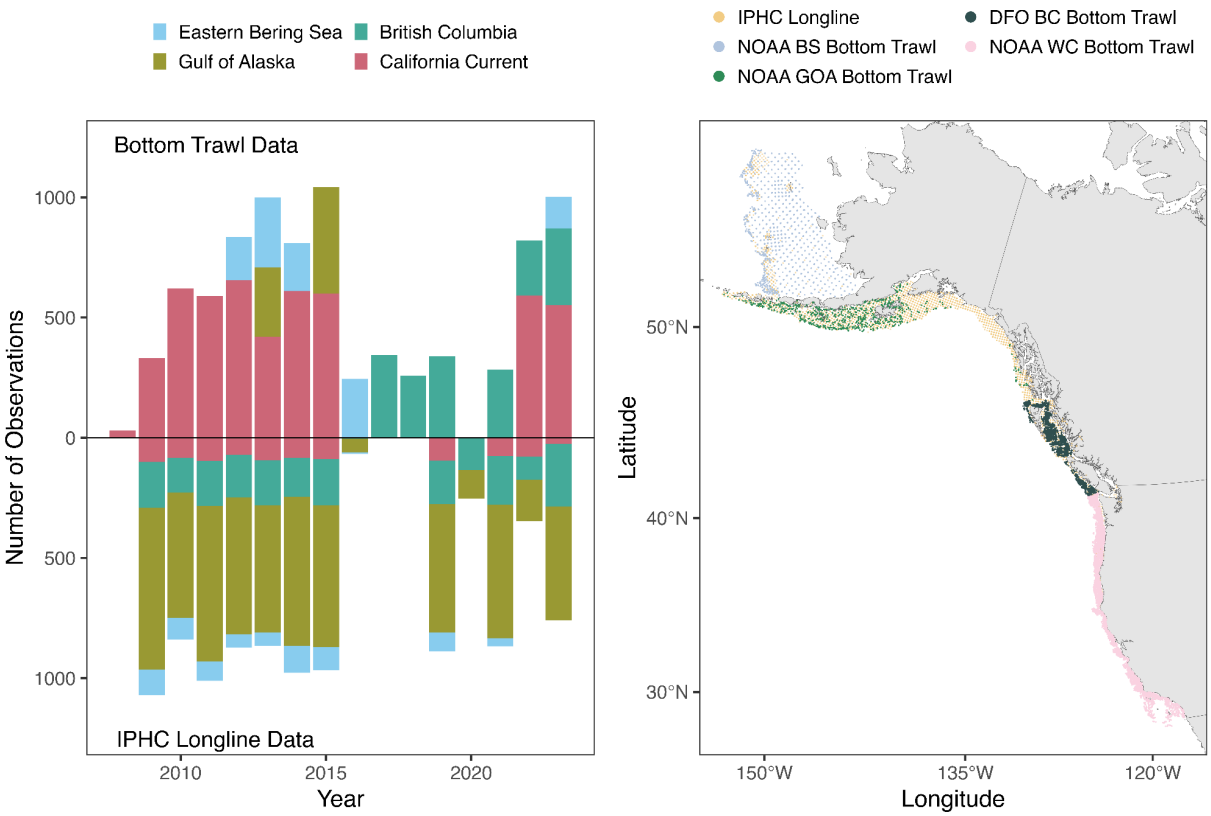

Figure S1. A) Compiled observations of fish catch available for model fitting in each region in each year. Each observation is a single sampling event. Colors indicate the region, with bars above the line observations from bottom trawl data (U.S. National Oceanic and Atmospheric Administration [NOAA] and Department of Fisheries and Oceans Canada [DFO]) and bars below the line from International Pacific Halibut Commission (IPHC) longline data. B) Map of fish catch data, with colors indicating the data source: International Pacific Halibut Commission longline data, NOAA Bering Sea (BS), Gulf of Alaska (GOA), and West Coast (WC); and DFO British Columbia (BC) bottom trawl surveys.

Table S1. Species tested for threshold effects of temperature-corrected oxygen on fish density. Taxonomic Group refers to the taxonomic group that the temperature-dependence of oxygen tolerance parameter (E_0) was pulled from in the phylogenetic imputation. Depth limit (in meters) is the depth at 99% of the cumulative catch biomass of the species in the catch data. Southern limits are the latitude at the 99% for the southern extent of cumulative biomass in the California Current, and northern limits at the latitude at the 99% for northern extent of cumulative biomass in the eastern Bering Sea. Species without a northern or southern limit did not have clear range limits.

Common Name	Scientific Name	Taxonomic Group	Depth limit (m)	Southern limit (°N)	Northern limit (°N)
Southern rock sole	*Lepidopsetta bilineata*	pleuronectidae	297	42.15	--
Big skate	*Raja binoculata*	elasmobranchii	525.8791	--	--
Canary rockfish	*Sebastes pinniger*	scorpaenidae	261.3	42.42	--
Yellowtail rockfish	*Sebastes flavidus*	scorpaenidae	313.17	--	--
Pacific sanddab	*Citharichthys sordidus*	paralichthyidae	302.9	37.76	--
Pacific cod	*Gadus macrocephalus*	gadidae	363.9	37.65	--
Yelloweye rockfish	*sebastes ruberrimus*	scorpaenidae	200.3087	--	--
Redstripe rockfish	*Sebastes proriger*	scorpaenidae	237.744	39.88	--
Walleye pollock	*Gadus chalcogrammus*	gadidae	311.7181	--	--
Silvergray rockfish	*Sebastes brevispinis*	scorpaenidae	310.7657	--	--
Sharpchin rockfish	*Sebastes zacentrus*	scorpaenidae	131	--	55.68
English sole	*Parophrys vetulus*	pleuronectidae	403.058	37.92	--
Lingcod	*Ophiodon elongatus*	perciformes	386.4	35.97	--
Petrale sole	*Eopsetta jordani*	pleuronectidae	276.1488	40.17	--
Spiny dogfish	*Squalus suckleyi*	elasmobranchii	446.3967	--	--
Redbanded rockfish	*Sebastes babcocki*	scorpaenidae	229.2	36.96	--
Darkblotched rockfish	*Sebastes crameri*	scorpaenidae	526.095	34.50	59.66
Spotted ratfish	*Hydrolagus colliei*	elasmobranchii	503	42.99	58.66
Pacific halibut	*Hippoglossus stenolepis*	pleuronectidae	431	--	--
Slender sole	*Lyopsetta exilis*	pleuronectidae	433	38.91	--
Flathead sole	*Hippoglossoides elassodon*	pleuronectidae	514.9	--	--
Arrowtooth flounder	*Atheresthes stomias*	pleuronectidae	370	43.58	--
Pacific hake	*Merluccius productus*	gadidae	546.9	--	--
Blackbelly eelpout	*Lycodes pacificus*	zoarcidae	384.048	40.49	--
Rougheye rockfish	*sebastes aleutianus*	scorpaenidae	325.5264	35.04	--
Rex sole	*Glyptocephalus zachirus*	pleuronectidae	283.464	43.83	--

Sandpaper skate	*Bathyraja kincaidii*	elasmobranchii	262	--	--
Longnose skate	*Raja rhina*	elasmobranchii	1060.939	--	57.34
Dover sole	*Microstomus pacificus*	carangiformes	587	--	--
Sablefish	*Anoplopoma fimbria*	perciformes	1150.8	--	59.81
Shortspine thornyhead	*Sebastolobus alascanus*	scorpaenidae	1215.4	--	--
Longspine thornyhead	*Sebastolobus altivelis*	scorpaenidae	998.52	--	59.81

Table S2. Marginal Akaike Information Criteria (ΔAIC) for each of the five models fit to each species and dataset combination. For species and datasets with one of the pO_2' models identified as best-fitting (i.e. ΔAIC=0), the breakpoint and slope estimate is calculated as the mean ensemble ± standard deviation from the three pO_2' models (low, median, and high E_0) weighted by marginal Akaike Information Criteria (ΔAIC) across 100 Monte Carlo simulations of the maximum likelihood estimation of the breakpoint and slope parameters. N obs is the number of observations in the model fitting, N region is the number of regions included, and N years the number of years of data included. Dashed lines in the ΔAIC columns indicate the model failed to pass diagnostics checks, and dashed lines in the parameter estimate columns indicate a pO_2' model was not identified as best-fitting.

			ΔAIC					Parameter estimates						
Species	Region	Data type	Base	Temp	pO2' low	pO2' med	pO2' high	Breakpoint mean	Breakpoint SD	Slope mean	Slope SD	N obs	N years	N regions
silvergray rockfish	bc	bottom trawl only	45.886	26.871	0	--	6.571	6.885	0.275	2.456	0.325	832	1	6
blackbelly eelpout	cc	bottom trawl only	39.21	29.505	15.244	14.017	0	2.138	1.923	0.552	0.243	1114	1	10
blackbelly eelpout	bc	bottom trawl only	16.379	0	--	--	--	--	--	--	--	356	1	6
blackbelly eelpout	coastwide	bottom trawl only	--	--	12.066	0	5.814	--	--	--	--	1470	2	14
redstripe rockfish	cc	bottom trawl only	0.92	--	--	0	0.051	--	--	--	--	88	1	9
redstripe rockfish	bc	bottom trawl only	6.048	2.522	4.911	--	0	--	--	--	--	436	1	6
redstripe rockfish	coastwide	bottom trawl only	27.742	17.519	0	6.716	6.324	2.575	1.199	1.572	0.449	524	2	13
lingcod	cc	bottom trawl only	0.931	--	--	0	--	4.95	1.334	0.262	0.139	1716	1	10

lingcod	bc	bottom trawl only	15.559	14.895	0	6.263	4.908	5.574	0.607	1.173	0.229	734	1	6
lingcod	coastwide	bottom trawl only	8.46	--	0	1.454	--	4.787	1.344	0.263	0.118	2448	2	14
sharpchin rockfish	cc	bottom trawl only	--	--	--	0	0.385	--	--	--	--	292	1	9
sharpchin rockfish	bc	bottom trawl only	5.679	0	3.374	3.113	--	--	--	--	--	440	1	6
sharpchin rockfish	coastwide	bottom trawl only	0	3.079	6.13	8.241	6.768	--	--	--	--	729	2	13
yellowtail rockfish	cc	bottom trawl only	17.924	15.817	0	0.409	1.019	5.974	0.297	1.412	0.203	367	1	9
yellowtail rockfish	bc	bottom trawl only	--	--	0	--	--	--	--	--	--	477	1	6
yellowtail rockfish	coastwide	bottom trawl only	48.028	47.632	--	0	9.337	5.817	0.351	2.234	0.276	843	2	13
pacific sanddab	cc	bottom trawl only	34.993	14.017	--	0	--	3.272	1.392	0.224	0.091	1683	1	10
pacific sanddab	bc	bottom trawl only	--	--	0	0.933	15.012	--	--	--	--	421	1	6
pacific sanddab	coastwide	bottom trawl only	--	--	--	0	--	--	--	--	--	2103	2	14
yelloweye rockfish	cc	bottom trawl only	--	0	4	--	4	--	--	--	--	95	1	9
yelloweye rockfish	bc	bottom trawl only	0	2.512	5.909	--	--	--	--	--	--	174	1	6
yelloweye rockfish	coastwide	bottom trawl only	0	3.568	6.847	5.984	7.219	--	--	--	--	269	2	13
yelloweye rockfish	cc	bottom trawl & IPHC	0	3.409	7.409	7.409	--	--	--	--	--	194	1	11
yelloweye rockfish	bc	bottom trawl & IPHC	0	3.244	5.788	5.638	5.017	--	--	--	--	706	1	15
yelloweye rockfish	goa	bottom trawl & IPHC	3.374	0.769	1.429	0	1.143	--	--	--	--	1085	1	13

yelloweye rockfish	coastwide	bottom trawl & IPHC	8.791	0	3.776	12.487	4	--	--	--	--	1985	3	15
english sole	cc	bottom trawl only	28.119	0	4	--	3.536	--	--	--	--	2104	1	10
english sole	bc	bottom trawl only	--	--	3.403	0	--	3.27	1.975	0.485	0.19	868	1	6
english sole	goa	bottom trawl only	0	2.898	3.025	3.244	2.943	--	--	--	--	56	1	2
english sole	coastwide	bottom trawl only	--	0	--	--	1.142	--	--	--	--	3029	3	14
petrale sole	cc	bottom trawl only	--	--	0	--	5.34	2.896	1.196	0.214	0.092	2165	1	10
petrale sole	bc	bottom trawl only	--	--	--	--	0	--	--	--	--	974	1	6
petrale sole	coastwide	bottom trawl only	147.028	0	0.498	0.3	1.055	--	--	--	--	3139	2	14
southern rock sole	cc	bottom trawl only	0	3.457	7.174	6.631	5.997	--	--	--	--	256	1	10
southern rock sole	bc	bottom trawl only	--	--	5.535	--	0	7.555	3.741	0.457	0.223	397	1	6
southern rock sole	goa	bottom trawl only	0	2.803	--	--	--	--	--	--	--	180	1	2
southern rock sole	coastwide	bottom trawl only	2.457	0	3.46	3.147	2.954	--	--	--	--	833	3	14
darkblotched rockfish	cc	bottom trawl only	--	0	4	4	--	--	--	--	--	839	1	9
darkblotched rockfish	bc	bottom trawl only	--	0	--	3.346	4	--	--	--	--	265	1	6
darkblotched rockfish	coastwide	bottom trawl only	19.835	0	--	--	--	--	--	--	--	1105	2	13
redbanded rockfish	cc	bottom trawl only	--	--	2.895	0.395	0	--	--	--	--	374	1	9
redbanded rockfish	bc	bottom trawl only	--	--	0.649	0	1.682	--	--	--	--	709	1	6
redbanded rockfish	coastwide	bottom trawl only	48.423	0.084	--	--	0	--	--	--	--	1084	2	13

big skate	bc	bottom trawl only	10.37	--	0.198	0	2.796	--	--	--	--	195	1	6
big skate	cc	bottom trawl & IPHC	0	1.986	--	--	2.469	--	--	--	--	132	1	11
big skate	bc	bottom trawl & IPHC	6.522	0	0.809	--	2.161	--	--	--	--	486	1	15
big skate	goa	bottom trawl & IPHC	51.75	0	0.144	0.581	--	--	--	--	--	1362	1	13
big skate	coastwide	bottom trawl & IPHC	37.953	8.685	0	--	--	11.215	1.468	0.549	0.179	1980	3	15
slender sole	cc	bottom trawl only	232.394	13.684	0	2.748	8.563	--	--	--	--	2371	1	10
slender sole	bc	bottom trawl only	4.77	0	--	--	--	--	--	--	--	975	1	6
slender sole	coastwide	bottom trawl only	--	65.47	0	8.415	18.951	--	--	--	--	3345	2	14
canary rockfish	cc	bottom trawl only	--	--	0	--	0.524	--	--	--	--	400	1	9
canary rockfish	bc	bottom trawl only	7.979	10.535	--	1.402	0	11.135	0.729	2.155	0.401	381	1	6
canary rockfish	coastwide	bottom trawl only	5.826	--	--	0	--	7.463	1.238	0.792	0.289	782	2	13
rex sole	cc	bottom trawl only	41.055	0	--	--	--	--	--	--	--	2723	1	10
rex sole	bc	bottom trawl only	--	--	21.17	21.094	0	--	--	--	--	1486	1	6
rex sole	goa	bottom trawl only	0	3.375	3.329	2.906	3.099	--	--	--	--	415	1	2
rex sole	ebs	bottom trawl only	0.8	0.227	--	--	0	--	--	--	--	266	1	6
rex sole	coastwide	bottom trawl only	44.894	0	1.583	1.134	2.438	--	--	--	--	4891	4	15
rougheye rockfish	bc	bottom trawl only	12.564	0	4	4	--	--	--	--	--	404	1	6

rougheye rockfish	goa	bottom trawl only	0	3.888	0.406	0.858	2.071	--	--	--	--	88	1	2
rougheye rockfish	coastwide	bottom trawl only	--	--	--	--	--	--	--	--	--	491	2	8
rougheye rockfish	cc	bottom trawl & IPHC	4.906	0	--	--	--	--	--	--	--	65	1	12
rougheye rockfish	bc	bottom trawl & IPHC	--	0	--	--	--	--	--	--	--	242	1	15
rougheye rockfish	goa	bottom trawl & IPHC	--	--	--	--	--	--	--	--	--	217	1	13
rougheye rockfish	coastwide	bottom trawl & IPHC	1.24	0	4	--	4	--	--	--	--	524	3	15
spotted ratfish	cc	bottom trawl only	--	--	--	0	--	--	--	--	--	2398	1	10
spotted ratfish	bc	bottom trawl only	83.563	0	2.076	--	3.218	--	--	--	--	1574	1	6
spotted ratfish	coastwide	bottom trawl only	115.398	4.954	0	2.529	0.717	6.5	0.744	0.28	0.067	3972	2	14
arrowtooth flounder	cc	bottom trawl only	9.67	0	3.729	1.174	1.791	--	--	--	--	1603	1	9
arrowtooth flounder	bc	bottom trawl only	--	--	--	--	0	--	--	--	--	1457	1	6
arrowtooth flounder	goa	bottom trawl only	0	0.503	1.556	2.264	--	--	--	--	--	623	1	2
arrowtooth flounder	ebs	bottom trawl only	20.004	0	--	4	4	--	--	--	--	640	1	6
arrowtooth flounder	coastwide	bottom trawl only	36.717	0	--	3.378	4	--	--	--	--	4322	4	14
pacific hake	cc	bottom trawl only	150.211	59.366	--	--	0	--	--	--	--	1858	1	10
pacific hake	bc	bottom trawl only	32.701	31.576	0.932	3.542	0	--	--	--	--	663	1	6
pacific hake	coastwide	bottom trawl only	34.25	0	--	--	--	--	--	--	--	2521	2	14

flathead sole	cc	bottom trawl only	--	--	0.441	--	0	--	--	--	--	403	1	9
flathead sole	bc	bottom trawl only	41.116	7.242	--	0.3	0	--	--	--	--	752	1	6
flathead sole	goa	bottom trawl only	0	2.331	6.315	6.331	6.255	--	--	--	--	443	1	2
flathead sole	ebs	bottom trawl only	0	2.252	--	--	2.921	--	--	--	--	813	1	6
flathead sole	coastwide	bottom trawl only	11.886	--	0	--	--	--	--	--	--	2408	4	14
longnose skate	cc	bottom trawl only	83.056	5.682	0	3.712	--	--	--	--	--	2828	1	10
longnose skate	bc	bottom trawl only	0	3.596	--	--	--	--	--	--	--	608	1	6
longnose skate	coastwide	bottom trawl only	95.947	16.674	9.232	0	8.983	--	--	--	--	3436	2	14
longnose skate	cc	bottom trawl & IPHC	68.136	12.83	0	2.367	6.815	--	--	--	--	3125	1	13
longnose skate	bc	bottom trawl & IPHC	4.182	0	3.614	3.977	3.924	--	--	--	--	1459	1	15
longnose skate	goa	bottom trawl & IPHC	--	--	--	--	--	--	--	--	--	3611	1	13
longnose skate	coastwide	bottom trawl & IPHC	199.596	0	--	--	--	--	--	--	--	8195	3	16
pacific halibut	cc	bottom trawl only	18.173	17.205	0	1.914	2.636	5.345	0.384	0.813	0.158	394	1	9
pacific halibut	bc	bottom trawl only	1.398	0.804	0.343	0	0.894	6.792	0.755	0.667	0.191	658	1	6
pacific halibut	goa	bottom trawl only	0	3.153	--	--	--	--	--	--	--	610	1	2
pacific halibut	ebs	bottom trawl only	0	3.732	2.108	1.646	2.764	--	--	--	--	753	1	6
pacific halibut	coastwide	bottom trawl only	9.721	1.46	1.828	1.026	0	13.285	4.489	0.265	0.13	2417	4	14

pacific halibut	cc	bottom trawl & IPHC	67.784	63.043	3.843	2.257	0	6.386	0.214	1.067	0.119	989	1	12
pacific halibut	bc	bottom trawl & IPHC	56.322	47.051	11.23	2.912	0	9.283	0.344	0.724	0.089	2500	1	14
pacific halibut	goa	bottom trawl & IPHC	32.381	13.573	5.277	0	3.806	25.92	5.761	0.055	0.021	5984	1	12
pacific halibut	ebs	bottom trawl & IPHC	34.648	--	6.939	0	--	8.222	3.062	0.2	0.063	1362	1	11
pacific halibut	coastwide	bottom trawl & IPHC	59.892	34.459	0.61	42.145	0	10.266	0.58	0.272	0.031	10835	4	15
spiny dogfish	cc	bottom trawl only	35.221	0	3.414	--	3.079	--	--	--	--	937	1	9
spiny dogfish	bc	bottom trawl only	41.783	0	4	--	--	--	--	--	--	823	1	6
spiny dogfish	coastwide	bottom trawl only	75.942	44.268	0	16.193	43.712	--	--	--	--	1759	2	13
spiny dogfish	cc	bottom trawl & IPHC	28.616	0	0.094	3.931	--	--	--	--	--	1330	1	11
spiny dogfish	bc	bottom trawl & IPHC	59.093	3.845	2.097	0.178	0	4.76	2.64	0.222	0.086	2354	1	15
spiny dogfish	goa	bottom trawl & IPHC	55.649	0	4	2.884	3.896	--	--	--	--	3063	1	13
spiny dogfish	coastwide	bottom trawl & IPHC	192.335	0	1.418	189.419	4	--	--	--	--	6747	3	15
pacific cod	cc	bottom trawl only	22.123	25.632	--	0	--	5.587	0.466	1.391	0.343	255	1	9
pacific cod	bc	bottom trawl only	0.233	0	--	--	--	--	--	--	--	976	1	6
pacific cod	goa	bottom trawl only	0	1.691	--	3.94	--	--	--	--	--	544	1	2

pacific cod	ebs	bottom trawl only	--	0	3.999	3.735	3.426	--	--	--	--	1007	1	6
pacific cod	coastwide	bottom trawl only	16.225	11.787	0	0.971	0.82	14.197	2.501	0.333	0.086	2783	4	14
pacific cod	cc	bottom trawl & IPHC	29.657	31.942	0.775	--	0	6.441	0.466	1.565	0.268	269	1	11
pacific cod	bc	bottom trawl & IPHC	0	3.066	--	3.234	3.503	--	--	--	--	947	1	15
pacific cod	goa	bottom trawl & IPHC	188.848	81.253	0	1.059	3.171	15.43	0.4	0.412	0.03	4606	1	13
pacific cod	ebs	bottom trawl & IPHC	44.541	19.453	10.58	5.46	0	--	--	--	--	1588	1	11
pacific cod	coastwide	bottom trawl & IPHC	232.058	104.943	0	174.167	4.749	11.853	0.483	0.613	0.057	7410	4	15
walleye pollock	bc	bottom trawl only	17.112	0	2.791	--	1.228	--	--	--	--	950	1	6
walleye pollock	goa	bottom trawl only	--	5.243	--	0	5.678	11.849	2.341	1.009	0.313	543	1	2
walleye pollock	ebs	bottom trawl only	0.969	0	--	2.854	2.713	--	--	--	--	1025	1	6
walleye pollock	coastwide	bottom trawl only	43.197	14.029	0	6.693	9.313	--	--	--	--	2519	3	11
dover sole	cc	bottom trawl only	312.648	2.705	0	2.38	5.168	--	--	--	--	4116	1	10
dover sole	bc	bottom trawl only	35.789	9.184	0	--	--	--	--	--	--	1403	1	6
dover sole	goa	bottom trawl only	0	3.175	--	6.174	6.356	--	--	--	--	156	1	2
dover sole	coastwide	bottom trawl only	292.687	36.543	0	6.871	11.151	--	--	--	--	5675	3	14
sandpaper skate	bc	bottom trawl only	0	2.675	--	--	--	--	--	--	--	240	1	6

sandpaper skate	goa	bottom trawl only	0	2.102	--	--	6.069	--	--	--	--	76	1	2
sandpaper skate	ebs	bottom trawl only	0	0.802	4.802	3.984	1.61	--	--	--	--	297	1	6
sandpaper skate	coastwide	bottom trawl only	14.419	6.386	1.352	0.274	0	22.117	5.503	0.561	0.21	611	3	11
shortspine thornyhead	cc	bottom trawl only	211.292	57.418	--	--	0	15.184	5.707	0.24	0.111	2422	1	10
shortspine thornyhead	bc	bottom trawl only	--	0	--	--	--	--	--	--	--	642	1	6
shortspine thornyhead	goa	bottom trawl only	0	3.378	6.378	6.463	6.464	--	--	--	--	129	1	2
shortspine thornyhead	ebs	bottom trawl only	20.07	0	--	--	--	--	--	--	--	203	1	6
shortspine thornyhead	coastwide	bottom trawl only	168.578	83.738	23.787	0	13.412	4.023	0.603	1.642	0.17	3395	4	15
longspine thornyhead	cc	bottom trawl only	13.527	0	--	--	4	--	--	--	--	1677	1	10
sablefish	cc	bottom trawl only	0	--	--	--	--	--	--	--	--	2957	1	10
sablefish	bc	bottom trawl only	54.269	25.466	10.799	0	--	--	--	--	--	1189	1	6
sablefish	goa	bottom trawl only	--	--	--	--	--	--	--	--	--	189	1	2
sablefish	ebs	bottom trawl only	30.957	0	--	--	--	--	--	--	--	148	1	6
sablefish	coastwide	bottom trawl only	204.097	190.737	0	11.821	84.848	--	--	--	--	4482	4	15
sablefish	cc	bottom trawl & IPHC	--	--	--	--	--	--	--	--	--	3297	1	13
sablefish	bc	bottom trawl & IPHC	53.251	17.204	8.221	3.52	0	--	--	--	--	1533	1	15
sablefish	goa	bottom trawl & IPHC	--	--	--	0	--	--	--	--	--	2209	1	13

sablefish	ebs	bottom trawl & IPHC	--	7.317	0	8.894	9.896	--	--	--	--	194	1	11
sablefish	coastwide	bottom trawl & IPHC	275.972	240.204	0	44.781	1.947	--	--	--	--	7233	4	16

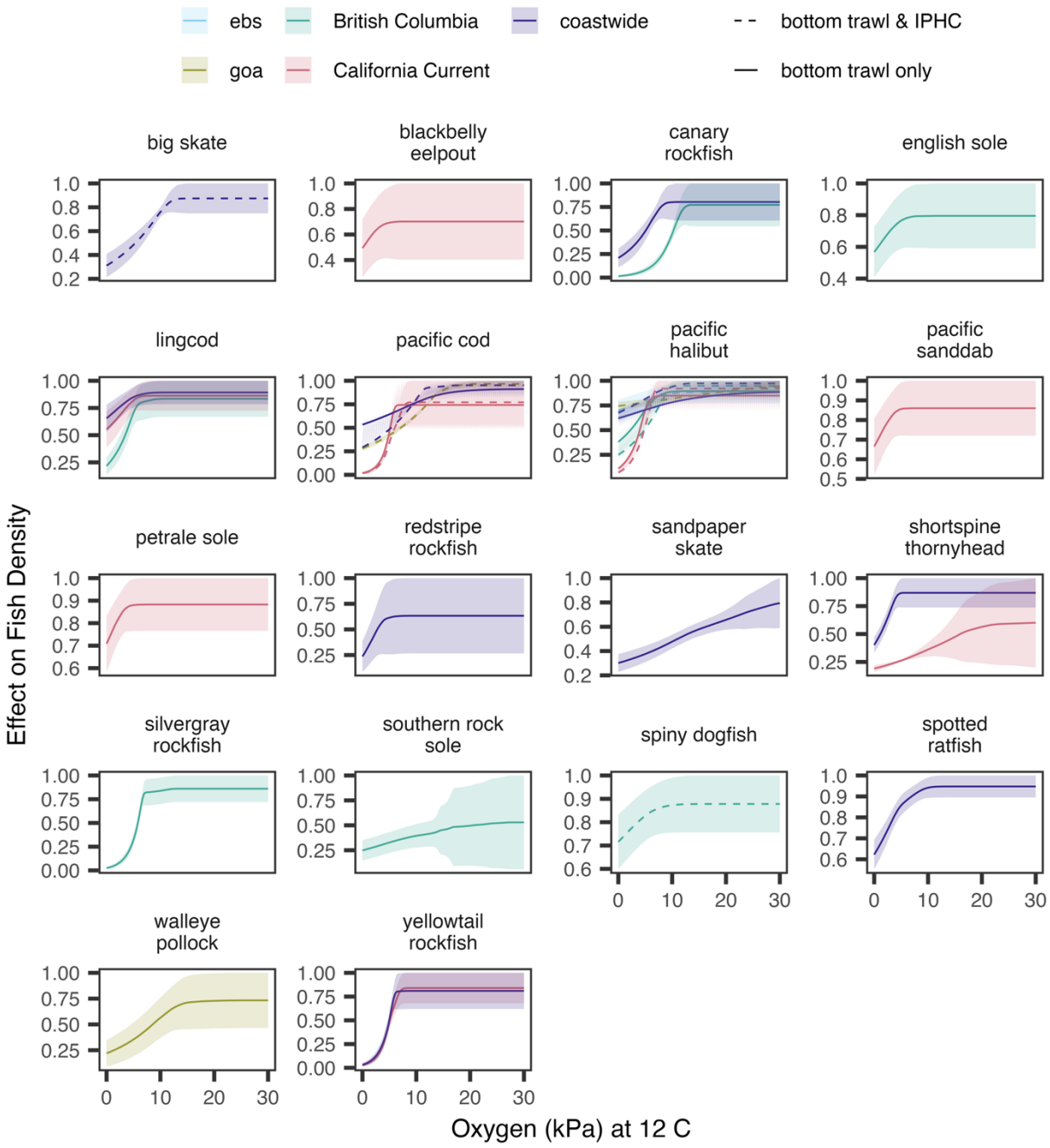

Figure S2. Mean ensemble conditional effect ± standard deviation of the partial pressure of oxygen (pO_2') (kPa) at 12 degrees C on local fish density, scaled to the maximum effect size. mean conditional effects ensembled across the five models—base, temperature, and the three breakpoint(pO2')—with conditional effects weighted by conditional Akaike Information Criteria (AIC) across 100 Monte Carlo simulations of the maximum likelihood estimation of the breakpoint and slope parameters. All other fixed (year, survey, region) and random fields (spatial and spatio-temporal variation) are set to zero. Color indicates the geographic extent of the model (region-specific or coastwide) Solid line indicates species was fit to only bottom trawl data, and dashed line that species was fit to combined bottom trawl and IPHC longline data.

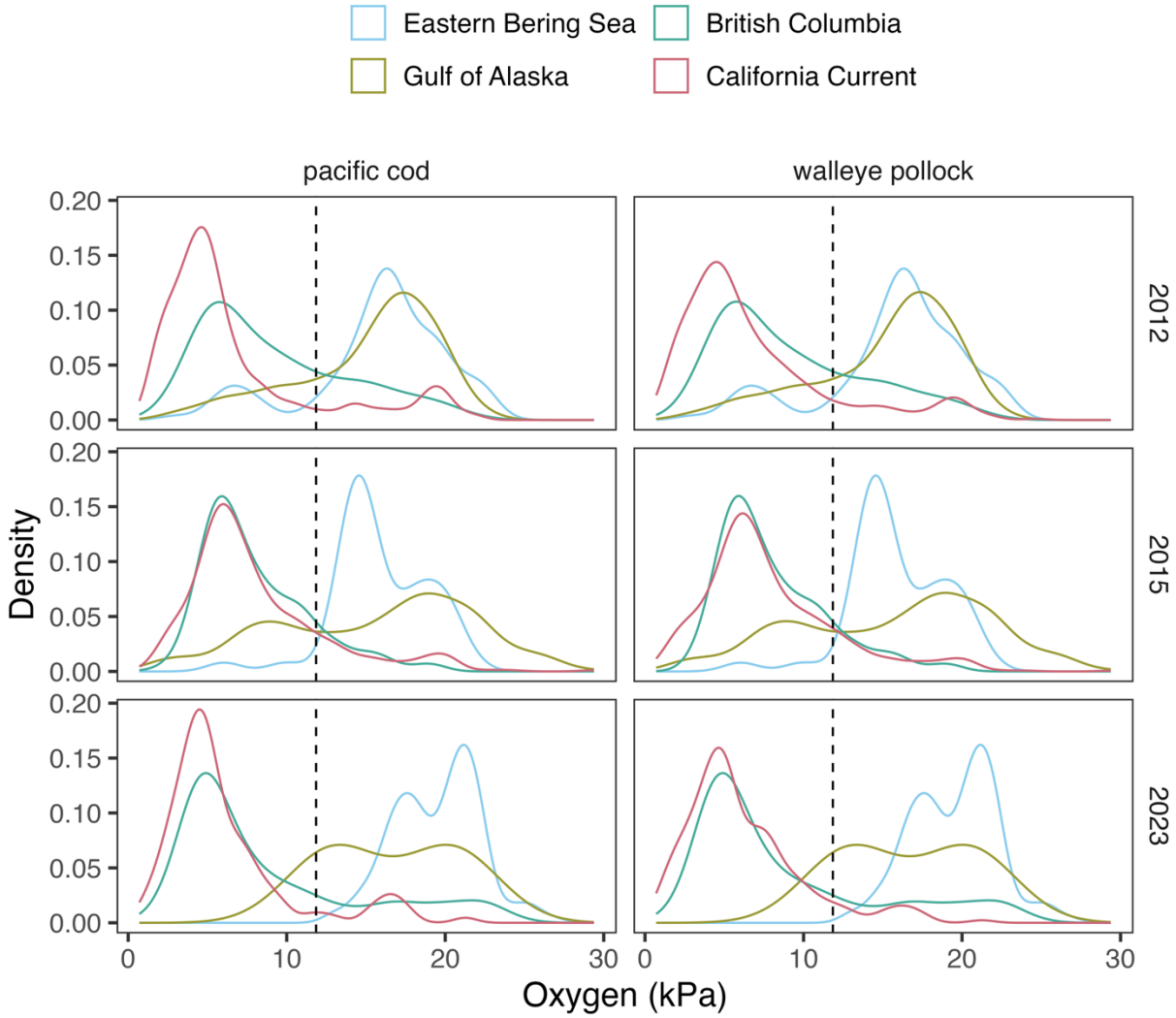

Figure S3. Density of oxygen observations in each region in three example years (2012, 2015, 2023) for two example species (pacific cod and walleye pollock), with dashed lines showing the mean ensemble temperature-corrected oxygen threshold. California Current and British Columbia are consistently generally below this threshold, while oxygen observations in the Gulf of Alaska and Eastern Bering Sea are generally above the threshold.

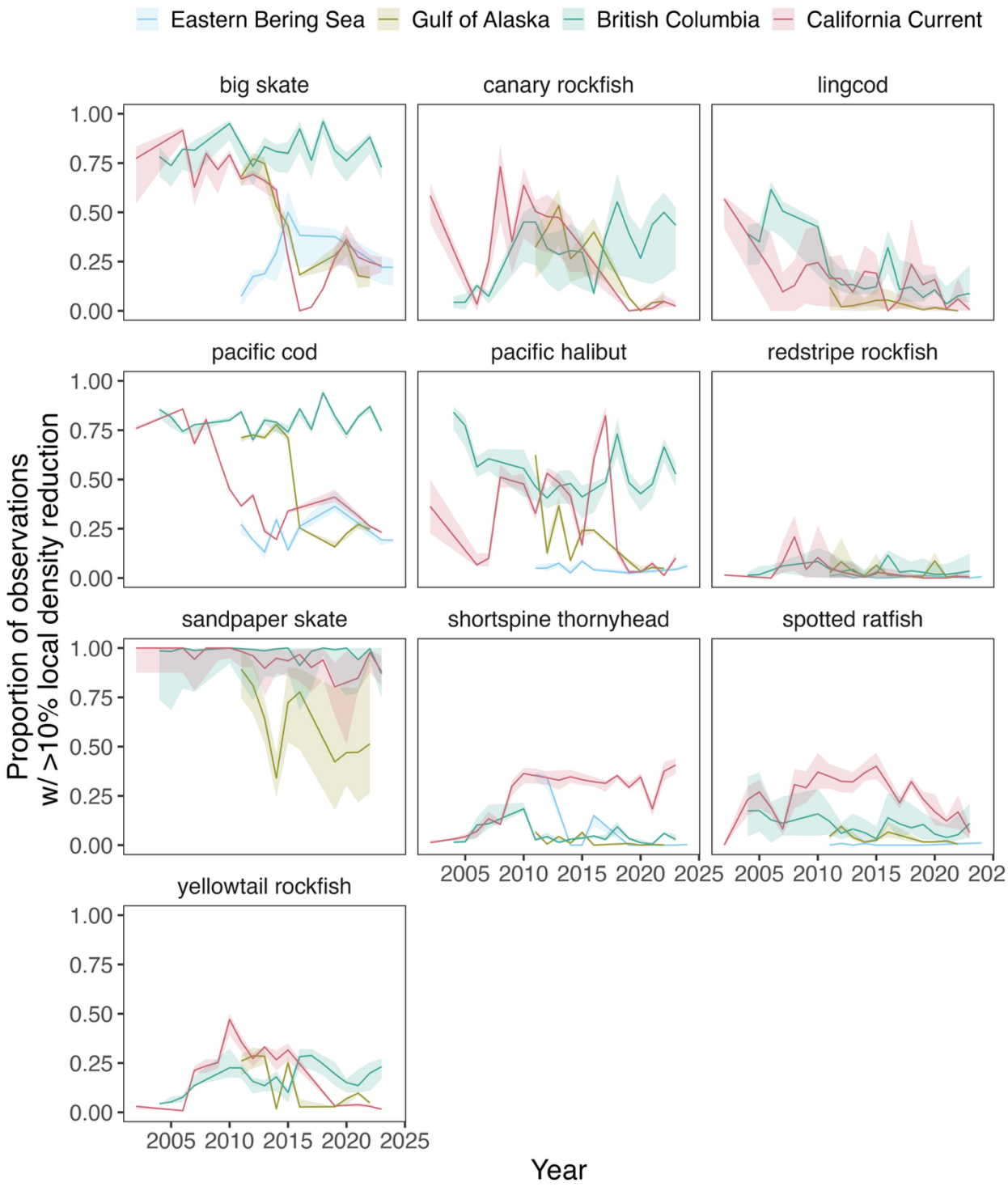

Figure S4. Proportion of historical oxygen observations ± standard error in each year and region at which mean ensemble reduction in fish density due to oxygen is estimated to be greater than 10%. Observations are constrained to the latitudinal range and typical depth habitat (200m buffer deeper than 99% cumulative catch) of each species. Reductions in biomass were calculated as the mean conditional effects ensembled across the five models–null, temperature, and the three

breakpoint(pO_2')--with conditional effects weighted by marginal Akaike Information Criteria (AIC) across 100 Monte Carlo simulations of the maximum likelihood estimation of the breakpoint and slope parameters. All other fixed (year, survey, region) and random fields (spatial and spatio-temporal variation) are set to zero. While there is some fluctuation between years, there is no clear trend.

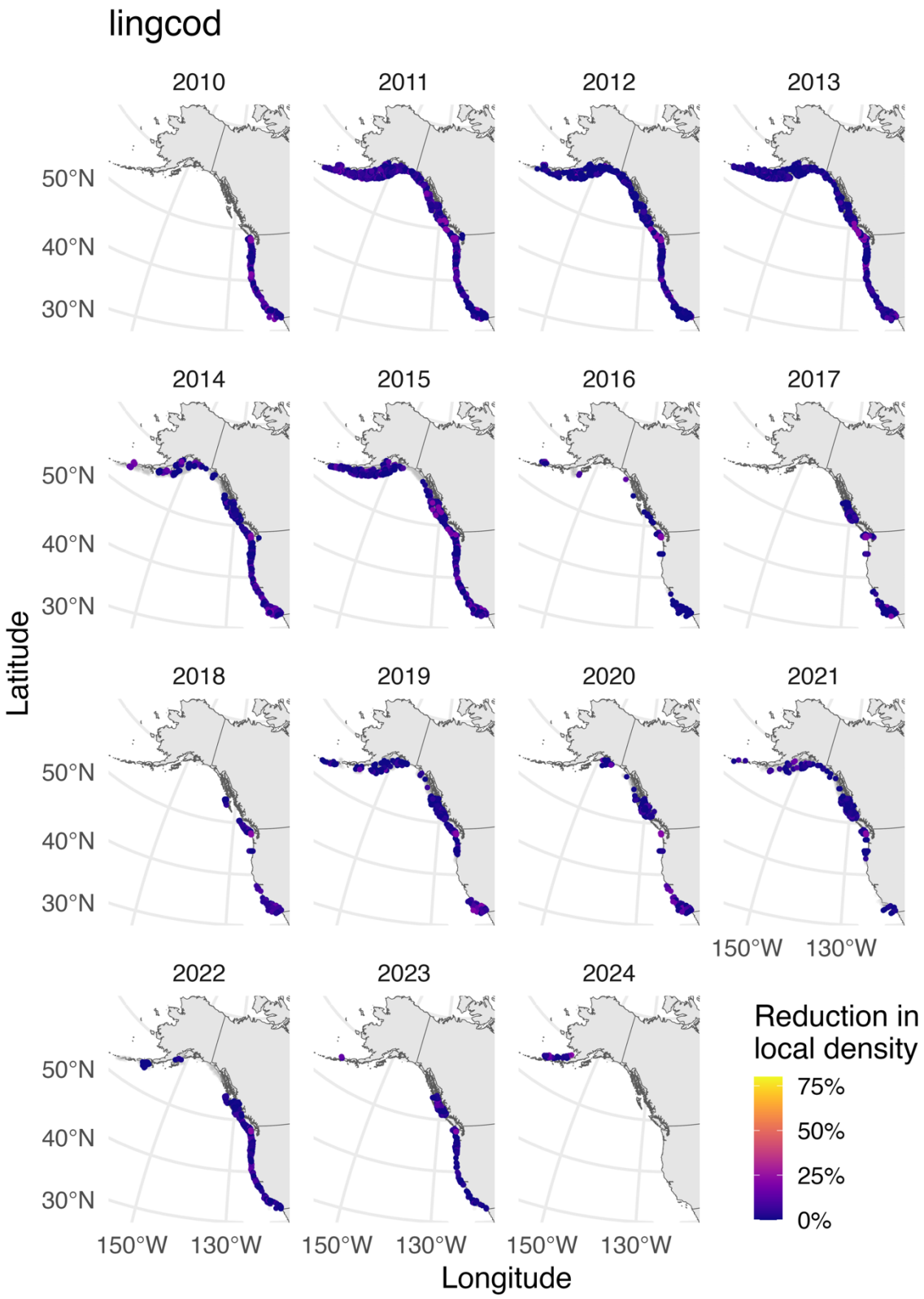

Figure S5. Percentage reduction in local fish density due to oxygen at oxygen observations compiled coastwide in each year for lingcod. While spatial area of observations available in each year varies, the overall spatial pattern in estimated reductions in density are similar and stable

across years. Reductions in density were calculated as the mean conditional effects ensembled across the five models–base, temperature, and the three breakpoint(pO_2')–with conditional effects weighted by marginal Akaike Information Criteria (AIC) across 100 Monte Carlo simulations of the maximum likelihood estimation of the breakpoint and slope parameters. Only species with a coastwide pO_2' model are included. All other fixed (year, survey, region) and random fields (spatial and spatio-temporal variation) are set to zero. Observations are constrained to the latitudinal range and typical depth habitat (200m buffer deeper than 99% cumulative catch) of each species. Pacific halibut models were fit to combined bottom trawl and IPHC longline survey biomass data (kg ha^{-1}). Grey points indicates there was no estimated biomass reduction from oxygen at that oxygen observation.

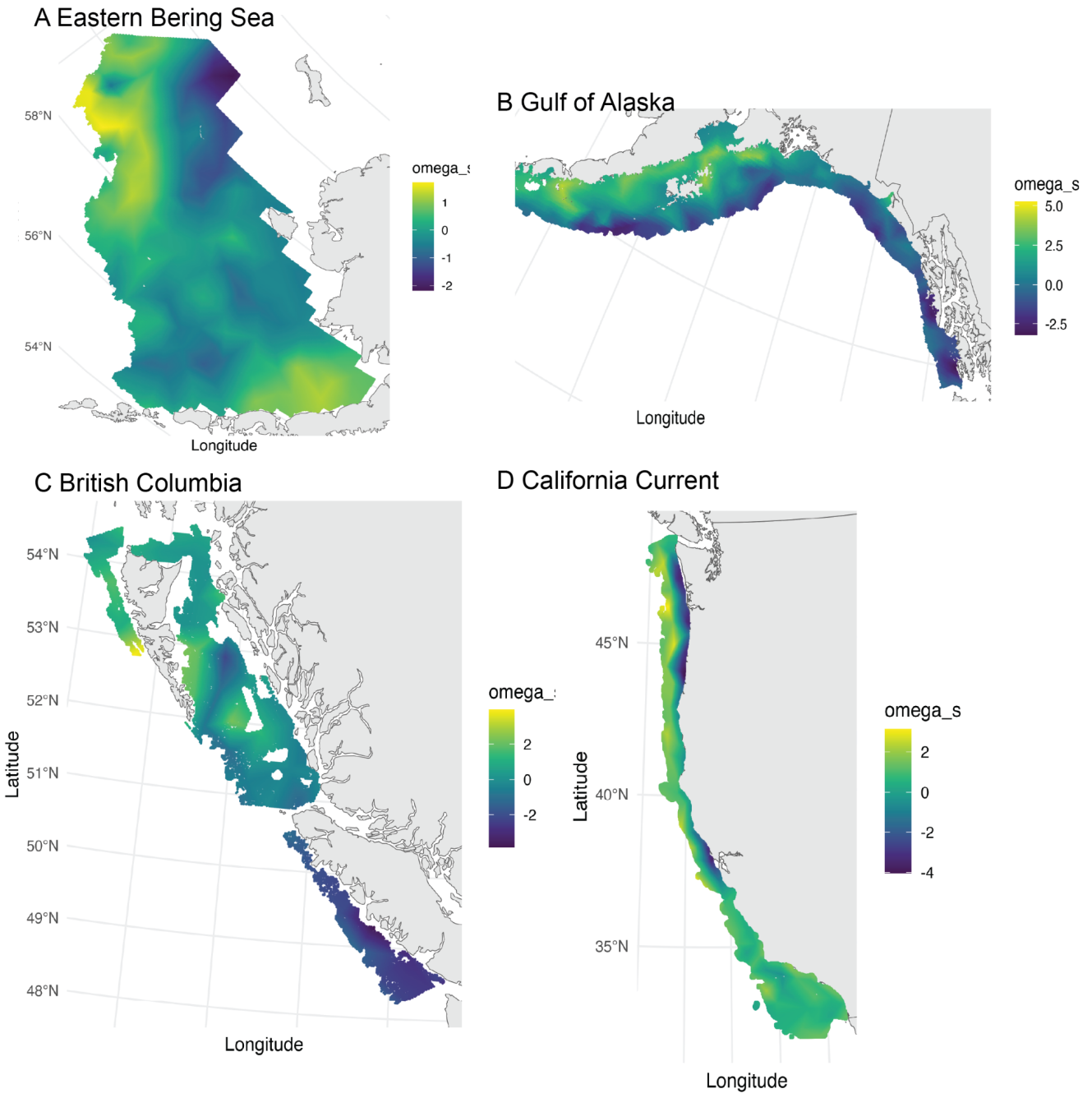

Figure S6. A-D) Estimated persistent spatial variation (i.e. omega) of dissolved oxygen of period in each region in A) California Current, B) British Columbia, C) Eastern Bering Sea, and D) Gulf of Alaska. Overall spatial variation in each region was larger than estimated spatio-temporal variation.

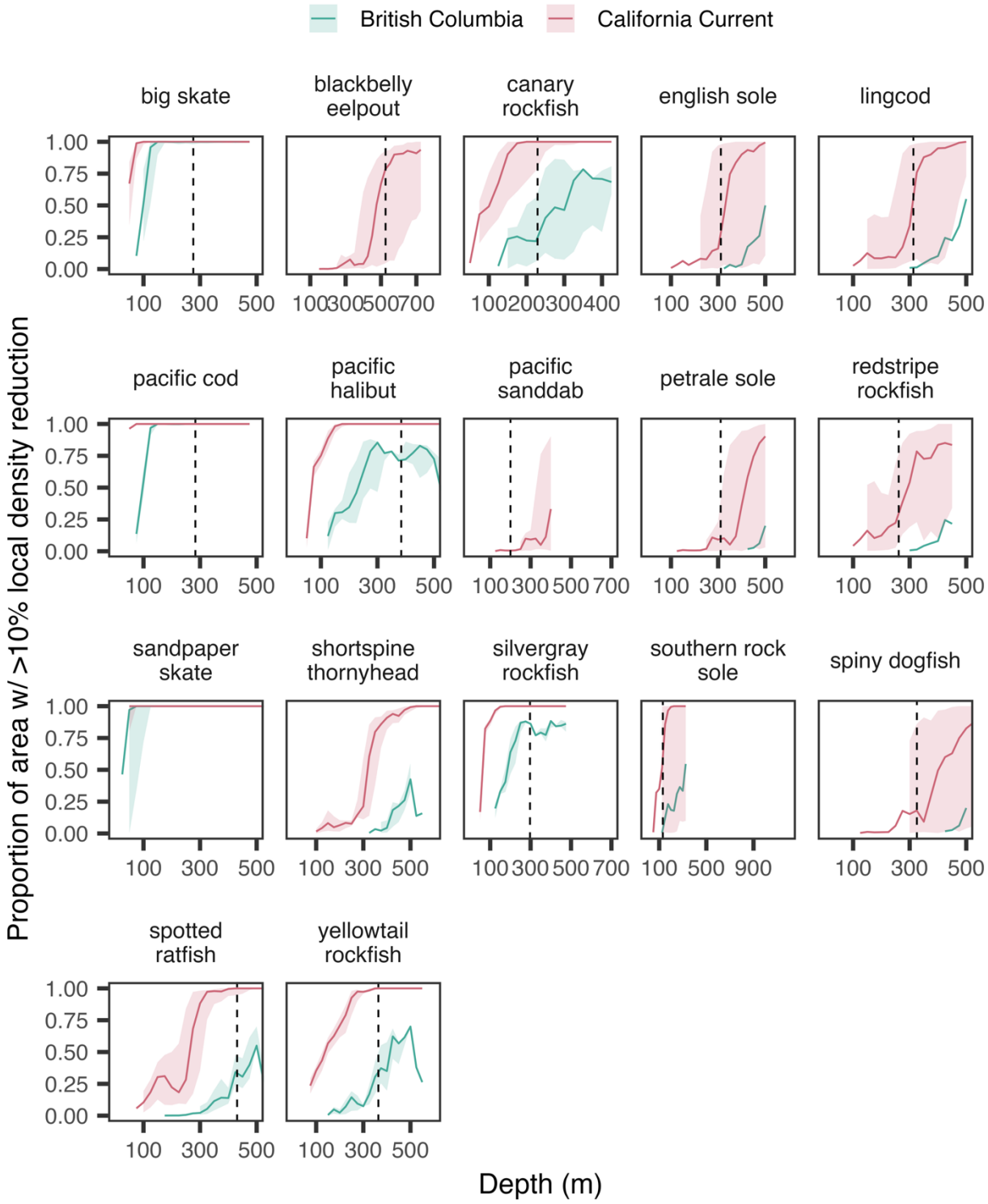

Figure S7. Proportion of area ± standard deviation in 2021 at which mean ensemble reduction in fish density was estimated to be greater than 10% across depth (50m bins) in each region. Dashed lines indicate the depth limit at which species were typically found in data (at 99% of cumulative fish catch). Grid is constrained to the latitudinal range and typical depth habitat

(200m buffer deeper than 99% cumulative catch) of each species. Reductions in biomass were calculated as the mean conditional effects ensembled across the five models–base, temperature, and the three breakpoint(pO_2')–with conditional effects weighted by marginal Akaike Information Criteria (AIC) across 100 Monte Carlo simulations of the maximum likelihood estimation of the breakpoint and slope parameters. All other fixed (year, survey, region) and random fields (spatial and spatio-temporal variation) are set to zero.

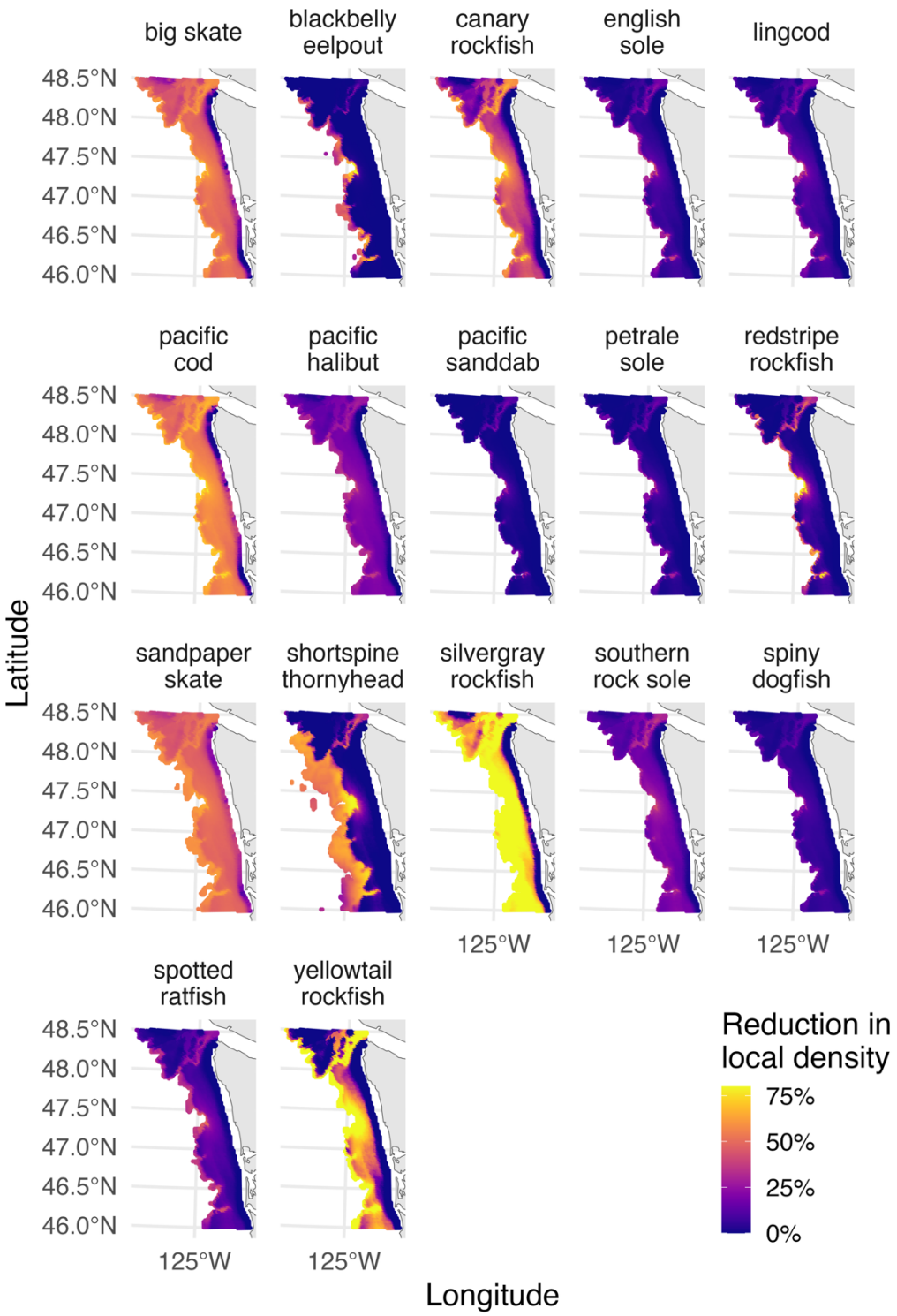

Figure S8. Reduction in local fish density due to oxygen in 2021 (a year with hypoxic conditions, Barth et al 2024) off the coast of Washington state. Reductions in biomass were calculated as the mean conditional effects ensembled across the five models–null, temperature, and the three breakpoint(pO_2')–with conditional effects weighted by marginal Akaike Information Criteria (AIC) across 100 Monte Carlo simulations of the maximum likelihood

estimation of the breakpoint and slope parameters. All other fixed (year, survey, region) and random (spatial and spatio-temporal variation) effects were set to zero. Grid is constrained to the latitudinal range and typical depth habitat (200m buffer deeper than 99% cumulative catch) of each species. For each species, the model fit to coastwide data and including IPHC data were used if available, otherwise region-specific models were used. Pacific halibut and Pacific cod models were fit to combined bottom trawl and IPHC longline survey, and the remainder of species were fit to only bottom trawl data (NOAA and DFO). Pacific cod was fit to abundance (numbers of fish) data, and the remainder of species were fit to biomass data (kg ha^{-1}). Grey indicates there was no estimated biomass reduction from oxygen. Oxygen was statistically interpolated across the grid from compiled *in situ* oxygen observations (Indivero et al., 2025).

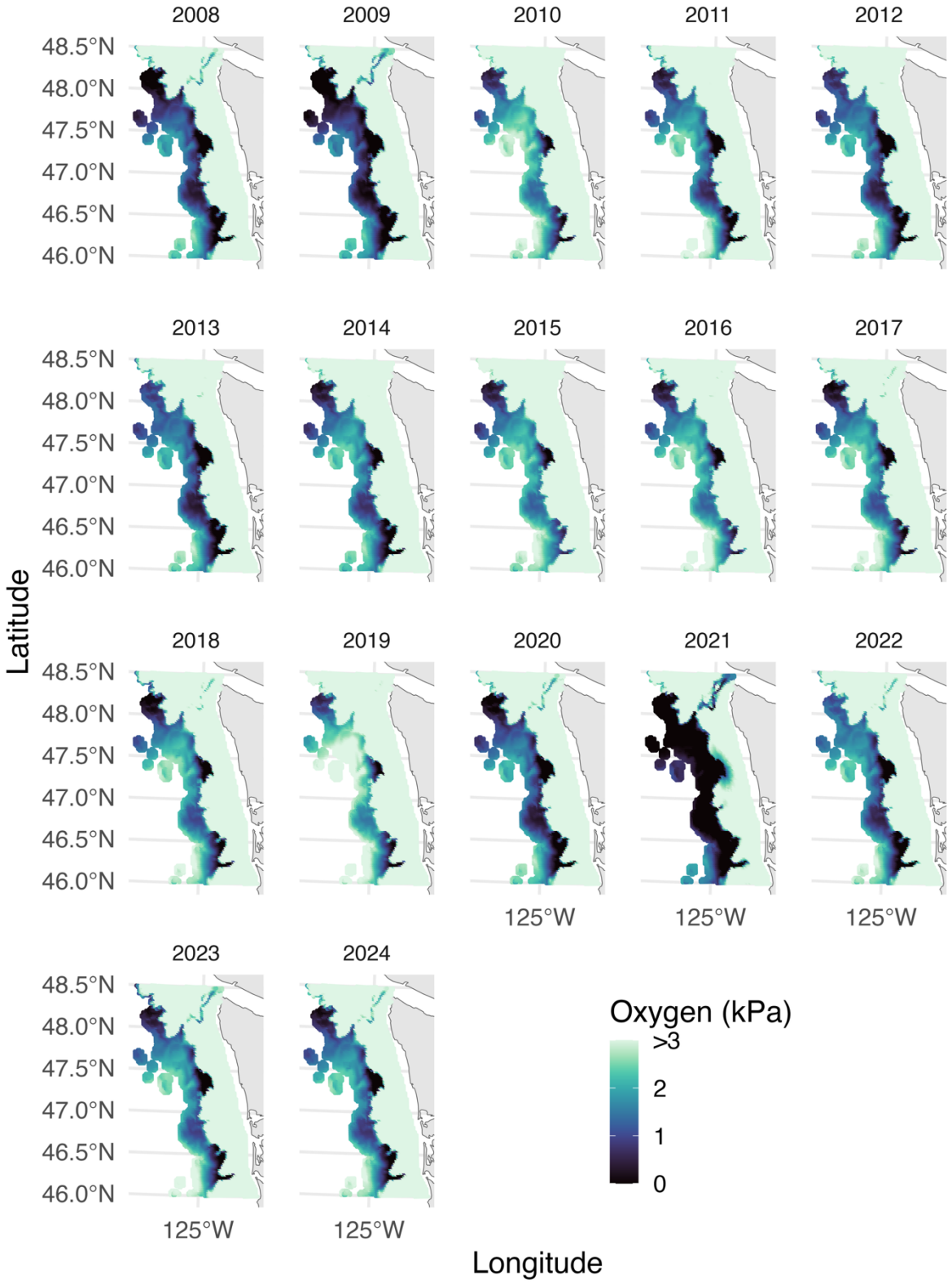

Figure S9. Oxygen across grid of California Current and British Columbia

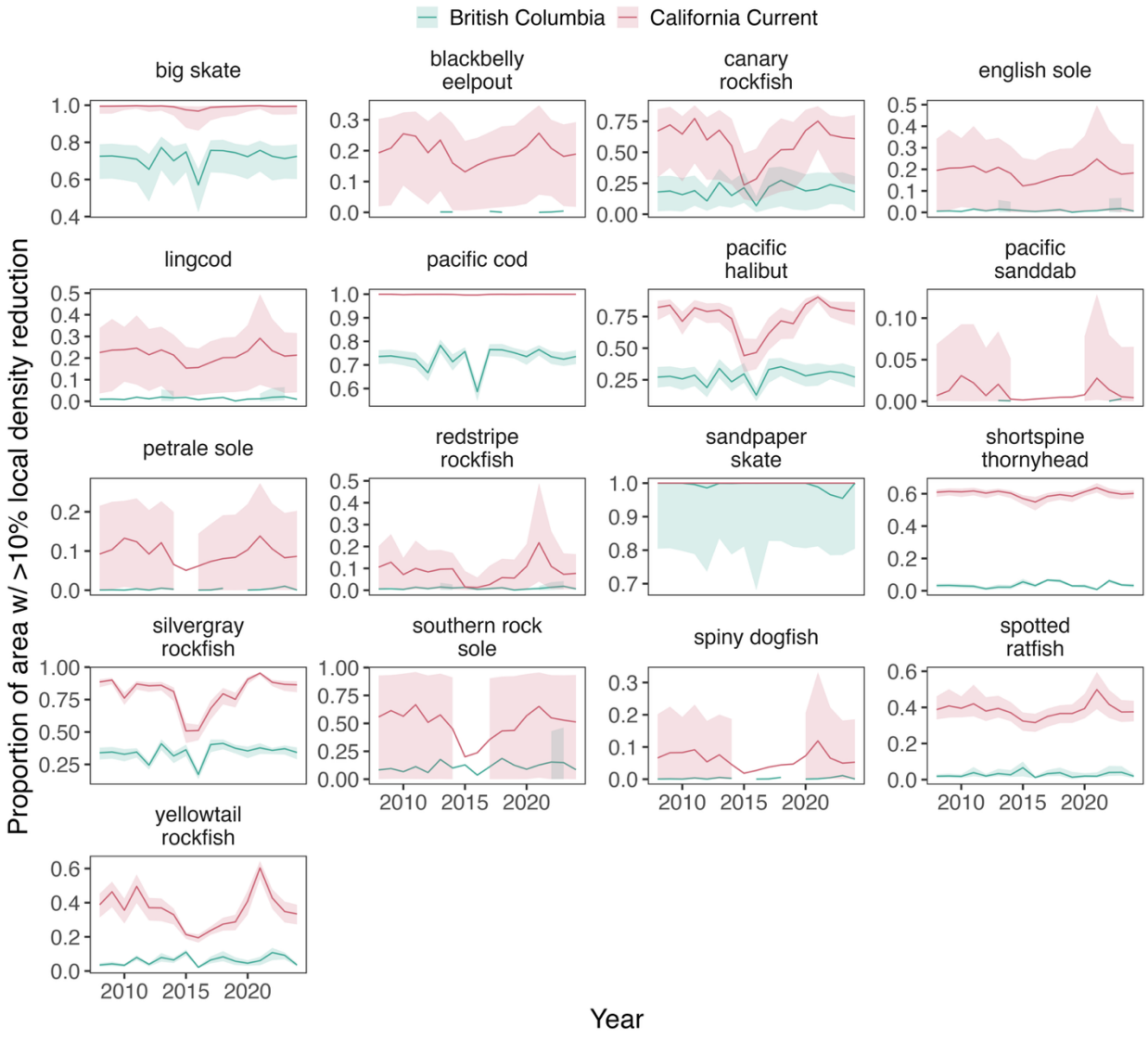

Figure S10. Proportion of area in survey grid ± standard deviation that historical oxygen is estimated to cause greater than 10% reduction in local fish density. Grid cells are constrained to the latitudinal range and typical depth habitat (200m buffer deeper than 99% cumulative catch) of each species. Reductions in density were calculated as the mean conditional effects ensembled across the five models–null, temperature, and the three breakpoint(pO2')–with conditional effects weighted by marginal Akaike Information Criteria (AIC) across 100 Monte Carlo simulations of the maximum likelihood estimation of the breakpoint and slope parameters. All other fixed (year, survey, region) and random fields (spatial and spatio-temporal variation) are set to zero.

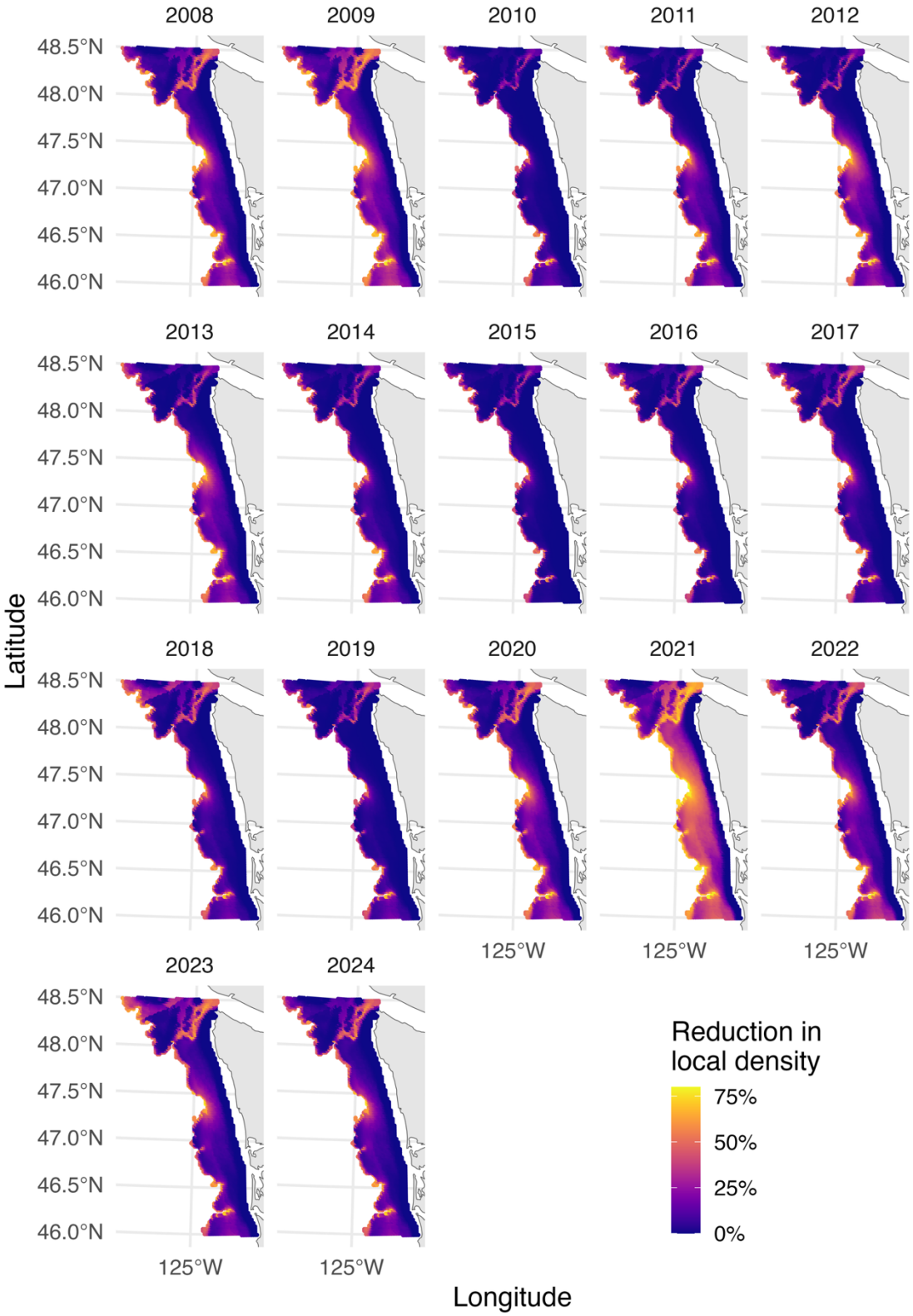

Figure S11. Estimated percentage reduction in local fish density due to oxygen off Washington coast each year of study period for an example species (canary rockfish). Estimated reductions were calculated as the mean conditional effects ensembled across the five models–basel,

temperature, and the three breakpoint(pO_2')--with conditional effects weighted by marginal Akaike Information Criteria (AIC) across 100 Monte Carlo simulations of the maximum likelihood estimation of the breakpoint and slope parameters. All other fixed (year, survey, region) and random fields (spatial and spatio-temporal variation) are set to zero. Grid is constrained to the latitudinal range and typical depth habitat (200m buffer deeper than 99% cumulative catch) of each species. Oxygen was statistically interpolated across the grid from compiled *in situ* oxygen observations (Indivero et al, 2025).

Figure S12. Proportion of area in survey grid in each U.S. state and British Columbia that historical oxygen ± standard deviation is estimated to cause greater than 10% reduction in local fish density. Grid cells are constrained to the latitudinal range and typical depth habitat (200m buffer deeper than 99% cumulative catch) of each species. Reductions in density were calculated as the mean conditional effects ensembled across the five models–null, temperature, and the three breakpoint(pO_2')–with conditional effects weighted by marginal Akaike Information Criteria (AIC) across 100 Monte Carlo simulations of the maximum likelihood estimation of the

breakpoint and slope parameters. All other fixed (year, survey, region) and random fields (spatial and spatio-temporal variation) are set to zero.

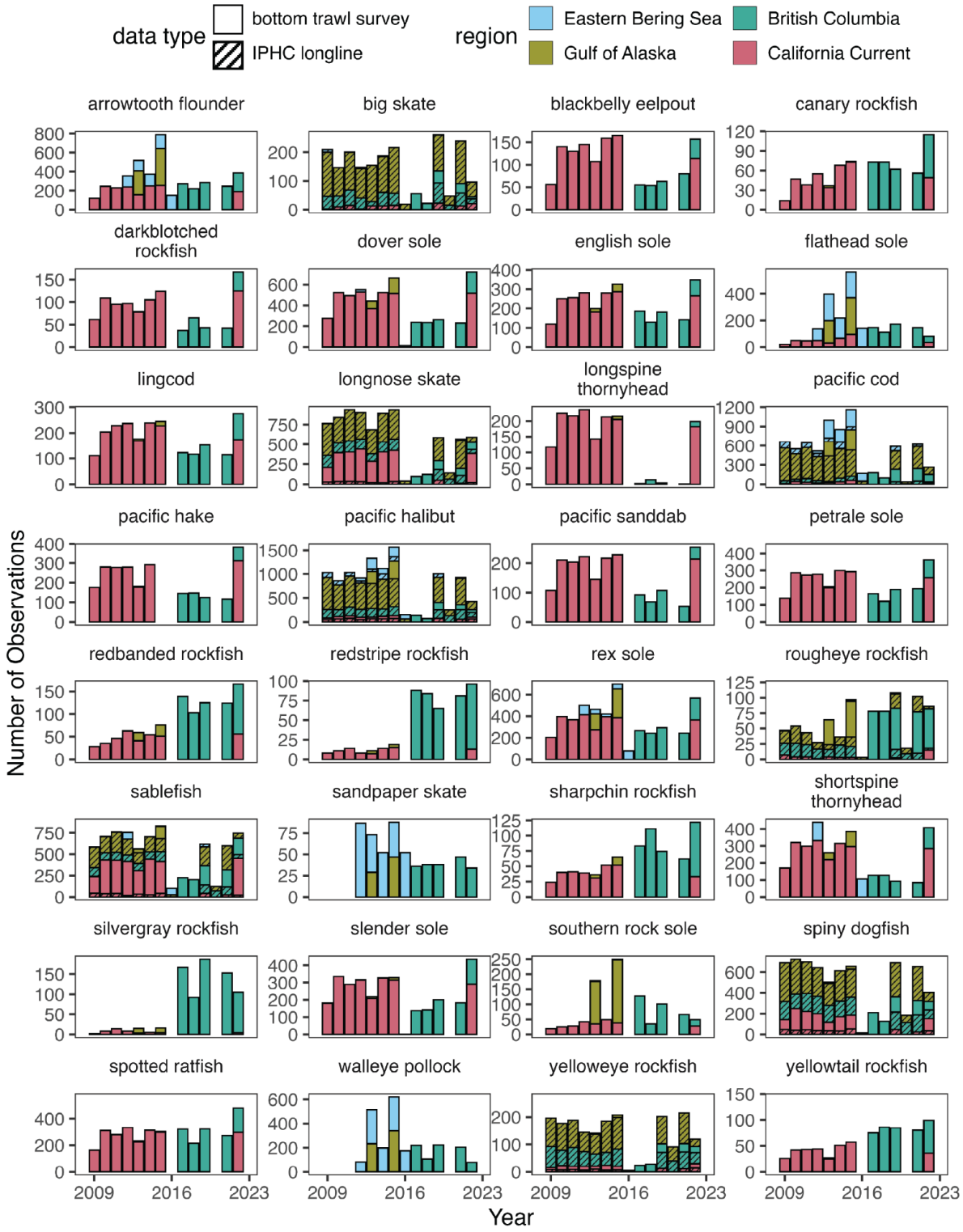

Figure S13. Number of observations with positive catch for each species in each region and year. Bars are colored by region, and dashed lines indicate data from the International Pacific Halibut Commission longline survey and solid bars from bottom trawl data (U.S. National Oceanic and Atmospheric Administration and Department of Fisheries and Oceans Canada).

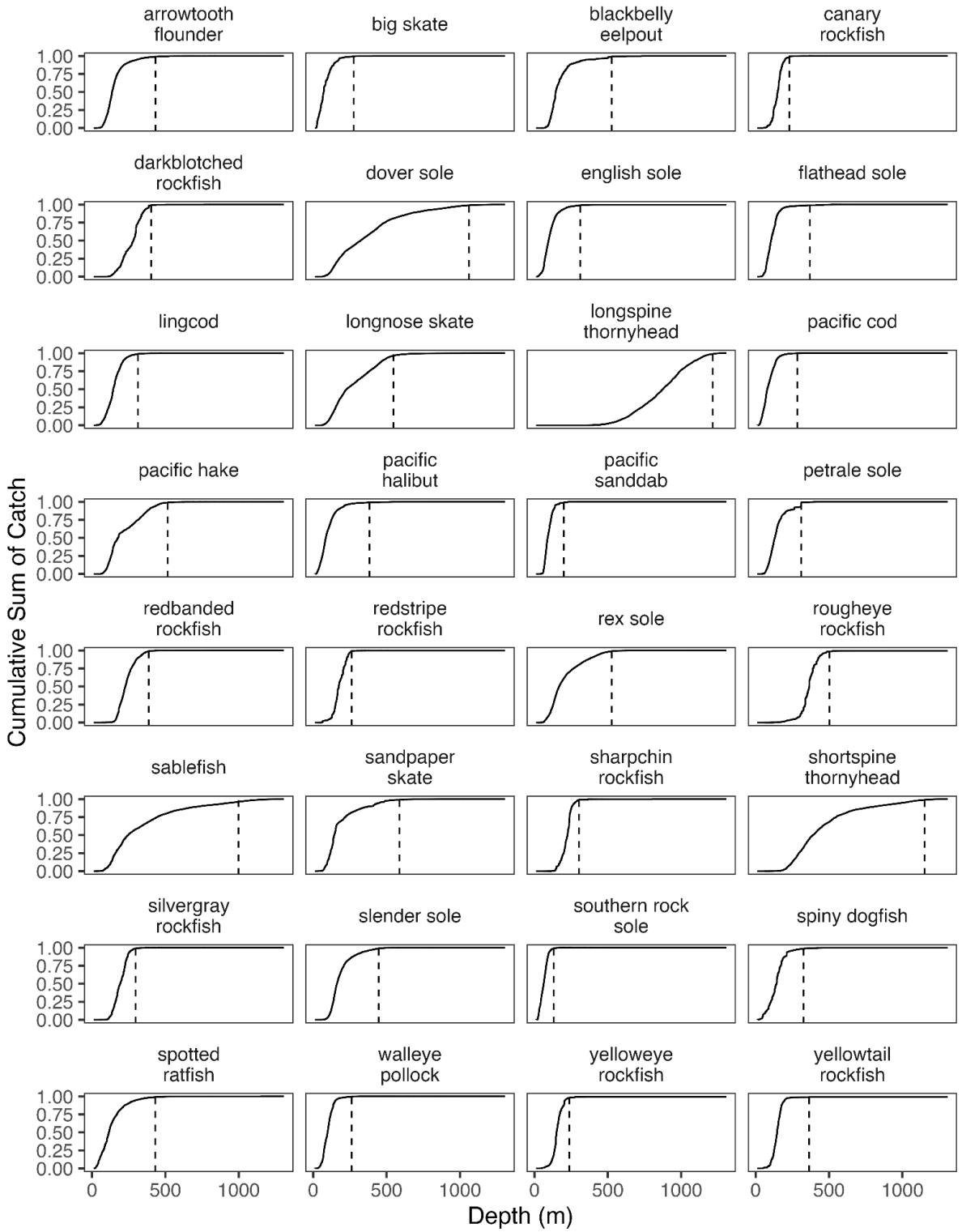

Figure S14. Cumulative sum of species catch (biomass) across depth, with dashed lines indicating the depth at 99% of cumulative sum. Data were filtered to above this depth limit for model fitting.

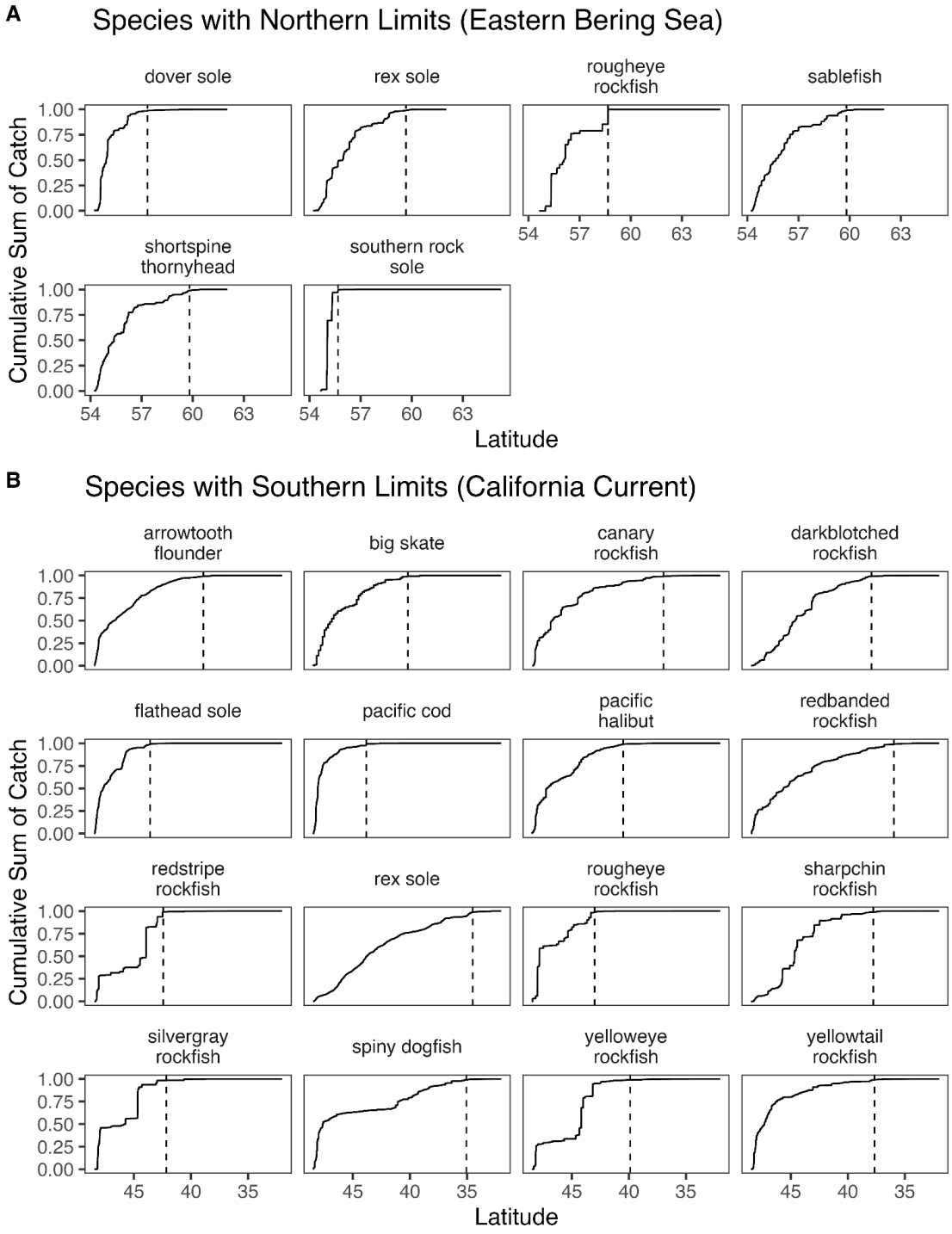

Figure S15. Cumulative sum of species catch (biomass) across latitude in the northern (A) and southern (B) regions,, with dashed lines indicating the depth at 99% of cumulative sum. Data were constrained to latitudinal ranges when there were clear range limits.

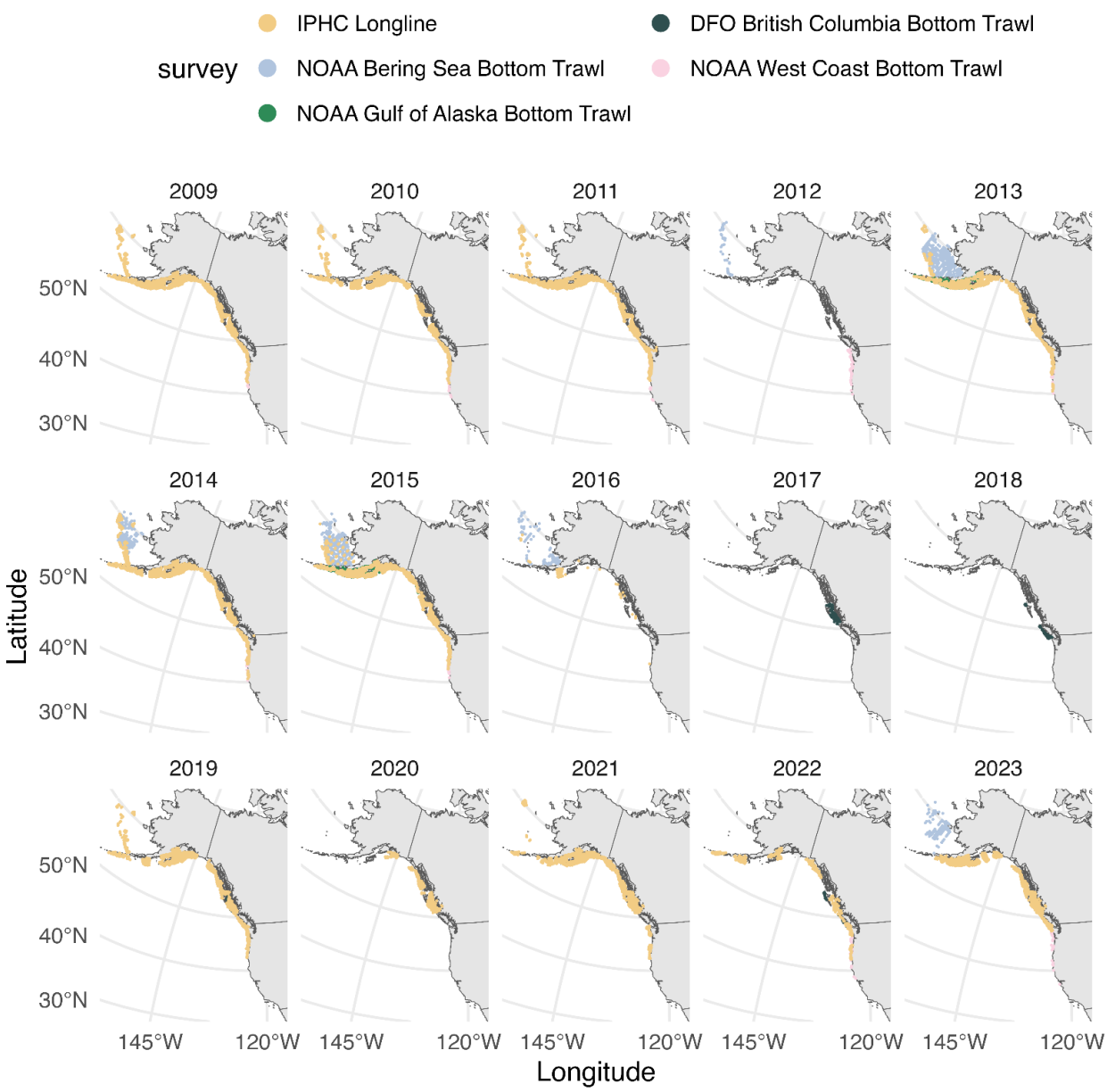

Figure S16. Example of observations (positive catch only) in data used in model fitting for Pacific halibut, with coastwide data including all bottom trawl surveys and the International Pacific Halibut Commission longline data.